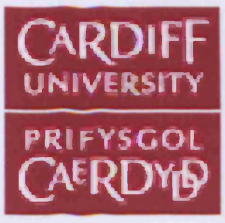

DISSECTING A NOVEL INVERTEBRATE PATHWAY IMPLICATED IN HEAVY METAL MEDIATED TRANSCRIPTIONAL CONTROL

BY SAMANTHA LOUISE HUGHES

Thesis submitted to Cardiff University for the degree of Doctor of Philosophy

ProQuest LLC
789 East Eisenhower Parkway
P.O. Box 1346
Ann Arbor, MI 48106-1346

"The most exciting phrase to hear in science, the one that heralds the most discoveries, is not "Eureka!" (I found it!) but "That's funny..."

Isaac Asimov

ACKNOWLEDGEMENTS

Foremost I would like to thank my supervisor, Dr Stephen Stürzenbaum, for his patience, experience and research insight. I also thank Dr Peter Kille for his advice and support. Thanks are also due to several other researchers: Dr Jacob Bundy for his help, support and encouragement and Dr Elizabeth Want, both of Imperial College London, Dr Barry Panaretou, King's College London and Dr Jodie Wren, now at Bristol University.

The work undertaken over the last 3 years could not have been achieved without the help and support from a variety of collegues, friends and family members. It is simple to name all the people who have helped and supported me but it will be difficult to thank them enough. Special mentions are required for my parents who supported and encouraged me during periods of stress and have survived to tell the tale. Special thanks go to Danny for putting up with my irregular hours and spoiled weekends. Thank you.

My PhD was funded by a Natural Environmental Research Council (NERC) studentship (NERC/S/A/2005/13135) and the Royal Society.

DECLARATION

This work has not previously been accepted in substance for any degree and is not concurrently submitted in candidature for any degree.

Signed  .....(candidate)

Date ...28th November 2008.....

STATEMENT 1

This thesis is being submitted in partial fulfillment of the requirements for the degree of PhD

Signed  .....(candidate)

Date ...28th November 2008.....

STATEMENT 2

This thesis is the result of my own independent work/investigation, except where otherwise stated. Other sources are acknowledged by explicit references.

Signed  .....(candidate)

Date .....28th November 2008.....

STATEMENT 3

I hereby give consent for my thesis, if accepted, to be available for photocopying and for inter-library loan, and for the title and summary to be made available to outside organisations.

Signed  .....(candidate)

Date ...28th November 2008.....

STATEMENT 4: PREVIOUSLY APPROVED BAR ON ACCESS

I hereby give consent for my thesis, if accepted, to be available for photocopying and for inter-library loans **after expiry of a bar on access previously approved by the Graduate Development Committee.**

Signed  .....(candidate)

Date ...28th November 2008.....

ABSTRACT

The genome of *Caenorhabditis elegans* contains two metallothionein isoforms and a functional phytochelatin synthase. All three proteins have roles in metal detoxification and metal homeostasis. Although a great deal is known with regards to vertebrate metallothioneins and their transcriptional control, little is understood about *C. elegans* metallothionein. In addition, phytochelatin synthase was only discovered within the last decade and as a consequence little is known about this enzyme and its product, phytochelatins. The use of green fluorescent protein expressing transgenes *C. elegans* allows the expression pattern for all genes to be investigated. The GFP transgenic strains were also utilised in the RNA mediated knockdown of a selection of transcription factors to identify two candidate genes involved in metallothionein transcription. The generation of a combination of single, double and triple mutants permitted the investigation into the function of metallothioneins and phytochelatins on elevated and depleted levels of essential and non-essential heavy metals via their phenotypic effects. Metabolomic analysis of these mutants provided an indication that cadmium affected the transsulfuration pathway and ultimately suggested that phytochelatins have a significant role in cadmium detoxification. Quantitative PCR analysis showed that there was minimal compensatory up regulation of metallothionein when one isoform is removed. Conversely, the removal of *pcs-1* results in significant up regulation of both MT isoforms following exposure to cadmium. In conclusion, this research was able to demonstrate that in *C. elegans,* phytochelatins play an important and significant role in metal detoxification, possibly more than metallothioneins.

Abbreviations and conventions

aa	Amino acids
AAS	Atomic absorption spectroscopy
ANOVA	Analysis of variance
amp	Ampicillin
BCS	Bathocuproinedisulfonic acid disodium salt
bp	Base pair
carb	Carbamycin
cDNA	Complementary DNA
CGC	*Caenorhabditis* genetics centre
Da	Daltons
dH_2O	Deionised water
DNA	Deoxyribonucleic acid
dNTPs	Deoxyribonucleotide triphosphates
ds	Double stranded
EC_{50}	Median effective concentration (of a toxin)
FA	Formic acid
GFP	Green fluorescent protein
HPLC	High purified liquid chromatography grade water
LC_{50}	Half the lethal concentration (of a toxin)
ICP/OES	Inductively coupled plasma - optical emission spectrometer
IPTG	Isopropyl β-D-thiogalactopyranoside
LB	Luria broth
LEU2	Leucine selection marker
M	Molar
MCS	Multiple cloning site
miRNA	Micro RNAi
ml	Millilitre
mM	Millimolar
MMuLV	Moloney murine leukemia virus reverse transcriptase
mRNA	Messenger RNA
MS	Mass spectrometry
MT	Metallothionein

MTF-1	Metal responsive transcription factor 1
Mw	Molecular weight
NMR	Nuclear magnetic resonance spectroscopy
°C	Degrees, in centigrade
oligo dT	Oligonucleotide of thymidine residues
OPNG	*Ortho*-nitrophenyl-β-d-galactoside
PC	Phytochelatin
PC	Principle components
PCA	Principle component analysis
PCR	Polymerase chain reaction
PCS	Phytochelatin synthase
PLS-DA	Partial least square discrimination analysis
P*mtl*::GFP	Promoter of either *mtl-1* or *mtl-2* fused to GFP
psi	Pounds per square inch
Q-PCR	Quantitative polymerase chain reaction
RISC	RNA induced silencing complex
RNA	Ribonucleic acid
RNAi	RNA interference
RNase	Ribonuclease
ROS	Reactive oxygen species
RT	Reverse transcriptase
shRNA	Short hairpin RNA
siRNA	Short interfering RNA
ss	Single stranded
TAE	Tris-acetic acid buffer
Taq	*Thermus aquaticus* polymerase
Tm	Annealing temperature
TOF	Time of flight
TSP	Trimethylsilyl-2,2,3,3-d4-propionic acid, NMR internal standard
Y1H	Yeast one hybrid
YPD	Yeast peptone dextrose
µg	Microgram(s)
µM	Microlitre(s)

CONTENTS PAGE

CHAPTER ONE

GENERAL INTRODUCTION

1.1. Heavy metals

Heavy metals are present in the terrestrial and aquatic environment as a result of natural and man-made processes (Swain *et al.* 2004). Heavy metals are those elements which have a density of 5 g/cm^3 or more, have a high molecular weight and are generally located in groups Ib and IIb of the periodic table. Biological systems require trace amounts of certain heavy metals such as zinc and copper for vital functions (Rea *et al.* 2004; Valko *et al.* 2005). Zinc is an essential heavy metal and it provides catalytic, structural and regulatory functions (Camakaris *et al.* 1999; Maret 2005). Copper, another important heavy metal, is utilised in many cellular processes throughout the animal and plant kingdom including respiration, iron metabolism and photosynthesis (Valko *et al.* 2005). Non-essential heavy metals occur in the environment frequently in conjunction with essential metals. The presence of these metals such as cadmium, mercury and lead can interfere with biological systems, specifically by disrupting the essential cofactor from enzymes (Rea *et al.* 2004). As a result, the physiological concentrations of essential, and non-essential, heavy metal ions in an organism are tightly regulated. Even a small deviation from the norm can cause various toxicological problems and may ultimately lead to death (Valko *et al.* 2005).

1.1.1. Zinc

Zinc is an essential metal and has specific roles in an organism. Zinc is used as a cofactor in enzymes (Blencowe and Morby 2003), aids in membrane stability (Prasad 1985), and functions in immunity (Valko *et al.* 2005). Cellular zinc levels are tightly controlled by complex regulatory pathways involving many different proteins including sensor proteins, membrane proteins, transporter proteins and metallothioneins (MT) (Maret 2005). Physiological concentrations of zinc must be tightly maintained. Too little of the ion is detrimental, for example, humans deficient in dietary zinc are susceptible to neuronal and immune problems (Cousins *et al.* 2003). An excess of the metal is toxic to cells, especially neuronal cells (Choi *et al.* 1988). Cation diffusion proteins and ZIP (Zrt- and Irt- like proteins) transporters regulate cytosolic zinc levels via transcriptional changes in gene expression (Cousins *et al.* 2003). Two members of the ZIP transporter family, ZIP1 and ZIP2, are upregulated in the absence of zinc to increase the cellular uptake of Zn^{2+} and return the cell to the optimal zinc level (Cousins *et al.* 2003). In contrast, during periods of excess zinc which is toxic to cells the ion can be transferred to lysosomes for removal (Valko *et al.* 2005).

1.1.2. Copper

Copper is an essential metal that has ion levels maintained by transporters such as *ctr-1*. Expression of transporters is increased following excess copper to increase the ion efflux and vice versa to return the cell to optimal copper concentrations (Ogra *et al.* 2006).

Excess copper conditions are detrimental to the cell due to the formation of free radicals and reactive oxygen species (ROS) via the Fenton Reaction (Camakaris *et al.* 1999; Mattie and Freedman 2004). The extremely reactive free radicals and ROS will cause irreversible damage to DNA as well as inducing conformational changes in proteins which may inactivate them (Camakaris *et al.* 1999; Mattie and Freedman 2004). Depleted copper environments result in the failure of copper dependent enzymes to function as there are no cofactors available (Ogra *et al.* 2006). Two genetic diseases in humans illustrate how important the maintenance of intracellular copper levels are to the cell and organism. Wilson's Disease is a consequence of copper accumulation in the liver as a result of the inability to transport ions across the apical membranes of liver cells (Klaassen *et al.* 1999; Larin *et al.* 1999). The hallmark of Menkes' Disease is an uneven or copper deficient environment. A copper deficient cellular environment is a result of a reduction in the ion efflux from the intestine into the blood stream (Klaassen *et al.* 1999; Larin *et al.* 1999).

1.1.3. Cadmium

Cadmium is a non-essential heavy metal which is found in natural sources and as a result of industrial activities such as the burning of fossil fuels and emissions from factories (Suzuki *et al.* 2002; Waisberg *et al.* 2003). As cadmium is not an essential metal, prolonged exposure to the ion is toxic to an organism. In humans extended periods of exposure to cadmium results in many varied pathologies; osteomalacia, anaemia and proteinurea are just a few (Waisberg *et al.* 2003). At the cellular level cadmium is able to inhibit DNA

repair mechanisms (specifically base excision repair), induce apotosis, prevent cell-to-cell adhesion, and generate reactive oxygen species (Waisberg *et al.* 2003). In addition, cadmium can indirectly generate free radicals via the displacement of copper and zinc from proteins which are then available to form free radicals via the Fenton reaction (Valko *et al.* 2005).

Full genome microarrays identified a change in expression of 290 genes in *Caenorhabditis elegans* as a result of cadmium exposure (Cui *et al.* 2007). Such genes include those involved in cellular and ion trafficking, metabolic enzymes, proteolysis, metallothioneins, heat shock proteins and glutathiones (Cui *et al.* 2007; Waisberg *et al.* 2003). All these mechanisms are in place to try and remove the ion from the cell to maintain viability.

1.2. Mechanisms of metal detoxification

Too much or too little of an essential metal can be harmful to the cell and as such there are various regulatory proteins to control the trace metal concentration. Iron regulatory proteins are critical in controlling the synthesis of proteins involved in ion homeostasis (Eisenstein 2000). The multi-subunit protein Ferritin is synthesised when the physiological iron concentration increases. Ferritin is a protein able to bind and store up to 4500 iron atoms (Eisenstein 2000). The binding of iron to Ferritin is a short term solution to reduce intracellular iron concentration. Copper and zinc regulatory mechanisms are extremely complex and involve a coordinated effort of increased transcription of various transporters and proteins. Copper is maintained, in part, by copper regulatory proteins such as superoxide

dismutatses (Camakaris *et al.* 1999). Superoxide dismutase is post-transcriptionally modified in response to physiological copper levels whereby an increase in cellular copper increases the activity of superoxide dismutase (Steinkühler *et al.* 1994). There are various mechanisms in place to reduce metal and ROS toxicity including glutathiones (Mendoza-Cózatl *et al.* 2005) and trehalose (Roth *et al.* 2006).

Glutathione is involved in free radical detoxification (Mendoza-Cózatl *et al.* 2005; Sugiura *et al.* 2005; Sura *et al.* 2006). Cadmium and other metals are bound to glutathione and removed from the cell and may also activate metal requiring enzymes (Mendoza-Cózatl *et al.* 2005). Trehalose is a sugar which has been shown to confer protection from various stressors in bacteria, yeast and invertebrates (Garg *et al.* 2002; Roth *et al.* 2006). Stress protection from trehalose arises from its ability to stabilise enzymes and membranes (Garg *et al.* 2002).

1.2.1. Metallothioneins

MTs were first isolated from horse kidney in 1957 (Margoshes and Vallee 1957) and have since been identified in most prokaryotes and eukaryotes (Kugawa *et al.* 1994). MTs are 6-7kDa proteins which are rich in cysteine residues. MTs are usually found to be associated with zinc or copper (Kägi and Vallee 1960; Klaassen *et al.* 1999; Moilanen *et al.* 1999; Rea *et al.* 2004; Riordan and Vallee 1991; Valko *et al.* 2005). The polypeptide chain contains no, or few, aromatic or heterocyclic amino acids whilst consisting of a high number of invariant cysteine residues (Kägi and Schaffer 1988; Riordan and

Vallee 1991). In addition serine, lysine and arginine are semi-conserved throughout the polypeptide chain (Kägi and Schaffer 1988; Kojima *et al.* 1976). Mammalian MTs have been extensively studied and the structure determined (Stillman *et al.* 1992). The binding of metal ions to the cysteine residues in the polypeptide chain causes two distinct domains to form as shown in Figure 1.1 (Stillman *et al.* 1992).

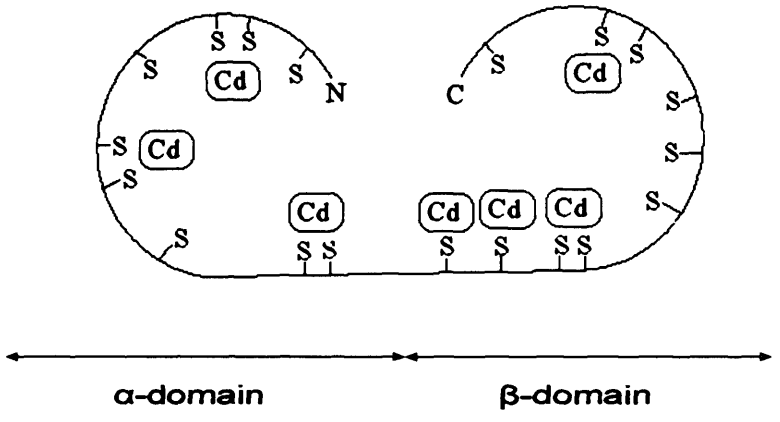

Figure 1.1: The structure of mammalian metallothionein. The α-domain is made from 30 residues of the N-terminal of the polypeptide chain and will bind three cadmium or zinc ions. The β-domain binds four cadmium or zinc ions in the 30 residues making up the C-terminus of the amino acid chain. The Figure was adapted from Klaassen *et al.* (1999)

The α-domain forms from the carboxy terminal and contains 11 cysteine residues. It is connected by a linker of 2-3 amino acids to the β-domain (Stillman *et al.* 1992). The β-domain contains 30 amino acids at the amino terminus of the polypeptide and comprises 9 cysteines (Stillman *et al.* 1992). The two domains do not interact with each other and are able to function separately, for example the β-domain can bind zinc to provide the ion for enzymes while the α-domain is able to scavenge toxic cadmium ions (Stillman *et al.* 1992).

The ability of MTs to bind metal ions arises from the presence of thiolate clusters (Palmiter 1998). The coordination of cations to cysteine residues in the thiolate clusters occurs via mercaptide linkages (Klaassen *et al.* 1999; Kojima *et al.* 1976; Riordan and Vallee 1991). Each cysteine has a different affinity for a cation and the three main metals which bind to MTs, namely copper, zinc and cadmium, also have different binding affinities for the cysteines (Stillman *et al.* 1992; Vallee 1995). As a result an ion can be displaced from the MTs by another metal ion. Zinc is normally found bound to MTs and can be displaced by copper. Both zinc and copper ions can be displaced by cadmium (Stillman *et al.* 1992). The ability to bind and release metals with differing affinities provide MTs with the exact property required for its roles in heavy metal detoxification and metal homeostasis (Palmiter 1998; Riordan and Vallee 1991). In addition to metal detoxification, MTs provide protection against reactive oxygen species as the thiolate clusters can be readily oxidised (Palmiter 1998).

MTs are divided into three classes as determined by the locations of cysteines and how the proteins are generated (Riordan and Vallee 1991; Stillman *et al.* 1992). Class I MTs have a similar structure to equine renal MT (Riordan and Vallee 1991) and include human MTs. The MTs in this group contain approximately 33% cysteines, and 13-14% serine, lysine and arginine (Riordan and Vallee 1991). The conserved cysteines are arranged in the polypeptide chain in particular structures namely as C-C dipeptides, C-X-C tripeptides and C-X-X-C peptides (Kojima *et al.* 1976). MTs which are distantly related to equine MT are grouped in class II and include

Caenorhabditis elegans MT. Both class I and class II MTs are transcriptionally generated. Generally, class I and II MTs have a polypeptide chain of approximately 61 amino acids although there are exceptions (Riordan and Vallee 1991). The earthworm *Lumbricus rubellus* MT has 72 amino acids (Stürzenbaum *et al.* 1998) whereas the bread mould *Neurospora crassa* has a short MT chain comprising of only 25 amino acids (Riordan and Vallee 1991). Class III MTs are different from those in classes I and II. Class III MTs are enzymatically synthesised and differ in structure (Riordan and Vallee 1991). Class III MTs are typically not referred to as metallothionein but termed phytochelatins or cadystins.

The un-conserved amino terminus has been shown to contain a higher number of mutations, although the locations of the cysteines remain constant (Kägi and Schaffer 1988). This results in the formation of isoforms which may have differing biological and physiological functions. MTs from class I generally consist of two or more isoforms (Dallinger 1996; Klaassen *et al.* 1999; Stillman *et al.* 1992). For example humans have 14 functional class I MTs which are all closely linked on chromosome 16 (West *et al.* 1990) and which have diverse distributions and functions (Riordan and Vallee 1991). The four commonly found MTs have very different locations in the human body. MT-1 and MT-2 are ubiquitous, MT-3 is localised to the brain and MT-4 is found only in stratified tissues (Riordan and Vallee 1991; Vasak 2005). The different isoforms have various functions depending upon their location. The presence of MT in the gastrointestinal tract aid in the absorption of dietary metals (Riordan and Vallee 1991) while kidney MT assist in the intracellular

accumulation of metals and their conversion into non-toxic forms prior to removal (Liao *et al.* 2002; Riordan and Vallee 1991).

MTs have a range of functions. MTs provide a source of zinc during low intracellular ion concentrations and act as an ion chelator during periods of elevated metal (Maret 2005; Vallee 1995). MTs are also thought to function in the maintenance of copper at optimal physiological concentration and also function as an antioxidant (Klaassen *et al.* 1999). MTs are thought to play an important role in the detoxification of non-essential metals, specifically cadmium (Palmiter 1998). Cadmium is only present in small amounts in the natural environment and therefore it is not efficient for organisms to have a cadmium-specific mechanism to prevent toxicity (Vallee 1995). In consequence, MTs are also utilised for cadmium detoxification (Roesijadi 1992).

1.2.2. Transcriptional control of metallothioneins

Class I and II MTs are transcriptionally controlled. Regulation is affected by metals, hormones and other factors acting on the *cis*-acting responsive element within the promoters (Figure 1.2) (Roesijadi 1992). A large number of factors can bind and regulate the MT promoter, indicating that MT regulation is complex. Of particular interest is the induction of MT via metals.

Studies in many species have shown that the generation of MT is increased following exposure to heavy metals, for example, in the snail, *Helix pomatia,* (Dallinger 1996), the mouse, *Mus,* (Wimmer *et al.* 2005) and zebrafish, *Danio*

rerio, (Yan and Chan 2004). Likewise, the basal level of MT synthesis is increased in the springtail *Orchesella cincta* in environments where there is a high cadmium concentration (Timmermans *et al.* 2005). The fruit fly, *Drosophila melanogaster,* synthesises more MT during periods of metal stress (Maroni *et al.* 1987). During continued exposure to high levels of toxic metal ions *Drosophila* quickly becomes tolerant to the environment (Maroni *et al.* 1987). This is achieved via an MT gene duplication which allows more protein to be synthesised quickly using the same mechanism (Maroni *et al.* 1987).

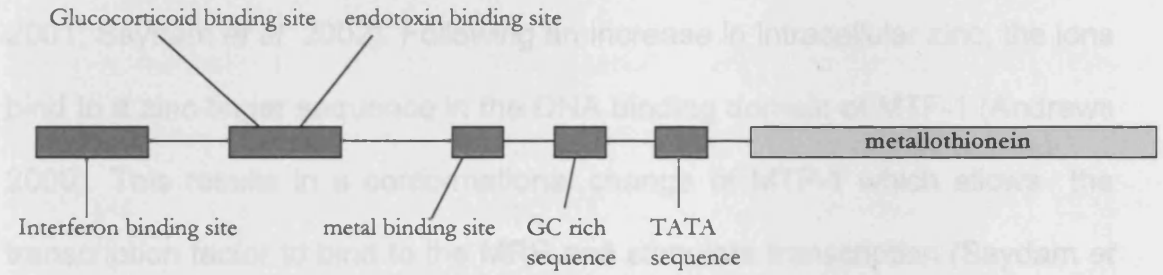

Figure 1.2: Schematic representation of the factors that can bind the metallothionein *cis*-acting element. Re-drawn from Roesijadi (1992). In vertebrates there are various factors which act on the promoter of metallothionein to stimulate transcription.

In vertebrates, the regulation of MT arises from the presence of metal responsive elements (MRE) in the promoters (Andrews 2000; Freedman *et al.* 1993; Saydam *et al.* 2002; Stuart *et al.* 1984). MREs are composed of a 7 base pair core sequence flanked by a semi-conserved set of bases (Gedamu *et al.* 1999). Thus the MRE sequence is ctnTGC(G/A)CNCggccc, where the uppercase letters are the 7 base pair conserved core sequence with the semi-conserved sequence in lower case (Andrews *et al.* 1999). The binding of a metal regulatory transcription factor (MTF-1) to the MRE sequence stimulates MT transcription (Andrews *et al.* 1999; Saydam *et al.* 2002). MTF-1 is required

for the basal and heavy metal induced MT gene expression (Lichtlen and Schaffner 2001). The removal of MTF-1 results in embryonic death *in utero* probably as a result of the embryo being unable to respond to heavy metal toxicity (Andrews 2000; Lichtlen and Schaffner 2001).

Three possible modes of action of MTF-1 binding to MREs to stimulate MT transcription have been hypothesised. All of these are based on the fact that MTF-1 has both DNA binding and activation domains which interact (Lichtlen and Schaffner 2001; Saydam *et al.* 2002). The first and most popular mode of action is based on MTF-1 acting as a zinc sensor (Lichtlen and Schaffner 2001; Saydam *et al.* 2002). Following an increase in intracellular zinc, the ions bind to a zinc-finger sequence in the DNA binding domain of MTF-1 (Andrews 2000). This results in a conformational change of MTF-1 which allows the transcription factor to bind to the MRE and stimulate transcription (Saydam *et al.* 2002). Conversely a decrease in zinc concentration prevents the conformational change and binding of MTF-1 to the MT promoter. Binding of other cationic heavy metals such as cadmium to the zinc-fingers would also induce a conformational change to stimulate binding to the MRE. A second proposed method is that a zinc sensitive protein binds to, and inhibits the action of, MTF-1 until a threshold level of zinc, or other metal ion, is reached (Saydam *et al.* 2002). The binding of the ion causes the release of the inhibitor and MTF-1 is free to bind to the MRE (Saydam *et al.* 2002). The third proposed mechanism is that MTF-1 controls MT transcription via signal transduction cascades as a consequence of the phosphorylation of MTF-1 (Saydam *et al.* 2002). MTF-1 contains conserved serine and tyrosine residues which can be phosphorylated by phosphorylases such as casein kinase II,

protein kinase C and c-jun N terminal kinases (Jiang *et al.* 2004). The degree of MTF-1 phosphorylation depends on metal exposure and kinase inhibitors. Metals, such as cadmium, increase the level of phosphorylation which activates MTF-1 resulting in an increase in MT transcription (Saydam *et al.* 2002). Conversely kinase inhibitors decrease MTF-1 phosporylation but not MTF-1 activity (Jiang *et al.* 2004). Consequently the MT gene is not stimulated to generate more protein but the basal level of transcription remains unchanged (Jiang *et al.* 2004).

1.2.3. Phytochelatin synthase

Another mechanism of cadmium detoxification is via phytochelatins (PC). PCs are short polypeptide chains rich in cysteine residues and are grouped into the class III metallothioneins (Cobbett 2000a; Riordan and Vallee 1991). PCs are similar to MTs as they are able to bind and chelate heavy metals in the same way as class I and II MTs (Vatamaniuk *et al.* 2005). However, the difference in classification arises as PCs are not transcriptionally synthesised but generated enzymatically by the action of phytochelatin synthase (Lee and Korban 2002).

Expressed sequence tag analysis has identified phytochelatin synthase (PC synthase) or a homologous genes in numerous bacteria and plants; however few animals have had functional PC synthase identified (Cobbett 2000a). The C-terminal of PC synthase is highly variable but does contain multiple cysteines and it has been proposed that this is a metal-sensing domain (Cobbett 2000a; Vatamaniuk *et al.* 2000). Bound metals at the C-terminal can

be brought into contact with the N-terminal domain which has catalytic activity (Cobbett 2000a; Vatamaniuk *et al.* 2000). The catalytic domain has the γ-Glu-Cys dipeptididyl transpeptidase activity (Cobbett 2000a). PC synthase catalyses the transpeptidation of a γ-Glu-Cys group to form PC (Cobbett 2000b).

As shown in Figure 1.3, PCs are generated at a catalytic triad within the PC synthase formed from a conserved cysteine together with an aspartate and histidine (Clemens 2006). Following acylation of the cysteine, glycerine is cleaved from a glutathione in a metal independent step. The peptide is transferred to a new glutathione, generating PC_2, or an existing PC chain, PC_{n+1}, in a metal dependent step and finally a new peptide bond is formed (Clemens 2006). PC synthase must be activated to synthesise PCs and activation requires metal ions and energy (Grill *et al.* 1989). Cadmium ions are potent activators of PC synthase with copper, zinc, mercury and lead also stimulating the enzyme (Clemens 2006). The heavy metals are thought to interact with the five cysteines in the N-terminal of PC synthase which create the catalytic domain (Cobbett 2000a).

It is also possible that activation of PC synthase arises from the presence of a metal bound glutathione. In *Arabidopsis thaliana*, activation of PC synthase arises from the presence of a metal-glutathione thiolate and free glutathione are required to synthesise PC_2 (Vatamaniuk *et al.* 2000). The metal-glutathione thiolate provides the essential metal ion for the formation of the peptide bond between itself and the free glutathione (Vatamaniuk *et al.* 2000).

In the same way as metal-glutathione conjugates are used to generate PC, it is possible that xenobiotic-glutathione conjugates can be degraded (Beck *et al.* 2003).

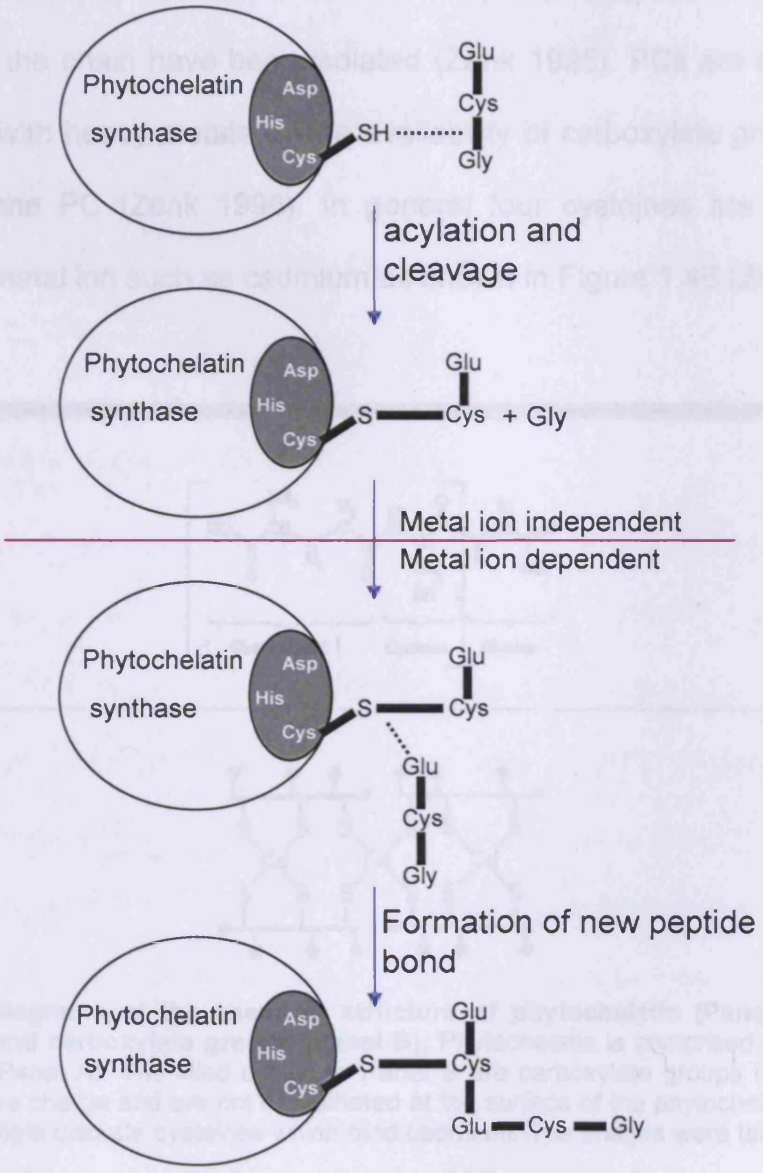

Figure 1.3: The action of phytochelatin synthase. A cysteine within the PC synthase catalytic triad is acetylated. Glutathione is cleaved to a dipeptide and glycine in a metal independent step. Metal ions are required to form new bond between the dipeptide and a new glutathione to generate the phytochelatin polypeptide chain. Cadmium, copper and zinc are all stimulators of PC synthase. Re-drawn from Clemens (2006).

1.2.4. Phytochelatins

PCs are a polypeptide repeat of $(\gamma\text{-Glu-Cys})_n$-Gly (Figure 1.4A), where n is the number of repeated γ-Glu-Cys units and can be between two and 11 (Lee and Korban 2002; Zenk 1996). Glycine is commonly found at the end of the PC chain, however phytochelatins with alanine, serine, glutamic acid at the terminus of the chain have been isolated (Zenk 1996). PCs are able to form complexes with heavy metals by the availability of carboxylate groups on the outside of the PC (Zenk 1996). In general four cysteines are required to complex a metal ion such as cadmium as shown in Figure 1.4B (Zenk 1996).

A.

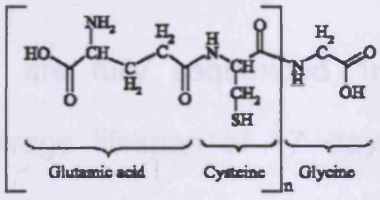

B.

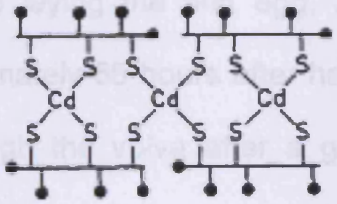

Figure 1.4: Diagrams of the chemical structure of phytochelatin (Panel A) and the cadmium bound carboxylate groups (Panel B). Phytochelatin is comprised of 2-11 γ-Glu-Cys repeats (Panel A). The filled circles in Panel B are carboxylate groups (COOH) which have a negative charge and are not coordinated at the surface of the phytochelatin molecule. There are multiple discrete cysteines which bind cadmium. The images were taken from Zenk (1996).

It is not believed that PCs have any function other than that of metal detoxification (Cobbett and Goldsbrough 2002). Therefore it is surprising that some organisms contain both MT and PC – two metal detoxifiying proteins.

Plants and fungi, such as *Candida glabrata, Saccharomyces cerevisiae* and *Neurospora crassa,* are examples of organisms which contain both MT and PC (Gonzalez-Mendoza *et al.* 2007; Zenk 1996). It is possible that having both detoxification systems becomes useful when one of the systems is compromised in some way. The primary detoxification system in *Schizosaccharomyces pombe* is via MT unless the MTs are absent or fully metal bound in which case PC synthase is activated to synthesise PC for metal sequestration (Zhang *et al.* 2005; Zhou and Goldsbrough 1994). *Caenorhabditis elegans* is another organism which contains both MT and a functional PC.

1.3. *Caenorhabditis elegans*

Caenorhabditis elegans are fully sequenced 1mm long free living soil nematodes with an average lifespan of 17 days at 20°C (Johnson and Hutchinson 1993; Wood 1988). *C. elegans* has a three day egg-to-egg cycle, the time from hatching to laying the first egg, at 20°C (Figure 1.5). Egg production begins approximately 65 hours after hatching (Byerly *et al.* 1976). Eggs are deposited through the vulva after a gastrulation period of three hours (Wood 1988) and the nematode hatches seven to nine hours after the egg is laid, as a first stage larva, L1 (Byerly *et al.* 1976; Wood 1988). Over the following forty hours the worm develops through a series of larval stages which are separated by molts. Molts are four separate periods of growth and development corresponding to transitions of L1/2, L2/3, L3/4 and L4/adult (Wood 1988). When the worm is at the L4/adult transition, gonadogenesis and spermatogenesis stop and oogenesis begins re-setting the cycle.

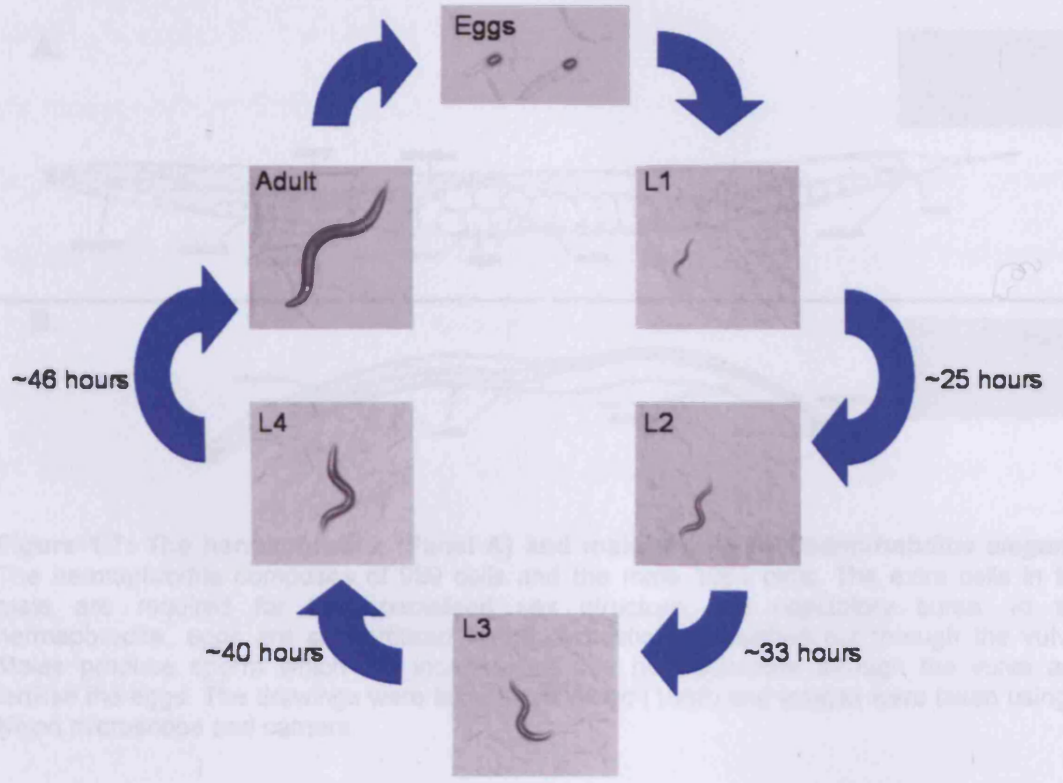

Figure 1.5: The lifecycle of *Caenorhabditis elegans* at 20°C. The nematode lives for 17 days at 20°C with a 3 day egg to egg cycle. Eggs are deposited and 7-9 hours later an L1 stage nematode emerges. The worm progresses through four larval stages separated by molts which are periods of growth and development. The time, in approximate hours, are the lengths of time from hatching the nematode takes to reach the molt. Images were taken using a Nikon microscope and camera.

If the nematode is subjected to unfavourable conditions during development, such as limited food supply, it will enter facultative diapause at the L2 stage (Wood 1988). Dauer larva do not feed and development halts (Wood 1988). *C. elegans* can survive as a dauer larva for four to six months. When favourable conditions return the nematode exits dauer and continues to develop as normal (Wood 1988).

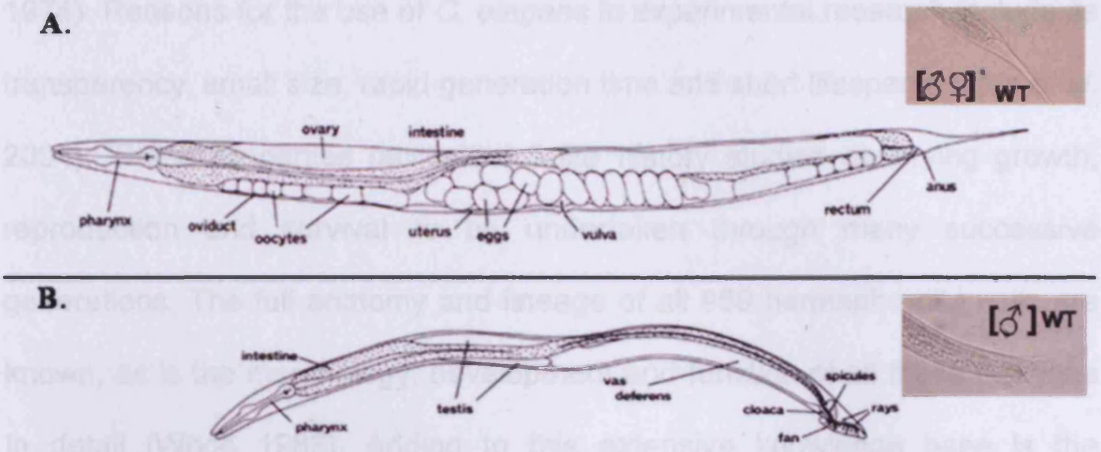

Figure 1.7: The hermaphrodite (Panel A) and male (Panel B) *Caenorhabditis elegans*. The hermaphrodite composes of 959 cells and the male 1051 cells. The extra cells in the male are required for the specialised sex structure, the copulatory bursa. In the hermaphrodite, eggs are self-fertilised in the ovotestis and pushed out through the vulva. Males produce sperm which are inserted into the hermaphrodite through the vulva and fertilise the eggs. The drawings were taken from Wood (1988) and images were taken using a Nikon microscope and camera.

The majority of *C. elegans* are hermaphrodites, comprising 959 cells (Figure 1.7A). The male and female reproductive organs are in an ovotestits which allows for self-fertilisation of between 200 and 300 viable offspring (Byerly *et al.* 1976; Jager *et al* 2005; Kadandale and Singson 2004; Wood 1988). Male nematodes are formed by spontaneous non-disjunction of chromosomes (Kadandale and Singson 2004). Due to the addition of specialised male reproductive organs, males have 1031 cells (Figure 1.7B). The additional 72 cells form the copulatory bursa containing sensory receptors and spicules, the latter are used to hold the two worms in place while sperm are inserted (Wood 1988). Hermaphrodites will self fertilise, however during mating with a male, the sperm from the male nematode will preferentially fertilise eggs over the hermaphrodites own (Wood 1988).

C. elegans has been used as an experimental organism since 1974 (Brenner 1974). Reasons for the use of *C. elegans* in experimental research include its transparency, small size, rapid generation time and short lifespan (Harris *et al.* 2004). These properties facilitate full life history studies observing growth, reproduction and survival to be undertaken through many successive generations. The full anatomy and lineage of all 959 hermaphrodite cells are known, as is the morphology, development and function of all these cell lines in detail (Wood 1988). Adding to this extensive knowledge base is the genome which has been sequenced and is publicly available via www.wormbase.org (Harris *et al.* 2004). Together, all these factors contribute to ensuring *C. elegans* as an important research tool.

Changes in life history traits such as reproduction and growth reflect the ability of *C. elegans* to deal with adverse living conditions (Kammenga *et al.* 1996) and can be related to changes at the molecular level. *C. elegans* is readily utilised to understand and test the toxicity of various toxins and heavy metals at the molecular and organism level. As the full genomic sequence is known, *C. elegans* can also be of benefit in genomic and proteomic studies (Harris *et al.* 2004).

1.3.1. *C. elegans* and metallothioneins

C. elegans contains two class I MT isoforms, *metallothionein-1 (mtl-1)* and *metallothionein-2 (mtl-2)* both located on chromosome V (Freedman *et al.* 1993). The MTs from *C. elegans* differ from the extensively studied mammalian MTs. The main difference is in the gene organisation. Both

mammalian and *C. elegans* MT have two domains which in mammals are coded by two separate exons, while the domains of *C. elegans* MT are not (Freedman *et al.* 1993). The single intron present in the *C. elegans* MT gene just splits the gene into two coding regions which both contribute to each protein domain (Freedman *et al.* 1993). A difference at the polypeptide level is that *C. elegans* MT contains a tyrosine residue between the 2 domains which is absent in mammalian MT (Freedman *et al.* 1993).

Both mammalian and *C. elegans* MT are transcriptionally controlled. In mammals, transcriptional control of the MT gene is due to the presence of numerous MRE sequences (Section 1.2.2). The MREs are bound by the transcription factor MTF-1 in the presence of a metal which induces a conformational change to stimulate MT transcription (Andrews 2000; Freedman *et al.* 1993; Moilanen *et al.* 1999). However, only one MRE has been identified in *C. elegans* MT promoters, namely in *mtl-2* (Freedman *et al.* 1993). In addition, the *C. elegans* genome does not contain an MTF-1 and as a result an interaction between MRE and MTF-1 may not be required for cadmium stimulation of the nematode MT genes (Freedman *et al.* 1993). Other small molecules may be present in the nematode which confer metal inducibility of MT, but at present it is not understood what these may be.

1.3.2. *C. elegans* and phytochelatins

C. elegans contains a functional PC synthase coded by *pcs-1* on chromosome II (Clemens *et al.* 2001; Vatamaniuk *et al.* 2001). A PC-null *Schizosaccharomyces pombe* was sensitive to cadmium toxicity with the

phenotype rescued with the expression of *C. elegans pcs-1* in the yeast (Clemens *et al.* 2001). Knockdown of *C. elegans pcs-1* by RNAi suppressed the phenotype and offspring showed developmental abnormalities, evidence of cell death and sterility (Vatamaniuk *et al.* 2002). The loss of *pcs-1* in nematodes resulted in a dose dependent hypersensitivity to cadmium (Vatamaniuk *et al.* 2002). At low cadmium concentrations *pcs-1* null nematodes showed reduced egg laying and some evidence of intestinal necrosis (Vatamaniuk *et al.* 2001; Vatamaniuk *et al.* 2005). At slightly elevated cadmium concentrations nematodes started to become sterile, while at cadmium concentrations greater than 50 µM nematodes arrested during early larval development (Vatamaniuk *et al.* 2001). As a consequence, *pcs-1,* and therefore PC, was shown to be crucial for cadmium tolerance in the nematode (Vatamaniuk *et al.* 2001).

In *S. pombe,* cadmium bound PCs are removed from cells by vacuolar sequestration. The process is catalysed by a transporter located in the vacuolar membrane, SpHMT-1, or *S. pombe* heavy metal tolerance factor (Vatamaniuk *et al.* 2005). There is an ortholog of SpHMT-1 in *C. elegans* located in intestinal cells which shows 51% sequence similarity (Vatamaniuk *et al.* 2005). CeHMT-1 null nematodes are highly sensitive to cadmium and will arrest at cadmium doses as low as 5 µM, thus this factor must be required for cadmium detoxification.

1.4. Overall aims of the project

- Bioinformatic analysis of *C. elegans mtl-1, mtl-2* and *pcs-1* genes.
- Obtain single *mtl-1, mtl-2* and *pcs-1* mutant strains and use these to generate double and triple knockouts.
- Obtain promoter::green fluorescent protein transgenic *C. elegans* lines for *mtl-1, mtl-2* and *pcs-1* and observe the location and inducibility of these genes.
- Investigate the metabolome of the MT mutants to observe changes in the small molecule component of the nematode.
- Identify phytochelatins *in vivo* in *C. elegans.*
- Expose all mutant strains to an excess of essential and non-essential heavy metals and an environment depleted in essential metals.
- Use quantitative polymerase chain reaction (Q-PCR) to measure the change in gene expression of *mtl-1* and *mtl-2* following cadmium exposure in each of the mutant genotypes.
- Screen the *C. elegans* genome for potential regulators of metallothionein transcription.
- Validate any potential regulators of transcription using Q-PCR and investigate the inductive potential of these regulators by yeast one-hybrid analysis.

CHAPTER TWO

MATERIALS AND METHODS

2.1 Materials, reagents and solutions

A list of consumables and the suppliers are given in Table 2.1 while the sources of reagents are shown in Table 2.2. Reagents were purchased of a molecular biology grade, unless stated otherwise. Specific solutions and buffers were prepared according to the compositions given in Table 2.3.

Supplier	Consumables
ABGene, UK	0.2 ml PCR tubes 1.5 ml PCR tubes
Alpha Laboratories, UK	Cryogenic vials
Applied Biosystems, UK	Q-PCR plates Q-PCR optical lids
BD (Becton, Dickinson and Company), UK	15 ml FALCON™ conical polystyrene tubes 50 ml FALCON™ round bottom polystyrene tubes
Fisher Scientific, UK	96-well multiwell plates with lids
GOSS Scientific Instruments Ltd, UK	5 mm NMR tubes
Greiner Bio-One, USA	55 mm diameter Petri dishes 90 mm diameter Petri dishes
LSL, UK	Soda glass specimen tubes with stopper
Millipore, USA	Millex™ nucleopore filters
Nuncleon, USA	12-well multiwell plates 24-well multiwell plates
Sigma Chemical Company, UK	Acid washed glass beads
StarLabs, UK	2 ml micro-centrifuge tubes Pipette tips of various sizes
Sterilin Ltd, UK	30 ml polystyrene containers (universals) Serological pipettes (10 ml, 25 ml)
Waters Corporation, USA	Sample glass vials

Table 2.1: A list of suppliers of consumables.

Supplier	Chemical
AB Gene, UK	Absolute QPCR ROX mix, Reverse Transcription Kit, MMuLV reverse transcriptase
Anala R, VWR Intenational Ltd, UK	Sodium carbonate (Na_2CO_3), Sodium phosphate (Na_2HPO_4), Sodium phosphate (NaH_2PO_4), Zinc sulphate ($ZnSO_4$), Nitric acid
BD (Becton, Dickinson and Company), UK	Bactoagar, Bactopeptone
BioRad Laboratories, UK	Biorad protein assay
Bioron, Germany	DNA markers
Calbiochem, UK	Tween
Difco Laboratories, USA	Bacto-peptone, Bacto-yeast extract
Fisher Scientific, UK	Acetone, iso-propanol, Sodium chloride (NaCl), Magnesium chloride ($MgCl_2$), Potassium chloride (KCl), Potassium phospahte (KPO_4), Ethanol, Chloroform, Acetonitrile, Methanol
Foremedium Ltd, UK	Yeast nitrogen base without amino acids, Glucose
Invitrogen Ltd, UK	*DH5α* competent cells, 10x TAE buffer
Melford Laboratories Ltd, UK	Agar, o-nitrophenyl-b-D-galactoside (OPNG)
MP Biochemicals, France	High Performance Liquid Chromatography (HPLC) water, Glycerol, Agarose, Ethidium bromide (EtBr), Proteinase K
MWG, UK	Custom synthesised primers, Fluorescent labelled probes
Promega Corporations	GoTaqFlexi Taq Polymerase and associated buffers, Restriction enzymes with associated buffers, dNTPS, 10x alkaline phosphatase, Wizard Plus SV miniprep DNA purification System, Wizard SV gel and PCR cleanup system, pGemT vector, T4 DNA ligase
Roche Diagnostics, UK	Tris, PhosSTOP protease cocktail inhibitor
Sigma Chemical Company, UK	Dimethyl sulfoxide (DMSO), Copper Chloride (Cu[I]Cl), Cadmium Chloride ($CdCl_2$), cholesterol, Calcium chloride ($CaCl_2$), Potassium phosphate (KH_2PO_4), Sodium phosphate ($Na_2H_2PO_4$), Magnesium sulphate ($MgSO_4$), Sodium hydroxide (NaOH), Luria Broth (LB) tablets, Sodium hypochlorite (NaOCl), Tri-reagent, Isopropyl β-D-thiogalactopyranoside (IPTG), Carbenicillin, Ampicillin, Nystatin, GenElute Gel Extractin kit, Custom synthesised primers, Bathocuproinedisulfonic acid disodium salt (BCS), Single stranded carrier DNA (salmon sperm), Lithium Acetate, Polyethylene glycol (PEG), OligodTs, Leucine ankephalin, trimethylsilyl-2,2,3,3-d4-propionic acid (TSP), NP40 (Tergitol®), Gelatin, Adenine, Arginine, Methionine, Tryptophan, Histidine, Leucine, Lysine, Uracil, Formic acid, Sodium formate

Table 2.2: Table of reagents and their suppliers.

Method	Solution	Components
Agar plates	NGM Agar	50 mM NaCl, 0.25% (w/v) Bactopeptone, 1.7% (w/v) bactoagar. Autoclave and add 1 mM $CaCl_2$, 1 mM $MgSO_4$, 25 mM K_2HPO_4 (pH6), 0.1% (v/v) cholesterol, nystatin.
	Cholesterol	5% (w/v) dissolved in ethanol.
Egg preparation	Bleaching solution	5% NaOH (10M), 20% NaOCl (4%).
	M9 buffer	22 mM KH_2PO_4, 42 mM Na_2HPO_4, 85.5 mM NaCl and 1 mM $MgSO_4$.
Nematode Freezing Solution	Freezing solution	100 mM NaCl, 50 mM KPO_4 (pH6), 30% glycerol. Autoclave and add 0.3 mM sterile $MgSO_4$.
Genomic DNA extraction	1x Worm lysis buffer	25 mM KCl, 25 mM Tris (pH8.2), 1.25 mM $MgCl_2$, 0.1% (v/v) NP40, 0.1% (v/v) Tween-20 and 0.005% gelatine. Add 25% (w/v) proteinase K prior to use.
Wizard Plus SV Miniprep DNA purification System	Cell lysis solution	0.2 M NaOH, 1% SDS.
	Cell resuspension solution	50 mM Tris-HCl (pH7.5), 10 mM EDTA, 100 µg/ml RNase A.
	Neutralisation solution	4.09 M guanidine hydrochloride, 0.759 M potassium acetate, 2.12 M glacial acetic acid (pH4.2).
	Column wash	60% ethanol, 60mM postassium acetate, 8.3mM Tris-HCl (pH7.5), 0.04mM EDTA (pH8.0).
Wizard SV gel and PCR Clean up system	Membrane wash solution	10mM potassium acteate (pH5.0), 80% ethanol, 16.7µM EDTA (pH8.0).
	Membrane binding solution	4.5M guanidine isothiocyanate, 0.5M potassium acetate (pH5.0).
Yeast Peptone Dextrose	YPD	20 g peptone, 20 g glucose, 10 g yeast extract in 1l dH_2O.
Yeast Media	Agar	20 g agar in 500 ml dH_2O.
	Minimal media	20 g glucose, 6.7 g yeast nitrogen base without amino acids in 400 ml dH_2O. Add selected amino acids from adenine, arginine, methionine, tryptophan, lysisne, histidines, leucine and uracil.
Yeast Freezing Solution	1x YFS	20 g glucose, 20 g peptone, 10 g yeast extract in 1l dH_2O and 30% glycerol.
LacZ assay	2x Z buffer	120 mM Na_2HPO_4, 120 mM NaH_2PO_4, 10 mM KCl and 1 mM $MgSO_4$ in 50 ml dH_2O.
	Extraction buffer	In 50 ml $dH2_0$, 1 ml Tris-HCl (1 M, pH8.0), 500 µl NaCl (1 M) and ½ a tablet of protease cocktail inhibitor.
	OPNG	For 10 ml, 5 ml 2x Z buffer, 5 ml dH_2O and 0.02 g OPNG (1 mg/ml).
	BioRad protein assay	1:5 dilution of BioRad protein assay with dH_2O.
	STOP buffer	1 M Na_2CO_3 in dH_2O.
NMR phosphate buffer	Phosphate buffer	Na_2HPO_4 (pH7.0, 0.2 M), NaH_2PO_4 (pH7.0, 0.2 M), 1.6 mM TSP, 4.7 mM sodium azide, 70% D_2O.

Table 2.3: List of solutions and buffers and their compositions.

2.2 Preparation of equipment

All pipette tips and micro-centrifuge tubes were autoclaved at 121°C and 15 psi for 20 minutes. Equipment used for RNA work was autoclaved twice. Heat sensitive components, such as antibiotics, were sterilised by filtration through a 0.22 µm Nucleopore™ filter into fresh sterile containers. Worm picks were dipped in 100% ethanol prior to use.

For nitric acid digestion, glassware was acid washed. Glassware was placed in a solution of 10% sodium dodecyl sulphate and scrubbed. Following several water rinses the glassware was placed in 6.9% nitric acid solution and scrubbed. After rinsing, the glass was dried overnight in an oven at 60°C.

2.3 Antibiotics

Aliquots of antibiotic were prepared in filtered HPLC water and then sterilised again by filtering though a 0.22 µm Nucleopore™ filter. The aliquots were stored at -20°C until use. Table 2.4 lists the antibiotics used in this study.

Antibiotic	Concentration
Ampicillin	100 mg/ml
Carbenicillin	25 mg/ml
Tetracycline	25 mg/ml

Table 2.4: List of antibiotics. All antibiotics were dissolved in filtered HPLC water and filter sterilised. Aliquots were stored at -20°C.

2.4 Nematode Growth Medium

Nematode growth medium, NGM, was made by preparing the agar as described in Table 2.3. The agar was kept liquid by placing in a water bath and poured into Petri dishes using stripettes (serological pipettes, Sterilin, UK) in a laminar flow cabinet. The 90 mm diameter Petri dishes contained 20 ml agar and 55 mm diameter Petri dishes contained 10 ml agar. An automated plate pourer (Masterfex, Cole-Parmer Instrument Companny) was used to dispense a set volume (2.5 ml or less) into 12- and 24- well plates (Nuncleon, USA).

2.5 *Escherichia coli* strains

The main strain used in all experiments was the OP50 strain *of Escherichia coli*. Used as a nematode food source, OP50 is a uracil deficient mutant which prevents overgrowth of the bacterial lawn. In addition the RNAi *E. coli* strain HT115(DE3) was used in all RNAi experiments.

2.5.1 OP50 Food source

E. coli OP50 was cultured overnight in a shaking (180 rpm) 37°C incubator in Luria broth (LB) (10 ml) made according to manufacturer's instructions (Sigma, UK) (1 tablet per 50 ml dH_20). Cultures were stored at 4°C for 2 weeks. Frozen stocks were prepared by growing a single OP50 colony at 37°C in LB. The following day 500 µl of 80% glycerol was mixed with 500 µl OP50 culture. After a brief vortex the stocks were stored at -80°C.

Bacteria were seeded onto NGM plates and spread using a flame sterilised glass rod. On 90mm Petri dishes 200 µl OP50 was dispensed (90 µl OP50 on 55mm Petri dishes). OP50 (25 µl) was dropped onto 12- and 24- well plates without spreading. All seeding of NGM plates was undertaken in the laminar flow cabinet to ensure sterility. Plates were left to dry for 20 minutes and incubated at room temperature overnight prior to use.

2.6 *Caenorhabditis elegans* husbandry

2.6.1 Strains of *C. elegans*

Strain name	Allele	Genotype	Supplier
N2 – Bristol		WT	CGC
mtl-1(tm1770)	tm1770	Δ*mtl-1*	Mitani Laboratory
mtl-2(gk125)	vc128	Δ*mtl-2*	*C. elegans* KnockOut Consortium and the CGC
mtl-1;mtl-2(zs1)	tm1770;gk125	Δ*mtl-1*Δ*mtl-2*	S. L. Hughes
mtl-1;mtl-2;pcs-1(zs2)	tm1770;gk125;tm1748	Δ*mtl-1*Δ*mtl-2*Δ*pcs-1*	S.L. Hughes
pcs-1(tm1748)	tm1748	Δ*pcs-1*	Mitani Laboratory
P*mtl-2*::GFP		*mtl-2* promoter::GFP fusion	S.R. Stürzenbaum
P*mtl-1*::GFP		*mtl-1* promoter::GFP fusion	S.R. Stürzenbaum
P*pcs-1*::GFP		*pcs-1* promoter::GFP fusion	I. Hope
RB1592	ok1957	Δ*nhr-64* (C45E1.1)	CGC
VC1310	ok1805	Δ*cey-1* (F33A8.3)	CGC

Table 2.5: Strains of *Caenorhabditis elegans*. The *Caenorhabditis* Genetics Centre (CGC) is funded by the National Institutes of Health National Centre for Research Resources. The Mitani Laboratory is at the Tokyo Women's Medical University School of Medicine in Japan.

Sydney Brenner in 1974 pioneered the use of Bristol N2 as a common laboratory control (Brenner 1974). Consequently, the Bristol N2 wild type strain was used as a control in all experiments (obtained from the

Caenorhabditis Genetics Centre at the University of Minnesota, USA). The strains *of C. elegans* used in this study are listed in Table 2.5.

2.6.2 Maintenance of *C. elegans* strains

Stocks of nematodes were maintained on NGM agar in 55 mm Petri dishes (Greiner Bio-One, USA) at 20°C in a constant temperature incubator (Sanyo Instruments). Temperatures of 15°C were also used to slow down the *C. elegans* life cycle. To sustain *C. elegans* populations, a large number of nematodes were transferred to new plates by 'chunking' weekly. Chunking is where a small cube of agar was cut from a plate of nematodes using a flame sterilised scalpel and transferred to fresh OP50 seeded NGM agar. Smaller numbers and individual *C. elegans* were transferred between plates using a worm pick which was made from a hair glued onto a small wooden cocktail stick.

2.6.3 Freezing stocks of *C. elegans*

To maintain *C. elegans* stocks, aliquots of strains were stored at -80°C. Nematodes, predominantly L1s, were used one day after the food source was exhausted. The nematodes were washed off plates with M9 buffer into a 15 ml conical centrifuge tube and centrifuged at 2500g for 2 minutes. The supernatant was reduced to 1.5 ml and an equal volume of freezing solution was added. Following mixing, the nematodes were aliquoted (500 µl) into 1.8 ml cryogenic tubes (Alpha Laboratories, UK) and placed in a styrofoam rack at -80°C to ensure slow freezing. The following day, one aliquot was defrosted

at room temperature, pipetted onto an agar plate and the viability of the nematodes evaluated.

2.6.4 Generation of males

Male nematodes are required for use in backcrossing and for genetic crosses. Hermaphrodite nematodes (5) at L4 stage were placed onto NGM agar at 30°C for 5.5, 6 and 6.5 hours before transferring back to 20°C. Following reproduction and hatching, male offspring were selected and isolated.

2.6.5 Backcrossing *C. elegans* strains

New strains were backcrossed to remove background mutations. This was achieved by generating males as in Section 2.6.4. Five wild type males were placed with a single mutant L4 hermaphrodite and left until eggs were produced. Male offspring were selected and a new cross set up using 5 males and one wild type L4 hermaphrodite. The offspring from the second cross were thus backcrossed twice.

2.6.6 Egg preparation

Egg preparation was performed to age synchronise nematodes at the L1 stage. Gravid adult *C. elegans* were washed off agar plates with M9 buffer (Table 2.3) into 15 ml centrifuge tubes. Centrifugation at 2500g for 2 minutes pelleted the nematodes and the supernatant was discarded. Bleaching solution (Table 2.3) was added to the pellet and vigorously shaken for 3 minutes. The tubes were then centrifuged at 2500g for 1 minute and the supernatant removed. The pellet was washed in M9 buffer (10 ml),

centrifuged at 2500g for 1 minute and the supernatant removed. The washing step was repeated three times. The supernatant from the final wash was discarded and 10 ml of M9 buffer added. The tubes were rotated overnight at room temperature which allowed eggs to hatch but halted development at the L1 stage. Following centrifugation at 2500g for 2 minutes, the pellet containing L1 nematodes were pipetted onto a fresh agar plate.

2.7 *C. elegans* life cycle toxicity testing

2.7.1 Dosing media

Stock solutions of each of the heavy metals were made using filter sterilised HPLC water and stored at 4°C. An appropriate volume of heavy metal or chelator was added to liquid NGM (Section 2.4) when the agar had cooled to 50°C prior to pouring the plates. Metals used were cadmium chloride ($CdCl_2$, with a molecular weight (Mw) of 183.316), zinc sulphate ($ZnSO_4.7H_20$, Mw 161.441) and copper chloride (Cu[I]Cl, Mw99.0). Bathocuproinedisulfonic acid (BCS, Mw 564.54) was added to the media to generate a copper deficient environment.

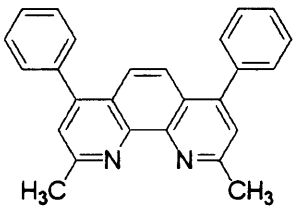

Figure 2.1: The structure of BCS, 2,9-Dimethyl-4,7-diphenyl-1,10-phenantroline disulfonic acid disodium salt. The molecular weight of BCS is 564.54. BCS was supplemented to liquid agar to chelate Cu^{2+} ions.

The structure of BCS is shown in Figure 2.1. BCS is a negatively charged ligand which has the ability to bind and chelate copper ions (Zhu and Chevion 2000). BCS can only form a complex with cupric ions (Cu^{2+}) and not cuprous ions (Cu^{+}) (Zhu and Chevion 2000). BCS is unable to enter cells and thus cannot interfere with the action of any chaperones or cuprous enzymes (Ogra *et al.* 2006).

2.7.2 Experimental design

For standard toxicity tests, nematodes were age synchronised and plated as L1s onto metal dosed NGM plates. After 24 hours, single L4 nematodes were transferred to individual wells of multi-well plates with an appropriate number of replicates. Nematodes were transferred daily until egg laying had been completed (Figure 2.2).

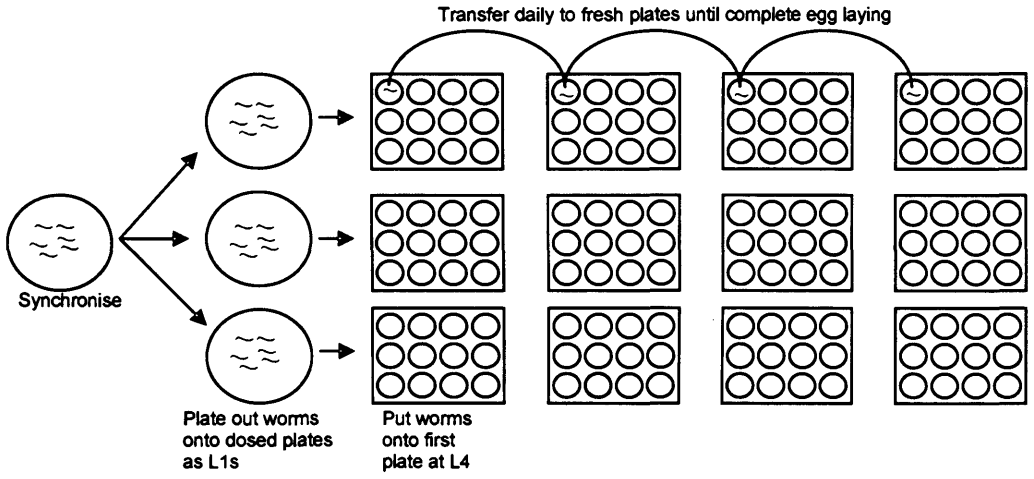

Figure 2.2: A schematic representation of the life cycle toxicity test. In brief, nematodes were age synchronised and plated as L1s onto dosed 60 mm Petri dishes. At the L4 stage, nematodes were transferred to a single well in a 12- or 24- well dish. Each *C. elegans* was transferred to a new well daily until egg laying was complete. All offspring in each well was counted manually to provide the daily reproductive output and total brood size.

Total brood size and daily reproductive output was determined for each nematode. Counts were performed manually. Nematodes were monitored daily throughout development and post-reproduction to determine the day of death. Death was recorded when no movement was observed following repeated probing with a hair. Each experiment was performed at 20°C unless stated otherwise.

2.7.3 Image analysis

C. elegans were photographed at set time intervals throughout development. T_0 was taken as the time at which nematodes were plated out as L1s on to the NGM plate. Digital images were acquired using a digital camera attached to a microscope (both Nikon UK Ltd., Kingston upon Thames, UK). Image ProExpress v4.5.1.2 (Media Cybernetics, Wokingham, UK) software allowed the perimeter of each nematode to be traced on computer and volumetric length was calculated as half of this value, i.e. the cubic root of body volume as shown in Box 2.1.

$$((1/8 * \pi * A2) / (l))1/3$$

where A is area of the worm
and l is maximum length

Box 2.1: The calculation of volumetric length. Length was calculated via digital images of nematodes taken with a camera attached to a microscope (Nikon). On a computer, the outline of nematodes was traced. Image ProExpress software calculates the volumetric length as half of this value, i.e. the cubic root of body. This is detailed in Alvarez *et al.* (2005).

2.8 Determination of metal content by nitric acid digestion

2.8.1 Determination of agar metal content

The concentration of metal ions present within the NGM was determined by inductively coupled plasma-optical emission spectrometry (ICP/OES). Analysis was undertaken by Dr Mark Hodson (Reading University). Metal was supplemented to the media as previously described (Section 2.4 and 2.7.1). A sample (0.5 g) of agar was digested in 10 ml nitric acid. Following an overnight digest at room temperature, the sample was heated at 60°C for 3 hours and then 6 hours at 110°C. The digested sample was diluted to 100 ml with deionised water and then further diluted by a factor of 2 prior to ICP/OES analysis.

2.8.2 Determination of nematode metal content

The concentration of accumulated metal within the nematodes was quantified using graphite furnace atomic absorption spectroscopy (AAS). Age synchronised nematodes were placed on metal or chelator supplemented plates at L1 stage. When the nematodes had developed to L4 stage they were washed off the plates with M9 buffer. The nematodes were washed to remove excess bacteria and pelleted. Samples were stored at -80°C until required for acid digestion. Concentrated nitric acid (500 µl) was added to the pellet in acid washed flat bottom glass tubes (LSL, UK) and the tubes placed in a water bath at 70°C. After 5 hours the tubes were transferred to 4°C. The following day 4.5 ml HPLC water was added to each sample and 20 µl of this was used for AAS (41102L PerkinElmer, Waltham Massachusetts, USA).

2.8.3 Determination of yeast metal content

Cultures of yeast were exposed to cadmium for 30 minutes and AAS was performed to determine the metal ion content of the yeast cells. Yeast cultures were grown overnight at 30°C in 200 ml YPD (Table 2.3). An aliquot (1 ml) of culture was measured for exponential growth by measuring the absorbance at 600nm. When the cultures were in exponential phase, at an absorbance of between 0.6 and 0.8, cadmium (12 µM) was added to half (100 ml) of the culture. Both flasks were incubated for 30 minutes at 30°C on a shaking platform (180 rpm).

Cells were counted and harvested by centrifugation (2000g, 5 minutes). The supernatant was discarded and cell pellets resuspended in 20 ml of deionised water. The cells were re-pelleted by centrifugation (2000g, 5 minutes), the supernatant discarded and stored at -80°C until required for digestion. Concentrated nitric acid (500 µl) was added to the pellet in acid washed flat bottom glass tubes (LSL, UK) and the tubes placed in a water bath at 70°C. After 7 hours, the tubes were transferred to 4°C overnight. Following overnight condensation, 4.5 ml HPLC water was added to each sample and 20 µl used for graphite furnace AAS (41102L PerkinElmer, Waltham Massachusetts, USA).

2.9 Polymerase chain reaction

2.9.1 Extraction of genomic DNA using single worm PCR

Individual *C. elegans* were placed into a 0.2 ml PCR tube (AB Gene, UK) containing 2.5 µl of worm lysis buffer (Table 2.3). Samples were placed at -80°C for a minimum of 20 minutes. Following freezing, the samples were placed in a PCR block at 65°C for one hour followed by a 10 minute enzyme inactivation step at 95°C. The sample (2.5 µl) was then ready for genomic DNA (gDNA) PCR.

2.9.2 Primer design

Primers were designed to a specific DNA sequence flanking the DNA sequence of interest. The primer sequence was designed to contain 50-60% GC bases with an oligo length between 20 bp and 25 bp. Paired primers were designed to have near identical annealing temperatures of in the range of 55°C and 60°C. In addition, the freely available software OligoAnalyzer 3.1 (http://scitools.idtdna.com/analyzer/Applications/OligoAnalyzer/) was used to reduce the risk of hairpin-loop formation (self-complementary sequences) and primer-dimer formation (primer-primer complementary sequences) of the primers. Primers were synthesised by MWG or Sigma.

2.9.3 PCR amplification

The standard mix for PCR reactions was as follows: 10% (v/v) 10x GoTaq Flexi buffer (Promega), 2.5 mM $MgCl_2$, 0.2 mM dNTPs, forward and reverse

primer each at 1 pM, DNA template at 1 µg and filtered HPLC water to a final volume of 10, 20 or 50µl. PCR amplifications were performed in a ThermoCycler (PTC 225 Peltier ThermoCycler, MJ Research, USA) with optimised conditions depending on the primer set. The basic cycling conditions were as below:

95°C for 5 minutes
95°C for 30 seconds
x°C for 30 seconds } y cycles
72°C for z time
72°C for 5 minutes
hold at 4°C

Where x is the annealing temperature specific to each primer set, y is the number of amplification cycles (usually between 25 and 35) and z is the extension time. Typically 1 minute of extension time allows the amplification of 1 kb of DNA.

2.9.4 DNA ladders

The DNA markers were used to calculate the sizes of DNA run on agarose gels. The ladders were either 1 kb or 100 bp in size and purchased from Bioron, Germany. The fragment sizes of the markers are given in Table 2.6.

DNA marker	Fragment sizes (bp)
100bp	1500, 1000, 900, 800, 700, 600, 500, 400, 300, 200, 100
1kb	10000, 8000, 6000, 5000, 4000, 3000, 2500, 2000, 1500, 1000, 750, 500, 250

Table 2.6: The band sizes of the DNA ladders. Markers were purchased from Bioron, Germany. The bands at 1000bp had double intensity as the other bands. The fragments at 500 and 100 bp in the 100 bp ladder and 3000 bp in the 1 kb ladder were also twice as bright.

2.9.5 Agarose gel electrophoresis

DNA was routinely visualised on agarose gels. Gels were typically 1-2% (w/v) agarose in 1x TAE buffer containing 0.5 µg/ml ethidium bromide. Samples (5 µl) were loaded into the wells. Appropriate DNA ladders (Table 2.6) were also run in a separate well on the gel to determine the size of fragments. An electric current was applied at 150 volts for 15-20 minutes in 1x TAE buffer. Bands were visualised under UV light and a UV trans-illuminator camera was used to photograph the gel.

2.9.6 DNA purification from gels and PCR

To purify DNA from an agarose gel, the PCR product was separated on a 1% agarose gel and visualised under low intensity UV light. The PCR product band of the required size was cut out using an ethanol cleaned scalpel and placed in a 1.5 ml micro-centrifuge tube. An equal volume of membrane binding solution from the Wizard SV gel and PCR clean-up system (Promega) was added to the gel slice. The solution/gel slice was heated at 60°C for 10 minutes with occasional brief vortexing. In addition, PCR products could be directly purified using the Wizard SV gel and PCR clean-up system (Promega). In this instance, an equal volume of membrane binding solution was added to the PCR product and incubated at room temperature for 1 minute.

The gel/PCR mixture was transferred to an SV column in a micro-centrifuge tube and incubated at room temperature for 1 minute. The columns were centrifuged (16000g, 1 minute) and the flow through discarded. Membrane

wash solution (700 µl) was added to the column and centrifuged (16000g, 1 minute) followed by a second wash with 500 µl of membrane wash solution. The samples were centrifuged (16000g, 5 minutes), the flow through discarded and then centrifuged a second time (16000g, 1 minute). The SV column was transferred to a fresh micro-centrifuge tube and 50 µl nuclease free water added to the membrane. The samples were incubated at room temperature for 1 minute followed by centrifugation (16000g, 1 minute). The flow through contained the purified DNA.

2.10 Cloning

2.10.1 Restriction digest

Digestion of a vector and PCR product requires the use of specific restriction digestion enzymes at specific DNA sequences. In general, purified vectors (200 - 500 ng) were digested with 5 units of restriction enzyme and 10% (v/v) 10x digestion buffer in a total reaction volume of 40 µl. In some instances double digests were undertaken in which case a buffer was chosen which provided the best efficiency for both enzymes. The components were mixed briefly and placed at 37°C for 2 hours. Approximately 30 minutes prior to the end of the digest, 2 µl alkaline phosphatase (Promega, UK) was added to the vector digests to prevent re-circularisation. DNA was digested with commercially available restriction enzymes and those used in this study were *BamHI, HindIII, ApaI, ClaI, EcoRI, PstI, SpeI, BalII, XbaI* and *SalI*.

2.10.2 Ligation of DNA into vectors

Purified PCR products were ligated into vectors. The ligation reaction contained 50% (v/v) 2x ligation buffer, 3 units of T4 ligase, 50 ng of vector and an appropriate amount of DNA as calculated in Box 2.2. The mixture was made up to a total volume of 10 µl using filter sterilised HPLC water. After a brief mixing, the ligation was incubated at room temperature for 1 hour and a second parallel ligation was incubated at 4°C overnight.

(50ng vector * size (kb) of insert / size (kb) vector)* 1/3 = ng of insert

note: 1/3 is the insert:vector molar ratio

Box 2.2: Calculation of the required volume of purified DNA. The ligation mixture contained 50 ng vector and a calculated volume of insert together with 2x ligation buffer and T4 DNA ligase. The mixture was made up to 10 µl and left on at room temperature for 1 hour or at 4°C overnight prior to transformation into competent cells.

2.10.3 Transformation into competent cells

All ligations were transformed into the competent *E. coli* strain *DH5α* (Invitrogen, UK). Aliquots (50 µl) of cells were thawed slowly on ice. The ligation mixture (Section 2.10.2) was added to the competent cells, gently mixed and left on ice for 40 minutes. The cells were then heat shocked for 90 seconds at 42°C and afterwards placed back on ice for 3 minutes. Sterile Luria broth (600 µl) was added and cells incubated at 37°C for 1 hour. The cells were then centrifuged (5000g, 30 seconds) and 400 µl of supernatant discarded. The remaining transformed cells were spread on a dry solid LB agar plate containing ampicillin. Plates were incubated at 37°C overnight.

2.10.4 Selection of positive colonies and plasmid extraction

Positive colonies were selected as those which grew on LB/ampicillin plates after 24 hours. These *E. coli* colonies bearing plasmids were picked by stabbing a sterile p10 tip into the centre of the colony and transferring the tip to 10 ml LB broth with 1 µl ampicillin liquid medium. Cultures were grown overnight at 37°C in a shaking incubator (180 rpm).

The following day, plasmids were extracted using the Wizard SV Miniprep DNA purification system (Promega, UK) following the manufacturer's instructions. Briefly, a cleared lysate was prepared by centrifuging 1 ml of plasmid culture (10000g, 10 minutes). The supernatant was discarded and the pellet resuspended in cell resuspension solution (250 µl). Cell lysis solution was added (250 µl) and samples inverted four times and incubated at room temperature for 5 minutes. Alkaline protease solution (10 µl) was added and incubated for a further 5 minutes After this step, neutralisation solution (350 µl) was added to the solution and after inversion, the samples were centrifuged (14000g, 10 minutes). The lysate was transferred to a spin column in a micro-centrifuge tube and centrifuged at maximum speed for 1 minute (room temperature). The flow through was discarded and column wash solution (750 µl) added to the column. The samples were centrifuged (maximum speed, 1 minute), the flow through discarded and a second aliquot of column wash solution (250 µl) added. Following centrifugation (maximum speed, 2 minutes) the column was transferred to a new micro-centrifuge tube and 55 µl nuclease free water added to the membrane. The samples were centrifuged (maximum speed, 1 minute) and the solution containing the

purified plasmid transferred to a fresh micro-centrifuge tube. The plasmid DNA was stored at -20°C.

2.11 Total RNA extraction

All pipette tips and micro-centrifuge tubes were double autoclaved. *C. elegans* were washed off the NGM plates with M9 buffer into 15 ml centrifuge tubes and centrifuged (2500g, 2 minutes) to pellet the nematodes. The supernatant was removed and the remaining pellet was shock frozen in liquid nitrogen and stored at -80°C. RNA was extracted using the standard Tri®-reagent (Sigma, UK) protocol. Briefly, the nematode pellets were thawed on ice and an equal volume of acid washed glass beads (Sigma) added to Tri-reagent (1 ml per 100 µl nematode pellet). The samples were vortexed for 3 minutes and the supernatant transferred to a 1.5 ml micro-centrifuge tube being careful not to carry over glass beads. Following incubation at room temperature for 5 minutes, chloroform (200 µl) was added, vortexed and incubated for 10 minutes at room temperature. The samples were then centrifuged at 12000g for 15 minutes and the supernatant transferred to a clean micro-centrifuge tube containing 500 µl *iso*-propanol. Tubes were inverted twice and incubated for 10 minutes at room temperature prior to centrifugation (12000g, 10 minutes). The supernatant was discarded and the RNA pellet washed in 75% ethanol (1 ml). Following centrifugation at 12000g for 5 minutes, the ethanol was removed and the pellet left to air dry at room temperature for 5 minutes. Filtered HPLC water was used to resuspend the pellet.

2.12 Assessment of quality and purity of DNA and RNA

A nanodrop (ND-100 Spectrophotometer, NanoDrop Technologies Inc, USA) was used to assess the quality and quantity of DNA and RNA. The sample (1.2 µl) was placed onto the spectrophotometer which provided a sample concentration in ng/µl. The A260/A280 ratio indicated protein or phenol contamination and the A260/A230 ethanol or salt contamination. In each case, the optimum value for the ratio should be 1.9-2.0, although values greater than 1.8 can still be used successfully in many downstream applications.

2.13 Reverse transcription

The purpose of reverse transcription was to generate cDNA from RNA. The RNA samples were defrosted slowly on ice and 500 ng of each sample was used in the reverse transcription reaction. In each reaction 5x buffer was added, dNTPs at 10 mM and oligodT primer (100 pmol/µl). The reverse transcriptase enzyme, MMuLV (Promega, UK), was added (1 µl) and the reaction made up to 20 µl. The tubes were incubated at 37°C for 50 minutes and then at 80°C for 10 minutes. The cDNA was stored at -20°C.

2.14 RNA interference

The method used to introduce dsRNA into nematodes was adapted from Kamath and Arhringer (2003). A 96-pin stainless steel replicator (Fisher Scientific, UK) was used to spike bacteria from a 96-well plate of bacterial glycerol stocks into a fresh 96-well plate containing LB broth and ampicillin (50 mg/ml). The glycerol stocks were provided by the Medical Research

Council GeneService (Cambridge, UK). The bacteria cultures were left to grow overnight at 37°C without shaking. Agar was prepared as previously described (Section 2.4 and Table 2.3). When the liquid agar had cooled to below 50°C, isopropyl β-D-thiogalactopyranoside (IPTG) (10 μg/ml) and carbamycin (25 μg/ml) were added. Half the plates were supplemented with cadmium (12 μM). Agar was dispensed into 96-well multi-well plates (Fisher, UK). The HT115(DE3) strain of *E. coli* was pipetted directly onto the RNAi NGM (30 μl). The plates were left to dry for 20 minutes and then incubated at room temperature overnight.

2.14.1 RNAi by feeding screen

RNA interference (RNAi) screens by feeding used the transgenic strains P*mtl*::GFP (provided by Dr Stephen Stürzenbaum). Gravid nematodes were bleached and plated onto regular NGM plates as L1s. Nematodes were left to the L3 stage. At this point nematodes were transferred to RNAi NGM. Transfer was performed by washing L3 nematodes off the NGM plates with M9 buffer. Nematodes were pelleted by centrifugation (2000g, 2 minutes) and resuspended in sufficient M9 buffer for 1-2 nematodes/μl. The nematodes (5 μl) were added to the RNAi NGM and the plates left to dry in a laminar flow for 20 minutes. The plates were incubated at 20°C to allow the nematodes to lay eggs. After two days, the offspring were monitored for fluorescence by visual inspection of the relative fluorescent level and any phenotypic changes.

2.15 Quantitative Polymerase chain reaction

2.15.1 Primer and probe design

Both primers and probes for TaqMan® qPCR were designed using the PrimerExpress™ software package (PE Applied Biosystems). Each oligonucleotide was synthesised by MWG Biotech (UK). Primers were purified oligonucelotides while the probes were modified with a FAM dye covalently linked to the 5' and TAMRA covalently linked to the 3' end of the probe. The generalised guidelines for the design of the primer, probe and amplicon are summarised in Box 2.3.

- Primer design
  - The melting temperature, Tm, of primers should be between 58-60°C
  - The primers should ideally have a GC content between 20-80% with more C bases than G bases
  - The length of the primers should be approximately 20 bases
  - The difference in Tm between the two primers should be less than 2°C
  - The last 5 bases of the 3' end of primers should have no more than two G or C bases to increase specificity

- Probe design
  - The Tm of the probe should be 8-10°C higher than the primers
  - The GC content of the probe should be 20-80%
  - The length of the probe should be approximately 20 bases
  - There should be no G on the 5' end of the probe
  - Probes should be designed over intron/exon boundaries to prevent genomic
  - DNA amplification
  - Probes should be located 3-10 bases away from primers

- Amplicon
  - Target size should be 70-150 bases

Box 2.3: Guidelines for the design of primers and probes in quantitative PCR reactions.

2.15.2 Preparation of standards

Plasmid standards were generated containing an insert corresponding to the target sequence to be amplified. The target cDNA sequence was amplified by PCR (Section 2.9.3). The PCR product was transformed into the pGemT vector (Promega) as detailed in section 2.10.2. Purified plasmids were diluted to 0.2 ng/µl and a standard 10-fold serial dilution from was prepared.

2.15.3 Preparation of samples

Nematodes at the L4 stage were washed off Petri dishes and total RNA was extracted using the Tri®-reagent method as detailed in Section 2.11. cDNA was generated using MMuLV reverse transcriptase (Section 2.13). In all cases, each sample was diluted 1:10 prior to use in the Q-PCR reaction. There were multiple (3-4) biological replicates per sample.

2.15.4 TaqMan® Q-PCR experiments

Optimisation of both primer and probe concentrations was required for TaqMan® Q-PCR analysis. The manufacturer's instructions provided with the Absolute QPCR ROX MIX kit (AB Gene, UK) indicated optimal conditions which were used. Ultimately in each 25 µl reaction the concentration of primers (forward and reverse) was 0.4 µM with 0.2 µM probe. The volume of cDNA was 5 µl of a 1:10 dilution. Absolute ROX master mix (12.5 µl) was added and the remaining volume made up with filter sterilised HPLC water.

The Q-PCR amplifications were performed in 96-well Q-PCR plates using optical lids. Calibration standards and samples were quantified in parallel and all in triplicate. The Q-PCR machine was an Applied Biosystems ABI Prism 7000 (UK) with the following cycling parameters used for each run:

50°C for 2 minutes
95°C for 15 minutes
95°C for 15 seconds } 40 cycles
60°C for 1 minutes

Product formation was monitored at the end of each amplification by measuring the fluorescence emitted from the TaqMan® probes. The C_T values were calculated automatically by the analysis package 7000 system SDS software core application, Sequence Detection Software v1.2.3.

2.16 Yeast media

2.16.1 Yeast Peptone Dextrose

YPD is a broth optimised for culturing yeast. The components of YPD, as detailed in Table 2.3, were dissolved in water using a magnetic stirrer and bar. The solution was divided into 200 ml aliquots in conical flasks and autoclaved. Flasks were stored at 4°C until required.

2.16.2 Minimal media

Yeast was maintained on minimal media. The omission of selected amino acids from the media provides a simple method to identify positive transformants. A 2% agar solution (Table 2.3) was prepared in 400 ml dH_2O.

Following complete mixing with a magnetic stirrer, the liquid was topped up to 500 ml. In a second flask containing 400 ml dH_2O, glucose and yeast nitrogen base without amino acids were added and dissolved. The appropriate amino acids were added, namely arginine, methionine, tryptophan, lysine, histidine and leucine together with the nucleoside bases adenine and uracil. Both agar and minimal media were autoclaved. Once cooled to 50°C, the minimal media was slowly added to the agar and the solution gently mixed on a heated magnetic stirrer. The agar (approximately 25 ml) was then poured into 90 mm Petri dishes.

2.17 High efficiency yeast transformation

To incorporate a gene of interest into yeast, the vector containing the gene was purified (Section 2.10.4) and then transformed into the strain Y0000 (Provided by Dr Barry Panaretou, King's College London, UK). The lithium acetate and polyethylene glycol (PEG) solutions were sterilised by filtration through a 0.2 µm membrane prior to use. Yeast cells were inoculated in liquid YPD media and grown overnight in a shaking incubator (30°C, 180 rpm). When cell density of the culture reached the exponential phase of growth, 0.7-5x10^6 cells/ml, cells were harvested by centrifugation (2000g, 5 minutes). The supernatant was discarded and cell pellets resuspended in 20 ml of 100 mM lithium acetate. The cells were re-pelleted by centrifugation (2000g, 5 minutes), the supernatant discarded, and resuspended in 20 ml of lithium acetate and centrifuged again (2000g, 5 minutes) and the supernatant discarded. The cell pellets were resuspended in 100 mM of lithium acetate to give a final cell density of 4x10^9 cells/ml. From this, 50 µl per transformation

was aliquoted into sterile microcentrifuge tubes and incubated at 30°C for 30 minutes. During this incubation, single stranded carrier DNA (from salmon sperm) was incubated at 95°C for 5 minutes and then chilled on ice.

Following the 30 minute incubation of yeast cells, 240 µl of 50% (w/v) PEG, 36 µl 1M lithium acetate, 25 µl of single stranded DNA and 50 µl DNA (containing 1.5 µl of each miniprepped vector and 47 µl of dH_2O) were added to the cells. In addition, a negative control was prepared by adding 50 µl dH_2O in place of the DNA. The solutions were incubated for 30 minutes at 30°C and heat shocked at 42°C for 20 minutes allowing for the vectors to enter cells. Cells were harvested by centrifugation (2000g, 5 minutes) and the supernatant discarded. Cells were resuspended in 1 ml of YPD and added to 15 ml centrifuge tubes containing 7 ml of YPD. The tubes were shaken for 90 minutes at 30°C and then harvested by centrifugation (2000g, 5 minutes) and the supernatant discarded. Cells were resuspended in 450 µl of dH_2O and 150 µl was spread on the appropriate media plates and incubated at 30°C for two days. Following incubation, the yeast was streaked to single colonies on minimal media plates. Plates were incubated at 30°C for two days after which stock patches could be made.

2.18 Maintenance of yeast

Stock plates of yeast were maintained as "patches". An autoclaved wooden stick was used to transfer a single colony to a fresh minimal media plate and a small "patch" made. These stock plates were incubated at 30°C for two days and stored at room temperature for a further two to three days. Every 4-5

days or prior to a new experiment being undertaken, a new stock plate was prepared.

Yeast stocks were stored at -80°C. To freeze yeast, a single colony was resuspended in 1 ml of yeast freezing solution (Table 2.3) in a cryogenic vial. The vials were briefly vortexed and then placed at -80°C.

2.19 Yeast spot assays

Yeast cultures were grown overnight in 200 ml YPD in a shaking incubator (30°C, 180 rpm). An aliquot of culture (12 µl) was removed and the cells counted. When the cell count was in exponential phase 0.7-5x10^7 cells/ml, the cultures were prepared for dilution. To ensure that the same number of cells were preset in the starting concentration (1x10^7 cells/ml) the calculation in Box 2.4 was used.

$$(1x10^7 \times 1.2) / \text{cell count} = \text{volume in ml}$$

Box 2.4: The calculation of initial concentration of yeast cells. A sample (12 µl) of yeast culture is counted and when in exponential phase (0.7-5x10^7) can be used for the assay. The calculation provides the volume of yeast culture to pellet to ensure 1x10^7 cells in 1 ml YPD.

The calculated volume was centrifuged (2000g, 5 minutes) to pellet the cells and the supernatant discarded. The pellet was resuspended in 1.2 ml freshly autoclaved YPD. The cells were transferred to the first well of the replicator (custom made, provided by Dr B. Panaretou) and 1 ml YPD added to the remaining wells. From the first well 200 µl were transferred to the second and gently mixed by pipetting. Then 200 µl was taken from the second well and

added to the third. This continued to the final well where 200 µl cells are discarded. Thus there was a 5-fold serial dilution across the replicator.

The replicator was placed in the wells containing the yeast solution. The replicator was transferred to a minimal media plate ensuring the sides of the wells were not touched. The replicator was then gently pressed down onto the media plate to transfer cells. The spots were allowed to dry for 20 minutes in the laminar flow, sealed and placed at 30°C for 2 days.

2.20 *LacZ* assay

Yeast cultures were grown overnight (30°C, 180 rpm) in 200 ml YPD. An aliquot (1 ml) of culture was measured for exponential growth by measuring the absorbance at 600 nm. When absorbance was between 0.6-0.8, cadmium (12 µM) was added to half (100 ml) of the culture. Both dosed and non-dosed flasks were incubated for 30 minutes at 30°C on a shaking platform at 180 rpm. Following incubation, the cells were pelleted by centrifugation (2000g, 5 minutes). The supernatant was discarded and the pellet resuspended in 20 ml dH_2O. The supernatant was removed after centrifugation (2000g, 5 minutes) and the pellet resuspended in 1 ml of extraction buffer. The solution was transferred to screw top micro-centrifuge tubes, centrifuged (maximum speed, 2 minutes) and the supernatant was removed. An equal volume of acid washed glass beads (Sigma, UK) and extraction buffer (Table 2.3) were added to the pellets. The samples were then shaken in a bead beater (Mini Beadbeater-8, BioSpec Products, USA) for 45 seconds and transferred to ice for 45 seconds. This was repeated 3 times before the samples were

centrifuged (4°C, maximum speed, 3 minutes). The supernatant was transferred to new tube and kept on ice.

BioRad protein assay reagent (5 ml of 1:5 dilution) was added to round bottom polystyrene tubes. Protein (5 µl) was added to the BioRad and the mixture submitted to a brief vortex. The samples were left at room temperature for 10 minutes and the absorbance at 595 nm measured. If the OD was greater than 0.6, the protein was diluted with dH_2O until the OD was within the range. The concentration of the protein was calculated using a standard curve (Figure 2.3). The standard curve absorbance is equivalent to a 1:20 dilution. Thus the concentration of protein is multiplied by the dilution factor of 20 to give a final protein concentration in mg/ml (µg/µl).

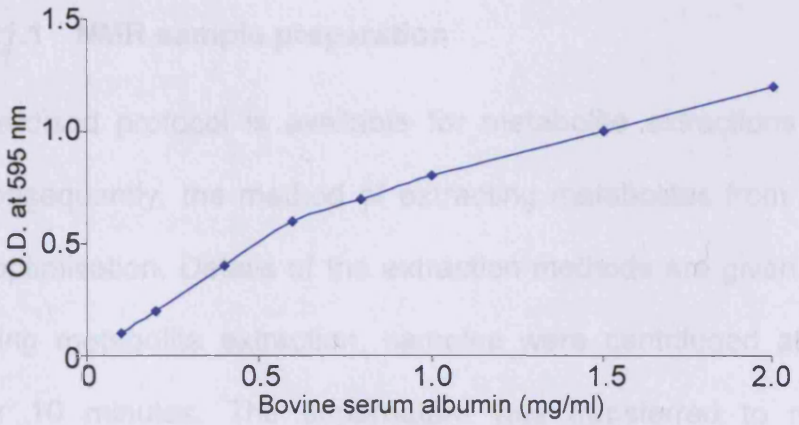

Figure 2.3: Calibration curve to calculate the extracted protein concentration. The calculated protein is a 1:20 dilution.

Following the BioRad protein assay, OPNG, o-nitrophenyl-b-D-galactoside, (700 µl) was added to micro-centrifuge tubes for each sample in triplicate.

Protein (10 µl) was added to each tube, inverted 3 times and incubated at 30°C. After 10-15 minutes 500 µl STOP buffer (Table 2.3) was added to each sample, inverted and placed at room temperature. The absorbance was measured at 420 nm. Enzyme activity was calculated as shown in Box 2.5. The calculations took into account the dilution factor of the protein from the BioRad protein assay, the volume of protein used with the OPNG and the length of incubation time the protein had with OPNG.

$$\frac{1000 \times OD@420\ nm\ /\ length\ assay\ in\ minutes\ of\ assay}{(protein\ volume \times protein\ concentration\ in\ \mu g/\mu l)} = units/min/\mu g$$

Box 2.5: Calculation of enzyme activity (units/min/µg). Where OD is optical density and OPNG is o-nitrophenyl-β-D-galactoside. The calculations take into account the protein concentration, the length of time of the OPNG exposure and the volume of protein used in the assay.

2.21 NMR spectroscopy

2.21.1 NMR sample preparation

No standardised protocol is available for metabolite extractions (Lin *et al.* 2007). Consequently, the method of extracting metabolites from *C. elegans* required optimisation. Details of the extraction methods are given in Chapter 4. Following metabolite extraction, samples were centrifuged at maximum speed for 10 minutes. The supernatant was transferred to new micro-centrifuge tubes with holes punched in the lids. An aliquot (100 µl) was removed and stored at -80°C. Samples were placed in a rotary vacuum concentrator (45°C, 10 millibar, 8 hours) following which the pellets were resuspended in 650 µl of NMR phosphate buffer (Table 2.3). Once the pellets

had resuspended they were placed in a sonic bath for 2-5 minutes and then centrifuged (maximum speed, 10 minutes). From the supernatant, 600 µl aliquots were transferred into glass NMR tubes (GOSS, UK).

Samples were analysed essentially as described in Beckonert *et al.* (2007). Briefly, all samples were analysed on a 600 MHz Bruker Avance DRX600 spectrometer equipped with a triple-axis inverse-geometry probe (Bruker BioSpin, Rheinstetten, Germany). The samples were held at 300K during acquisition. A Bruker Avance 'NOESYPRESAT' pulse sequence with 100 ms mixing time was used to suppress the peak from residual water protons; an appropriate $\pi/2$ pulse length was calculated using a typical sample. Data were acquired over a 12 kHz spectral width into 32K data points; an additional 3.5 s relaxation recovery delay was included for each pulse, giving a 5.0 s recycle time. The number of scans was adjusted to give an appropriate signal:noise ratio, namely 256 scans per sample, giving an approximate acquisition time of 22 minutes per sample.

2.21.2 NMR data processing.

Spectra were initially processed in iNMR v.2 (Nucleomatica, Molfetta, Italy). Free induction decays were zero-filled by a factor of 1.5 and an exponential apodization function of 0.5 Hz applied, followed by Fourier transformation. Phase correction and first-order polynomial baseline correction were carried out using the software proprietary algorithms. Spectra were manually binned for further data analysis into 96 separate regions, using the iNMR integration function (a list of bins are given in Appendix 1). For the method-development

and extraction comparison experiments, all spectra were normalized to TSP, as this allowed direct comparison of the compound intensities.

Further selected compounds were analysed in detail using the software package NMR Suite 5.0 (Chenomx, Edmonton, Canada). This software enables computer-aided fitting of spectra of individual compounds (based on authentic standards) to the mixture spectra, thus allowing both deconvolution and quantification of specific metabolites (in this case, alanine, betaine, cystathioneine, glutamate, glutathione, methionine, succinate and trehelose).

2.21.3 NMR pattern recognition analysis

Binned data were loaded into SIMCA-P+ v11.5 (Umetrics, Sweden). Regions around the residual water peak and the TSP peak were removed and mean centred scaling applied. Centring of the variable is where the average value of all the data points is subtracted from each variable. Results were analysed by the unsupervised principle component analysis (PCA) followed by a regression extension analysis called partial least squares discrimination analysis (PLS-DA). Outputs were initially scores plots which indicated the differentiation of classes samples followed by loadings plots which indicated regions of the NMR spectra which were important with respect to the scores plot classification (Bailey *et al.* 2003).

2.22 Mass spectrometry

2.22.1 Mass spectrometry sample preparation

Metabolites were extracted from nematodes following an optimised protocol (Chapter 4). Samples were centrifuged at maximum speed for 10 minutes. An aliquot of the supernatant was placed in a sample glass vial (Waters, USA) and maintained at 4°C prior to injection of 5 µl onto the column.

Chromatographic separations were performed on a Waters 2.1mm x 100mm ACQUITYTM (Waters, USA) 1.7 µm C18 BEH column maintained at 40 °C. Reverse phase chromatography conditions were employed using a 26 minute gradient with mobile phase A being 0.1% formic acid in water and mobile phase B 0.1% formic acid in acetonitrile. The composition was maintained at 99.9% A for the first 2 minutes, then increased linearly from 0.1 to 50% B over 10 minutes. A 50% composition of B was held for 1 minute and then increased to 99.9% B over the next 4 minutes. Mobile phase B was held at 99.9% for 4 minutes and then returned to 99.9% A and held until 26 minutes.

Electrospray (ESI) mass spectrometry experiments were performed on a Micromass LCT Premier (Waters, USA) operated in both positive and negative ionisation modes. The mass spectrometer was calibrated across the mass range 50-2000 Da using a solution of sodium formate. All analyses were acquired using the lock spray to ensure accuracy and reproducibility; 200 pg/µl leucine-enkephalin in water:acetonitrile at a 50:50 ratio was used as the lock mass with a flow rate 30 µl/min. Data were collected in centroid mode,

the lockspray frequency was set at 5 seconds, and data were averaged over 10 scans. The mass spectrometer was operated with a capillary voltage of 2.4 kV in negative ion mode and 3.2 kV in positive ion mode, using a cone voltage of 35 V, nebulizer gas flow of 900 l/h, desolvation temperature of 350°C, and source temperature of 120°C. The instrument was set to acquire over the mass range *m/z* 50-2000 with acquisition time of 1 second and an interscan delay of 100 ms.

2.22.2 Mass spectrometry data processing

Raw data was inputted into the open-source freeware XCMS which is able to detect and align metabolite peaks. After correcting for retention time, the relative metabolite ion intensities were directly compared (Smith *et al.* 2006). Following data input the samples were divided into 8 groups (based on strains with the genotype wild type (N2), *mtl-1(tm1770), mtl-2(gk125)* and *mtl-1;mtl-2(zs1)* in the presence and absence of cadmium) and the chromatograms directly compared.

2.22.3 Mass spectrometry pattern recognition analysis

Data was reduced to those integrals between the time points 1.5 minutes and 17 minutes. Reduced data was inputted into SIMCA-P+ v11.5 (Umetrics, Sweden). Mean centred scaling was applied to all data. Both positive and negative mode data were analysed by PCA and PLS-DA.

CHAPTER THREE

THE GENERATION OF *C. ELEGANS* STRAINS

3.1. Introduction

The fully sequenced genome of the nematode *C. elegans* was completed in 1998 (Consortium 1998). The genome is 97 Mb in size and contains over 19,000 genes which have been mapped (Consortium 1998). The complete genome sequence can be found via WormBase, an internet based database specifically developed for the *C. elegans* community (www.wormbase.org) (Harris *et al.* 2004). WormBase contains the basic genetic information but also information regarding genetic markers, mutant phenotypes, gene expression at the single cell level and results from RNA interference and microarray large scale screens (Harris *et al.* 2004).

WormBase is an example of a database which can be used for bioinformatic study of a gene of interest. Bioinformatics is the use of *in silico* analysis to further understand molecular biology. Large databases such as the European Bioinformatics Institute (www.ebi.co.uk) and the National Centre for Biotechnology Information (www.ncbi.nlm.nih.gov) provide an interface for the integrated study of gene and protein information. Commonly, databases are used to obtain gene or protein sequence information about a gene of interest from one or more organisms and align them to asses the level of similarity and sequence identity between them. Bioinformatics has become a popular method for initial analysis of a gene prior to laboratory work.

3.2. Aims

WormBase confirmed that the genome of *C. elegans* contains 2 isoforms of metallothionein (MT) and a gene coding for the enzyme phytochelatin synthase, *pcs-1* (Clemens *et al.* 2001; Vatamaniuk *et al.* 2001). Information about each gene was gathered from the literature available and analysed using a bioinformatics approach. Following analysis, single *mtl-1* and *mtl-2* mutant nematodes were obtained (Table 2.5) and used to generate a double MT deletion strain of *C. elegans*. In addition, a *pcs-1* deletion strain was obtained. A mutant was generated which was null for both metallothioneins and phytochelatins. For each of the three genes, *C. elegans* expressing a green fluorescent protein transgene were acquired to provide *in vivo* details of gene expression.

3.3. Results

3.3.1 The genes

Firstly, bioinformatics was performed on the genetic information acquired from WormBase and Ensembl (www.ensembl.org). The *mtl-1* gene (WormBase ID 00003473, sequence name K11G9.6) resides on the antisense (-) strand of chromosome V and is flanked by genes for alkaline ceramidase (sequence name W02F12.2) and a permease (sequence name K11G9.5). The *mtl-1* gene consists of 2 exons and 1 intron. The first exon is 16 base pairs (bp) in length while the second is 211 bp. Further downstream on the antisense strand of chromosome V resides *mtl-2* (WormBase ID 00003474, sequence name T08G5.10). The genes for tyronsine kinases (T08G5.2) and olfactory G proteins (F58E10.6) flank *mtl-2*. The *mtl-2* gene also consists of 1 intron and 2 exons. The exons are 16 bp and 175 bp, respectively.

Promoters of *mtl-1* and *mtl-2* genes have been extensively characterised (Freedman *et al.* 1993). Manual *in silico* comparisons were performed using BioEdit (Ibis Biosciences, USA). BioEdit is a computer aided alignment program which utilises ClustalW to align multiple DNA or amino acid sequences and calculate their percentage identity and similarity. Sequence identity relates to the percentage of invariant residues between the sequences and similarity is a measure of how related the sequences are. Comparisons of the first 700 bp of each *C. elegans* MT promoter show that there is a 50.8% sequence identity between *mtl-1* and *mtl-2* (Figure 3.1). Some differences between the promoters included the presence of a TATAA box and CCAAT box in *mtl-2* but not *mtl-1* (Freedman *et al.* 1993). The *cis*-acting elements

AP-1 (Activator Protein 1) and VPE-2 (Vitellogenin Promoter Element-2) are present in promoters of both *C. elegans* MTs, although in slightly different locations as indicated in Figure 3.1 (Freedman *et al.* 1993).

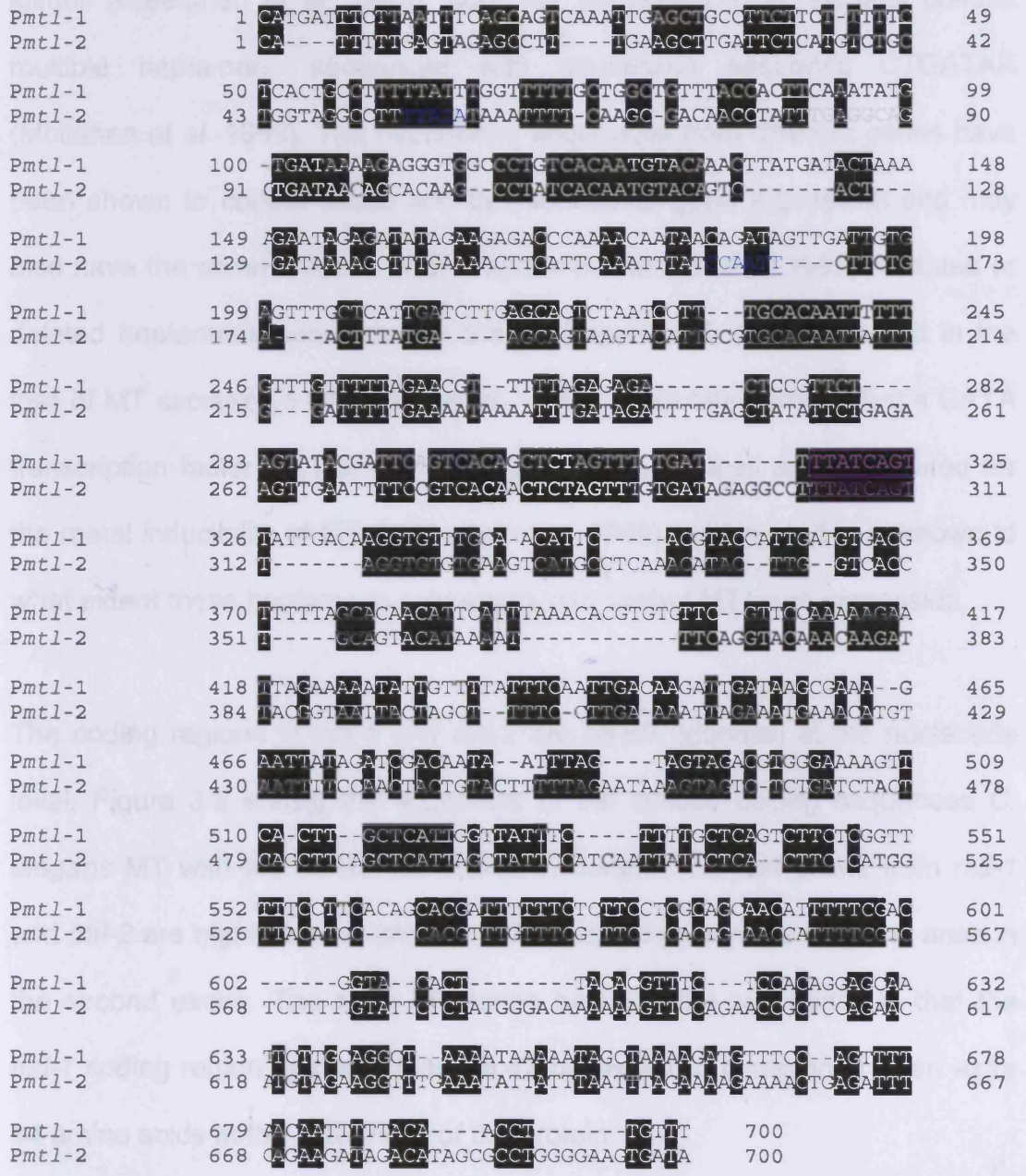

Figure 3.1: Comparison of the promoters of *C. elegans mtl-1* and *mtl-2*. There was 50.8% sequence identity between the MT promoters. Both contain some *cis*-acting elements, such as AP-1 and VPE-2 highlighted and underlined in dark purple and light purple text respectively. Only *mtl-2* contains a CCAAT and a TATAA box indicated by blue underlined text. Note: 1 is the first base before the ATG start codon of the gene.

Further upstream, the *mtl-1* promoter contains sequences which are similar to a glucocorticoid response element and *mtl-2* a cyclic AMP regulatory element (Freedman *et al.* 1993). These *cis*-acting elements may provide some transcriptional control of *C. elegans* MT via intracellular and environmental stimuli (Freedman *et al.* 1993). Both MT promoters in *C. elegans* contain multiple heptameric sequences with consensus sequence CTGATAA (Moilanen *et al.* 1999). The heptameric sequences from different genes have been shown to control tissue and developmental gene expression and may also have the same function in *C. elegans* (Moilanen *et al.* 1999). Mutated or deleted heptameric sequences in the *C. elegans* MT promoter result in the loss of MT expression (Moilanen *et al.* 1999). It has been shown that a GATA transcription factor, ELT-2, can bind to these sequences and is required for the metal inducibility of MT (Moilanen *et al.* 1999). However, it is unknown to what extent these heptameric sequences can control MT gene expression.

The coding regions of *mtl-1* and *mtl-2* are 58.6% identical at the nucleotide level. Figure 3.2 shows the alignment of the spliced coding sequences *C. elegans* MT with the conserved bases indicated. The first exons from *mtl-1* and *mtl-2* are highly similar and the differences between the isoforms arise in the second exons. The main difference between the two genes is that the *mtl-1* coding region has an additional 42 bases which correspond to an extra 14 amino acids at the N-terminal of the protein.

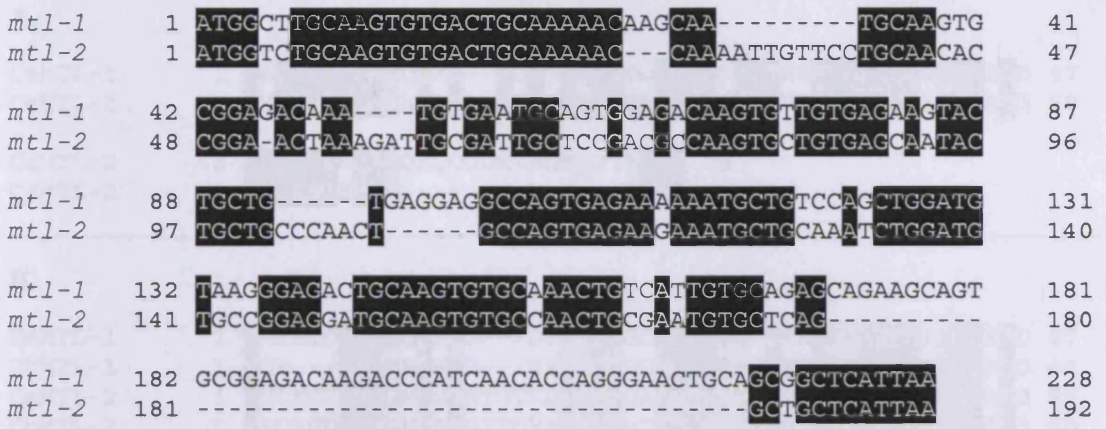

Figure 3.2: Comparison of *C. elegans* coding region of *mtl-1* and *mtl-2*. There was 58.6% sequence identity between the two sequences. The *mtl-1* gene is longer as at the C-terminal there are additional bases coding for 14 amino acids.

The longer polypeptide chain of MTL-1 reduces the percentage identity with MTL-2 to 46.2% (Figure 3.3A). Both amino acid sequences have 18 conserved cysteines residues, a hallmark of the MT protein. The cysteines are highly conserved between *C. elegans* MT isoforms and also MT from a related species *Caenorhabditis briggsae* (Figure 3.3B). The extent to which *C. elegans* MTL-1 and *C. briggsae* MTL-1 are related is 88% while the similarity between *C. elegans* MTL-2 and *C. briggsae* MTL-2 is 79.4%. Ultimately the similarity is greater between species than between isoforms within the same species.

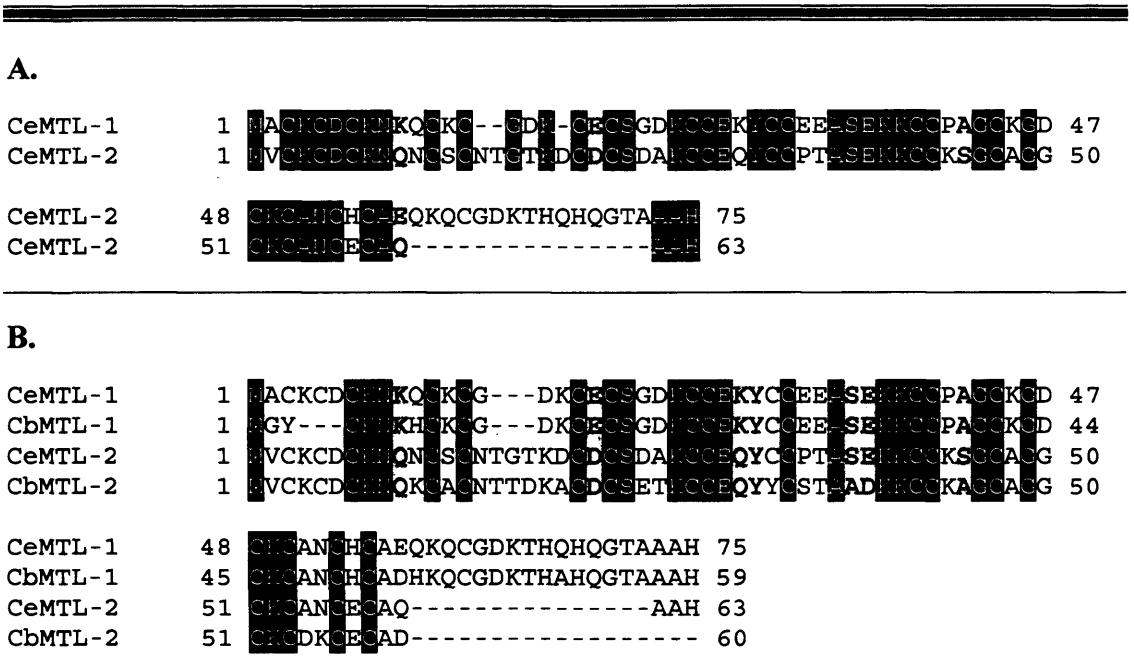

Figure 3.3: Comparison of *C. elegans* amino acid sequences of *mtl-1* and *mtl-2* (Panel A) and the *C. elegans* and *C. briggsae* MT proteins (Panel B). Amino acids shaded black are identical and those which are shaded grey are similar. A comparison of *C. elelegans* (Ce) MTL-1 and CeMTL-2 show that there is only 46.2% identity between the two proteins (Panel A). *C. briggsae* MT isoforms have a similar identity (35.9%) as *C. elegans* MT isoforms. Alignments of MTL-1 from both species show that the protein is highly conserved (88%) as is MTL-2 (79.4%) (Panel B).

The gene for phytochelatin synthase, *pcs-1* (WormBase ID 00003960, sequence name F54D5.1) is on the antisense (-) strand of chromosome II at approximately 1.15 Mb. The gene is flanked by two uncharacterised genes (sequence names F54D5.2 and F54D5.14). Details about *pcs-1* are scarce, particularly in *C. elegans*. Most information comes from plant and yeast studies (Cobbett 2000a; Cobbett 2000b; Rea *et al.* 2004; Yu *et al.* 1994). However, amino acid sequence homology searches have found that the phytochelatin (PC) synthase enzyme is present in many species including yeast, nematodes, bacteria and plants (Cobbett and Goldsbrough 2002; Clemens 2006). The *C. elegans pcs-1* DNA sequence has 44% sequence identity when compared to the yeast *Schizosaccharomyces pombe* whereas

C. elegans and the plant *Arabidopsis thaliana* have 46% sequence identity and similarity. In contrast, the amino acid sequences of *S. pombe* and *A. thaliana* have 64% similarity to the *C. elegans* PC synthase polypeptide chain (Figure 3.4).

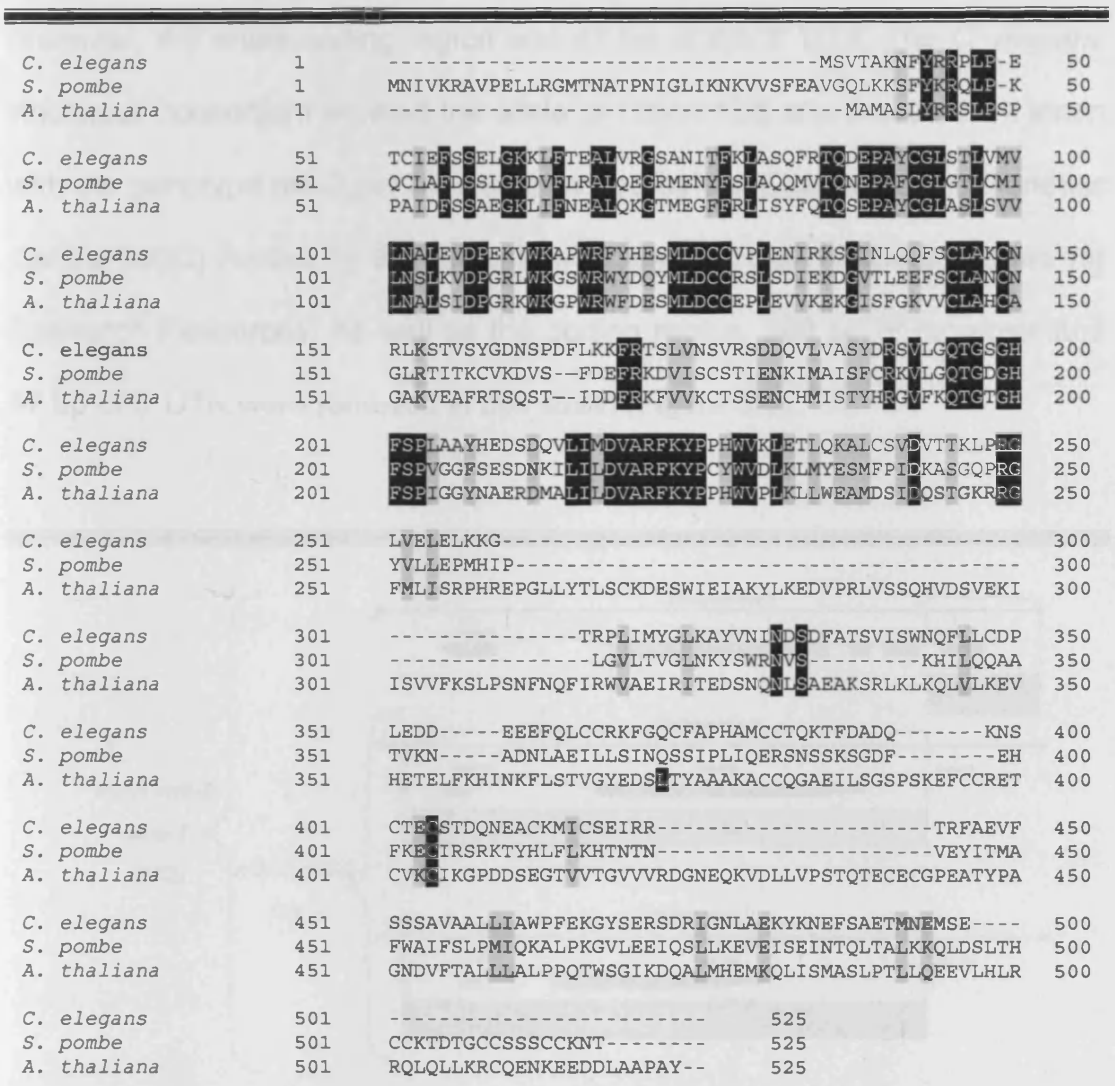

Figure 3.4: Comparison of phytochelatin synthase protein in different species. A BioEdit (Ibis Biosciences, USA) alignment of the amino acid sequence for phytochelatin synthase from *Schizosaccharomyces pombe, Arabidopsis thaliana and C. elegans.* Black shading indicates identical amino acids and grey shading shows similar amino acids. There is 64% sequence similarity between the phytochelatin synthase enzymes. *C. elegans* and *S. pombe* share 44% sequence identity and *C. elegans* and *A. thaliana* 46% identity.

3.3.2 The deletion mutants

Chromosomal deletions of the genes of interest were obtained. The isolation of the mutant allele *mtl-1*(*tm1770*) was provided by the Mitani Laboratory, Tokyo Women's Medical University School of Medicine, Japan. In detail, as shown in Figure 3.5, *mtl-1*(*tm1770*) comprises of the removal of 186 bp promoter, the entire coding region and 47 bp of the 3' UTR. The *C. elegans* Knockout Consortium isolated the allele *gk125(vc128)* and the resultant strain with the genotype *mtl-2*(*gk125*) was provided by the *Caenorhabditis* Genetics Centre (CGC) funded by the National Institutes of Health National Centre for Research Resources. As well as the coding region, 208 bp of promoter and 47 bp of 3' UTR were removed in this strain (Figure 3.5).

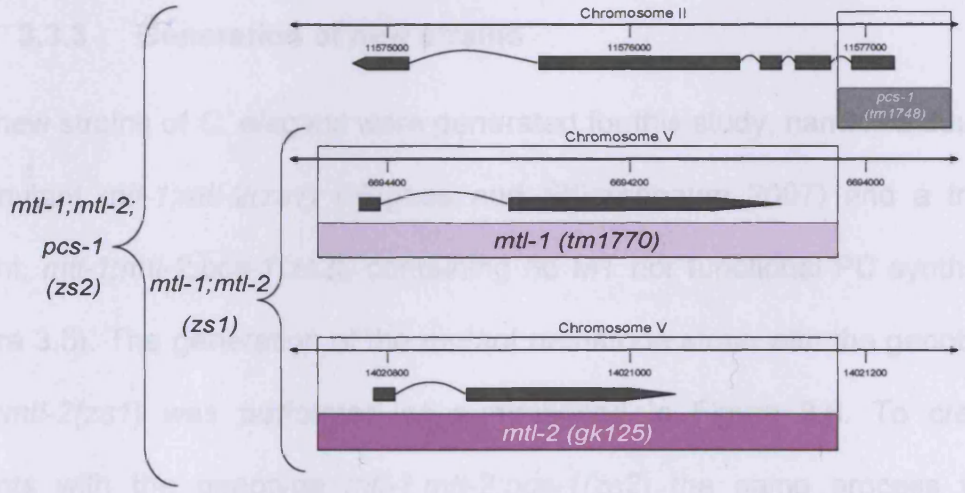

Figure 3.5: Schematic representation of the location of *mtl-1, mtl-2* and *pcs-1* and the locations of the respective deletions. The *mtl-1* and *pcs-1* mutants were isolated and provided by the Mitani Laboratory, Tokyo Womens Medical University School of Medicine, Japan. The *C. elegans* Knockout Consortium isolated the *gk125(vc128) mtl-2* mutant allele and the strain was provided by the *Caenorhabditis* Genetics Centre. In the case of *mtl-1(tm1770)* and *mtl-2(gk215)* the whole coding region was deleted (chromosomal deletions) while only one exon was deleted in *pcs-1(tm1748)*.

The Mitani Laboratory provided a mutant for *pcs-1* which has a deletion of the allele *tm1748*. Unlike the MT mutants the genotype *pcs-1(tm1748)* is only a partial deletion of the gene locus, namely of 416 bp of promoter, the whole of the first exon and 45 bp of the first intron resulting in a truncated protein (Figure 3.5). The loss of a significant portion of the promoter and 42 amino acids from the start of the polypeptide chain for PC synthase is likely to be a null deletion.

All strains were backcrossed with N2 to remove any background mutations. The strain with the genotype *mtl-1(tm1770)* was backcrossed twice, *mtl-2(gk125)* backcrossed six times and *pcs-1(tm1748)* backcrossed four times. Details of backcrossing are in Section 2.6.5.

3.3.3 Generation of new strains

Two new strains of *C. elegans* were generated for this study, namely a double MT mutant *mtl-1;mtl-2(zs1)* (Hughes and Stürzenbaum 2007) and a triple mutant, *mtl-1;mtl-2;pcs-1(zs2)*, containing no MT nor functional PC synthase (Figure 3.5). The generation of the mutant nematode strain with the genotype *mtl-1;mtl-2(zs1)* was performed as summarised in Figure 3.6. To create mutants with the genotype *mtl-1;mtl-2;pcs-1(zs2)* the same process was applied but using males containing the genotype *pcs-1(tm1748)* and hermaphrodites with the genotype *mtl-1;mtl-2(zs1)*.

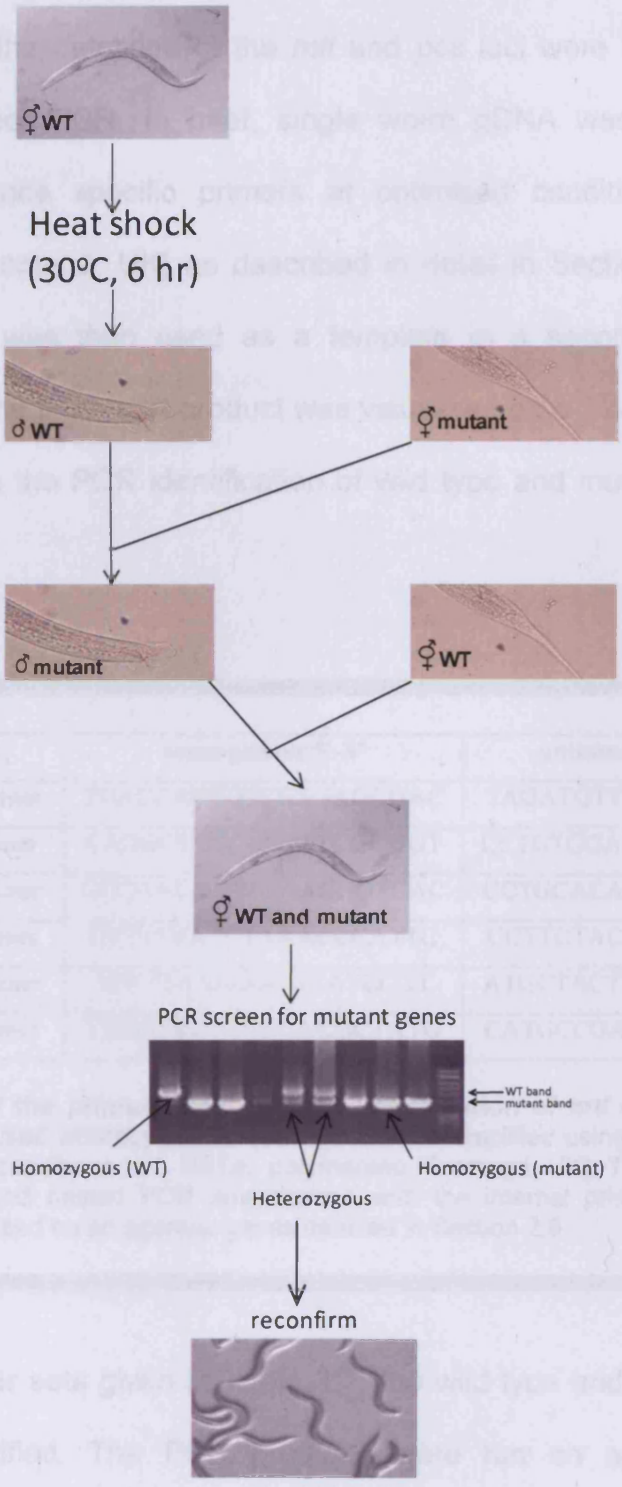

Figure 3.6: Diagram to show the generation of mutant strains of *C. elegans*. Hermaphrodite nematodes were heat shocked (30°C, 6 hours) and left to lay eggs. The offspring were then screened for males and these used in a cross with a mutant hermaphrodite (5 males to one hermaphrodite). Following reproduction, the adult was tested by polymerase chain reaction for the gene of interest. Four successive rounds of crossing were undertaken and a homozygous mutant identified.

3.3.4 PCR identification of strains

Wild type and the deletions of the *mtl* and *pcs* loci were identified using a two-step (nested) PCR. In brief, single worm gDNA was amplified using external sequence specific primers at optimised conditions with GoTaq polymerase (Promega, UK) as described in detail in Section 2.9. The PCR product (1 µl) was then used as a template in a second, internal, PCR amplification. The final PCR product was visualised on a 1% agarose gel. The primers used in the PCR identification of wild type and mutants are given in Table 3.1.

gene	sense primer 5'-3'	antisense primer 5'-3'
mtl-1 External primer	TGACCAGTGTCGTGAGCGAC	TAGATGTTTCAGACGTCACC
mtl-1 Internal primer	CAGGGTTTCATAGTCGGGGT	CCTGTGGAGAAACGTGTAAG
mtl-2 External primer	CCGAACAATTGAACGGTCAC	CCTGCACAAAGAGTTCCTGG
mtl-2 Internal primer	GTTTCCATCTAAACCCATTC	CCTTCTACATGTTCTGGAGC
pcs-1 External primer	TCTTTAAAGGCGCATCCGT	ATGCTACTACCATGCGGGAC
pcs-1 Internal primer	TTTCGAATGGCCACGCTATG	CATGCCGACTCGAGCTGTTA

Table 3.1: List of the primers used in PCR identification of *mtl* and *pcs-1* mutants. Nested PCR was used whereby single worm gDNA was amplified using the external primers at optimised PCR conditions with GoTaq polymerase (Promega, UK). The PCR product was used for the second nested PCR amplification with the internal primers. The final PCR product was visualised on an agarose gel as detailed in Section 2.9.

Using the primer sets given in Table 3.1, the wild type and deletion mutants could be identified. The PCR products were run on agarose gels and visualised with UV light (Figure 3.7). The PCR products of wild type *mtl-1* and *mtl-2* were 1800 bp and 1510 bp, respectively. In nematodes null for *mtl-1* which are those with the genotypes *mtl-1(tm1770)*, *mtl-1;mtl-2(zs1)* and *mtl-1;mtl-2;pcs-1(zs2)*, the amplicon size was reduced to 1041 bp. Nematodes

null for *mtl-2* had a reduction in the size of the PCR product from 1800 bp to 759 bp. The wild type *pcs-1* amplicon was 2516 bp and was observed in all strains bar those with the genotypes *pcs-1(tm1748)* and *mtl-1;mtl-2;pcs-1(zs2)*. Strains null for *pcs-1* had a reduced amplicon size of 1407 bp.

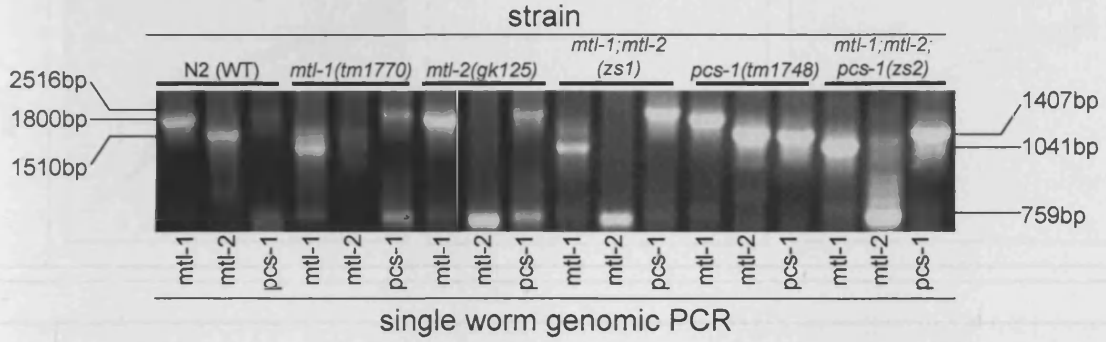

Figure 3.7: Agarose gel of PCR identification of wild type and mutant *C. elegans*. Each strain was amplified using the relevant primers for *mtl-1, mtl-2* and *pcs-1*. N2 is wild type for all genes. The strain *mtl-1(tm1770)* is a *mtl-1* deletion and *mtl-2* is deleted in *mtl-2(gk125)*. Both MT isoforms are removed in *mtl-1;mtl-2(zs1)*. The strain *pcs-1(tm1748)* is null for *pcs-1* but wild type for MT isoforms. Both MT isoforms and PC are deleted in *mtl-1;mtl-2;pcs-1(zs2)*.

3.3.5 Green Fluorescent Protein strains

Promoter constructs of green fluorescent protein (GFP) were generated for each gene of interest and the transgenic lines P*mtl-1*::GFP and P*mtl-2*::GFP were provided by Dr S. Stürzenbaum (King's College London, UK). Strains were generated as detailed in Swain *et al.* (2004), where the *mtl* promoter (1171 bp of *mtl-1* and 856 bp of *mtl-2* promoter) was amplified from gDNA. The PCR product was cloned into the vector pPD95.75 generating C-terminal GFP fusion constructs. The construct was co-injected with pRF-4, a *rol-6* gene, into the somatic cells of the nematode gonad.

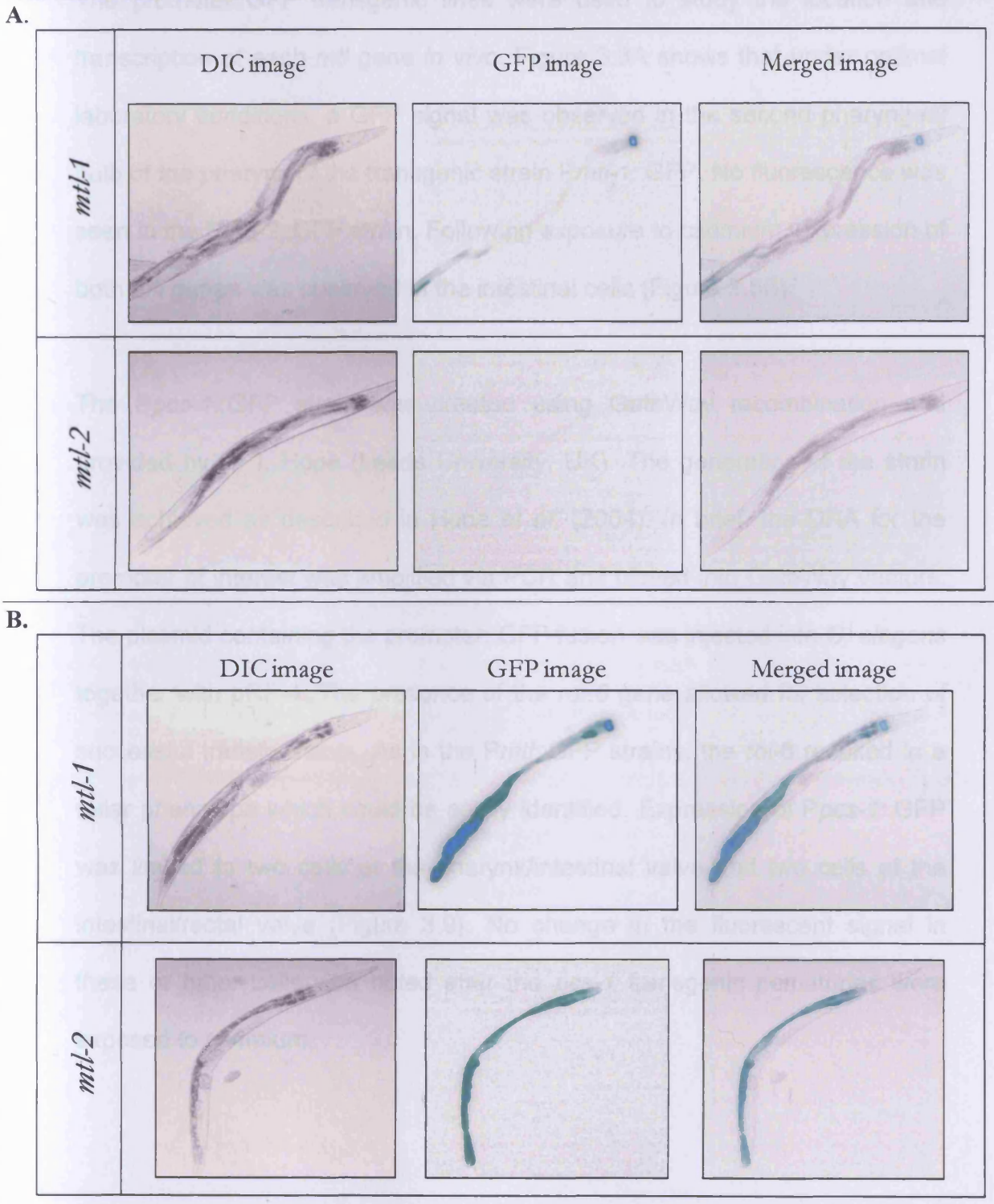

Figure 3.8: Digital images of P*mtl-1*::GFP and P*mtl-2*::GFP in the absence (Panel A) and presence (Panel B) of cadmium. Photographs were taken of L4/adult staged GFP fusion strains under the DIC microscope at a magnification of x10 on the Nikon system. GFP images were also taken at the same camera settings but with a UV filter. Images were merged using the freeware software, ImageMerger. There was expression of *mtl-1* in the pharynx but no expression of *mtl*-2 under control conditions (Panel A) and cadmium stimulates *mtl-1* and *mtl-2* gene transcription in intestinal cells (Panel B). Strains were provided by Dr Stürzenbaum, King's College London, UK.

The promoter::GFP transgenic lines were used to study the location and transcription of each *mtl* gene *in vivo*. Figure 3.8A shows that under optimal laboratory conditions, a GFP signal was observed in the second pharyngeal bulb of the pharynx of the transgenic strain P*mtl-1*::GFP. No fluorescence was seen in the P*mtl-2*::GFP strain. Following exposure to cadmium, expression of both *mtl* genes was observed in the intestinal cells (Figure 3.8B).

The P*pcs-1*::GFP strain was created using GateWay recombination and provided by Dr I. Hope (Leeds University, UK). The generation of the strain was achieved as described in Hope *et al.* (2004). In brief, the DNA for the promoter of interest was amplified via PCR and cloned into GateWay vectors. The plasmid containing the promoter::GFP fusion was injected into *C. elegans* together with pRF-4. The presence of the *rol-6* gene allowed for selection of successful transformants. As in the P*mtl*::GFP strains, the rol-6 resulted in a roller phenotype which could be easily identified. Expression of P*pcs-1*::GFP was limited to two cells at the pharynx/intestinal valve and two cells at the intestinal/rectal valve (Figure 3.9). No change in the fluorescent signal in these or other cells was noted after the *pcs-1* transgenic nematodes were exposed to cadmium.

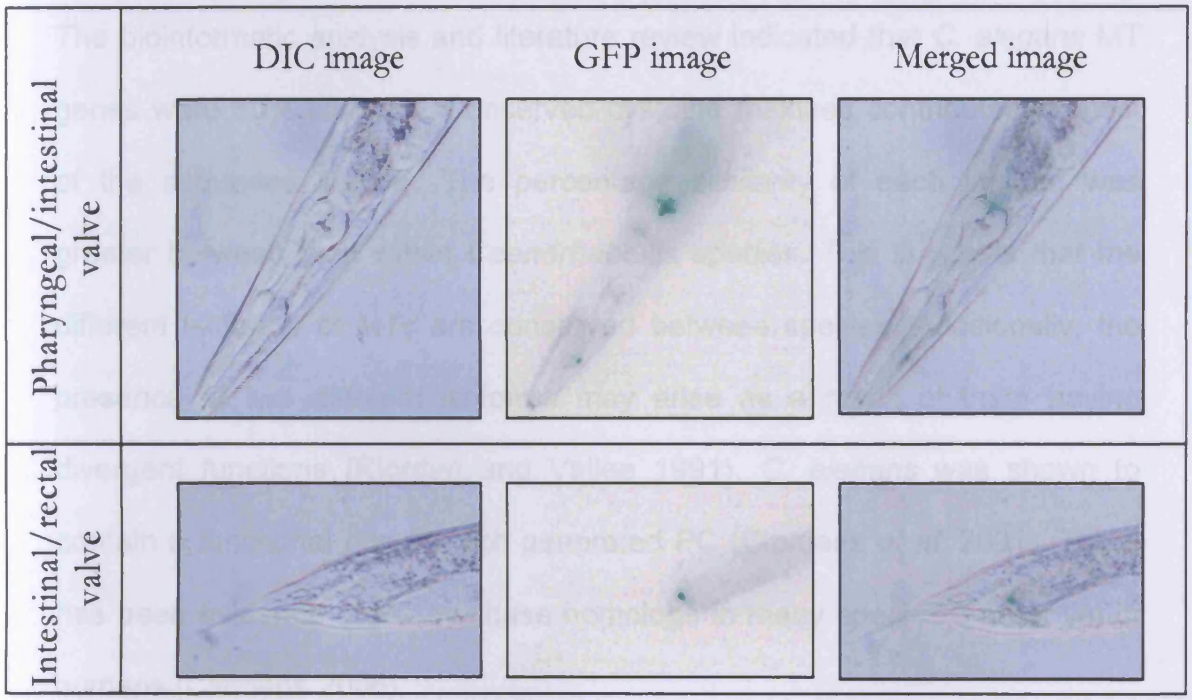

Figure 3.9: Images of P*pcs-1*::GFP. Photographs were taken of L4/adult staged P*pcs-1*::GFP fusion strain provided by Dr Hope, Leeds University (Hope *et al.* 2004). The fusion strains were generated by GateWay cloning. Images were taking using a DIC format at x40 magnification. The valves at either end of the intestine are the location of *pcs-1*.

3.4 Discussion

The bioinformatic analysis and literature review indicated that *C. elegans* MT genes were 50% identical. Conserved cysteine residues contributed to most of the sequence identity. The percentage similarity of each isoform was greater between than within *Caenorhabditis* species. This suggests that the different isoforms of MTs are conserved between species. Additionally, the presence of two different isoforms may arise as a result of them having divergent functions (Riordan and Vallee 1991). *C. elegans* was shown to contain a functional *pcs-1* which generated PC (Clemens *et al.* 2001). There has been evidence of PC synthase homologs in many species but not yet in humans (Clemens 2006).

The deletion strains of *mtl-1(tm1770)* and *mtl-2(gk125)* are true chromosomal deletions with the whole gene, approximately 200 bp of each promoter and 3' UTR removed in both cases. The generation of *mtl-1;mtl-2(zs1)* was achieved by genetic crosses of nematodes with the genotypes *mtl-1(tm1770)* and *mtl-2(gk125)*. The viability of the double knockout (genotype *mtl1;mtl-2(zs1)*) indicates that MT are not essential for life. A strain of nematode with the genotype *pcs-1(tm1748)* was obtained, which although not a full length deletion, transcribes a truncated PC synthase protein. The truncated protein is not thought to be functional and consequently phytochelatins can not be synthesised. As a consequence, the genotype *pcs-1(tm1748)* is said to be null for *pcs-1*. The newly generated double MT knockout strain and pcs-*1(tm1748)* was used to generate a triple mutant *mtl-1;mtl-2;pcs-1(zs2)*).

Using promoter::GFP fusion transgenic nematodes, it was confirmed that *mtl-1* is constitutively expressed in the pharynx. Intestinal gene expression of *mtl-1* was induced upon exposure to cadmium. The expression of *mtl-2* was only observed following stimulation by cadmium, as shown previously by Swain *et al.* (2004). The location of *pcs-1* expression was restricted to two cells of the valves at either end of the intestine. The expression pattern of *pcs-1* was not affected by cadmium at the transcriptional level. The location of both MT and PC synthase around the intestine support a hypothesis that the proteins are synthesised following the exposure to heavy metal. It is proposed that MTL-1 chelates metals upon immediate ingestion due to its location in the pharynx. Expression of both *mtl-1* and *mtl-2* in the intestine provide a mechanism by which metals can be bound before transport across apical membranes of the intestinal cells. PCs are produced by PC synthase at either end of the intestine where they can enter the gut and bind metals. PC bound metals can be transported across the apical membranes by transporters (Vatamaniuk *et al.* 2005). Once inside the cell, the metal-PC complex can be transported to a site where the metal is required or can be disposed of without the metal exerting its toxic effects.

3.5 Conclusion

C. elegans contains genes for two isoforms of MT, both located on chromosome V. There was constitutive expression of *mtl-1* in the second pharyngeal bulb. Following stimulation by cadmium, there is intestinal expression of *mtl-1* and *mtl-2*. A functional *pcs-1* gene is located on chromosome II. Expression of the gene is in two cells at the pharyngeal/intestinal valve and two cells at the intestinal/rectal valve. Single deletion mutants for the three genes were obtained and used to generate strains which contain the genotypes *mtl-1;mtl-2(zs1)* and *mtl-1;mtl-2;pcs-1(zs2)*. All the mutant genotypes are viable in control (i.e. cadmium devoid) conditions, indicating that neither MT nor PC are essential for life.

CHAPTER FOUR

CADMIUM TREATMENT NOT METALLOTHIONEIN STATUS CAUSES METABOLIC DIFFERENCES IN *C. ELEGANS*

4.1 Introduction

Metallothioneins (MT) are considered to be the primary cadmium detoxification mechanism in many organisms including *Caenorhabditis elegans*. The viability of the double *mtl* knockout, *mtl-1;mtl-2(zs1)*, contradicts the view that MTs are essential for life. To investigate the differences between mutant *mtl* strains at the cellular level, metabolomic profiling can be used. Metabolomics is a non-biased and non-targeted technique to quantify the small molecule component (metabolites) in a system (Goodacre *et al.* 2004). Specifically, metabolomics investigates the change in metabolites in response to biochemical events, environmental changes and disease (Bedair and Sumner 2008; Nicholson *et al.* 1999; Want *et al.* 2005). Changes in the metabolic profile allow an insight into the way in which an organism responds to stress (Bailey *et al.* 2003).

Raamsdonk *et al* (2001) identified "silent" phenotypes in the yeast, *Saccharomyces cerevisiae,* using metabolomics. The growth rate of *S. cerevisiae* was a sensitive method to measure the change in yeast cells as a result of the environment. However, some mutations do not show a change in the phenotype (Raamsdonk *et al.* 2001). In this case comparisons of the metabolite profiles indicate differences in the small molecule components

between mutants. This is referred to as the metabolic phenotype (Raamsdonk *et al.* 2001). Raamsdonk's 'proof of concept' paper proved that mutations in the metabolic pathway which do not result in a visual phenotype can be identified using metabolomics (Griffin 2006; Raamsdonk *et al.* 2001). Similar experiments have been undertaken in *C. elegans* to identify "silent" mutations as a result of oxidative stress (Blaise *et al.* 2007). Metabolomic profiling has therefore become a useful technique study the wide range of molecules present in the cell at a particular point in time (Griffin 2006). To date, the use of metabolomics in biomedical and clinical applications has been fruitful and has been extremely successful when applied to the field of ecotoxicology (Robertson 2005). The primary focus of ecotoxicology has been to identify and characterise the expression of proteins in response to a stress. It remains a constant challenge to equate changes in the environment to changes at the molecular level (Moore 2002). As the cell metabolome is highly sensitive to environmental changes, it is possible to investigate the effects of an environmental contaminant on an organism (Robertson 2005). Metabolic changes have been observed in the earthworm, *Lumbricus rubellus*, following copper exposure (Bundy *et al.* 2008) and metabolic responses to cadmium in mammalian cells have also been recorded (Jones *et al.* 2007; Sugiura *et al.* 2005).

Selecting suitable techniques to investigate the metabolomic changes in response to environmental stimuli is a complex choice. Speed, chemical selectivity and sensitivity are all important factors to consider (Bedair and Sumner 2008). The primary techniques used in metabolomics are nuclear

magnetic resonance (NMR) spectroscopy and mass spectrometry (MS) (Beckonert *et al.* 2007). NMR is fast, selective and non-destructive to samples while MS provides a good range of coverage with wide selectivity of compounds (Bedair and Sumner 2008). Both techniques can detect many tens of hundreds of metabolites during one sample run (Coen *et al.* 2008), and used in tandem to form a complete metabolic profile of an isolated system (Griffin 2006). Consequently, in the majority of cases NMR and MS are used in combination to probe the metabolome.

4.1.1 NMR background

The use of NMR for metabolite profiling soared during the 1990s due to the increased speed of analytical runs and the non-invasive and non-destructive nature of the technique (Reo 2002; Want *et al.* 2005). Other advantages of NMR is that there is no requirement for complicated sample preparation prior to an NMR run and that the detection of metabolites in the millimolar and micromolar range are possible (Grivet *et al.* 2003; Want *et al.* 2005). NMR relies on the property that atomic nuclei have a quantum nuclear spin. The spins orientate parallel to an applied magnetic field, like magnets, as shown in Figure 4.1 (Williams and Fleming 1995). The application of radio signals at the same frequency as the nuclear magnets cause some nuclei to "jump" from a low to high energy state. As the nuclei relax back to the lower energy state energy is released. The difference in frequency between the nuclear magnetic resonance frequency and the excitation frequency (the radio frequency causing the nuclei to "jump" energy states) is recorded as the NMR spectra (Williams and Fleming 1995). Modern NMR spectroscopy uses Fourier

Transform of a time-domain envelope of overlapping resonating frequencies to determine spectral frequency shifts.

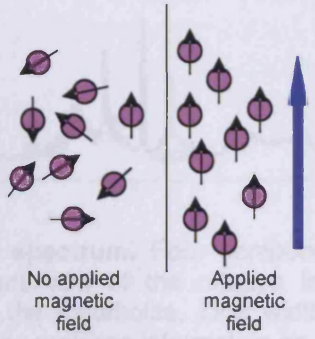

Figure 4.1: Diagram to show the orientation of nuclear magnets. In the absence of a magnetic field, nuclei have a spin with random orientation. When a magnetic field is applied, the nuclear spins align parallel to the magnetic field. Redrawn from Williams and Fleming (1995).

There are two common types of nuclei spectrum - ^{1}H and ^{13}C although one dimensional ^{1}H NMR is most frequently used. In the spectrum, peaks are characterised by four basic parameters as shown in Figure 4.2. Firstly, the relative frequency is given as an arbitrary unit ppm. The units are arbitrary as the input energy is in joules, the energy change is measured in tesla and the output is given in hertz. An arbitrary unit is required to normalise the frequency between NMR machines. Secondly, the intensity of peak height is proportional to the concentration of metabolites. The multiplicity, or splitting, of peaks provides information on neighbouring nuclei. Adjacent nuclei cause a single peak to be split into a characteristic doublet or triplet. Finally the line width provides information on the relaxation of the nuclei.

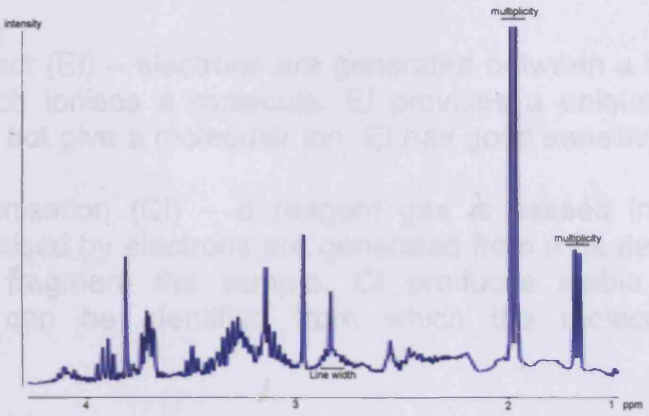

Figure 4.2: An example NMR spectrum. Four components comprise the spectra. The arbitrary unit, ppm, is a measurement of the relative frequency. The peak intensity is proportional to concentration of the metabolite. Line width indicates the relaxation of the nuclei. Finally multiplicity or splitting provides information on neighbouring nuclei.

4.1.2 Mass spectrometry background

A mass spectrometer is used to vaporise and ionise components from a sample which can then be separated based on the mass to charge ratio (*m/z*) of the ions. MS is a powerful tool to study metabolomics and has several advantages over NMR methods (Want *et al.* 2005). MS has a greater dynamic range than NMR, 10^6 compared to 10^3, and is more sensitive due to its ability to detect small molecules in the nanomolar range (Want *et al.* 2005). There are various ways in which vaporisation and ionisation of a sample is achieved (Box 4.1). The two common methods of ionisation are electron impact (EI) and electrospray ionisation (ESI).

Volatile samples

- Electron impact (EI) – electrons are generated between a heated filament and anode which ionises a molecule. EI provides a unique fragmentation pattern but may not give a molecular ion. EI has good sensitivity but a limited mass range.
- Chemical ionisation (CI) – a reagent gas is passed into the sample chamber and ionised by electrons are generated from a heated filament. The electrons then fragment the sample. CI produces stable ions and the molecular ion can be identified from which the molecular weight is determined.

Non-volatile samples

- Electrospray ionisation (ESI) – a potential difference is created between an electrode and capillary. A small volume of liquid sample (1-10 µl/min) is sprayed as a fine mist at atmospheric pressure into the chamber. The spray contains charged droplets which can be detected. Few molecular ions are generated but large polar compounds can be analysed. Adducts can form.
- Field desorption – electrons from the sample are transferred to a thin metal wire which has been heated. The ion is in the gas phase without thermal decomposition. Occasionally the molecular ion can be identified.
- Particle/radiation desorption
  - Laser desorption – the sample is dissolved in a matrix and energy from a laser is transferred to the sample. The sample does not decompose and will generate information to calculate molecular weights of molecules.
  - SIMS/FAB – a beam of ions/atoms are directed to the sample to fragment it. This ionisation provides structurally useful fragment ions.
  - Plasma desorption – uses radioactive californium to hit the sample deposited on nickel foil to ionise it. Spontaneous fission occurs, giving rise to two fragments which can be detected.

Box 4.1: Details of the ionisation methods used in mass spectrometry. EI is commonly used as an ionisation method with gas chromatography while ESI is commonly found with liquid chromatography mass spectrometry. Adapted from Williams and Fleming (1995) and Want *et al.* (2007).

EI is primarily used with gas chromatography mass spectrometry (GC/MS) and is referred to as "hard ionisation" due to the high energy which is required to ionise samples. A sample is heated and electrons bombard the sample as they pass through it to ionise molecules (Want *et al.* 2007). EI provides a unique fragment pattern but may not give a molecular ion fragment (Williams and Fleming 1995). ESI, so called "soft ionisation", is used to generate ions in

liquid chromatography mass spectrometry (LC/MS). Liquid is sprayed out of a capillary needle into a heated chamber. The spray is then charged by a current passing though the gas. This charges the liquid droplets which are carried through an electric field to an analyser (Williams and Fleming 1995). Few molecular fragments are produced using ESI, however adducts, most commonly with sodium and potassium can be formed (Want *et al.* 2007).

Mass analysers are critical to mass spectrometry and the two common types of analyser are quadrupole and time-of-flight (TOF) (Want *et al.* 2005; Want *et al.* 2007). Quadrupole analysers can detect molecules with a *m/z* of up to 4000 and can be coupled to different ion sources, commonly gas chromatography or high-pressure liquid chromatography (Want *et al.* 2005; Want *et al.* 2007; Williams and Fleming 1995). Quadrupole instruments are very robust and have a large dynamic range. They are tolerant of the high pressures required for ionisation of a single ion species which can be isolated and kept stable (Want *et al.* 2007; Williams and Fleming 1995). However, quadrupoles have low resolution and mass accuracy compared to TOF instruments. TOF analysers are much simpler, have an unlimited mass range, a high resolution and are accurate to 5 parts per million (Want *et al.* 2005; Want *et al.* 2007; Williams and Fleming 1995). The principal of TOF instruments is to extract ions following a high voltage pulse when a potential difference accelerates ions into a field-free tube (Figure 4.3) (Williams and Fleming 1995). The ions are separated according to the *m/z* ratio with large mass ions having a slower velocity and consequently a longer time in flight (Williams and Fleming 1995).

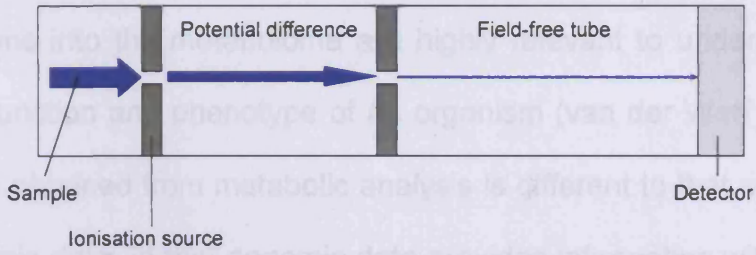

Figure 4.3: Diagram to show the time of flight (TOF) mass analyser. The TOF instrument allows detection of masses based on the *m/z* ratios. Ions are produced from the sample by a pulse of high voltage (the ionisation source) which are accelerated into a field-free tube. The ions are detected when they hit the detector. Ions with large masses have a lower velocity and so take longer to reach the detector whereas smaller ions reach the detector faster. Adapted from Williams and Fleming (1995).

High resolution gas chromatography coupled to mass spectrometry (GC/MS) was historically the preferential method of mass spectrometry in metabolomic studies (Want *et al.* 2005). Although GC/MS can provide high resolution chromatograms the sample preparation is complex and non-volatile polar molecules are not easily analysed (Want *et al.* 2005). As a result liquid chromatography mass spectrometry (LC/MS) has become increasingly popular, partly as sample preparation is much simpler and also as a larger mass range can be analysed (Want *et al.* 2005). The primary consideration in the choice of columns for LC/MS is important as some columns do not retain polar molecules (Want *et al.* 2007). Ultra-high performance LC/MS (UPLC/MS) uses columns with a packing material of 1.4-1.7 μm which increases the separation of metabolites compared to more traditional high performance liquid chromatography mass spectrometry (Want *et al.* 2007). UPLC/MS provides greater chromatographic resolution of peaks and supports high-throughput analytical approaches (Want *et al.* 2007).

4.1.3 NMR and UPLC/MS in metabolomics

Investigations into the metabolome are highly relevant to understanding the biological function and phenotype of an organism (van der Werf *et al.* 2005). Information obtained from metabolic analysis is different to that of genomic or transcriptomic data, in that genomic data provides information with regards to potential gene function while transcriptomic data is concerned with the functional response of proteins i.e. gene expression via mRNA levels (van der Werf *et al.* 2005). The data derived from the metabolome generates functional information about cellular metabolism in different environmental and phenotypic contexts (van der Werf *et al.* 2005).

Both NMR and UPLC/MS as individual techniques provide highly informative data sets. NMR was used to investigate the effect of cadmium on kidney cells using NMR (Jones *et al.* 2007) and used for metabotyping of *C. elegans* "silent" phenotypes (Blaise *et al.* 2007). The response of the *Arabidopisis thaliana* metabolome to cadmium was investigated using LC/MS (Sarry *et al.* 2006). In combination these techniques are even more powerful. Atherton *et al.* (2008) used a combined approach to study the metabolic changes of a *C. elegans* NHR-64 mutant. NMR was utilised to screen the soluble metabolites and GC/MS used to screen the fatty acid component (Atherton *et al.* 2008). Used together 86 metabolites were rapidly identified (Atherton *et al.* 2008). Thus an approach using several techniques in tandem to study the metabolome is highly informative.

4.2 Aims

The aim of this chapter was to investigate the global phenotypic effect as a result of cadmium exposure. ^{1}H-NMR was utilised to provide insight into the metabolic profile as a consequence of removal of MT and/or chronic cadmium exposure. Nematode metabolite extracts were subsequently analysed by UPLC-TOF/MS to identify any significant small metabolites. The genotypes used were the wild type strain Bristol N2, and nematodes with the genotypes *mtl-1(tm1770)*, *mtl-2(gk125)* and *mtl-1;mtl-2(zs1)* in the presence and absence of cadmium (12 µM).

4.3 Results

4.3.1 Sample extraction method

There are no universally accepted methods of sample preparation for NMR analysis (Lin *et al.* 2007). The most important aspect of sample preparation in metabolomic studies is to quickly stop enzyme activity and prevent the recovery of that activity (Lin *et al.* 2007). As such it is preferable to snap freeze a sample in liquid nitrogen to stop any enzyme activity immediately (Lin *et al.* 2007). In addition, samples should provide a high yield of metabolite with little variation between replicates (Le Belle *et al.* 2002). Several metabolite extraction methods were tested. In all cases, text extractions were performed on L4 stage nematodes with each replicate comprising five 90 mm Petri dishes (Greiner Bio-One). Age synchronised nematodes were left at 20°C for 48 hours to develop from L1 to L4 stage, at which point they were washed off the plates. The nematodes were pelleted by centrifugation (2000g, 2 minutes) and the supernatant removed. The pellet was resuspended in 200 µl M9 buffer (Table 2.3). The suspension was then used for metabolite extractions as described below.

The extraction methods tested were based on the direct disruption of the nematode pellet. In all extractions an 80% acetonitrile solution was used as the solvent. Firstly pellets were manually ground in a liquid nitrogen-cooled pestle and mortar. Additional liquid nitrogen was added to the sample to keep it frozen. The second extraction method tested was repeated freeze/thaw. In this method the pellets were snap frozen in liquid nitrogen then placed on ice

to thaw and re-frozen again three times. Finally, the use of acid washed glass beads (Sigma, UK) to disrupt nematodes mechanically was tested. An equal volume of glass beads was added to the nematode pellet and the sample was vortexed at high speed for 3 minutes. Following pellet disruption, 1 ml of 80% acetonitrile was added to the homogenised sample. The solvent was then transferred to a 2 ml micro-centrifuge tube prior to NMR analysis. Figure 4.4 shows the spectra of all the extraction methods tested. The spectra were all normalised to the internal control peak for TSP to allow sample comparison.

In general, the manual grinding method was less reproducible than the glass bead and freeze/thaw methods (Figure 4.4A). However, the prevalence of peaks and their intensities were similar across all extraction methods. The freeze/thaw method of extraction had lower intensity peaks in the aromatic region (Figure 4.4B) compared to the other extraction methods. In the aliphatic region (Figure 4.4C), at 1 ppm the freeze/thaw method had lost some peaks. The peaks in the glass bead extractions were of greater intensity than the other extraction methods (Figure 4.4A). There were more peaks present in the aromatic region of the glass bead extractions than either the manual or freeze/thaw extractions (Figure 4.4B). The glass bead extraction method was highly reproducible between sample replicates.

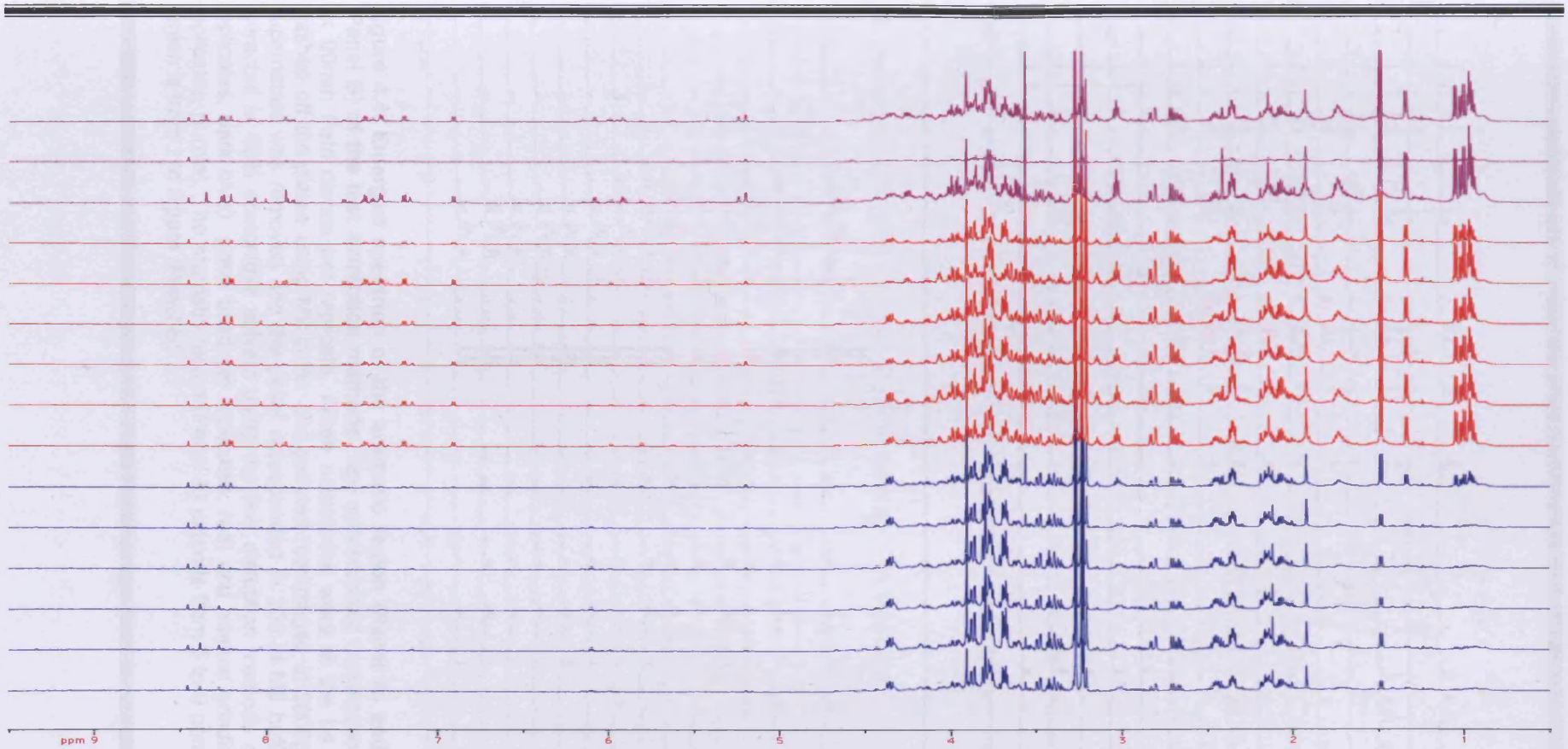

Figure 4.4A: The full NMR spectra of each test extraction method. Age synchronised nematodes were plated onto 5x 90mm Petri dishes per replicate. When nematodes were at the L4 stage, they were washed off the plates using M9 buffer and pelleted (centrifuged at 2000g, 2 minutes). The supernatant was removed and the pellet resuspended in 200 µl M9 buffer. Samples were extracted in 80% acetonitrile solvent using the test disruption methods of freeze/thaw (x6 replicates, dark blue), glass bead (x6 replicates, red) and manual grinding extractions (x3 replicates, purple).

A.

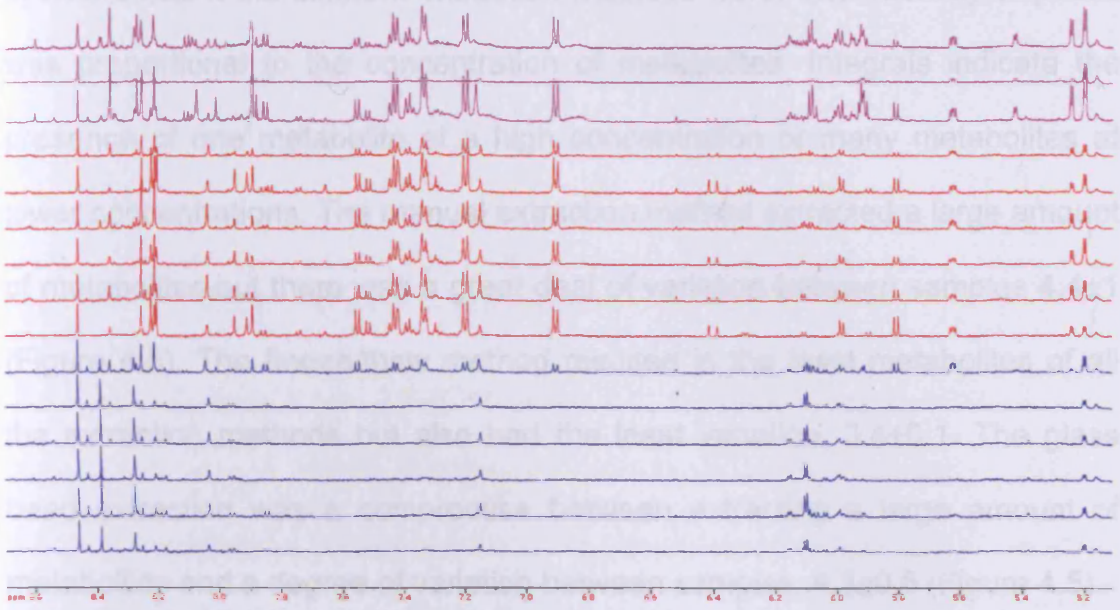

B.

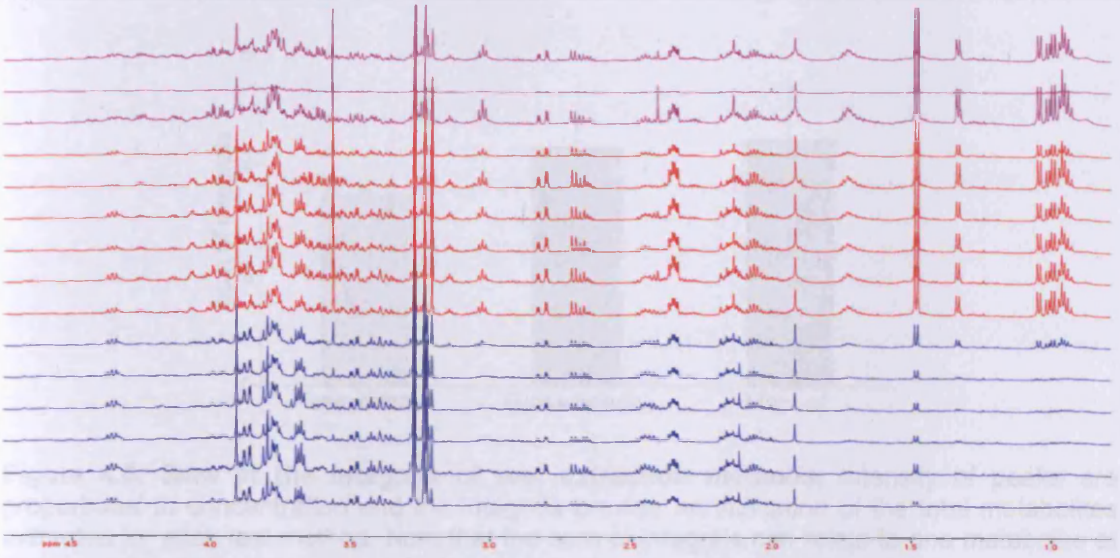

Figure 4.4: Enlarged spectrum of the aromatic region (Panel A) and aliphatic region (Panel B) of the test extraction methods. Age synchronised nematodes were plated onto 5x 90mm Petri dishes per replicate. When nematodes were at the L4 stage, they were washed off the plates using M9 buffer and pelleted (centrifuged at 2000g, 2 minutes). The supernatant was removed and the pellet resuspended in 200 µl M9 buffer. Samples were extracted in 80% acetonitrile solvent using the test disruption methods of freeze/thaw (x6 replicates, dark blue), glass bead (x6 replicates, red) and manual grinding extractions (x3 replicates, purple). The aromatic region (Panel A) extends from 5 to 9 ppm and the aliphatic region is from 1 to 5 ppm (Panel B).

Comparing the total integrals of each extraction method provides an indication of how efficient the different extraction methods were. The intensity of peaks was proportional to the concentration of metabolites. Integrals indicate the presence of one metabolite at a high concentration or many metabolites at lower concentrations. The manual extraction method extracted a large amount of metabolites but there was a great deal of variation between samples 4.4±1 (Figure 4.5). The freeze/thaw method resulted in the least metabolites of all the extraction methods but also had the least variation, 3.4±0.1. The glass bead extraction was a compromise between extracting a large amount of metabolites and a degree of variation between samples, 4.3±0.5 (Figure 4.5).

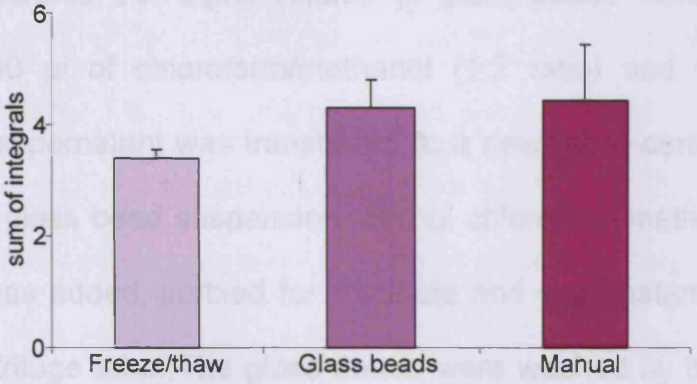

Figure 4.5: Sum of the integrals of test extraction methods. Intensity of peaks are proportional to concentration and the integrals provide an indication of the total metabolites extracted for each test method. Note that the sum of integrals can relate to one metabolite at high concentrations or many metabolites at much lower concentrations.

As the freeze/thaw extraction method generated the lowest sum of integrals and therefore the lowest number of metabolites, this method was discarded. The manual grinding of nematode samples using liquid nitrogen cooled pestle and mortar extracted a large number of metabolites (a high sum of integrals)

but with poor reproducibility. Using glass beads to extract metabolites provided a significant amount of metabolites and was reproducible between samples. As a consequence, the glass bead extraction method was chosen as the preferred method of homogenisation of the nematodes.

4.3.2 Solvent Optimisation

Solvents are required in aqueous extraction methods to lyse cells, remove cellular debris and isolate intracellular solutes (Sze and Jardetzky 1994). A chloroform/methanol solvent mixture had previously been used for *C. elegans* metabolite extractions and adapted for this study from Atherton *et al.* (2008) and Le Belle *et al.* (2002). Nematodes were pelleted to 200 µl in M9 buffer as previously described. An equal volume of glass beads were added to the pellet with 600 µl of chloroform/methanol (1:2 ratio) and vortexed for 3 minutes. The supernatant was transferred to a new micro-centrifuge tube. To the remaining glass bead suspension, 500 µl chloroform/methanol/water in a 1:2:0.9 ratio was added, vortxed for 1 minute and supernatant transferred to the micro-centrifuge tube. The glass beads were washed by briefly vortexing in a 1:1 ratio of chroloform/methanol (600 µl) with the supernatant transferred to the micro-centrifuge tube. Following centrifugation (12000g, 15 minutes) the metabolite containing supernatant was transferred to a fresh micro-centrifuge tube and stored at -80°C.

Other solvents tested were methanol, ethanol and acetonitrile. In each case, an equal volume of glass beads was added to the nematode pellet and 1 ml solvent added. The solvents were 100% with the exception of acetonitrile

which was 80% with water. The glass bead/pellet/solvent suspension was vortexed for 3 minutes and the supernatant transferred to a new micro-centrifuge tube. A second wash of solvent was added (0.8 ml of 80% methanol and acetonitrile in water and 0.8 ml of 75% ethanol in water). Following a brief vortex of 1 minute, the supernatant was added to the micro-centrifuge tube and centrifuged (3000g, 2 minutes). The supernatant was stored at -80°C.

A representative spectrum of each of the solvent extraction method tested is shown in Figure 4.6A. Overall there are very few differences between solvents tested with the exception that the ethanol extraction spectrum has a large glycerol peak in the aliphatic region which masks other peaks (Figure 4.6A and 4.6C). In addition the acetonitrile and ethanol solvents appear to extract more metabolites in the aromatic region than methanol and chloroform/methanol solvent extraction (Figure 4.6A and 4.6B). As there were only marginal differences between the solvent extraction spectra, any solvent could be used for the extraction. However, it was decided to choose a solvent which extracted a wide range of metabolites throughout the spectrum. Consequently, methanol was chosen as the solvent for metabolite extraction.

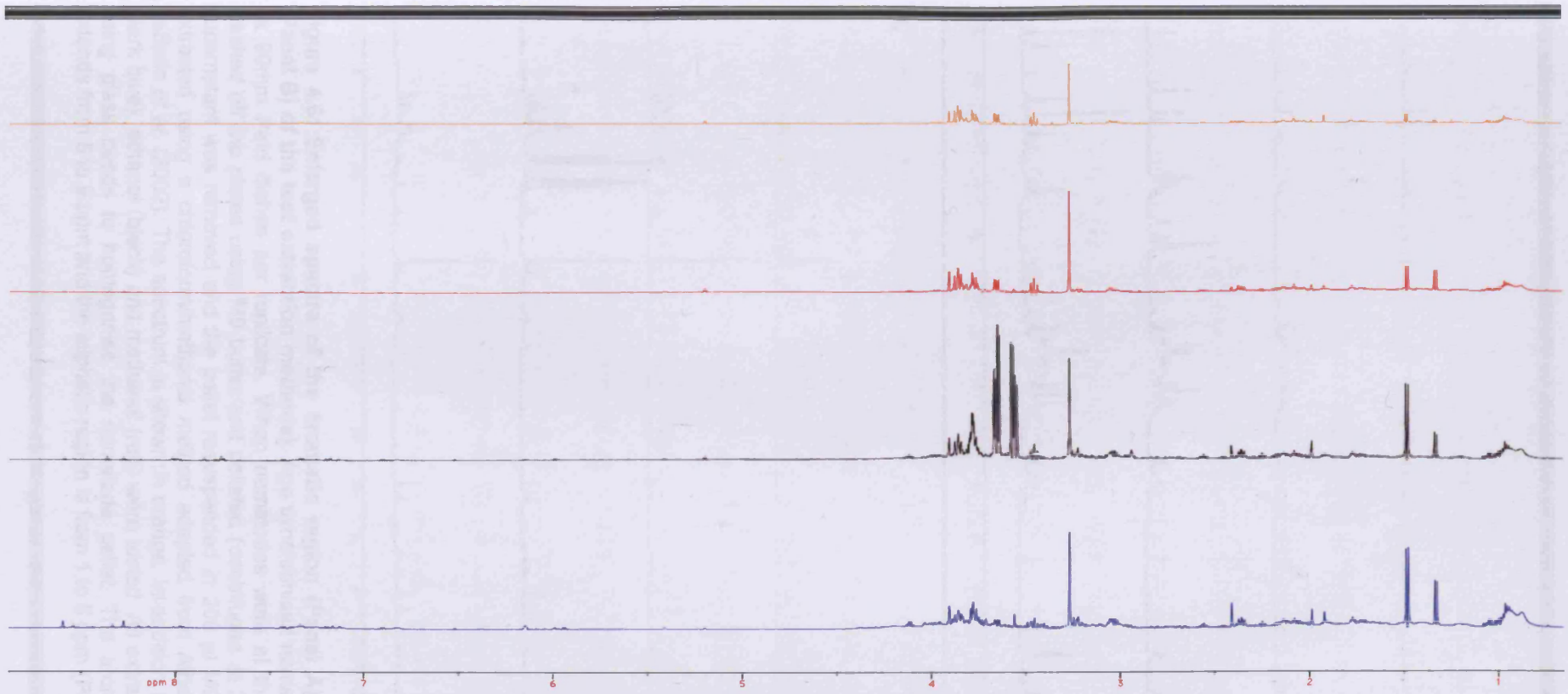

Figure 4.6A: Full spectra of solvent extraction optimisation. Age synchronised nematodes were plated onto 5x 90mm Petri dishes per replicate. When nematodes were at the L4 stage, they were washed off the plates using M9 buffer and pelleted (centrifuged at 2000g, 2 minutes). The supernatant was removed and the pellet resuspended in 200 µl M9 buffer. Samples were extracted using a chloroform/methanol method adapted from Atherton *et al.* (2008) and Le Belle *et al.* (2002) (orange spectrum). In addition the solvents acetonitrile (dark blue), ethanol (black) and methanol (red) were tested. All extractions were undertaken using glass beads to homogenise the nematode pellet.

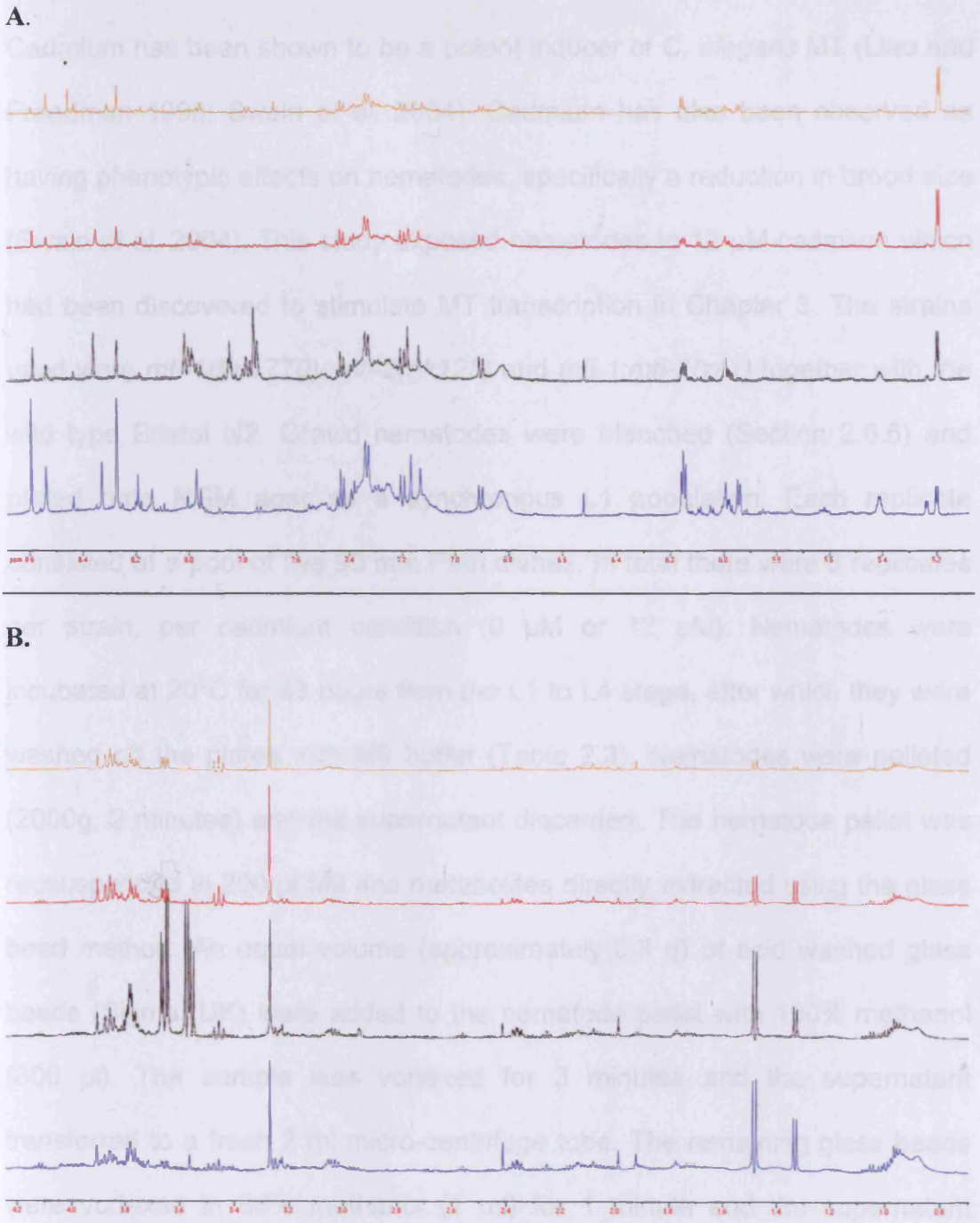

Figure 4.6: Enlarged spectra of the aromatic region (Panel A) and aliphatic region (Panel B) of the test extraction methods). Age synchronised nematodes were plated onto 5x 90mm Petri dishes per replicate. When nematodes were at the L4 stage, they were washed off the plates using M9 buffer and pelleted (centrifuged at 2000g, 2 minutes). The supernatant was removed and the pellet resuspended in 200 µl M9 buffer. Samples were extracted using a chloroform/methanol method adapted from Atherton *et al.* (2008) and LeBelle *et al.* (2002). The spectrum is shown in orange. In addition the solvents acetonitrile (dark blue), ethanol (black) and methanol (red) were tested. All extractions were undertaken using glass beads to homogenise the nematode pellet. The aromatic region (Panel A) extends from 5 to 9 ppm and the aliphatic region is from 1 to 5 ppm (Panel B).

4.3.3 Experimental design and metabolite extraction

Cadmium has been shown to be a potent inducer of *C. elegans* MT (Liao and Freedman 1998; Swain *et al.* 2004). Cadmium has also been observed as having phenotypic effects on nematodes, specifically a reduction in brood size (Swain *et al.* 2004). This study exposed nematodes to 12 µM cadmium which had been discovered to stimulate MT transcription in Chapter 3. The strains used were *mtl-1(tm1770), mtl-2(gk125)* and *mtl-1;mtl-2(zs1)* together with the wild type Bristol N2. Gravid nematodes were bleached (Section 2.6.6) and plated onto NGM agar as a synchronous L1 population. Each replicate consisted of a pool of five 90 mm Petri dishes. In total there were 8 replicates per strain, per cadmium condition (0 µM or 12 µM). Nematodes were incubated at 20°C for 48 hours from the L1 to L4 stage, after which they were washed off the plates with M9 buffer (Table 2.3). Nematodes were pelleted (2000g, 2 minutes) and the supernatant discarded. The nematode pellet was reususpended in 200 µl M9 and metabolites directly extracted using the glass bead method. An equal volume (approximately 0.3 g) of acid washed glass beads (Sigma, UK) were added to the nematode pellet with 100% methanol (800 µl). The sample was vortexed for 3 minutes and the supernatant transferred to a fresh 2 ml micro-centrifuge tube. The remaining glass beads were vortexed in 80% methanol (1 ml) for 1 minute and the supernatant transferred to the micro-centrifuge tube. Following centrifugation (3000g, 2 minutes) the supernatant was stored at -80°C until required.

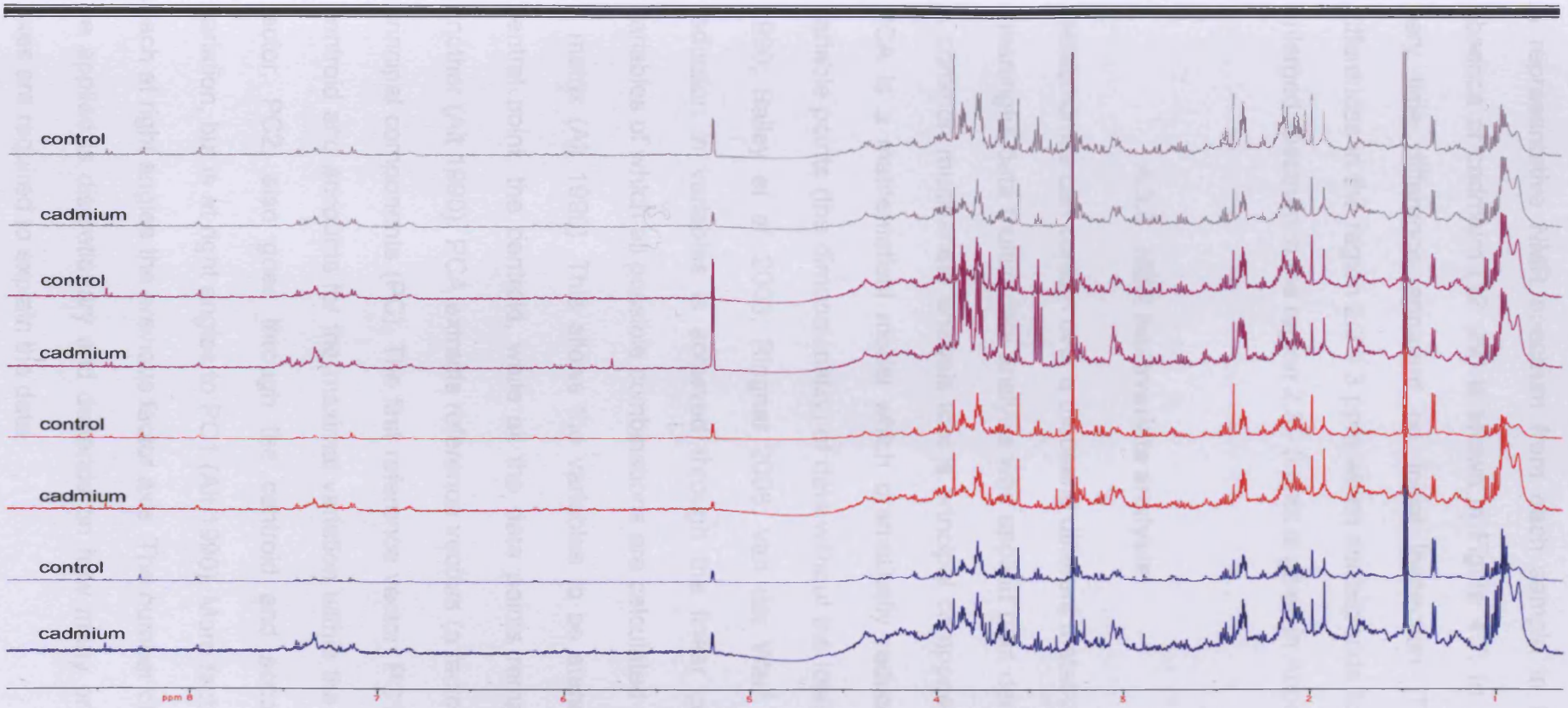

Figure 4.7: A representative spectrum from each of the sample extractions. Age synchronised nematodes were plated onto 5x 90mm Petri dishes per replicate. When nematodes were at the L4 stage, they were washed off the plates using M9 buffer and pelleted (centrifuged at 2000g, 2 minutes). The supernatant was removed and the pellet resuspended in 200 µl M9 buffer. Samples were extracted using the glass bead extraction method with methanol as the solvent. A representative spectra from the strain N2 (red), and those strain containing the genotypes *mtl-1(tm1770)* (purple), *mtl-2(gk125*) (blue) and mtl-*1;mtl-2(zs1)* (grey) are shown in the presence and absence of cadmium. The spectra have been normalised to alanine for comparison.

A representative NMR spectrum from each sample in the presence and absence of cadmium (12 μM) is shown in Figure 4.7. In general there was very little difference apparent on initial inspection. There were some differences in the region 2.3 - 3 ppm which corresponds to cystathionine. An enlarged spectrum in the region 2.3 - 3 ppm is given in Appendix 2.

4.3.4 NMR multivariate analysis

Metabolomes can contain over a thousand different metabolites and to extract meaningful data multivariate analysis was applied (van der Werf *et al.* 2005). A common multivariate analysis tool is principal component analysis (PCA). PCA is a mathematical model which dramatically reduces the number of variable points (the dimensionality) of data without the loss of information (Alt 1990; Bailey *et al.* 2003; Ringner 2008; van der Werf *et al.* 2005). The reduction in variables is achieved through the linear combinations of all variables of which all possible combinations are calculated and then plotted in a matrix (Alt 1990). This allows the variables to be standardised around a central point, the centroid, while all the data points remain relative to one another (Alt 1990). PCA extracts reference vectors (a factor) sequentially into principal components (PC). The first reference vector, PC1 goes through the centroid and accounts for the maximal variation within the data. The second factor, PC2, also goes through the centroid and accounts for maximal variation, but is at right angles to PC1 (Alt 1990). More factors can be applied each at right angles the previous factor axis. The number of factors which can be applied is discretionary and depends on how many principal component axes are required to explain the data.

PCA is an unsupervised analysis whereby relationships within data sets can be visualised without prior knowledge of the data (van der Werf *et al.* 2005). The binned NMR data (Section 2.21.2 and Appendix 1) were inputted into SIMCA-P+ v11.5 (Umetrics, Sweden) and analysed as described in Section 2.21.3. Briefly, the TSP and water spectral peaks were removed and all samples were mean centred. Samples were grouped on the basis of genotype in either the presence or absence of cadmium (two analyses comprising four groups). In addition samples were grouped with regards to cadmium exposure only and not genotype (two groups). The PCA scores plots provide a visualisation of the relationships between samples and can be used to establish differences and similarities of the samples (Bailey *et al.* 2003).

There was no clear clustering of genotypes in the absence of cadmium (Figure 4.8A) although *mtl-1;mtl-2(zs1)* nematodes were being drawn out to the left of the PCA plots and *mtl-2(gk125)* were distributed towards the top of the plot. In the presence of cadmium some clustering patterns emerged (Figure 4.8B). Wild type, N2, and *mtl-2(gk125)* genotypes were beginning to cluster towards the bottom left of the plot and there was some evidence that *mtl-1(tm1770)* may be forming a distinct cluster. When the genotypes were grouped solely on the basis of the presence or absence of the heavy metal, there was evidence indicative of a clustering pattern (Figure 4.8C). The R^2 value explains the amount of variance which is shared by the two variables (Alt 1990). In the PCA of samples in the presence and absence of cadmium (Figure 4.8C), the R^2 value was 0.87 indicating that 87% of the variance can be explained by the 2 components, PC1 and PC2. Thus the effects caused by

cadmium on the metabolome were larger than the metabolomic differences between genotypes within the dosed and control groups.

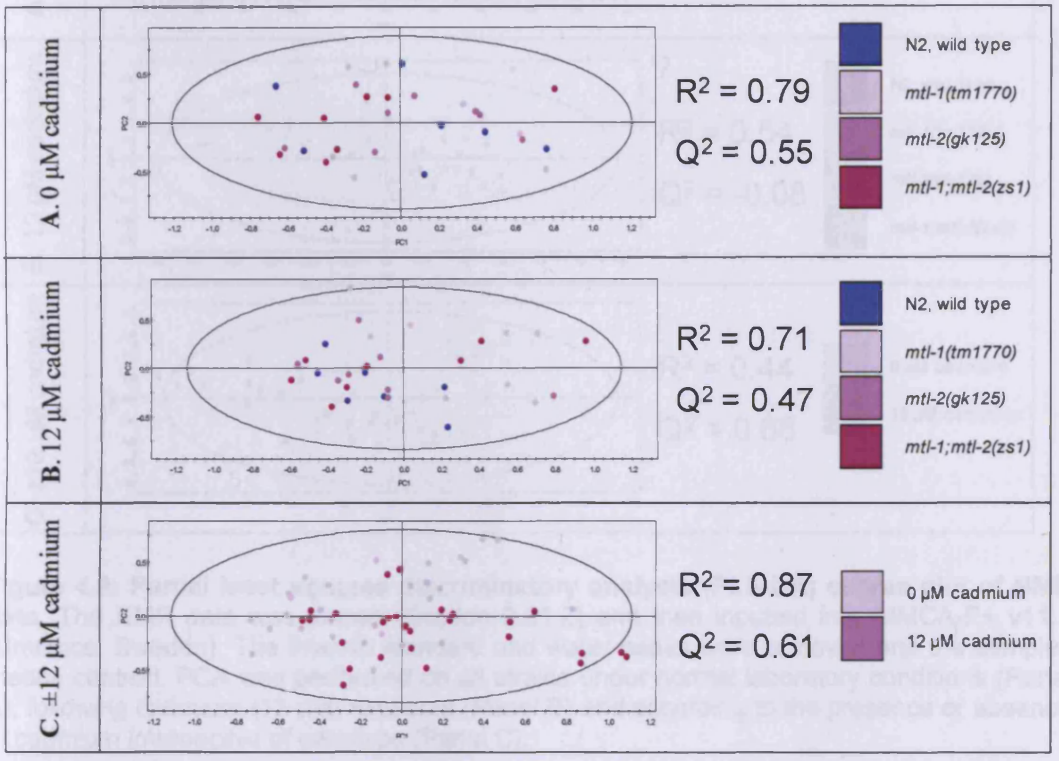

Figure 4.8: The principal component analysis (PCA) scores plots (PC1 vs PC2) for all samples. The NMR data was binned (Section 2.21.2) and then inputted into SIMCA-P+ v11.5 (Umetrics, Sweden). The internal standard and water peaks were removed and the samples means centred. PCA was performed on all nematode strains under normal laboratory conditions (Panel A), following cadmium (12 µM) exposure (Panel B) and grouped according to the presence or absence of cadmium irrespective of genotype (Panel C).

Partial least squares discrimination (PLS-DA) is a regression extension of PCA for a supervised analysis (Atherton *et al.* 2008). PLS-DA in a model which provides the means to visualise relationships within a data set based on previous knowledge of the biological properties of the data (van der Werf *et al.* 2005). Using the same groupings as in the PCA plots, PLS-DA scores plots are shown in Figure 4.9.

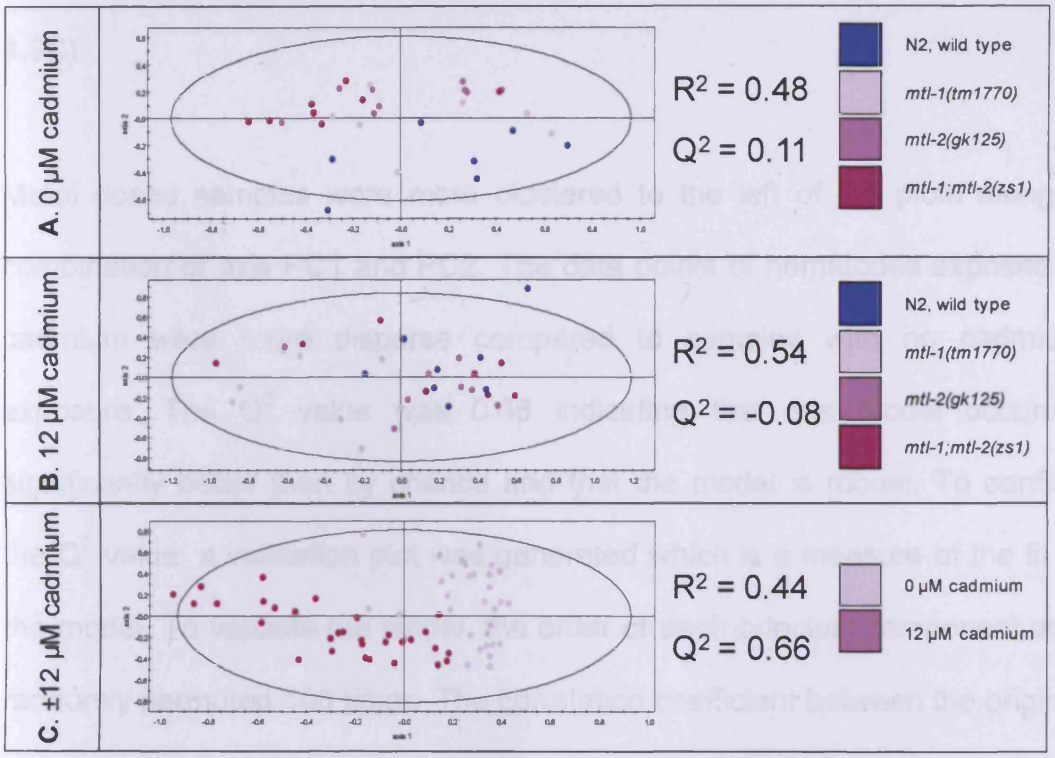

Figure 4.9: Partial least squares discriminatory analysis (PLS-DA) scores plot of NMR data. The NMR data was binned (Section 2.21.2) and then inputted into SIMCA-P+ v11.5 (Umetrics, Sweden). The internal standard and water peaks were removed and the samples means centred. PCA was performed on all strains under normal laboratory conditions (Panel A), following cadmium (12 µM) exposure (Panel B) and according to the presence or absence of cadmium irrespective of genotype (Panel C).

In the absence of cadmium, the four sample groups clustered only to a small degree, particularly N2 (bottom right of the plot) and *mtl-1;mtl-2(zs1)* to the top left of the plot (Figure 4.9A). The Q^2 value is a measure of the robustness of the model and also an indication of how likely the model would occur by chance. In Figure 4.9A, the genotypes in the absence of metal exposure had a Q^2 value of 0.11. The low Q^2 value indicated that the clustering of this data had occurred only slightly better than by chance and was not a robust model. Similarly, the Q^2 value of cadmium exposed samples was -0.08 (Figure 4.9B) and this model of separation was not robust. In contrast there was distinct

separation of data based on the presence or absence of cadmium (Figure 4.9C).

Metal dosed samples were more clustered to the left of the plots along a combination of axis PC1 and PC2. The data points of nematodes exposed to cadmium were more disperse compared to samples with no cadmium exposure. The Q^2 value was 0.66 indicating that this model occurred significantly better than by chance and that the model is robust. To confirm the Q^2 value, a validation plot was generated which is a measure of the fit of the model. To validate the model, the order of each principal component was randomly permuted 100 times. The correlation coefficient between the original and the permutated principal components were plotted against the cumulative R^2 and Q^2. The intercept of the regression line is the measure of validity and over-fit of the model and should be close to zero (Blaise *et al.* 2007). The validation plot of the genotypes in the presence and absence of cadmium show a regression line with the intercept at 0.15 for R^2 and a Q^2 intercept of -0.2 (Figure 10). The values are very close to zero and therefore confirms that the model is true and not due to chance. Thus there are significant differences in the samples, irrespective of genotype, following cadmium exposure.

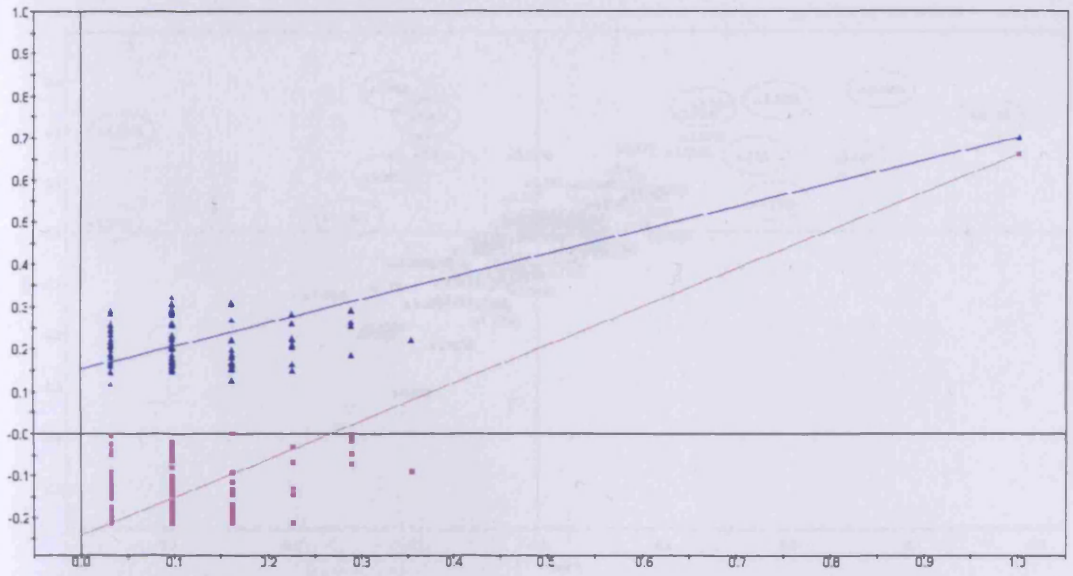

Figure 4.10: Validation plot from the supervised analysis based on the grouping according to metal exposure. Taken from the PLS-DA plot of genotypes exposed to control and cadmium supplemented environments, each principal component is permutated 100 times. The regression line for R^2 (blue) and Q^2 (purple) are plotted. The closer the y-axis intercept is to zero means a more valid model with less over-fit (Blaise *et al.* 2007).

Using the degree of association between the original variables and the direction of the model, the importance of each variable can be plotted as the variable loadings (Bailey *et al.* 2003). In the loadings plot each point corresponds to a spectral peak. The loadings plot from the samples separated on the basis of cadmium exposure can be analysed to identify which compounds are causing the formation of the two clusters in Figure 4.9C. Three metabolites were identified from the PLS-DA loadings plot with a correlation to the scores plot. Betaine had a negative correlation to scores along the PC1 while trehalose had a positive correlation with scores on axis PC2. Cystathionine was identified from the loadings plot as having a positive correlation to sores on both PC1 and PC2 axis (Figure 4.11). Thus, the presence of cystathionine is a major contributor to the clustering pattern observed in Figure 4.9C.

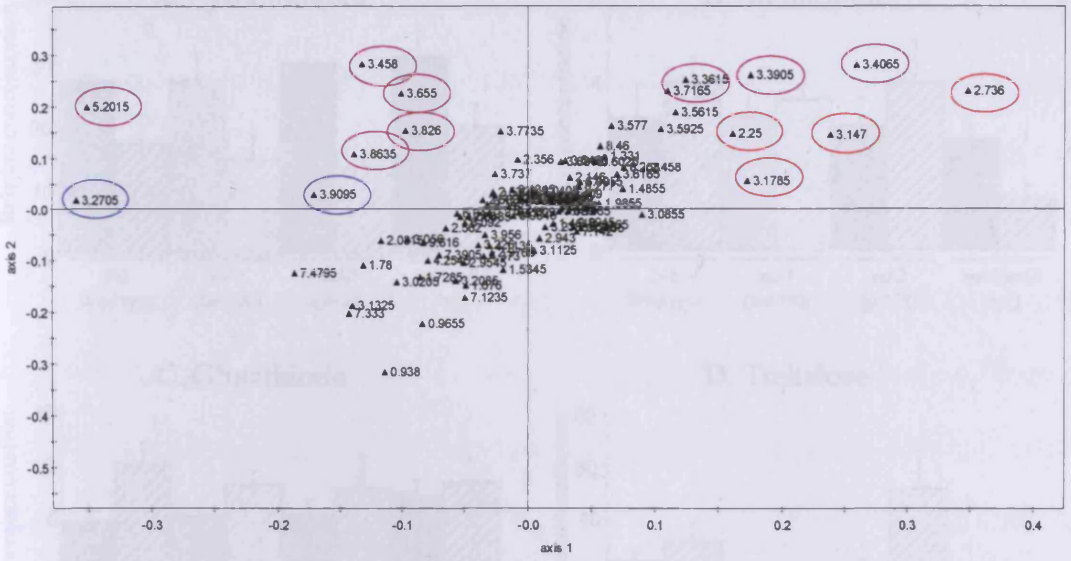

Figure 4.11: Loadings plot from the PLS-DA analysis of all genotypes in the presence and absence of cadmium. Those points highlighted in blue are betaine (points 3.2705 and 3.5095) and have a negative correlation to PC1, purple are trehalose with a positive correlation to PC2. Cystathionine (red) has a positive correlation of a combination of PC1 and PC2 which strengthens the argument that this metabolite is causing the separation of genotypes following cadmium exposure.

4.3.5 Metabolite concentrations

Following the positive identification of compounds which changed as a result of cadmium exposure, individual metabolites were identified and quantified using the software package NMR Suite 5.0 (Chenomx, Edmonton, Canada). In addition to cystathionine, betaine and trehalose which were identified from the PLS-DA loadings plot, glutathione, alanine, glutamate, succinate and methionine were also identified and quantified in all spectra. In all cases, the NMR suite 5.0 provides a method to fit spectra for individual reference metabolites to the sample spectra.

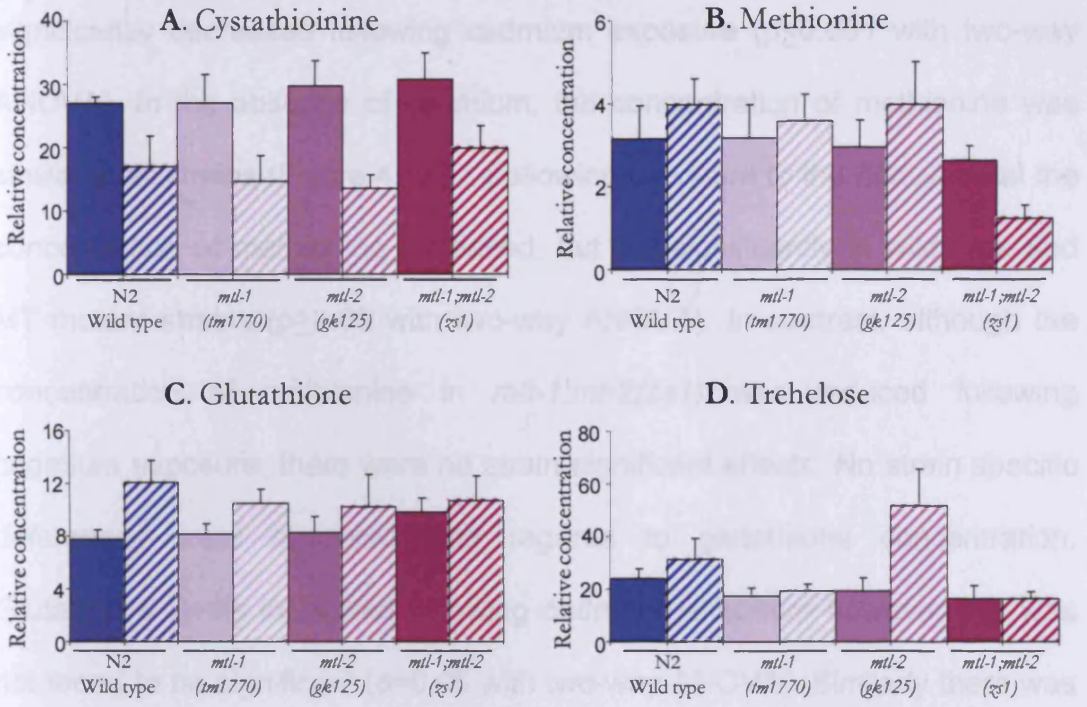

Figure 4.12: Graphs to show metabolite concentrations of cystathionine (Panel A), methionine (Panel B), glutathione (Panel C) and trehalose ((Panel D) identified from NMR spectra. The compounds were all identified and quantified using the NMR Suite 5.0 (Chenomx, Edmonton, Canada). The relative concentrations of metabolites were normalised to an average of the internal concentrations of succinate, alanine, betaine and glutamate. The error bars are SEM (n was 8 in all samples). Filled bars are non-metal exposures and hashed bars are nematodes exposed to 12 µM cadmium. The control, wild type strain is blue, the strains containing the genotype *mtl-1(tm1770)* are pale purple, *mtl-2(gk125)* are light purple and *mtl-1;mtl-2(zs1)* are dark purple. Note the difference in scale. The ANOVA two-way analysis indicates that in all there was no significant interaction between genotype and cadmium exposure. Only cystathionine showed a significant response in relative concentration based on cadmium exposure.

The metabolites alanine, betaine, glutamate and succinate did not appear to fluctuate following cadmium exposure. Using the Chenomx software this was confirmed and as a result the average of the four metabolites could be used as an internal control. The quantification of cystathionine, methionine, glutathione and trehalose was then normalised to the average of the internal controls and plotted as a ratio in Figures 4.12A-D. No strain specific differences were observed in the cystathionine levels in the presence or

absence of cadmium (Figure 4.12A). The concentration of cystathionine was significantly decreased following cadmium exposure ($p \leq 0.001$ with two-way ANOVA). In the absence of cadmium, the concentration of methionine was similar in all strains (Figure 4.12B). Following exposure to the heavy metal the concentration of methionine increased, but not significantly in wild type and MT mutant strains ($p \geq 0.05$ with two-way ANOVA). In contrast, although the concentration of methionine in *mtl-1;mt-2(zs1)* was reduced following cadmium exposure, there were no strain significant effects. No strain specific differences were observed with regards to glutathione concentration. Glutathione levels increased following cadmium exposure however this was not found to be significant ($p=0.06$ with two-way ANOVA). Similarly there was not a significant change in trehalose concentration following exposure to cadmium compared to basal levels. There was a genotype effect on trehelose concentration ($p \leq 0.05$ with two-way ANOVA) as a consequence of the high concentration of trehalose in *mtl-2(gk125)*.

4.3.6 Mass chromatograms

To attempt to identify the presence of phytochelatins in *C. elegans* metabolite samples, UPLC/MS was implemented. The chromatographic separations were performed on a Water AQUITY™ (Waters, USA) with a 26 minute gradient (Section 2.22.1). The data obtained was inputted into the freely available software XCMS and baseline normalised (Section 2.22.2) (Smith *et al.* 2006). Peaks obtained between 1.5 and 17 minutes were analysed as outside this region few metabolites were detected. In addition, at 18 or more minutes the re-equilibration of the column occurred with a distinctive high

organic solvent peak obscuring any further metabolite peaks. Samples were analysed in positive and negative modes. Peaks corresponding to PCs were identified only in the positive mode and therefore only these chromatograms are shown. The total ion chromatograms were baseline normalised.

A representative chromatogram from each strain (N2 wild type, *mtl-1(tm1770)*, *mtl-2(gk125)* and *mtl-1;mtl-2(zs1)*) in the absence of cadmium is shown in Figure 4.13. In the absence of cadmium the chromatograms of all samples were similar. In the chromatograms of the strains with the genotypes *mtl-2(gk125)* and *mtl-1;mtl-2(zs1)*, a peak at 7.5-8 minutes retention was prominent but in the *mtl-1* deletion mutant and wild type strains the amplitude of this peak was very low and almost absent in the case of *mtl-1(tm1770)*. The same was true of the series of peaks at 4.5-5 minutes. The retention time 11.5-13 minutes contained a series of peaks which had different amplitudes and ratios in *mtl-2(gk125)* and *mtl-1;mtl-2(zs1)* were more similar.

Figure 4.14 shows a representative chromatogram of each genotype strain following exposure to cadmium (12 µM). The retention time between 2-10 minutes was highly variable, with peaks present in *mtl-1(tm1770)* but not in the wild type and the same peaks had a lower amplitude in the *mtl-2* deletion *C. elegans* strains. In addition there was a significant peak observed in all strains with the exception of N2 at 11 minutes retention (Figure 4.14). There was very little difference in the pattern of peaks between the *mtl* deletion genotypes at the retention time 11-17 minutes.

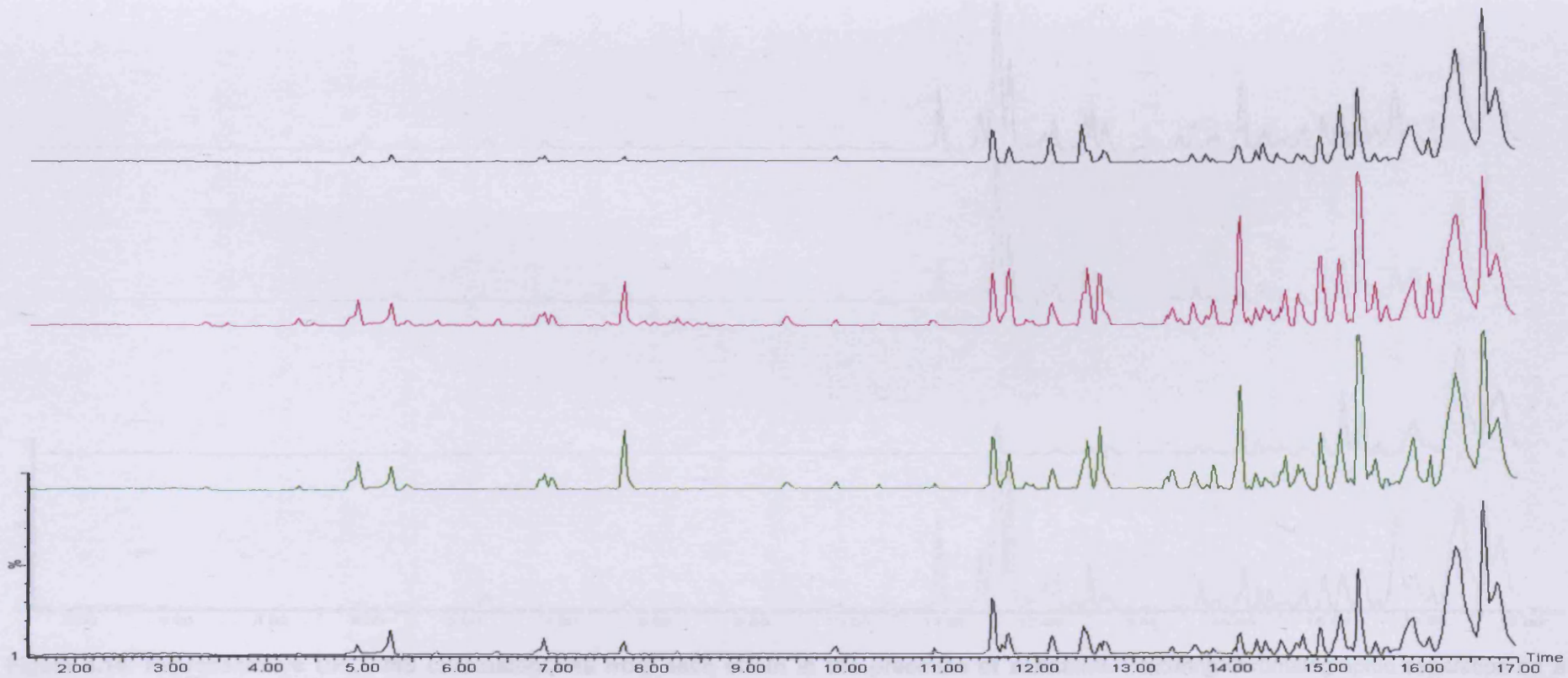

Figure 4.13: Representative UPLC-MS chromatograms from each strain in the absence of cadmium. Following chromatographic separation on a Waters ACQUITY^{TM} (Waters, USA) samples were inputted into XCMS for analysis. The chromatograms with the retention time of 1.5-17 minutes were baseline normalised in the positive mode with the y axis as a percentage of the concentration of the most intense ion in each scan. The bottom chromatogram in dark blue is *mtl-1;mtl-2(zs1)* followed by N2 wild type (green), *mtl-2(gk125)* (purple) and *mtl-1(tm1770)* (black) at the top.

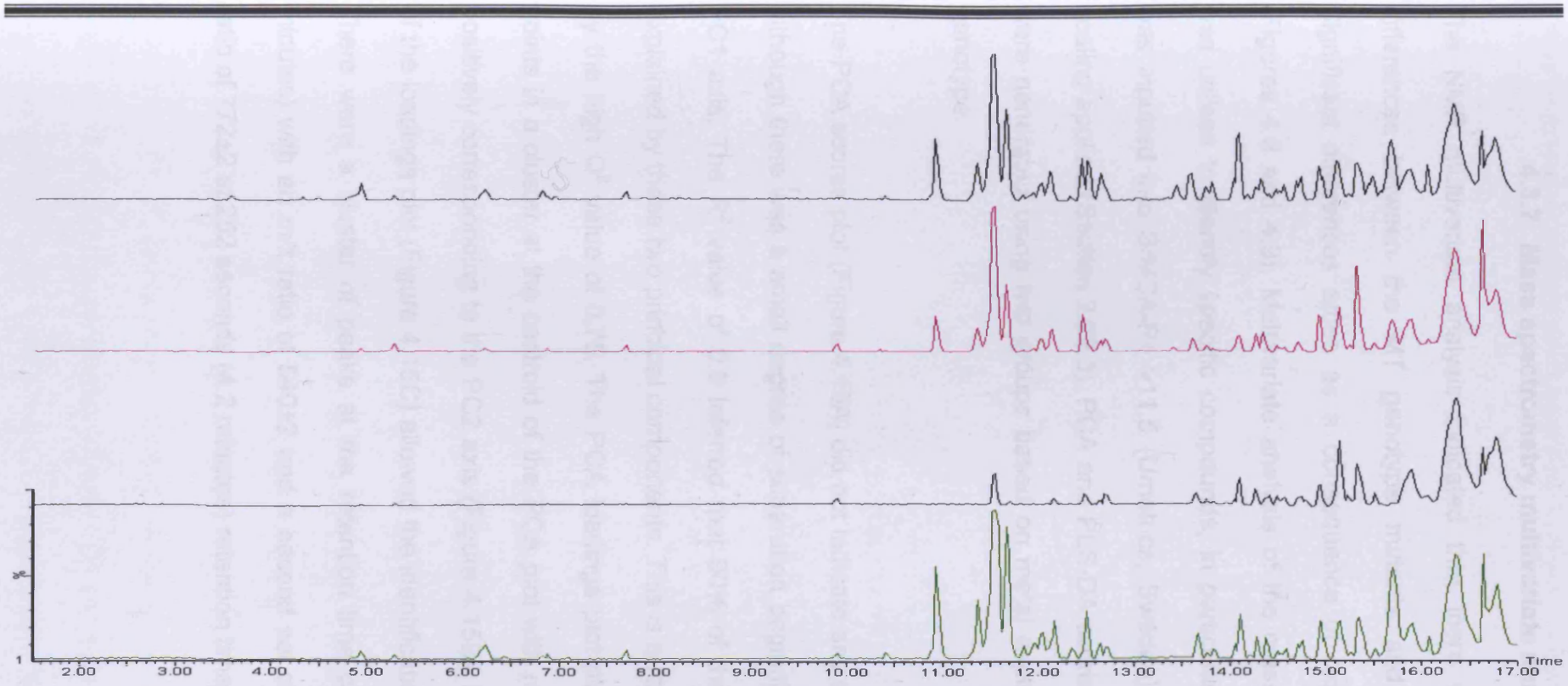

Figure 4.14: Representative UPLC-MS chromatograms from each strain in the presence of cadmium. Following chromatographic separation on a Waters ACQUITY^{TM} (Waters, USA) samples were inputted into XCMS for analysis. The chromatograms with the retention time of 1.5-17 minutes were baseline normalised in the positive mode with the y axis as a percentage of the concentration of the most intense ion in each scan. The bottom chromatogram in dark blue is *mtl-1;mtl-2(zs1)* followed by N2 wild type (green), *mtl-2(gk125*) (purple) and *mtl-1(tm1770*) (black) at the top.

4.3.7 Mass spectrometry multivariate analysis

The NMR multivariate analysis indicated that there were no significant differences between the MT genotype mutants and wild type strains. Significant differences arose as a consequence of exposure to cadmium (Figures 4.8 and 4.9). Multivariate analysis of the mass spectrometry data was utilised to identify specific compounds, in particular PC. The raw data was inputted into SIMCA-P+ v11.5 (Umetrics, Sweden) and mean centred scaling applied (Section 2.22.3). PCA and PLS-DA scores and loadings plots were generated using two groups based on metal exposure irrespective of genotype.

The PCA scores plot (Figure 4.15A) did not indicate any significant clustering, although there was a small degree of separation beginning to form along he PC1 axis. The R^2 value of 0.9 inferred that 90% of the variance could be explained by these two principal components. This is a robust model as given by the high Q^2 value of 0.75. The PCA loadings plot placed the majority of points in a cluster at the centroid of the PCA plot with more disperse points positively corresponding to the PC2 axis (Figure 4.15B). Enhancing the scale of the loadings plot (Figure 4.15C) allowed the identification of specific peaks. There were a cluster of peaks at the retention time of 212 seconds (3.5 minutes) with an *m/z* ratio of 540±2 and a second set of peaks with an *m/z* ratio of 772±2 at 252 seconds (4.2 minutes) retention time.

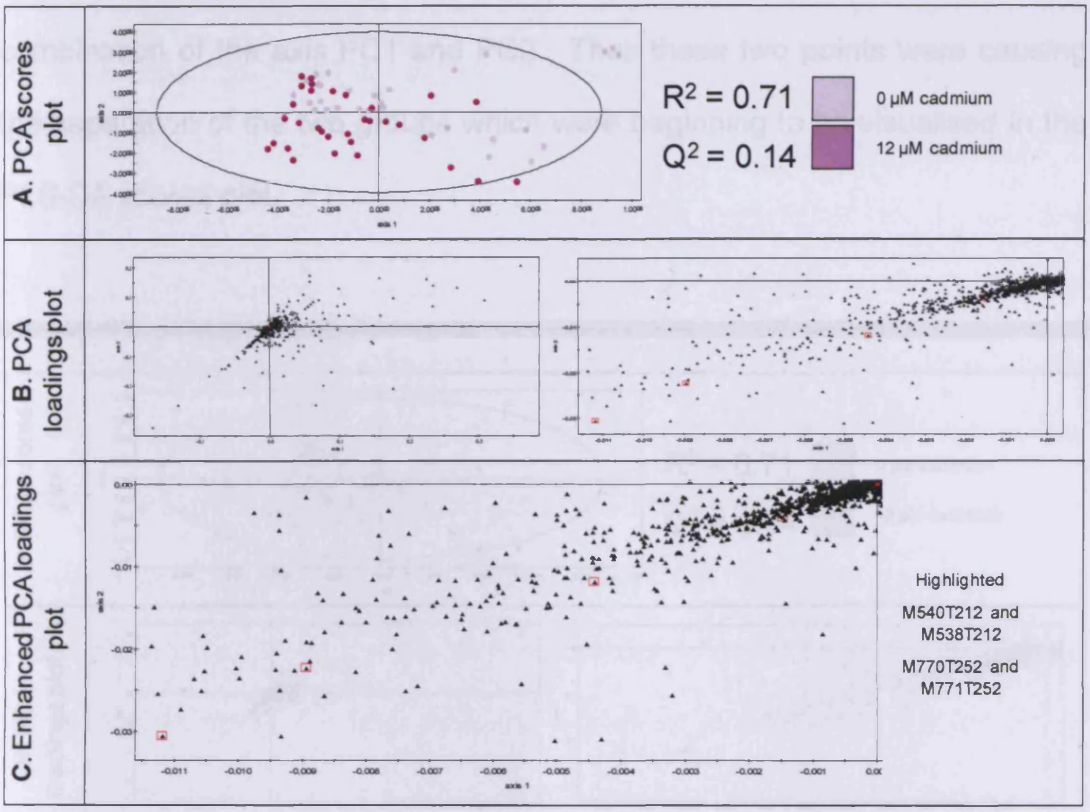

Figure 4.15: The principal component analysis (PCA) plots (PC1 vs PC2) in the presence and absence of cadmium. The data was normalised in XCMS (Section 2.212.2) and then inputted into SIMCA-P+ v11.5 (Umetrics, Sweden). The samples were means centred. PCA was performed on all genotypes grouped according to heavy metal exposure (Panel A). The loadings plot in Panel B shows most points clustered around the centroid. When this was enhanced as in Panel C, a series of points were indicated which correspond to an *m/z* ratio of 540 and 538 at 212 seconds and 770 and 772 at 252 seconds.

Supervised analysis was performed on the same data set as shown in Figure 4.16. There appeared to be two clusters forming from the PLS-DA scores plot along a combination of the PC1 and PC2 axis (Figure 4.16A). More than two thirds (71%) of the variance was explained by this model as indicated by the R^2 value. The Q^2 value was 0.14 indicating that this is not a robust model. The subsequent loadings plot was similar to that of the PCA loadings plot whereby there majority of points were clustered around the centroid with some disperse points along a combination of axis PC1 and axis PC2 (Figure 4.16B). When enhanced (Figure 4.16C) the same mass peaks were identified at 212

and 252 seconds retention time were identified with negative correlation of a combination of the axis PC1 and PC2. Thus these two points were causing the separation of the two groups which were beginning to be visualised in the PLS-DA scores plot.

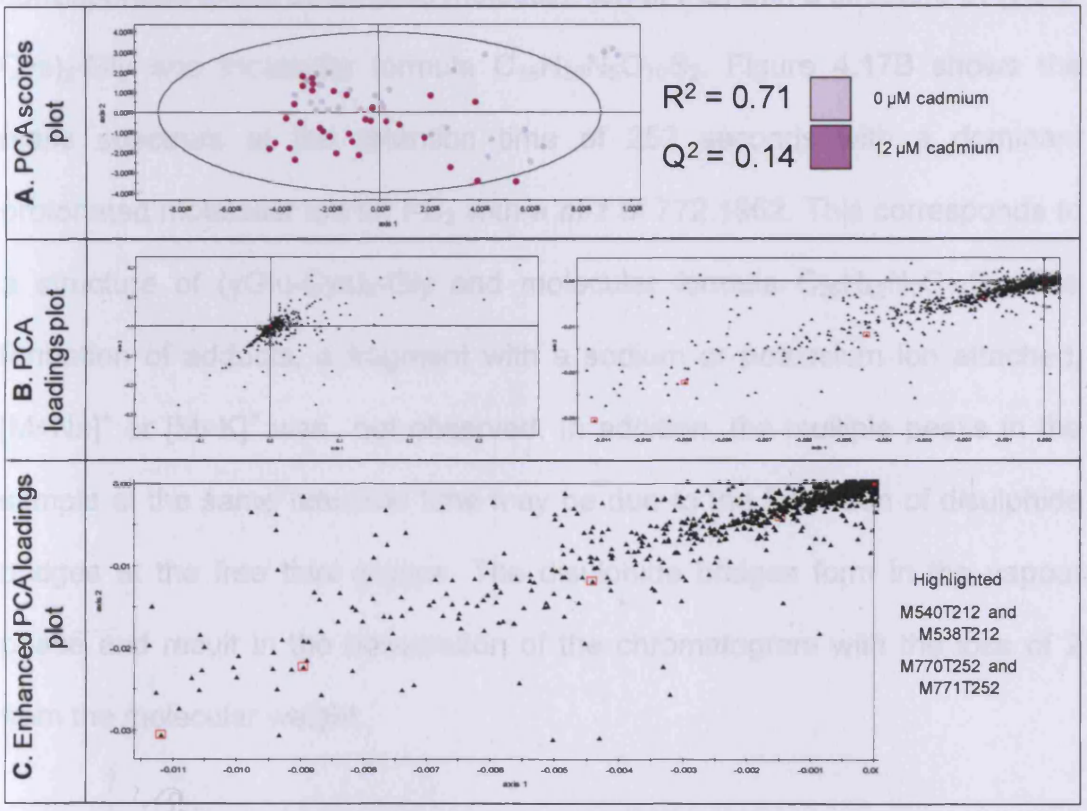

Figure 4.16: The partial least squares discrimination analysis (PLS-DA) plots in the presence and absence of cadmium. The data was normalised in XCMS (Section 2.212.2) and then inputted into SIMCA-P+ v11.5 (Umetrics, Sweden). The samples were means centred. PCA was performed on all genotypes grouped according to cadmium exposure (Panel A). The loadings plot in Panel B shows most points clustered around the centroid. When this was enhanced as in Panel C, a series of points were indicated which correspond to an *m/z* ratio of 540 and 538 at 212 seconds and 770 and 772 at 252 seconds.

4.3.8 Phytochelatin identification

Mass chromatograms of the peaks at retention times 212 and 252 seconds are shown in Figures 4.17A and 4.17B respectively. These compounds were only identified in the positive mode data, as protonated molecule ions ($[M+H]^+$). The dominant peak with an *m/z* of 540.142 in Figure 4.17A corresponded to the protonated molecular ion of PC_2 with a structure of $(\gamma Glu\text{-}Cys)_2\text{-}Gly$ and molecular formula $C_{18}H_{30}N_5O_{10}S_2$. Figure 4.17B shows the mass spectrum at the retention time of 252 seconds with a dominant protonated molecular ion for PC_3 with a *m/z* of 772.1962. This corresponds to a structure of $(\gamma Glu\text{-}Cys)_3\text{-}Gly$ and molecular formula $C_{26}H_{42}N_7O_{14}S_3$. The formation of adducts, a fragment with a sodium or potassium ion attached, $[M+Na]^+$ or $[M+K]^+$ was not observed. In addition, the multiple peaks in the sample at the same retention time may be due to the formation of disulphide bridges at the free thiol groups. The disulphide bridges form in the vapour phase and result in the observation of the chromatogram with the loss of 2 from the molecular weight.

A.

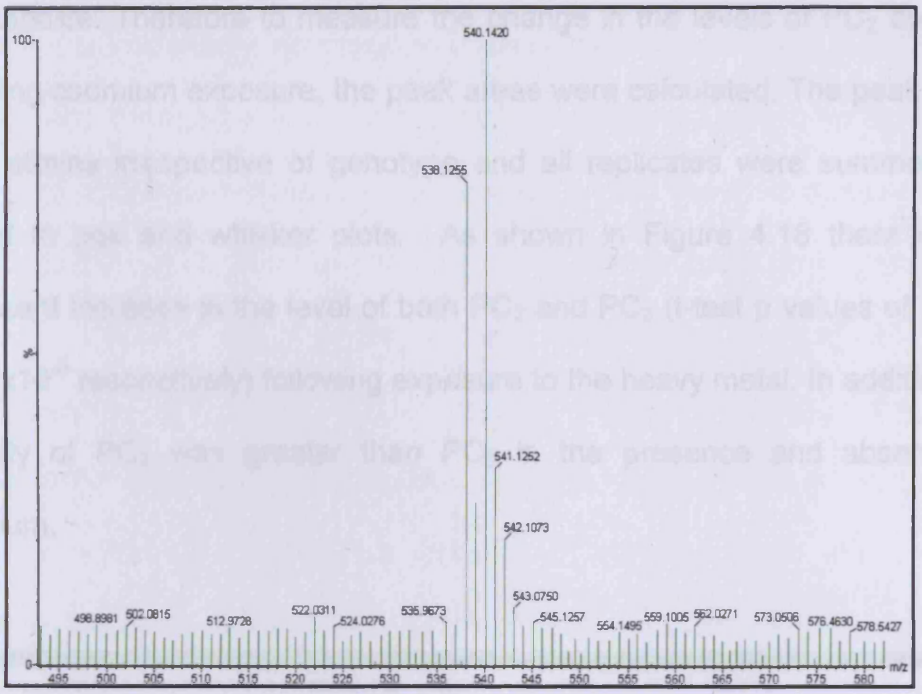

B.

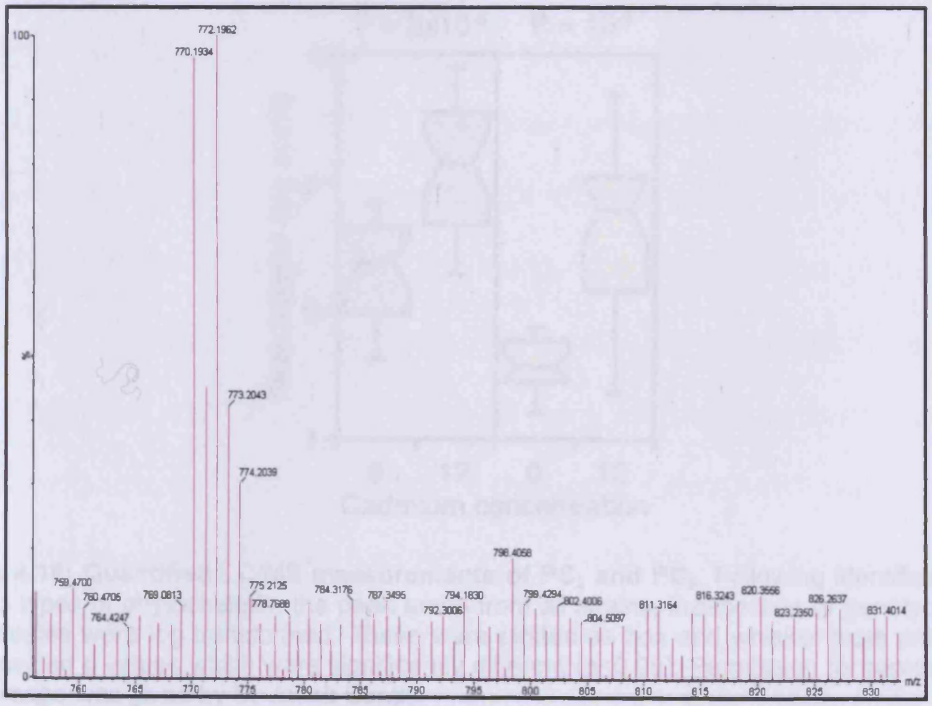

Figure 4.17: Mass spectrum of PC_2 (Panel A) and PC_3 (Panel B) from a representative sample. Panel A shows the $[M+H]^+$ ion at *m/z* 540.1420 with the retention time of 212 seconds. This corresponds to a calculated molecular formula of $C_{18}H_{30}N_5O_{10}S_2$. At retention time 252 seconds, PC_3 came off the column. Mass spectrum of PC_3 (Panel B) shows the $[M+H]^+$ ion at *m/z* 772.1962. This corresponds to the formula $C_{26}H_{42}N_7O_{14}S_3$.

The peak areas of the chromatogram correspond to relative concentrations of a metabolite. Therefore to measure the change in the levels of PC_2 and PC_3 following cadmium exposure, the peak areas were calculated. The peak areas of all strains irrespective of genotype and all replicates were summed and plotted in box and whisker plots. As shown in Figure 4.18 there was a significant increase in the level of both PC_2 and PC_3 (t-test p values of $3x10^{-8}$ and $1x10^{-9}$ respectively) following exposure to the heavy metal. In addition the quantity of PC_2 was greater than PC_3 in the presence and absence of cadmium.

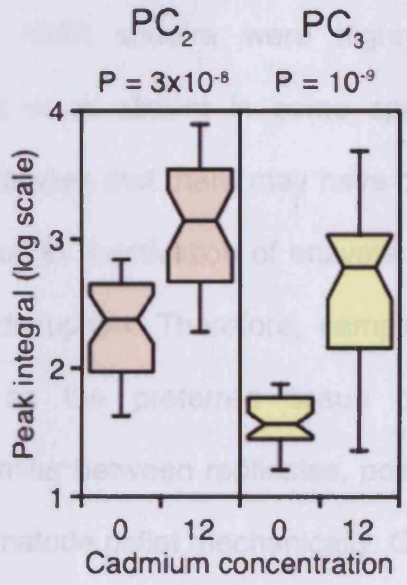

Figure 4.18: Quantified LC/MS measurements of PC_2 and PC_3. Following identification of the two types of phytochelatin, the peak areas from all strains, irrespective of genotype, and all replicates were log transformed. These were plotted as box and whisker plots and the t-test provided p values which were significantly different ($p \leq 0.05$). Permission for reproduction of the image was given by Dr Jacob Bundy.

4.4 Discussion

There is no universally accepted extraction method for NMR metabolomic analysis and consequently a suitable extraction method had to be optimised. Three homogenisation methods were chosen to find the most suitable tissue disruption technique. Manual grinding of the frozen pellet in a pestle and mortar was tested as this is a well established method of tissue homogenisation (Lin *et al.* 2007). However, manual grinding of the pellet proved to be unreliable in terms of sample to sample reproducibility. This arose as a result of non-uniform grinding of samples or as the result of inadvertent thawing of sample. In addition manual grinding was highly labour intensive. Repeated freeze/thaw was employed as a second extraction method. Although the NMR spectra were highly reproducible between replicates, some peaks were absent in some spectra, particularly in the aliphatic region. This indicates that there may have been some change in the metabolome possibly due to reactivation of enzyme during a thawing step or due to inefficient cell disruption. Therefore, sample disruption using glass beads was selected as the preferred tissue homogenisation method. Homogenisation was similar between replicates, possibly due to the use of a vortex to disrupt the nematode pellet mechanically. Glass bead extraction had a high reproducibility between samples with a good range of peaks throughout the spectra. In addition, the glass bead method was simple and less labour intensive than the other methods tested and one which could be easily adapted for small or large sample sizes.

The solvent used in extractions is important and the choice depends upon the metabolites of interest. Organic solvents such as chloroform are used to extract hydrophobic metabolites while aqueous solvents such as methanol and acetonitrile are preferred to extract hydrophilic compounds (Lin *et al.* 2007; Sze and Jardetzky 1994). There was little apparent difference between the solvents tested and the metabolic profile. The exception was ethanol extraction where the presence of a large glycerol peak masked metabolites. Although the chloroform/methanol extraction method had previously been used for *C. elegans* NMR analysis (Atherton *et al.* 2008) this technique proved to be time consuming and labour intensive. Methanol extractions were reproducible and provided a range of peaks throughout the spectrum. Consequently, the methanol solvent based glass bead exaction method was chosen as the most suitable method of metabolite extraction from *C. elegans*.

The aim of the investigation was to observe the change in global metabolite concentration following cadmium exposure between wild type and MT mutants (strains containing the genotypes *mtl-1(tm1770), mtl-2(gk125)* and *mtl-1;mtl-2(zs1)*). No major differences were observed between wild type and MT mutants in both the unsupervised PCA and supervised PLS-DA scores plots. Upon analysing the data grouped according to cadmium exposure (two groups) two significant clusters formed. The high Q^2 value obtained in the PLS-DA and validation plots indicated that this was a robust result. Cystathionine was a metabolite with a positive correlation between the loadings plot and the scores plot and was the cause of the observed pattern of clustering. Betaine and trehalose were also identified form the loadings

plot. The relative concentration of these metabolites as well as glutathione, succinate, alanine, glutamate and methionine were calculated following deconvolution and quantification using the software Chenomx (Section 2.21.2). Following identification of the metabolites, the values were normalised. TSP could not be used for normalisation of metabolite concentration for two reasons. Firstly, the number of nematodes per replicate varied although all were within the range 100,000 to 200,000. Also, normalisation by TSP does not take into account the error arising from the manual fitting of the reference peaks to the spectra. Consequently the concentrations of the four metabolites of interest (cystathionine, trehalose, methionine and glutathione) were measured and normalised by an average of four control metabolites (succinate, alanine, glutamate and betaine). The use of multiple control metabolites (ideally three or more) provide a more accurate and reliable normalisation (Vandesompele *et al.* 2002). Following normalisation, there was no significant change in the concentration of glutathione, methionine or trehelose while there was a significant decrease in cystathionine concentration following cadmium exposure. The only metabolite that was significantly affected by genotype was trehelose. This may be as a result of the increase in trehelose quantified in *mtl-2(gk125)*. It is unlikely that this is a true value based on the relative concentration of the metabolite in other strains and further extractions would be required to confirm this.

Glutathione concentration increased, but not significantly following cadmium exposure. An increase in glutathione would be expected as the metabolite is an antioxidant (Mendoza-Cózatl *et al.* 2005; Sugiura *et al.* 2005; Sura *et al.*

2006). The non-significant rise in the metabolite indicates that it may not be a significant mechanism of cadmium detoxification. Although there were no significant strain specific effects ($p \geq 0.05$), the non-cadmium stimulated double MT knockout genotype had a higher basal concentration of glutathione than other strains. This indicates that glutathione may be already up regulated in *C. elegans* in the absence of MTs. As MTs are able to protect against oxidative damage, nematodes with no MT may up regulate glutathiones to compensate (Moilanen *et al.* 1999; Palmiter 1998).

There was a significant decrease in cystathionine concentration in all strains following cadmium exposure. Cystathionine is the key intermediate in the transsulfuration pathway, a reaction by which cysteine and methionine can be generated (Rao *et al.* 1990; Sugiura *et al.* 2005). It is an important pathway as it is the only process by which cysteine, a non-essential amino acid is generated and requires the use of the essential amino acid methionine (Houghton and Cherian 1991). The transsulfuration pathway is shown in Figure 4.19 and involves the two key enzymes cystathionine-γ-lyase and cystathionine-β-synthase. It has been shown that cadmium causes a decrease in cystathionine levels in rat hepatocytes due to the inhibition of cystathionine-β-synthase (Sugiura *et al.* 2005). This was also thought to be the case in *C. elegans*. Cadmium can inhibit enzymes such as cystathionine-β-synthase as a result of the metal ions binding to free thiol [–SH] groups in the active site of the enzyme (Sura *et al.* 2006).

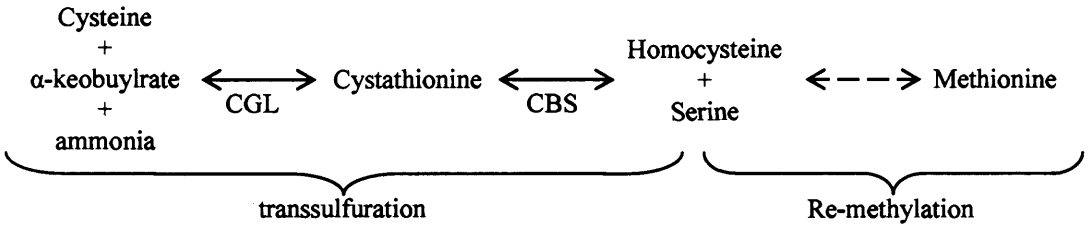

Figure 4.19: The transsulfonation and re-methylation pathway. The pathway is reversible (reverse transsulfonation). CGL is the enzyme cystathionine-γ-lyase and CBS is cystathionine-β-synthase. Cadmium is able to inhibit these enzymes by binding to –SH (thiol) groups at the active site and therefore preventing their mechanism of action. Adapted and redrawn from Mendoza-Cózatl *et al.* (2005) and Sugiura *et al.* (2005).

Following inactivation of cystathionine-β-synthase it would be expected that there would be a related increase in the concentration of cysteine. However in this experiment there was no observed change in cysteine levels. This was because cysteine was not detected during NMR spectral analysis. It is possible that cysteine peaks were masked by more prominent peaks and so the reference cysteine spectra could not be adequately assigned. Another possibility is that the concentration of cysteine in the nematode samples was below the detection limit of NMR. Although there would be an expected increase in cysteine the physiological concentration of the amino acid does not accumulate to levels greater than 0.2 mmol/litre in cells (Rao *et al.* 1990). If cysteine levels reach this threshold they are converted into proteins or degraded (Rao *et al.* 1990). The generation of cysteine rich proteins such as glutathiones, metallothioneins and phytochelatins may aid in the reduction of cysteine. In addition the presence of these proteins in excess would be beneficial as they are able to contribute to the reduction in oxidative stress and excess metal ions to reduce toxicity. The reduction in cadmium levels would therefore reactivate cystathionine-β-synthase.

Glutathione, a protein which can bind heavy metals, is synthesised by the action of γ-glutamylcysteine synthatase on cysteine and glutamate (Mendoza-Cózatl *et al.* 2005) as shown in Figure 4.20. By channelling excess generated cysteine into the formation of glutathione, the cysteine pool would be maintained at 0.2 mmol/l (Rao *et al.* 1990). However, glutathione is a rate limiting factor in its own generation (Rao *et al.* 1990). By channelling the newly generated glutathione into the synthesis of another protein the free glutathione pool remains constant and so there is no inhibition of the synthetase.

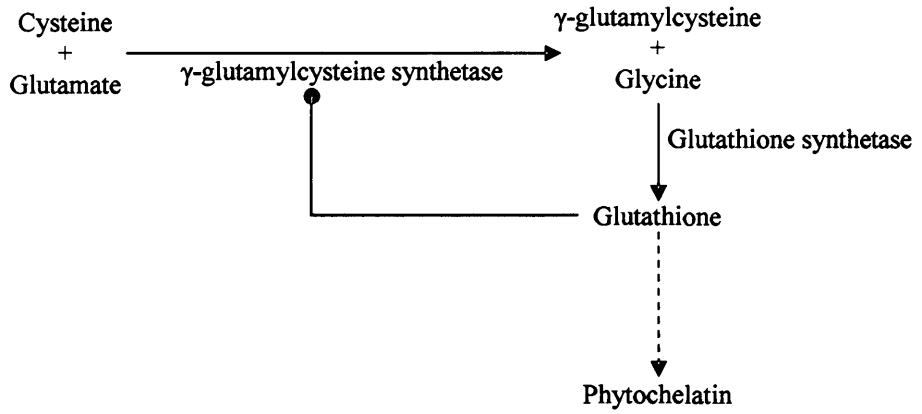

Figure 4.20: The generation of glutathione from cysteine. The rate limiting step in this pathway is glutathione by its inhibitory action on γ-glutamlycysteine sythetase. To prevent the shutting down of the pathway, glutathiones may be used in the generation of phytochelatins. Adapted from Mendoza-Cózatl *et al.* (2005).

Proteins, which glutathione could be a substrate for, are likely to be peptides which provide protection against heavy metal and free radical toxicity. One such protein is phytochelatin. The generation of the long chain polypeptide requires glutathione as it provides the metal ion requisite for the stimulation of the enzyme phytochelatin synthase (Clemens 2006). In addition glutathione is

cleaved to remove the glycine and the resulting dipeptide is used in the growing PC polypeptide (Clemens 2006).

To identify and quantify PC, UPLC/MS was performed. Two types of PC have been identified in *C. elegans* to date (Clemens *et al.* 2001; Vatamaniuk *et al.* 2001). In these previous studies, the *C. elegans* PC synthase gene, *pcs-1*, was cloned into *Schizosaccharomyces pombe.* The over-expression of *C. elegans pcs-1* in the yeast generated a large amount of PC following cadmium exposure which was extracted and purified prior to spectrometric analysis. In contrast the experiment described in this Chapter used metabolites extracted directly from *C. elegans* tissue and analysed by UPLC/MS. The subsequent PCA and PLS-DA scores analysis of the positive mode identified a strong separation of the samples grouped by cadmium exposure (71% variance was explained by two components). Analysis of the loadings plots identified multiple points which correspond to PC based on the previous mass spectrographic identification (Clemens *et al.* 2001; Vatamaniuk *et al.* 2001). Two mass regions had different retention times. A set of peaks at 212 seconds for *m/z* ratios of 538 and 540 and a second set of peaks at retention time of 252 seconds with mass ratios *m/z* 770 and 771 correspond to PC_2 and PC_3 respectively. No peaks corresponding to PCs were identified in negative mode. Thus, for the first time it was possible to identify the presence of PCs *in vivo* in *C. elegans.* The two species of PC both significantly increase in concentration following cadmium exposure. Notably PC_2 is present in greater concentrations than PC_3.

4.5 Conclusion

No differences were observed between *C. elegans* wild type and MT mutants. This indicated that there are very few metabolomic changes in these nematodes as a result of the different genotypes. However, whilst no differences were observed with regards to glutathione, methionine and trehalose concentrations, there was a significant decrease in cystathionine concentration upon cadmium exposure.

The proposed hypothesis states that the presence of cadmium decreases the concentration of cystathionine, a key intermediate in the transsulfuration pathway via the inhibition of cystathionine-β-synthase. Consequently cysteine levels are increased, but only to a physiological maximum of 0.2 mmol/l (Rao *et al.* 1990). To prevent the presence of excess cysteine, the amino acid is used in the synthesis of glutathione. To prevent the inhibition of glutathione production, the metabolite would be immediately channelled into the synthesis of proteins to prevent the feedback loop from stalling (Mendoza-Cózatl *et al.* 2005). One such protein that may be generated is PC. Measurements by mass spectrometry indicate that the concentrations of PC_2 and PC_3 increase significantly following cadmium exposure. This may be a result of cadmium bound glutathione providing the metal ion to stimulate phytochelatin synthase and glutathione acting as a substrate for PC synthesis.

This was the first time that PCs have been identified *in vivo* in *C. elegans*. Two PCs were isolated in the chromatograms based on previously published data for *C. elegans* PC (Clemens *et al.* 2001). One PC had a mass of 540.1

with a proposed structure of $(\gamma\text{-Glu-Cys})_2$-Gly. This was termed PC_2. A second PC, PC_3, with the structure $(\gamma\text{-Glu-Cys})_3$-Gly and a mass of 772.1 was also identified.

Metabolomics were initially performed as a non-targeted approach to identify phenotypic changes as a result of cadmium exposure on MT *C. elegans* mutants. This was an extremely useful approach to understand the changes occurring at the molecular level, although further research is required to confirm the proposed hypothesis. In general terms, the experiment was successful in providing an insight into the metal detoxification pathway of *C. elegans* and suggested that PC may play a more significant role in metal detoxification than previously thought.

CHAPTER FIVE

THE EFFECTS OF HEAVY METALS ON LIFE HISTORY TRAITS OF *C. ELEGANS*

5.1. Introduction

Following metabolomic analysis using NMR, no significant differences were apparent with regards to the metabolome between MT deletion strains (Chapter 4). However, there were differences based on exposure to cadmium irrespective of genotype. NMR studies provided the hypothesis that the presence of cadmium inhibited the transsulfuration pathway, ultimately resulting in an increase in cysteine which can be utilised in the generation of MT and PC, both cysteine rich proteins. Mass spectrometry quantified an increase in two types of PC following cadmium exposure. It can be inferred that in *C. elegans*, there are two metal detoxification systems (MT and PC). Other organisms, such as mangrove (Gonzalez-Mendoza *et al.* 2007), garlic (Zhang *et al.* 2005) and aquatic fungus (Jaeckel *et al.* 2005), express both MT and PC which act in conjunction during periods of metal stress. The yeast *Schizosaccharomyces pombe* also contains both metal detoxification systems (Gonzalez-Mendoza *et al.* 2007; Yu *et al.* 1994; Zhou and Goldsbrough 1994). In the case of *S. pombe* MT are used in preference over PC for metal detoxification unless the former is inhibited in some way (Yu *et al.* 1994; Zhou and Goldsbrough 1994). The elusive question is: to what extent are MT and PC utilised in metal detoxification?

MT and PC have been shown to bind zinc, copper and cadmium (Cobbett and Goldsbrough 2002; Klaassen *et al.* 1999; Palmiter 1998; Vallee 1995). Both proteins function in metal detoxification and in the case of MT also sequester reactive oxygen species. MT and PC are chelators which bind heavy metals during periods of metal excess and act as metal donors during metal depleted conditions to maintain physiological concentrations (Prasad 1985; Vallee 1995). *C. elegans* expresses two isoforms of MT and a functional PC synthase. It is known that *C. elegans* MT is required for metal detoxification however the function of PC synthase generated PC in metal detoxification is not yet fully known (Freedman *et al.* 1993; Swain *et al.* 2004; Vatamaniuk *et al.* 2001; Vatamaniuk *et al.* 2005). Thus the study of the phenotypes of mutant nematodes exposed to essential and non-essential heavy metals will provide an indication of how MT and PC contribute to metal detoxification.

5.2. Aims

The main aim was to study the effects of essential metals (copper and zinc) and a non-essential heavy metal (cadmium) on life history traits of *C. elegans* using the end points brood size and lifespan. Growth throughout development was also monitored. The strains used in this study were the wild type Bristol N2, the MT mutant genotypes *mtl-1(tm1770)*, *mtl-2(gk125)* and *mtl-1;mtl-2(zs1).* In addition, phytochelatin synthase mutants, namely *pcs-1(tm1748)* and *mtl-1;mtl-2;pcs-1(zs2)*, were used.

5.3. Results

5.3.1. Metal content of media and nematodes

The quantity of trace metals within control and metal dosed media was assessed to confirm the specific concentration of cations experienced by the nematodes. Agar samples were sent to Dr Mark Hodson at Reading University for analysis using inductively coupled plasma optical emission spectrometry (ICP/OES) (Section 2.8.1). The concentrations of the essential copper and zinc ions present in the Bactoagar (Becton, Dickenson and Company) are stated to be less than 0.001% with no detectable cadmium. Following nitric acid digestion of the control nutrient source, NGM, the basal level of cadmium and copper was quantified to be below 0.1 mg/kg and zinc levels 0.42 mg/kg (Table 5.1).

NGM Supplement	Cd mg/kg	Cd µM	Cu mg/kg	Cu µM	Zn mg/kg	Zn µM
None	<0.02	0.11	<0.08	0.22	0.42	1.49
12 µM Cd	2.21	12.08	<0.02	0.15	0.08	0.48
190 µM Cu	<0.02	0.11	24.77	184.24	0.18	1.97
160 µM Zn	<0.02	0.11	<0.03	0.22	23.56	145.93
500 µM BCS	<0.01	0.05	<0.02	0.15	0.08	0.51

Table 5.1: The absolute metal concentration of media. The metal concentration was determined by measuring the nitric acid digested fraction with coupled plasma optical emission spectrometry (ICP/OES) (Section 2.8.1). Media was supplemented in the liquid phase with the nominal concentration of metal or chelator. A sample of agar (0.5 g) was dissolved in nitric acid and digested overnight at room temperature. Samples were heated to 60°C for 3 hours and then incubated at 110°C for 6 hours. The sample was diluted prior to running on the ICP/OES. Analysis was undertaken by Dr Mark Hodson (Reading University, UK).

ICP/OES confirmed that the measured exposure cadmium dose was in extremely good agreement with the nominal concentration of cadmium at 12

µM. There were trace levels of copper and zinc present in the cadmium seeded NGM agar, however, these are within the range expected from the basal NGM. The nominal concentration of copper and zinc dosed plates was 190 µM while the ICP/OES quantified concentration was 184 µM and 146 µM respectively. Bathocuprinedisulfonic acid (BCS) was supplemented to NGM to act as a copper chelator generating a copper deficient environment. The copper concentration in the nitric acid digested sample was 0.15 µM which was lower than the concentration of copper in non-supplemented NGM.

The concentration of metal ions associated with the nematodes, after being maintained on the range of metal supplemented media for 48 hours, was assessed to determine how genotype and metal exposure are related. A known quantity of nematodes was collected, washed and nitric acid hydrolysed (Section 2.8.2). Metal concentration was measured by atomic absorption spectrophotometry (AAS) using a graphite furnace (41102L, Perkin Elmer, USA) and expressed per 1000 individuals or µg/l. Unfortunately, zinc levels in all samples were below the detection limit of the furnace and therefore could not be quantified. The average concentration of cadmium observed in control (N2) and the mutant strains *mtl-1(tm1770)*, *mtl-2(gk125)* and *mtl-1;mtl-2(zs1)*, maintained on control media was below the detection limit of the technique, approximately 0.04 µM/1000 nematodes (Figure 5.1A). However, in all strains cadmium accumulated in the nematodes to a concentration of 0.36 µM/1000 nematodes following a 48 hour exposure to 12 µM of cadmium. No strain specific differences in cadmium accumulation were observed. The strains containing the genotypes *pcs-1(tm1748)* and

mtl-1;mtl-2;pcs-1(zs2) were not measured for cadmium as these strains did not survive on cadmium dosed NGM.

A.

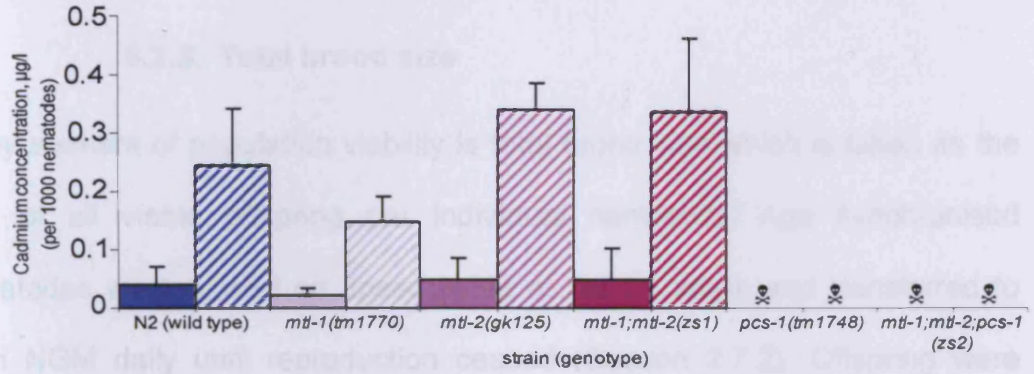

B.

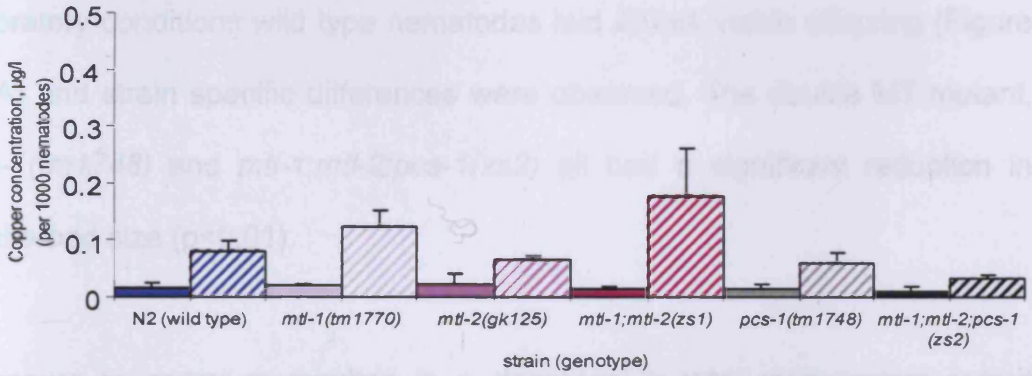

Figure 5.1: Nematode associated concentrations of cadmium (Panel A) and copper (Panel B) as determined by graphite furnace spectrophotometry (41102L Perkin Elmer, Waltham Massachusetts, USA). Wild type N2 (blue) nematodes together with single mutants *mtl-1(tm1770)*(pink), *mtl-2(gk125)* (mauve) and *pcs-1(tm1748)* (grey), the double mutant *mtl-1;mtl-2(zs1)* (purple) and the triple mutant *mtl-1;mtl-2;pcs-1(zs2)* (black) were maintained on control NGM (solid bars) and with the addition of 12 µM cadmium (Panel A) or 190 µM copper (Panel B) for 48 hours. Nematodes were subsequently washed off the plates and counted. Pelleted samples were acid hydrolysed in nitric acid (70°C for 6 hours) to liberate the total body metal content. Internal metal ion content was measured used atomic absorption spectroscopy.

The average copper concentration per 1000 nematodes increased from 0.018 to 0.114 µM/1000 nematodes following copper supplementation (190 µM) to media (Figure 5.1B). There were some strain specific differences while

mtl-1;mtl-2;pcs-1(zs2) accumulated copper at much lower levels than all other strains (0.033 µM/1000 nematodes) and the double MT knockout accumulated the highest levels of copper.

5.3.2. Total brood size

A key element of population viability is total brood size which is taken as the sum of all viable offspring per individual nematode. Age synchronised nematodes were placed on dosed NGM at the L1 stage and transferred to fresh NGM daily until reproduction ceased (Section 2.7.2). Offspring were allowed to grow to the L1/2 stage and then counted manually. Under optimal laboratory conditions wild type nematodes laid 232±4 viable offspring (Figure 5.2A) and strain specific differences were observed. The double MT mutant, *pcs-1(tm1748)* and *mtl-1;mtl-2;pcs-1(zs2)* all had a significant reduction in total brood size ($p \leq 0.01$).

Exposure to cadmium resulted in a decrease in total reproductive output compared to control conditions (Figure 5.2B). Single and double MT mutants laid significantly fewer viable eggs than wild type ($p \leq 0.01$) following exposure to cadmium. Nematodes null for *pcs-1* were hypersensitive to 12 µM cadmium. The strains *pcs-1(tm1748)* and *mtl-1;mtl-2;pcs-1(zs2)* did not develop past early larval stages (L1/L2 stage) and died prior to reaching reproductive maturity.

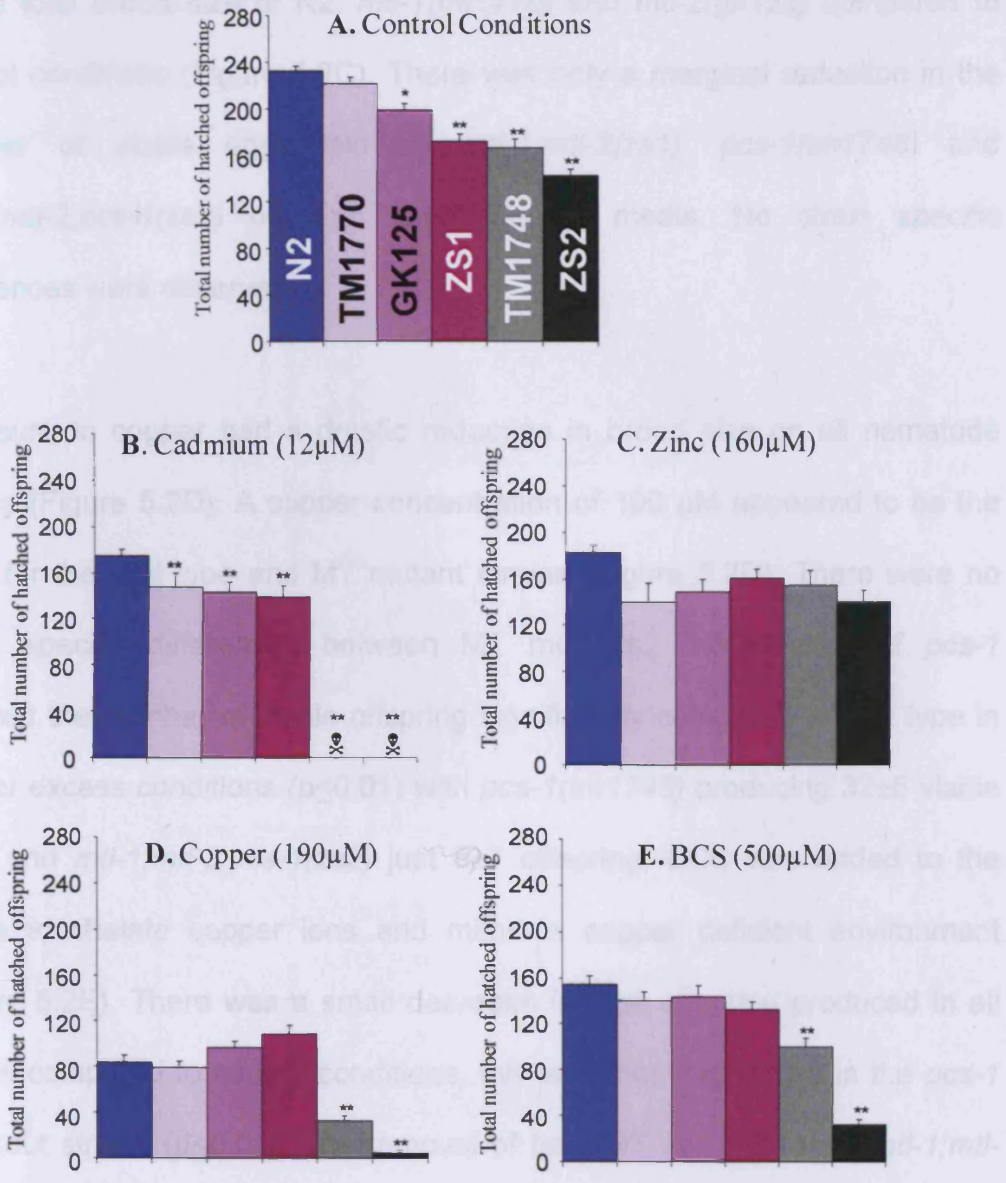

Figure 5.2: Comparative total brood size analysis of N2 (wild type) with mutants strains exposed to various metal conditions. Synchronised L1 wild type N2 (blue) nematodes together with strains containing the genotypes *mtl-1(tm1770)* (pale purple), *mtl-2(gk125)* (light purple), *mtl-1;mtl-2(zs1)* (dark purple), *pcs-1(tm1748)* (grey) and *mtl-1;mtl-2;pcs-1(zs2)* (black) were maintained on control NGM (Panel A) until death. During this time the eggs were collected and hatched to evaluate the total viable offspring (Section 2.7.2). This was repeated with the media supplemented with either 12 µM cadmium (Panel B), 160 µM zinc (Panel C), 190 µM copper (Panel D) or 500 µM of the metal chelator BCS (Panel E). Statistical analysis was performed using the ANOVA Test comparing to N2 at each metal concentration with confidence levels indicated by *p<0.05 **p<0.01. Error bars shown are standard error of the mean with an average n of 40. Genotypes *pcs-1(tm1748)* and *mtl-1;mtl-2;pcs-1(zs1)* did not develop past the L1/L2 in the presence of cadmium, therefore yielding no viable offspring (indicated by ☠).

Following zinc exposure (160 µM) there was a small, non-significant decrease in the total brood size of N2, *mtl-1(tm1770)* and *mtl-2(gk125)* compared to control conditions (Figure 5.2C). There was only a marginal reduction in the number of viable eggs laid by *mtl-1;mtl-2(zs1), pcs-1(tm1748)* and *mtl-1;mtl-2;pcs-1(zs2)* on zinc supplemented media. No strain specific differences were observed.

Exposure to copper had a drastic reduction in brood size on all nematode strains (Figure 5.2D). A copper concentration of 190 µM appeared to be the EC_{50} for the wild type and MT mutant strains (Figure 5.2D). There were no strain specific differences between MT mutants. The deletion of *pcs-1* reduced the number of viable offspring significantly compared to wild type in copper excess conditions ($p \leq 0.01$) with *pcs-1(tm1748)* producing 32±5 viable eggs and *mtl-1;mtl-2;pcs-1(zs2)* just 5±7 offspring. BCS was added to the media to chelate copper ions and mimic a copper deficient environment (Figure 5.2E). There was a small decrease in total offspring produced in all strains compared to control conditions, this was most significant in the *pcs-1* knockout strains ($p \leq 0.01$). The removal of both MT and PC (as in *mtl-1;mtl-2;pcs-1(zs2)*) rendered the nematode more sensitive to depleted copper than the single *pcs-1* knockout.

As shown in Figure 5.2B, the deletion of *pcs-1* resulted in cadmium hypersensitivity. At cadmium concentrations of 1 µM or greater, *pcs-1 (tm1748)* and *mtl-1;mtl-2;pcs-1(zs2)* died during early development. In the absence of cadmium (Figure 5.3A), wild type nematodes laid 238±4 viable

offspring. There were strain specific differences, with the triple knockout producing the smallest total brood of 143±6.

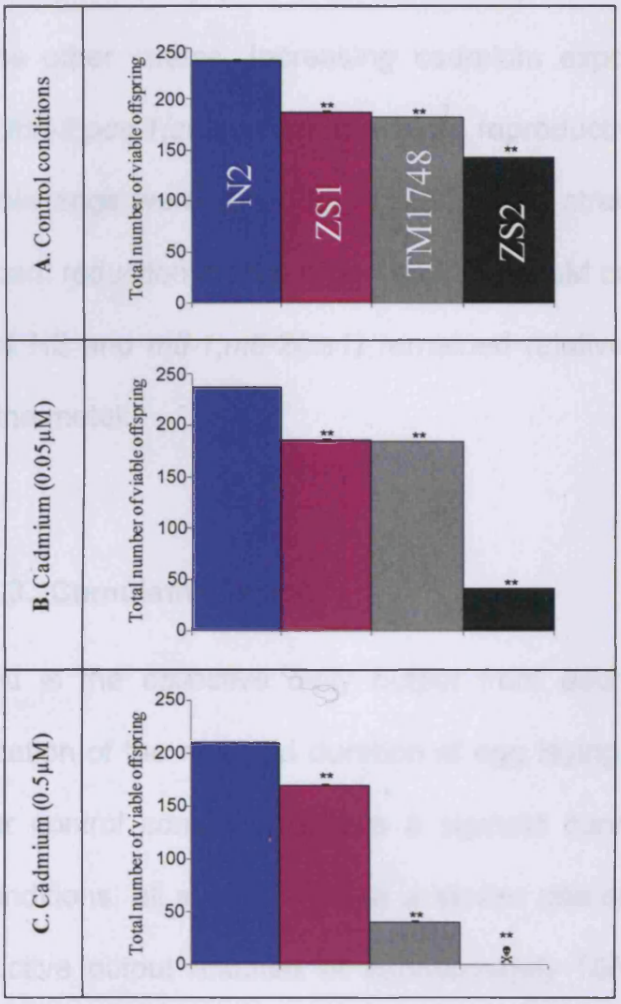

Figure 5.3: Total brood size of wild type and *pcs-1* null nematodes at low cadmium concentrations. Synchronised L1 wild type N2 (blue) nematodes together with strains containing the genotypes *mtl-1;mtl-2(zs1)* (dark purple), *pcs-1(tm1748)* (grey) and *mtl-1;mtl-2;pcs-1(zs2)* (black) were maintained on control NGM (Panel A) until death. During this time the eggs were collected and hatched to evaluate the total viable offspring (Section 2.7.2). This was repeated with the media supplemented with 0.05 µM cadmium (Panel B) or 0.5 µM cadmium (Panel C). Statistical analysis was performed using the ANOVA Test comparing to N2 at each metal concentration with confidence levels indicated by *p<0.05 **p<0.01. Error bars shown are standard error of the mean with an average n of 32. Nematodes which did not develop past the L2/L3 stage and did not yield viable offspring are indicated by ☠.

The addition of 0.05 µM cadmium to the media did not drastically affect wild type, the double MT knockout or the single *pcs-1* mutant (Figure 5.3B). These strains laid a similar number of viable eggs as under control conditions. In contrast, *mtl-1;mtl-2;pcs-1(zs2)* produced significantly fewer viable offspring ($p \leq 0.01$) than the other strains. Increasing cadmium exposure to 0.5 µM prevented *mtl-1;mtl-2;pcs-1(zs2)* from reaching reproductive maturity and therefore no viable eggs were laid (Figure 5.3C). The strain *pcs-1(tm1748)* showed a significant reduction in total brood size at 0.5 µM cadmium whereas the brood size of N2 and *mtl-1;mtl-2(zs1)* remained relatively unaffected by the presence of the metal.

5.3.3. Cumulative brood

Cumulative brood is the collective daily output from each nematode and provides an indication of the rate and duration of egg laying. The cumulative brood size under control conditions shows a sigmoid curve (Figure 5.4A). Under control conditions, all strains showed a similar rate of egg laying with maximal reproductive output reached at approximately 100 hours post L1. Brood period was three days.

The addition of cadmium did not significantly alter the rate of egg laying compared to control conditions however daily output was less than in control conditions (Figure 5.4B). Two of the strains are not represented in Figure 5.4B, namely *pcs-1(tm1748)* and *mtl-1;mtl-2;pcs-1(zs2)*. This is due to the hypersensitivity of these strains to cadmium which inhibits reproduction.

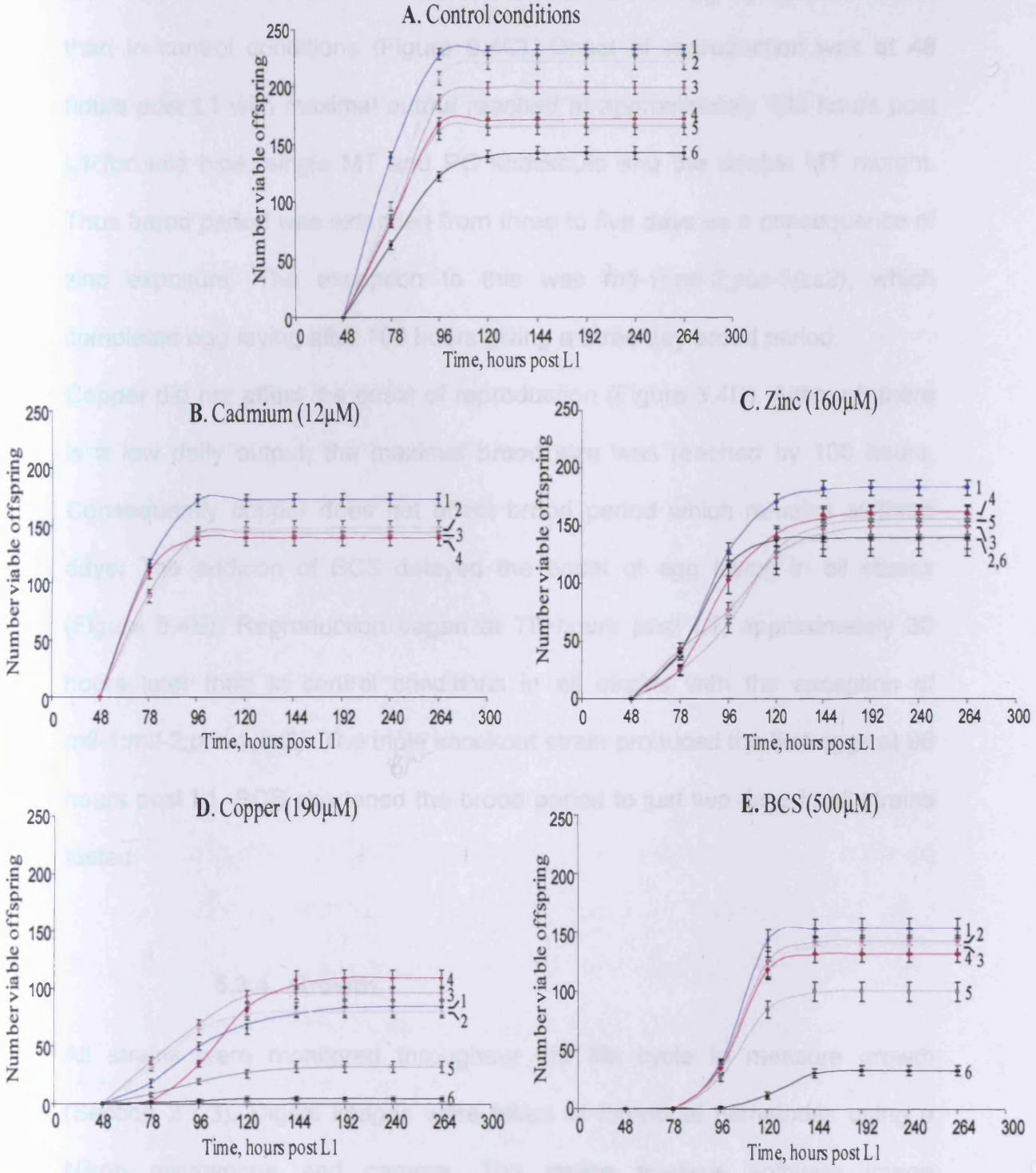

Figure 5.4: Rate of viable offspring production of N2 wild type and mutant nematode strains exposed to various metal conditions. Synchronised L1 wild type N2 (blue, 1) nematodes together with strains containing the genotypes *mtl-1(tm1770)* (pale purple, 2), *mtl-2(gk125)* (light purple, 3), *mtl-1;mtl-2(zs1)* (dark purple, 4), *pcs-1(tm1748)* (grey, 5) and *mtl-1;mtl-2;pcs-1(zs2)* (black, 6) were maintained on control NGM (Panel A) until death. Eggs were collected at regular intervals and hatched to evaluate the rate of viable offspring production (Section 2.7.2). This was repeated with the media supplemented with either 12 µM cadmium (Panel B), 160 µM zinc (Panel C), 190 µM copper (Panel D) or 500 µM of the metal chelator BCS (Panel E). Error bars indicate standard error of the mean (average n was 40).

Zinc supplemented media resulted in the initial rate of egg laying to be slower than in control conditions (Figure 5.4C). Onset of reproduction was at 48 hours post L1 with maximal output reached at approximately 130 hours post L1 for wild type, single MT and PC knockouts and the double MT mutant. Thus brood period was extended from three to five days as a consequence of zinc exposure. The exception to this was *mtl-1;mtl-2;pcs-1(zs2)*, which completed egg laying after 100 hours giving a three day brood period.

Copper did not affect the onset of reproduction (Figure 5.4D). Although there is a low daily output, the maximal brood size was reached by 100 hours. Consequently copper does not affect brood period which remains at three days. The addition of BCS delayed the onset of egg laying in all strains (Figure 5.4E). Reproduction began at 78 hours post L1, approximately 30 hours later than in control conditions in all strains with the exception of *mtl-1;mtl-2;pcs-1(zs2).* The triple knockout strain produced the first eggs at 96 hours post L1. BCS shortened the brood period to just two days in all strains tested.

5.3.4. Growth

All strains were monitored throughout the life cycle to measure growth (Section 2.7.3). Digital images were taken of individual nematodes using a Nikon microscope and camera. The image analysis software Image ProExpress v5.1 allowed the outline of each nematode to be traced and the software calculated volumetric area as detailed in Box 2.1. Figure 5.5 shows the change in volumetric area when nematodes were exposed to different metal environments. Under control conditions *mtl-1;mtl-2;pcs-1(zs2)* reaches

maximal volumetric area after approximately 75 hours post L1 whereas all other strains complete growth after 150 hours post L1 (Figure 5.5A). Ultimately the triple knockout was the smallest strain with *mtl-1(gk125)* having the largest volumetric size.

Cadmium reduced the volumetric area in all strains (Figure 5.4B). The strains *pcs-1(tm1748)* and *mtl-1;mtl-2;pcs-1(zs2)* were not measured as these nematodes were hypersensitive to cadmium and did not develop past the early larval stages. The wild type and MT mutants were all of a similar growth rate and final size of these nematodes were alike. Zinc did not drastically affect the area of the nematodes compared to control conditions (Figure 5.5C). The main difference was that the triple knockout was the strain with the greatest volumetric size, and was larger than in control conditions. The double MT mutant was the smallest strain.

Exposure to copper reduced the length of time over which growth occurred (Figure 5.5D). All strains had reached the final volumetric size after approximately 90 hours post L1, earlier than in control conditions. Wild type, single and double MT knockouts were smaller when exposed to copper compared to control conditions. The strains *pcs-1(tm1748)* and *mtl-1;mtl-2;pcs-1(zs2)* were the smallest nematodes in the presence of copper. Growth rate of N2, *mtl-1(tm1770)* and *mtl-1;mtl-2(zs1)* was slower than in control conditions following exposure to BCS (Figure 5.5E). These strains had the lowest volumetric area with the triple mutant having the largest area.

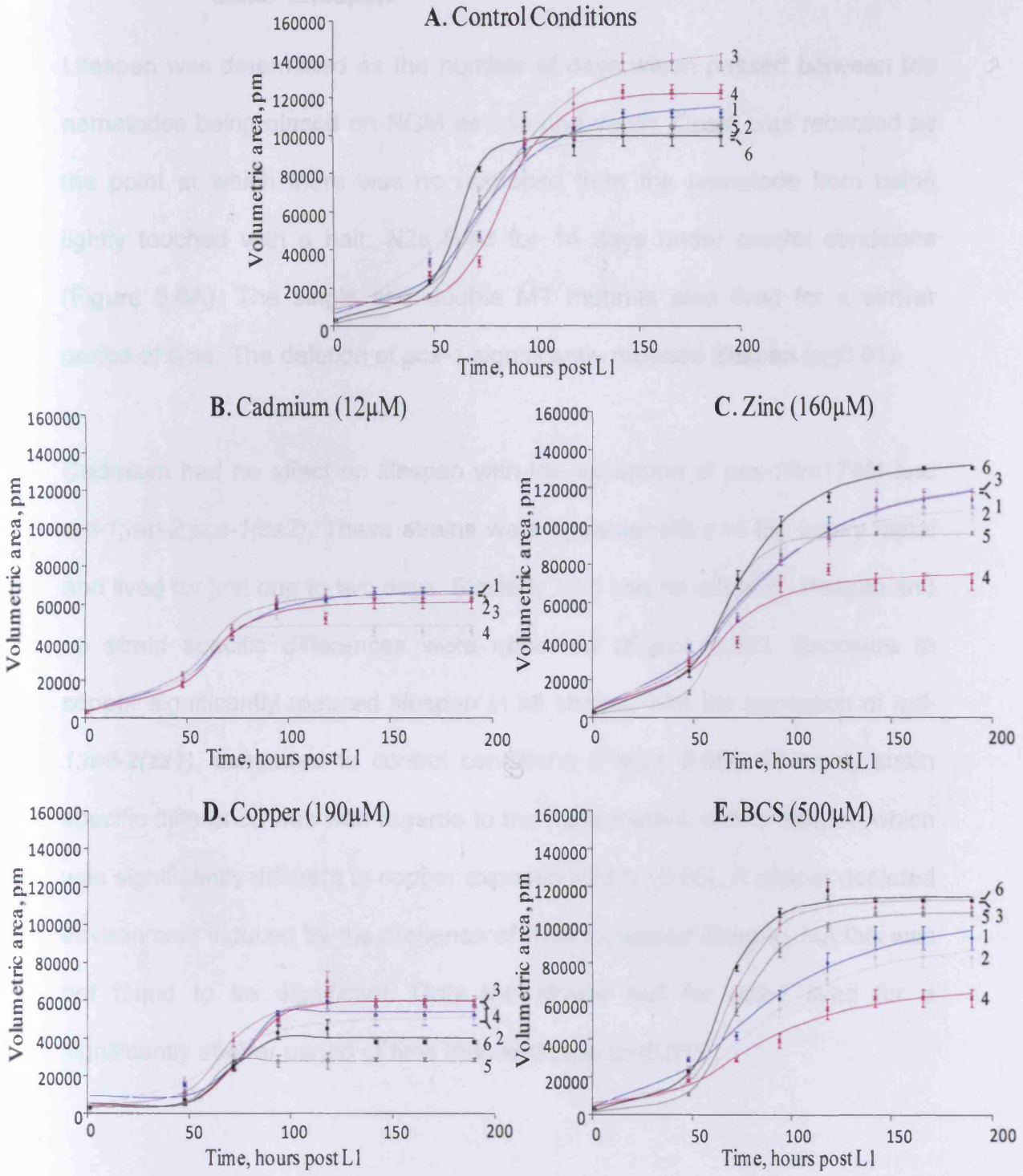

Figure 5.5: Volumetric area of N2 wild type and mutant nematode strains exposed to various metal conditions. Synchronised L1 wild type N2 (blue, 1) nematodes together with strains containing the genotypes *mtl-1(tm1770)* (pale purple, 2), *mtl-2(gk125)* (light purple, 3), *mtl-1;mtl-2(zs1)* (dark purple, 4), *pcs-1(tm1748)* (grey, 5) and *mtl-1;mtl-2;pcs-1(zs2)* (black, 6) were maintained on control NGM (Panel A) until death. Digital images of nematodes were taken throughout development and analysed with Image ProExpress software (Section 2.7.3). This was repeated with the media supplemented with either 12 µM cadmium (Panel B), 160 µM zinc (Panel C), 190 µM copper (Panel D) or 500 µM of the metal chelator BCS (Panel E). Error bars indicate standard error of the mean (n=10).

5.3.5. Lifespan

Lifespan was determined as the number of days which passed between the nematodes being placed on NGM as L1s and death. Death was recorded as the point at which there was no response from the nematode from being lightly touched with a hair. N2s lived for 14 days under control conditions (Figure 5.6A). The single and double MT mutants also lived for a similar period of time. The deletion of *pcs-1* significantly reduced lifespan ($p \leq 0.01$).

Cadmium had no affect on lifespan with the exception of *pcs-1(tm1748)* and *mtl-1;mtl-2;pcs-1(zs2)*. These strains were hypersensitive to the heavy metal and lived for just one to two days. Similarly zinc had no effect on lifespan and no strain specific differences were observed (Figure 5.6C). Exposure to copper significantly reduced lifespan in all strains, with the exception of *mtl-1;mtl-2(zs1)*, compared to control conditions (Figure 5.6D). The only strain specific difference was with regards to the triple mutant, with a lifespan which was significantly different to copper exposed N2s ($p \leq 0.05$). A copper depleted environment induced by the presence of BCS increased lifespan, but this was not found to be significant. Only the strains null for *pcs-1* lived for a significantly shorter period of time than wild type ($p \leq 0.01$).

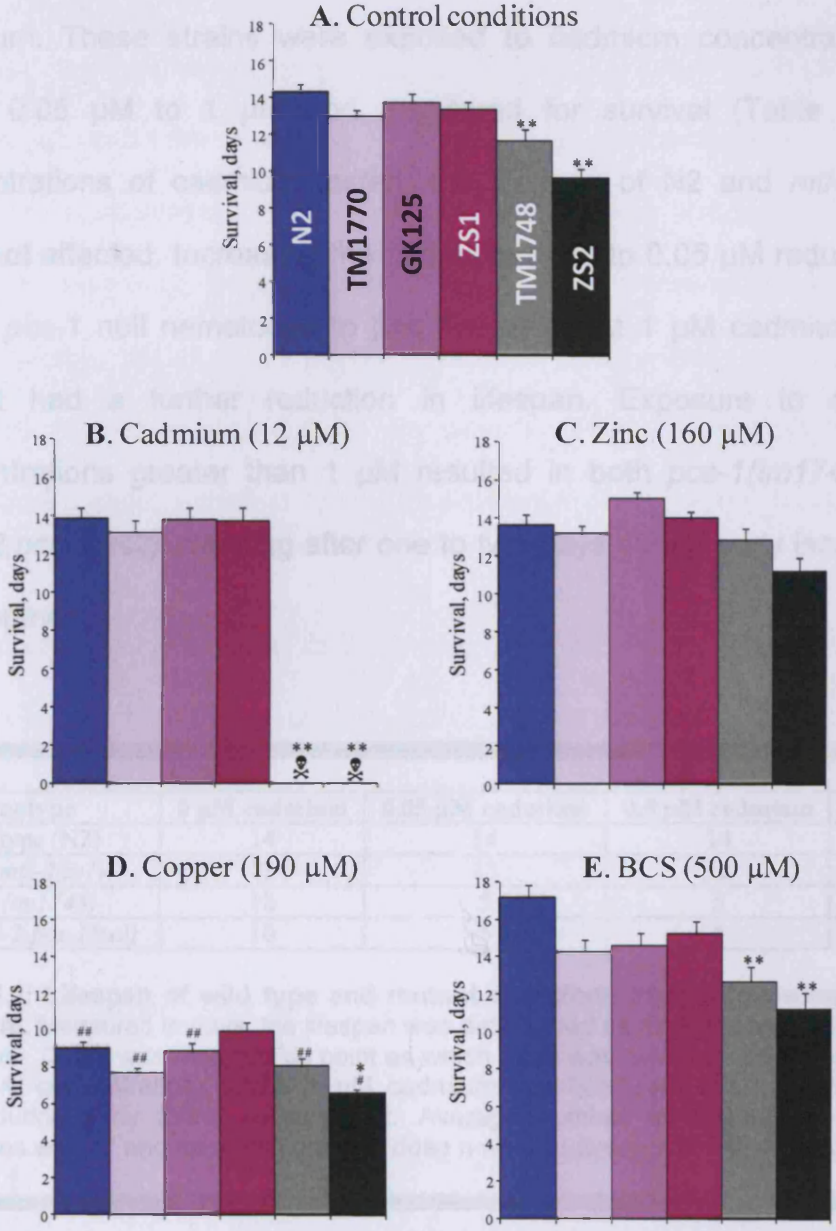

Figure 5.6: Lifespan of N2 wild type and mutant nematode strains exposed to various metal conditions. Synchronised L1 wild type N2 (blue) nematodes together with strains containing the genotypes *mtl-1(tm1770)* (pale purple), *mtl-2(gk125)* (light purple), *mtl-1;mtl-2(zs1)* (dark purple), *pcs-1(tm1748)* (grey) and *mtl-1;mtl-2;pcs-1(zs2)* (black) were maintained on control NGM (Panel A) until death. Death was recorded as the day when there was no response from the nematode to being tapped with a hair (Section 2.7.2). This was repeated with the media supplemented with either 12 µM cadmium (Panel B), 160 µM zinc (Panel C), 190 µM copper (Panel D) or 500 µM of the metal chelator BCS (Panel E). Statistical analysis was performed using the ANOVA Test comparing to N2 at each metal concentration with confidence levels indicated by $^{*}p<0.05$ $^{**}p<0.01$ and comparing to the same strain under control conditions indicated by $^{\#}p<0.05$ $^{\#\#}p<0.01$. Error bars indicate standard error of the mean (control n = 70, cadmium n = 14, zinc n = 60, copper n = 43, BCS n = 50). Genotypes *pcs-1(tm1748)* and *mtl-1;mtl-2;pcs-1(zs1)* did not develop past the L1/L2 in the presence of cadmium (indicated by ☠).

Figure 5.6B showed that *pcs-1* null nematodes were hypersensitive to cadmium. These strains were exposed to cadmium concentrations in the range 0.05 µM to 1 µM and monitored for survival (Table 5.2). At all concentrations of cadmium tested, the lifespan of N2 and *mtl-1;mtl-2(zs1)* were not affected. Increasing the cadmium dose to 0.05 µM reduced lifespan in the *pcs*-1 null nematodes to just five days. At 1 µM cadmium, the triple mutant had a further reduction in lifespan. Exposure to cadmium at concentrations greater than 1 µM resulted in both *pcs-1(tm1748)* and *mtl-1;mtl-2;pcs-1(zs2)* arresting after one to two days during early larval stages of development.

Genotype	0 µM cadmium	0.05 µM cadmium	0.5 µM cadmium	1 µM cadmium
Wild type (N2)	14	14	14	14
mtl-1;mtl-2(zs1)	13	13	12	12
pcs-1(tm1748)	12	5	5	5
mtl-1;mtl-2;pcs-1(zs2)	10	5	5	3

Table 5.2: Lifespan of wild type and mutant nematode strains following exposure to cadmium. Measured in days, the lifespan was determined as the number of days between L1 and death. Death was recorded as point as which there was no response to being touched by a hair. At concentrations above 1 µM cadmium *pcs-1(tm1748)* and *mtl-1;mtl-2;pcs-1(zs2)* arrest during early larval development. Average number for nematodes under control conditions was 47 and for each cadmium dose n was an average of 24 nematodes.

5.4. Discussion

The nitric acid digestion quantification of metal content from nematode and agar is an accurate measure of total metal concentration. Agar with no additional supplements had cadmium levels below the detection limit and negligible levels of copper and zinc. Likewise, nematodes on NGM agar accumulated cadmium at levels below the detection limit. Copper was detected in nematodes grown on control NGM (less than 0.1 µg/1000 nematodes) because the copper was present in the agar (<0.08 mg/kg).

The nominal concentration of cadmium supplemented in the media (12 µM) was comparable to the quantified concentration from ICP/OES analysis (12.8 µM). In addition, nematodes accumulated cadmium when grown on cadmium seeded plates. This indicates that cadmium is being taken up by nematodes from the agar via the OP50 food source. The nitric acid digested fraction of zinc supplemented agar was 146 µM as quantified by ICP/OES. This was marginally lower than the nominal concentration of 160 µM. The small difference in concentration is acceptable. Copper concentration was calculated as 184 µM compared to the nominal value of 190 µM. Nematode nitric acid digested fractions showed that copper accumulated as a result of metal uptake from the copper supplemented NGM. BCS was chosen to chelate the copper from the media to mimic a copper deficient environment. The nitric acid digested ICP/OES quantification showed that the measured concentration of copper was less than in control media and at the lower limit of detection. Nematode copper levels were not measured in BCS exposed samples.

All nematode strains were exposed to elevated or depleted metal environments from the L1 stage throughout life. The phenotypic response was recorded, namely brood size, brood period, growth and lifespan. Under optimal conditions, wild type *C. elegans* laid 232±4 viable eggs which was comparable to the reported norm (Alvarez *et al.* 2005; Byerly *et al.* 1976). The double MT mutant (*mtl-1;mtl-2(zs1)*) was viable and consequently MT cannot be essential for survival. The viability of the double MT knockout on NGM which contains trace essential metals indicates that MT is not required for metal homeostasis (Hughes and Stürzenbaum 2007). The presence of a functional PC synthase in *C. elegans* (Clemens *et al.* 2001) may provide a alternative mechanism for metal detoxification. The *pcs-1* null nematodes were viable, as was *mtl-1;mtl-2;pcs-1(zs2)* which contained no MT or functional PC synthase. Together these two knockout strains indicate that MT and PC are not fundamental to life and have minimal roles in essential metal homeostasis under optimal conditions.

Cadmium exposure resulted in a reduction in the number of viable offspring produced by N2 and MT mutants (Figure 4.2B) an effect also noted in *Drosophila* (Egli *et al.* 2006). Cadmium is a teratogenic agent and teratogens disrupt the growth and development of embryos (Alvarez *et al.* 2005). The nematode proceeds through the larval stages on cadmium seeded NGM and reaches reproductive maturity at the same time as non-cadmium exposed nematodes. Fertilisation of the eggs occurs in the hermaphrodite but cadmium may disrupt the formation of the embryo. Thus the number of viable eggs will be reduced. In addition, cadmium can decrease sperm count (Alvarez *et al.*

2005). Hermaphrodite *C. elegans* germ line cells produce a finite number of sperm and this is the limiting factor in reproduction (Alvarez *et al.* 2005; Jager *et al.* 2005). Low sperm counts would result in fewer successful fertilisations and ultimately a reduction in total brood size, as observed.

Deletions of the MT isoforms, in isolation or together, increased the sensitivity of *C. elegans* to cadmium (Figure 4.2B). MTs are widely considered to be the primary mechanism of cadmium detoxification. If this is true, the double MT knockout would be expected to suffer more drastically than observed during cadmium exposure. In contrast it is the *pcs-1* null strains which display cadmium hypersensitivity, even at cadmium concentrations as low as 1 µM. Hypersensitivity to cadmium has also been recorded in *Arabidopsis pcs-1* knockouts, where the plants were shown to be hypersensitive to 0.6 µM cadmium (Cobbett and Goldsbrough 2002). Similar findings have also been observed in yeast (Clemens *et al.* 1999; Cobbett 2000b). The hypersensitivity of *pcs-1* null organisms to cadmium indicates that PC is an important part of the detoxification route of cadmium, potentially more than MTs.

The nominal zinc concentration of 160 µM was chosen as it was at a previously identified *C. elegans* EC_{50} (Ibaim and Grant 2005). ICP/OES quantification of the zinc supplemented agar was 146 µM, which was slightly lower than the nominal concentration. However, even at 146 µM the nematodes were still being exposed to a zinc concentration close to the EC_{50}. Zinc excess results in a small, but not significant, decrease in brood size. Zinc also had little or no effect on lifespan and growth, a finding that corresponds

with previous reports utilising MT or PC knockouts in plants, flies and nematodes (Cobbett and Goldsbrough 2002; Cui *et al.* 2007; Egli *et al.* 2003; Ibaim and Grant 2005; Ha *et al.* 1999). It can be inferred that MT and PC synthase are not the key players in zinc homeostasis and other aspects of the zinc homeostatic pathway are likely to be utilised to keep cellular zinc at optimal levels. For example, during excess, zinc ion transporters may be upregulated to export the ions from the cell to reduce toxicity. The presence of zinc accelerates glutathione synthesis (Tsuji *et al.* 2003) which forms a complex with zinc. The glutathione-zinc complex can be transported out of the cell to reduce toxicity (Rea *et al.* 2004). A combination of this and other mechanisms would enable cells to continue to function in the presence of elevated zinc levels but in the absence of MT or PC.

Elevated copper concentrations had a drastic effect on *C. elegans* life history end points, namely a reduction in total brood size and an increase in brood period. In addition lifespan was significantly reduced in all strains with the exception of the triple knockout mutant. The effects caused by an increase in copper ions can be attributed to an increase in cytosolic copper (Tapia *et al.* 2004). In Drosophila, free copper was absorbed and shown to be readily soluble in the gut (Egli *et al.* 2006). It is conceivable that the same would be true in *C. elegans,* whereby copper is ingested via the OP50 growing on the copper supplemented NGM. The presence of elevated cytosolic copper results in cellular damage via the generation of free radicals and ROS via the Fenton Reaction (Shaw 1998). ROS prevent the correct folding and functioning of proteins as well as impairing DNA repair mechanisms.

Together, damaged DNA and proteins lead the cell towards the cell death pathways which may reflect the observed reduction in growth and lifespan.

Although there was a reduction in brood size and lifespan compared to control conditions, there was no statistical difference in these end points between MT knockout strains compared to wild type. However, the brood size and lifespan of *pcs-1(tm1748)* and *mtl-1;mtl-2;pcs-1(zs2)* was significantly affected during copper exposure. It can be proposed that PCs are used in preference to bind excess free copper ions to prevent them form exerting their toxic effects. MTs may only function in the absence of PC. Hypersensitivity to copper has been observed in other organisms null for *pcs-1* (Cobbett and Goldsbrough 2002; Clemens 2006). This indicates that PC may be a significant mechanism of copper detoxification. Consequently it can be hypothesised that although both MT and PC contribute to copper detoxification, PCs are potentially more important than MTs.

The volumetric area of all *C. elegans* strains exposed to copper was reduced by approximately 50% compared to the size of nematodes under control conditions. The final size of the copper exposed nematodes was similar to the size of nematodes exposed to cadmium. The decrease in volumetric area when exposed to copper and cadmium may be explained by the increase in the formation of ROS. Cadmium facilitates the formation of superoxide anions [$O_2^{\cdot}$-] and hydrogen peroxide [H_2O_2] which together react to form the extremely toxic hydroxyl [$^{\cdot}OH$] radical (Bertin and Averbeck 2006).

Additionally, copper ions react with hydrogen peroxide to generate more hydroxyl radicals and can generate ROS via the Fenton Reaction (Shaw 1998). The increase of toxic free radicals results in irreversible DNA damage and conformational changes in proteins which may affect cell growth and reduce lifespan. The presence of MT provides the cell with a mechanism to remove reactive oxygen species and free radicals via the oxidation of free thiolate clusters on the protein (Palmiter 1998). Copper is not a potent inducer of MT gene expression; consequently the gene may not be highly transcribed to generate enough protein to sequester the increased levels of radicals. Therefore there would be an excess of free radicals available to damage DNA and proteins.

Copper is an essential metal and used as a co-factor in many enzymes and cellular processes such as respiration (Valko *et al.* 2005). It has been proposed that during the absence of copper, non-essential cuprous enzymes are forced to degrade and release their associated copper (Suzuki *et al.* 2002). The free copper is used to supply essential enzymes such as cytochrome c oxidase and superoxide dismutatase to allow their continuing normal function (Suzuki *et al.* 2002). The cell wide degradation of cuprous enzymes results in a sudden increase in cytosolic copper. In effect this places the cell in a copper excess environment, but not at the same physiological concentration as that generated by excess environmental copper. Therefore the effects observed during copper deficient environments were similar but not as significant as those of copper excess conditions. Secondly, during copper deficient environments, there is an increase in oxidative stress. This in

turn up regulates the production of stress enzymes such as superoxide dismutase (Egli *et al.* 2006; Hirata *et al.* 2005). Superoxide dismutase and other stress enzymes can reduce oxidative stress generated free radicals and allow nematodes to survive in a copper deficient environment.

As in the copper excess environments *pcs-1* null nematodes were more significantly affected by a copper deficiency than mutants with the removal of one or both MT isoforms. This re-enforces the hypothesis that PCs may be more responsive to copper trafficking and detoxification than MTs. The importance of PC may arise from their ability to re-activate enzymes via their metal donating and accepting properties (Clemens 2006; Thumann *et al.* 1991). Diamine oxidase is an enzyme from the pea (*Pisum sativum*) which requires copper as a co-factor (Thumann *et al.* 1991). PCs were extracted from the pea and purified during copper excess environments. These PCs were able to re-activate diamine oxidase which was extracted from the plant during a copper deficient environment. Diamine oxidase was reactivated to 80% of its original activity due to the presence of copper supplied by the PC (Thumann *et al.* 1991). If *C. elegans* PCs also have this re-activation property, *pcs-1* null nematodes would not survive and reproduce in copper deficient environments as successfully as MT mutants. This was observed in these experiments via the larger brood size and longer lifespan of MT null strains compared to PC synthase null strains.

5.5. Conclusion

Firstly, neither MTs nor PCs were found to be pre-requisites for life or have a primary role in essential metal homeostasis. MTs have been considered to be the major component of heavy metal detoxification, specifically cadmium, and have, until recently, considered to be the only metal detoxification system in *C. elegans* (Vatamaniuk *et al.* 2001).

However, during this study it has become apparent that PC and MT have integrated roles in metal detoxification. It can be proposed that under normal physiological metal concentrations there is constitutive basal activity of PC synthase which provides a constant level of PC (Hirata *et al.* 2005). Metal ions can be easily and quickly sequestered by PCs. When metal concentrations become elevated, PC synthase is post-translationally stimulated to generate more PCs, which is a rapid process (Cobbett and Goldsbrough 2002; Rea *et al.* 2004; Vatamaniuk *et al.* 2000). However, in elevated metal environments there may be an excess of metal ions which cannot be sequestered by PC. In this instance, free metal is available to activate the transcription of MT to aid in metal detoxification. The stimulation of MTs may or may not be a direct result of the presence of free metal ions. In addition, the two detoxification systems may be mutually exclusive. Following the removal of one detoxification system, the remaining one may be up regulated to compensate.

CHAPTER SIX

QUANTITATIVE REAL TIME POLYMERASE CHAIN REACTION

6.1. Introduction

It is known that MT transcription is enhanced by a range of heavy metals (Kägi and Schffer 1988; Klaassen *et al.* 1999). Nematodes expressing green fluorescent protein (GFP) fusion constructs have been previously used to show that cadmium is a potent inducer of *mtl-1* and *mtl-2* (Swain *et al.* 2004). As described in Chapter 3, P*mtl-1*::GFP and P*mtl-2*::GFP promoter fusion constructs were available and these were used to investigate the extent of *mtl* induction by heavy metals. The previous chapter highlighted that cadmium and copper had a significant effect on *mtl* and *pcs-1* null nematodes while zinc did not. Using the P*mtl*::GFP transgenic nematodes which have been exposed to the metal and chelator, the inductive potential of the ions can be visualised. The *mtl* promoter drives expression of GFP when an ion binds the promoter, in an as yet unknown manner. Consequently a fluorescent signal can be observed using a UV light source. A stronger GFP signal would be observed with a more potent stimulator of *mtl* transcription.

The previous chapter implicated a co-ordinated response to heavy metals from PC and MT. Due to the hypersensitivity of *pcs-1* null nematodes to cadmium it was proposed that PC may the preferred route of cadmium detoxification. It was also hypothesised that PC and MT are mutually exclusive with the gene expression of one being up regulated in compensation for the removal of the other. To confirm the hypothesis,

quantitative PCR (Q-PCR) was performed. Q-PCR is a method which relies on the sequence specific detection of a PCR product using fluorescent probes to sensitively quantify transcript levels of a specific gene of interest (Giulietti *et al.* 2001; Wang and Brown 1999). Fluorescence is measured at the end of each PCR cycle in real time (Giulietti *et al.* 2001).

There are two main ways in which the fluorescence of the PCR product is achieved, as a result of fluorescent dyes or probes. An example of a fluorescent dye is SYBR® Green. SYBR® Green binds to double stranded DNA during the extension phase of PCR and emits a fluorescent signal (Qiagen 2006). SYBR® Green is useful for quantifying multiple targets but can result in non-specific PCR products and primer dimers (primer-primer self complementary sequence binding) (Qiagen 2006). There are 3 main probe types; Molecular beacons, LightCycler® hybridisation probes and TaqMan® probes (Qiagen 2006). Molecular beacons are a dual labelled probe with complementary ends. The probe forms a hairpin loop and quenches the fluorescent signal unless bound to DNA (Qiagen 2006). The LightCycler® hybridisation probes are two labelled oligonucleotides which bind head-to-tail on the PCR template (Qiagen 2006). Fluorescence is emitted only when the two probes have bound. The polymerase enzyme will remove the bound probe as it extends the new DNA strand. Due to the difficulty in design, molecular beacons and LightCycler® hybridisation probes are less frequently used. Like Molecular beacons and LightCycler® hybridisation probes, the commonly used TaqMan® probes are based upon fluorescence resonance energy transfer (FRET). A diagram showing the action of FRET in TaqMan® probes is shown in Figure 6.1.

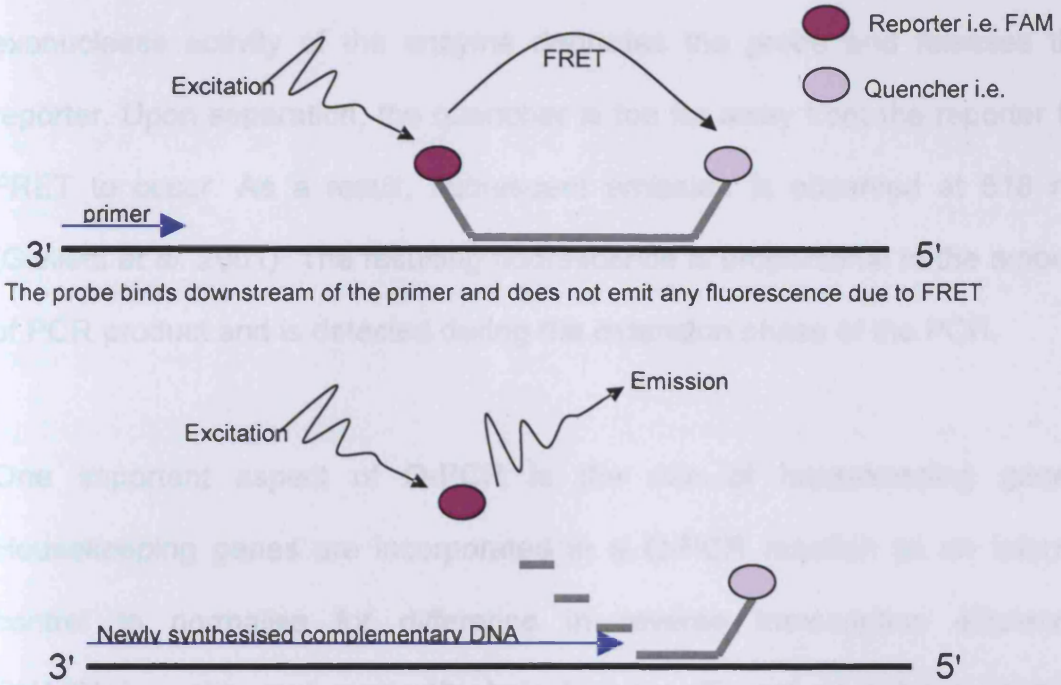

Figure 6.1: Fluorescence resonance energy transfer (FRET) in TaqMan® Q-PCR. A sequence specific probe with a reporter at one end and a quencher at the other binds to DNA. The presence of the quencher in close proximity to the reporter prevents the emission of a fluorescent signal. As a polymerase degrades the probe and extends the new DNA strand, the reporter is released due to the 5'-3' exonucelase activity. The reporter is not quenched and therefore is able to emit a fluorescent signal upon excitation. Adapted and re-drawn from Giulietti *et al.* (2001).

The TaqMan® probe is labelled at the 5' end with a fluorescent reporter, commonly FAM (6-carboxyfluorescein) and at the 3' end with a quencher such as TAMRA (6-carboxytetramethylrhodamine) (Giulietti *et al.* 2001). The probe is sequence specific and binds to the DNA where the reporter and quencher are in close proximity. When close together the quencher, in this case TAMRA, absorbs the fluorescent emission from the reporter, FAM and prevents emission of fluorescence. This is the process of FRET. A primer anneals to the DNA sequence upstream of the probe. A *Taq* polymerase is added to the mix and begins to generate a new DNA strand from the primer.

As the polymerase reaches the place where the probe is bound, the 5'→3' exonuclease activity of the enzyme degrades the probe and releases the reporter. Upon separation, the quencher is too far away from the reporter for FRET to occur. As a result, fluorescent emission is observed at 518 nm (Giulietti *et al.* 2001). The resulting fluorescence is proportional to the amount of PCR product and is detected during the extension phase of the PCR.

One important aspect of Q-PCR is the use of housekeeping genes. Housekeeping genes are incorporated in a Q-PCR reaction as an internal control to normalise for difference in reverse transcription efficiency, RNA/DNA quality and manual/technical errors. To act as a housekeeping gene, the gene must have two properties. Firstly, it must be ubiquitously expressed and secondly transcription of that gene should not be affected by the experimental conditions (Stürzenbaum and Kille 2001). There are many possible housekeeping genes to choose from depending on the organism of study and experimental design. Popular housekeeping genes are actin, glyceraldehyde-3-phosphate dehydrogenase and ribosomal genes (Stürzenbaum and Kille 2001). In Q-PCR with *C. elegans* samples, the housekeeping gene commonly used is a gene for a ribosomal protein, *rla-1* (Sequence name Y37E3.7, WBGene00004409).

6.2. Aims

The aim of this chapter was to investigate the change in gene expression of *mtl-1* and *mtl-2* in the presence and absence of heavy metals. Firstly, P*mtl*::GFP transgenic nematodes were used to investigate the inducibility of various essential and non-essential metals on *mtl-1* and *mtl-2*. Secondly, Q-PCR was performed on cadmium exposed and non-exposed MT and PC synthase mutants to quantify the change in gene expression of *mtl* genes.

6.3. Results

6.3.1. GFP exposures

The transgenic lines P*mtl-1*::GFP and P*mtl-2*::GFP were provided by Dr S. Stürzenbaum (King's College London). The generation of the promoter::GFP fusion constructs and their subsequent injection into *C. elegans* was detailed in Chapter 3 and Swain *et al.* (2004). Nematodes expressing the GFP were identified by the *roller* phenotype and were maintained on metal supplemented NGM (Section 2.7.1) from L1 to the L4 stage. The GFP signal was observed using low intensity UV light to stimulate fluorescence of the GFP. Images were taken in the presence and absence of UV light using a Nikon microscope and camera. For all GFP images the same microscope magnification and camera settings (gain and exposure time) were used to allow for direct comparison of GFP signal. The effect of cadmium, zinc, copper and BCS were observed on nematodes expressing P*mtl-1*::GFP (Figure 6.2A) and P*mtl-2*::GFP (Figure 6.2B).

There was basal expression of *mtl-1* in the pharynx which was enhanced following cadmium exposure (Figure 6.2A). There was also an increase in pharyngeal GFP signal in the presence of copper and zinc. In the absence of any heavy metal no *mtl-1* intestinal expression was observed (Figure 6.2A). Cadmium and zinc were strong inducers of intestinal expression. Although an elevated or depleted copper environment increased the GFP signal in the intestine, induction was not as potent as cadmium. Cadmium was a potent stimulator of intestinal *mtl-2* GFP expression followed by zinc whereas copper and BCS had only a marginal affect (Figure 6.2B).

A.

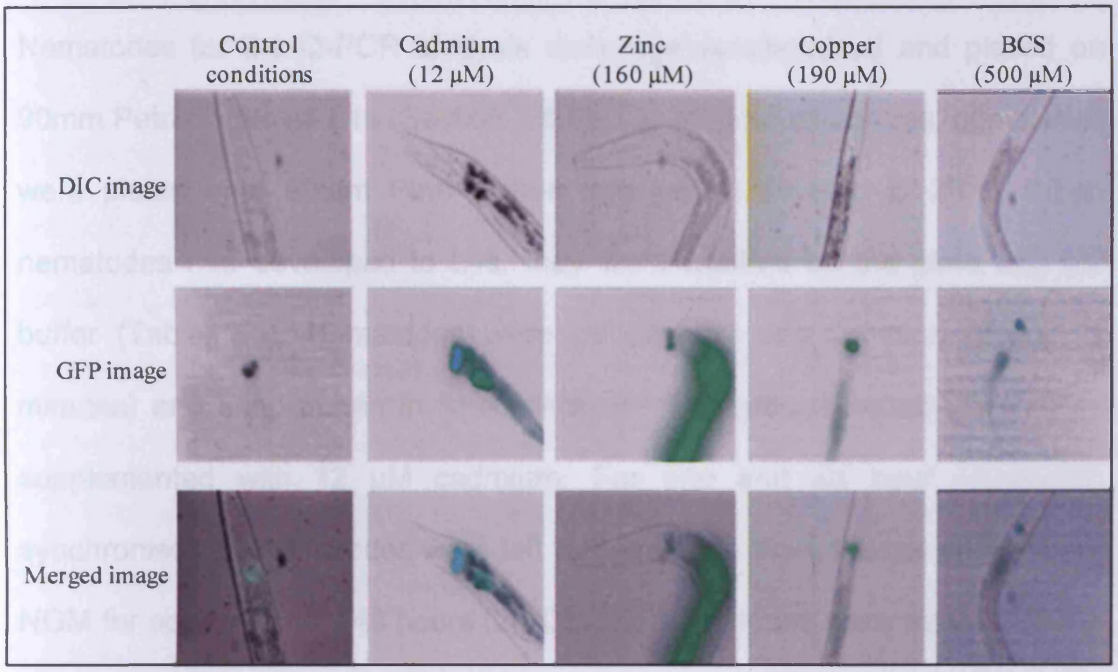

B.

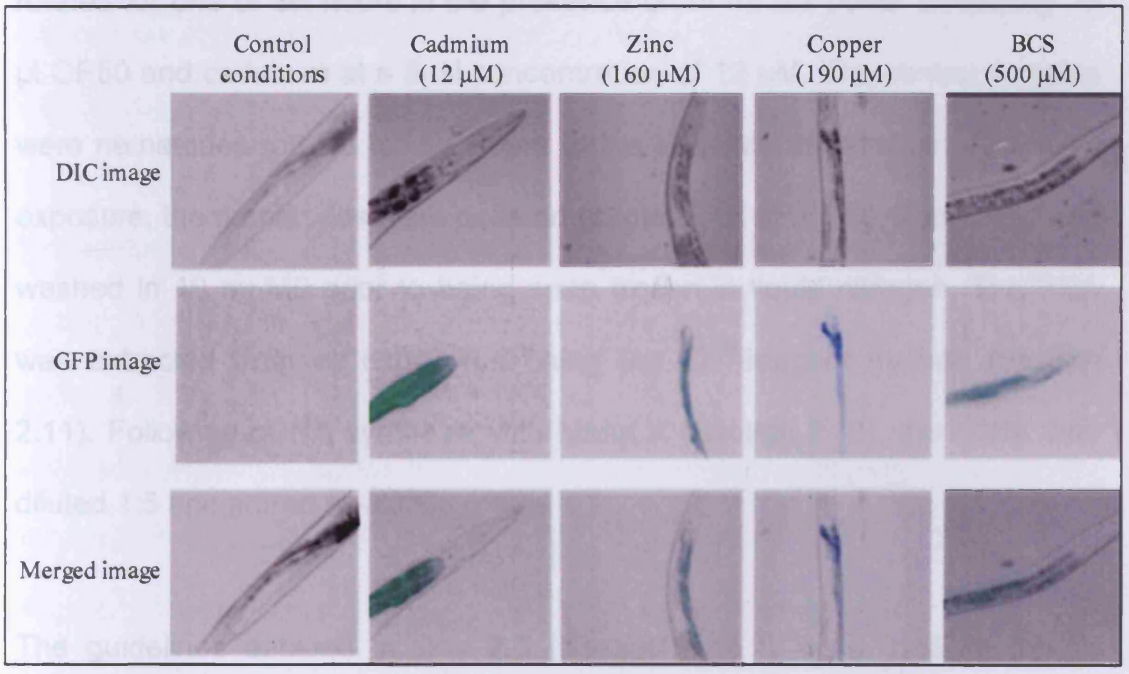

Figure 6.2: The effect of essential and non-essential heavy metals on the expression of *mtl-1* in P*mtl-1*::GP (Panel A) and in *mtl-2* in P*mtl-2*::GFP (Panel B). Transgenic lines were supplied by Dr Stürzenbaum (King's College London, UK). The nematodes were exposed to metals via metal supplemented NGM from L1 to L4 stages. Photographs were taken using a Nikon microscope and camera. The GFP images were taken under low intensity UV light at the same microscope and camera settings to allow a direct comparison between GFP signals.

6.3.2. TaqMan® Q-PCR

Nematodes for the Q-PCR analysis were age synchronised and placed on 90mm Petri dishes as L1s (Section 2.6.6). For 48 hour exposures, nematodes were plated onto 90mm Petri dishes and left to develop at 20°C. When nematodes had developed to L4s, they were washed off the plate with M9 buffer (Table 2.3). Nematodes were pelleted by centrifugation (2000g, 2 minutes) and snap frozen in liquid nitrogen. This was repeated using NGM supplemented with 12 µM cadmium. For one and six hour exposures, synchronised L1 nematodes were left to develop to the L4 stage on standard NGM for approximately 48 hours (20°C). The nematodes were washed off the plates with M9 buffer into 15 ml conical centrifuge tubes. The tubes were rotated for one or six hours in the presence of 10 ml M9 buffer containing 10 µl OP50 and cadmium at a final concentration of 12 µM. The control samples were nematodes rotated for six hours in the absence of cadmium. Following exposure, the nematodes were pelleted (centrifuged at 2000g, 2 minutes) and washed in 10 ml M9 prior to being snap frozen in liquid nitrogen. The RNA was extracted from all exposures using the Tri®-reagent method (Section 2.11). Following cDNA synthesis with MMuLV (Section 2.13), the cDNA was diluted 1:5 and stored at -20°C.

The guidelines detailed in Box 2.3 (Section 2.15.1) were used to design primers specific to each of the two genes of interest (*mtl-1* and *mtl-2*) and the housekeeping gene *rla-1*. Following amplification from N2 cDNA, the PCR product was purified and cloned into the vector pGemT (Promega) and used as a standard (Section 2.10 and 2.15.2). Purified plasmids were diluted to

ensure a starting concentration of 1 ng/µl and diluted in a 10-fold serial dilution. The same primers were used to amplify the test samples.

The TaqMan® Q-PCR experiment was performed on an ABI Prism using a 96-well plate format. As detailed in Section 2.15.4, each reaction was in 25 µl containing primers (MWG, UK), probe (MWG, UK), cDNA and Absolute ROX mix (AB Gene, UK) which was an internal standard. Data was analysed by normalising each gene to *rla-1*. A average of the three technical triplicates was taken and then used to calculate the average and standard deviation of the sample replicates. Gene expression was plotted as a ratio of *mtl/rla-1*. The gene expression at time zero was normalised to one. All gene expressions at time points one, six and 48 hours were calculated relative to the gene expression at time zero to provide a fold change in gene expression following cadmium exposure.

The relative gene expression of *mtl-1* and *mtl-2* increased with longer periods of cadmium exposure in control nematodes, N2 (Figure 6.3). The relative gene expression of wild type *mtl-1* and *mtl-2* increased over 6 hours of cadmium exposure to a relative gene expression 12±6 and 12±0.2 fold respectively. Exposure to cadmium throughout development from L1 to L4 stages, approximately 48 hours, did not significantly enhance *mtl-1* gene expression further. However, the relative gene expression of *mtl-2* at 48 hours did increase to 27.9±6.9 fold following (Figure 6.3).

There was no expression of *mtl-1* at any time point in *mtl-1(tm1770)* whereas the fold change in expression of *mtl-2* became larger following increased cadmium exposure (Figure 6.3). The fold change of *mtl-2* expression in *mtl-1(tm1770)* was approximately half that of N2 *mtl-2* at each time point. Maximal gene expression of *mtl-2* was observed after 48 hours of cadmium exposure and this was much lower than in wild type (9.1±0.3 in *mtl-1(tm1770)* compared to 27.9±6.9 in N2).

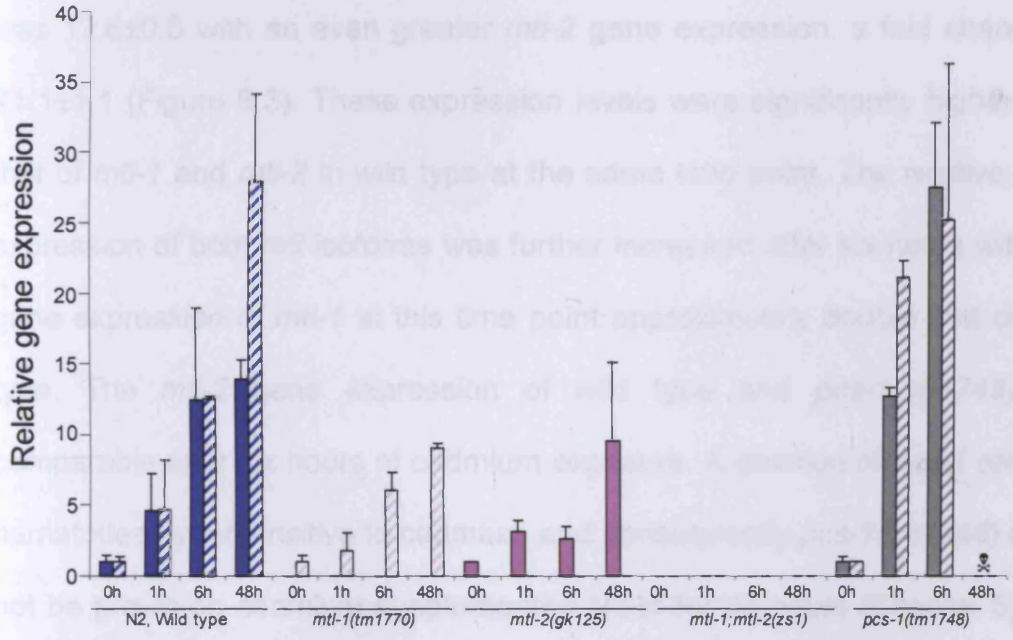

Figure 6.3: The relative expression values of *mtl-1* and *mtl-2* normalised to a housekeeping gene, *rla-1* measured using TaqMan® Q-PCR. The solid bars are *mtl-1/rla-1* and the hashed bars are *mtl-2/rla-1*. Age synchronised nematodes were placed on NGM as L1s. For 0, 1 and 6 hour exposure times, when the nematodes were at the L4 stage (approximately 48 hours) they were washed off the plates with M9 buffer into a 15 ml conical centrifuge tube. M9 buffer was added (10 ml) together with 10 µl OP50 and cadmium at a concentration of 12 µM. Samples were rotated for the stipulated time prior to washing and pelleting (centrifugation 2000g, 2 minutes). The 48 hour exposed nematodes were grown on 90mm Petri dishes seeded with 12 µM cadmium from L1 to L4 stage. When L4s the nematodes were washed off the plates and pelleted (centrifugation at 2000g, 2 minutes). All nematode pellets were snap frozen in liquid nitrogen. RNA from the pelleted nematodes was extracted by Tri®-reagent and cDNA synthesised (Sections 2.11 and 2.13). The TaqMan® Q-PCR was undertaken using specifically designed primers and probes (Section 2.15). Nematodes with the genotype *pcs-1(tm1748)* did not survive at 12 µM cadmium for 48 hours as indicated by an ☠.

The strain *mtl-2(gk125)* had a fold change in *mtl-1* gene expression which was similar after one and six hours of exposure to the heavy metal (Figure 6.3). The fold change in gene expression at these time points was much lower compared to wild type. Exposure of *mtl-2(gk125)* to cadmium for 48 hours resulted in a fold change in gene expression that was comparable to *mtl-1* in N2. There was no expression recorded for *mtl-2* in the strain *mtl-2(gk125)*. There was no expression of *mtl-1* or *mtl-2* in the double MT knockout.

In *pcs-1(tm1748), mtl-1* gene expression after one hour of cadmium exposure was 12.6±0.6 with an even greater *mtl-2* gene expression, a fold change of 21.1±1.1 (Figure 6.3). These expression levels were significantly higher than that of *mtl-1* and *mtl-2* in wild type at the same time point. The relative gene expression of both *mtl* isoforms was further increased after six hours with the gene expression of *mtl-1* at this time point approximately double that of wild type. The *mtl-2* gene expression of wild type and *pcs-1(tm1748)* are comparable after six hours of cadmium exposure. A deletion of *pcs-1* renders nematodes hypersensitive to cadmium and consequently *pcs-1(tm1748)* could not be grown on cadmium supplemented NGM for 48 hours (Chapter 5) and as a result no Q-PCR could be performed.

Figure 6.4 shows the fold change in relative expression of wild type *mtl-1* and *mtl-2* following exposure to 50 µM cadmium for 48 hours. The fold change of *mtl-1* and *mtl-2* were similar in the presence of cadmium (50 µM). There was a greater fold change in gene expression of *mtl-1* at 50 µM cadmium compared to that at 12 µM (Figures 6.4 and 6.5). The fold change in gene

expression of *mtl-2* was comparable at 12 µM and 50 µM cadmium. The majority of cadmium exposed samples (Figure 6.3 and 6.4) had large error bars. The errors were calculated from standard deviation. Generally, as nematodes were exposed to cadmium for longer periods of time, the size of the error bars increased.

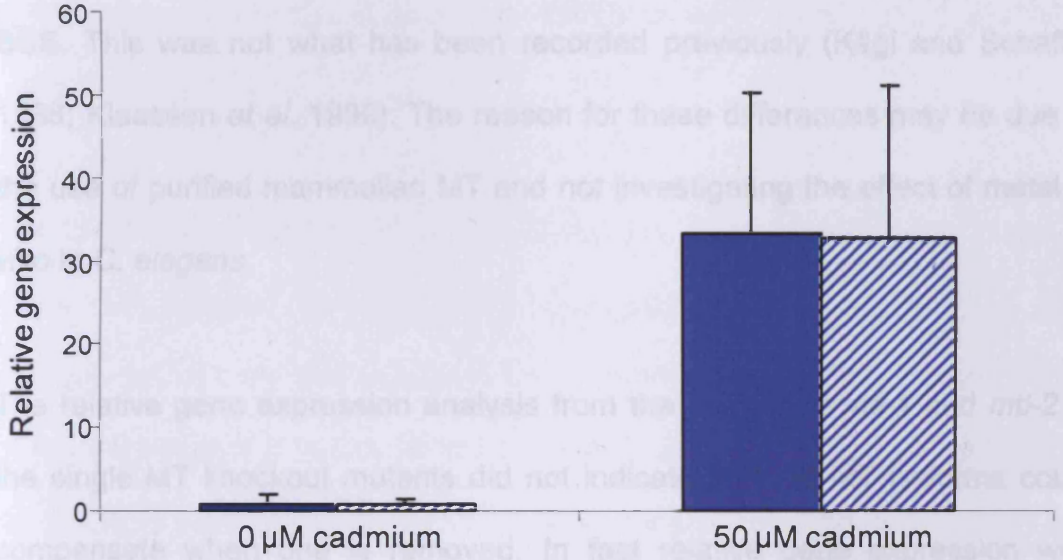

Figure 6.5: Relative gene expression of N2 to 50 µM cadmium levels for 48 hours. Filled bars are *mtl-1/rla-1* and hashed bars are *mtl-2/rla-1*. N2 nematodes were grown for 48 hours from the L1 to L4 stage on control NGM or NGM seeded with cadmium (50 µM). Nematodes were washed off the plate with M9 buffer when at the L4 stage. Nematodes were pelleted by centrifugation (2000g, 2 minutes) and snap frozen in liquid nitrogen. The RNA was extracted by Tri®-regent method and cDNA synthesised using MMuLV (Section 2.11 and 2.13). The TaqMan® Q-PCR was undertaken using specifically designed primers and probes (Section 2.15).

6.4. Discussion

The strong GFP signal from the transgenic nematodes confirmed that cadmium is a potent inducer of *mtl-1* and *mtl-2* (Figure 6.2). Thus the use of cadmium to stimulate *mtl* transcription in the Q-PCR experiment was justified. Zinc was also a potent enhancer of *mtl* transcription. Elevated or depleted copper environments did not significantly induce the transcription of either isoform of MT. Therefore the order of potency was cadmium $\geq$ zinc > copper $\geq$ BCS. This was not what has been recorded previously (Kägi and Schaffer 1988; Klaassen *et al.* 1999). The reason for these differences may be due to the use of purified mammalian MT and not investigating the effect of metal *in vivo* in *C. elegans*.

The relative gene expression analysis from the Q-PCR of *mtl-1* and *mtl-2* in the single MT knockout mutants did not indicate that the MT isoforms could compensate when one is removed. In fact relative gene expression was markedly reduced in the single MT knockout strains. It is possible that there was another mechanism which becomes up regulated in the absence of MT. The presence of a functional PC in *C. elegans* has been proposed in previous chapters as a preferred mechanism of metal detoxification above MT. However, the presence of two detoxification systems is not unusual. Plants and yeast have been shown to contain both MT and PC which are stimulated by cadmium (Gonzalez-Mendoza *et al.* 2007). In organisms where both complementary chelating proteins are present, one may be used in preference to the other unless that protein is compromised in some way (Gonzalez-Mendoza *et al.* 2007; Yu *et al.* 1994; Zhang *et al.* 2005; Zhou and

Goldsbrough 1994). If *C. elegans* MT and PC can work in combination, as in other organisms, it would explain why single MT mutants did not show a compensatory increase in gene expression of the remaining isoform. The change in MT gene expression in the *pcs-1* null strain *pcs-1(tm1748)* can be quantified using Q-PCR. This strain does not express a functional PC synthase and as a result cannot generate PC. Using a Ppcs-1::GFP transgenic strain, the PC synthase was not markedly upregulated by cadmium (Chapter 3), the change in gene expression of *pcs-1* could not be quantified using Q-PCR.

The Q-PCR analysis of *mtl-1* and *mtl-2* expression showed that expression of these two genes is significantly upregulated in *pcs-1(tm1748).* The upregulation of *mtl-1* and *mtl-2* may be a method of compensating for the loss of PC. Additionally if PCs were the preferred route of cadmium detoxification, there would be no requirement to increase *mtl* transcription in the single MT deletion strains, a result which was observed in the Q-PCR analysis. Another hypothesis to explain the low levels of *mtl* gene expression in *mtl-1(tm1770)* and *mtl-2(gk125)* is that when one *mtl* isoform is absent, more PCs are generated to chelate cadmium ions which results in a reduction in the stimulation of MT transcription. The only way to truly validate this hypothesis is to measure the level of PC directly or to measure the activity of PC synthase. One way in which this could be achieved would be using western blotting. Li *et al.* (2001) used monoclonal antibodies for a western blot and enzyme linked immunosorbant assay to study the activity of enzymes including PC synthase. Unfortunately there were not any antibodies specific to

C. elegans pcs-1 available to undertake this type of experiment. However, using mass spectrometry the overall levels of PC *in vivo* were calculated as described in detail in Chapter 4. Briefly, exposure to cadmium significantly increased the levels of PC. Thus, in the absence of one or both MT isoforms, PC may be used in the detoxification of cadmium in preference to MT. When PCs are not present then both MT isoforms are upregulated in response to elevated cadmium levels to enable the cell to return to optimal physiological conditions.

In the majority of cadmium exposed Q-PCR samples, there were large error bars (standard deviation). The error increased relative to the duration of cadmium exposure, with errors approximately 50% of the measured gene expression. For example, the relative gene expression of N2 *mtl-1* following one hour exposure to cadmium (12 μM) was 4.6±2.5 and after six hours was 12.4±6.4 (Figure 6.3). There are three aspects of the Q-PCR process that can generate error. Firstly, error can arise from technical or manual mistakes. The standard curve provides an indicator of technical error. Curves are generated from amplified cDNA cloned into pGemT. They are diluted in a 10-fold serial dilution and plated out in triplicate on the Q-PCR plate. Following amplification in the ABI Prism, the number of PCR cycles between each dilution should be 3.3 with all triplicates lying on top of one another. The slope of the standard curve should have an R^2 of 1, although most are between 0.95 and 0.99. Any significant deviation from this value is due to technical error. In all Q-PCR experiments, a standard curve was run on each plate and any runs with a standard curve slope where the R^2 deviated from 0.95 were discarded. This

reduced technical error between runs and due to the machine. Technical and human error was reduced further by running all samples in triplicate. The triplicate samples had to be within 0.5 C_T values of each other, which meant that one of the triplicates was occasionally removed. In addition the C_T values of the unknown samples should fall within the range as dictated by the standard curve (1 ng to 1 fg). Any C_T values outside this range were considered to be below the detection limit of the machine and discarded. If manual or technical faults were a significant factor, all samples (exposed and non-exposed) would be affected and this was not observed.

A second source of variation can be of biological nature. Biological variation may arise due to a different threshold level of MT activation between individual nematodes. It may be possible that a cadmium concentration of 12 µM is not sufficiently toxic to be able to activate transcription of *mtl* genes in all members of the population. To test this hypothesis, N2 were exposed to 50 µM cadmium (Figure 6.4). Following sample preparation and Q-PCR analysis as previously described, the error bars at 50 µM are still approximately 50% of the mean. Finally, error can be due to poor efficiency of the reverse transcriptase enzyme during RNA extraction. The concentration of RNA was quantified and an appropriate volume used to ensure that 500ng RNA was present in each reaction mix. This was done as accurately as possible but error could arise through pipetting. In conclusion, the error may arise as a combination of inefficient reverse transcription and biological variation.

6.5. Conclusion

Cadmium and zinc are potent inducers of *mtl* transcription. The presence of excess copper or an environment depleted in copper will enhance transcription, but not to the same extent as cadmium or zinc ions. In both *mtl-1* and *mtl-2*, the presence of heavy metal is required to induce transcription in the intestine. The length of time from six to 48 hours is typical for a transcriptional response to occur and expression of MT, in particular *mtl-2*, increased most dramatically within this time frame. It can be hypothesised that as PCs are already present in the cell at physiological metal concentrations (Grill *et al.* 1987; Grill *et al.* 1989), there is a pool of readily available PC to sequester heavy metals upon immediate metal challenge. In contrast *mtl* genes must be stimulated by an as yet unknown factor to increase transcription and produce more MT. This is a slower process and is not suitable as a mechanism for immediate detoxification of acute toxicity.

Q-PCR analysis indicated that there was no compensation between the two individual MT isoforms, indicating that the two isoforms function independently of each other. The relative gene expression of *mtl-1* and *mtl-2* was upregulated in the absence of a functional PC synthase. Although this provides *pcs-1* null nematodes with the means to survive acute cadmium toxicity it is not sufficient for survival for extended periods of metal exposure. Again, this indicates that PC are of vital importance in cadmium detoxification.

CHAPTER SEVEN

TRANSCRIPTIONAL CONTROL OF METALLOTHIONEIN

7.1 Introduction

As shown previously, organisms must regulate the physiological concentration of heavy metals for continued reproduction, growth and development. MTs have been shown in Chapter 6 to be up regulated following cadmium exposure. Control of MT occurs at the transcriptional level by the presence of cations such as cadmium, copper and zinc (Gonzalez-Mendoza *et al.* 2007; Swain *et al.* 2004; Zhang *et al.* 2005). In vertebrates, metal induction of MT is achieved via a metal responsive transcription factor, MTF-1. The MTF-1 binds metal ions and the complex binds sequence specific metal responsive elements located in the promoter regions of MT (Andrews 2000; Freedman *et al.* 1993; Saydam *et al.* 2002; Stuart *et al.* 1984). The *C. elegans* genome does not contain the transcription factor MTF-1 nor do the promoters of the gene contain functional metal responsive elements (Freedman *et al.* 1993). As a result it is still not fully understood what stimulates *C. elegans* MT transcription following metal challenge. Now that the genome has been fully sequenced (Consortium 1998), it is possible to screen the genome for any suitable genes which code for proteins affecting MT transcriptional regulation. To investigate the gene-specific loss-of-function phenotypes RNA interference (RNAi) can be performed (Kamath *et al.* 2000). RNAi is a mechanism which results in the sequence specific silencing of homologous messenger RNA (Sijen *et al.* 2001).

7.1.1 RNA interference approaches

In 1998 Andrew Fire discovered that the silencing of a gene occurred when the complementary double stranded RNA (dsRNA) was injected into *C. elegans* (Fire *et al.* 1998). This led to Fire and his co-worker Craig Mello being awarded the 2006 Nobel Prize in Physiology and Medicine for what is now known as RNAi. RNAi has become a widely used mechanism for targeted gene inactivation (Kamath and Arhringer 2003). RNAi functions on the basis of dsRNA being incorporated into a protein which will bind to complementary RNA and prevent its translation. The process is summarised in Figure 7.1. There are three types of dsRNA. Firstly, there are endogenous dsRNAs which arise from microRNAs. The nucleus contains microRNAs (miRNA) which are short sequences of RNA containing multiple hairpin loops. Individual loops are excised by an enzyme called Drosha resulting in a short hairpin loop RNA sequences (shRNA) of 21 nucleotides. The shRNA is transported out of the nucleus into the cytosol. Exogenous short interfering RNAs (siRNA) as a result of viral infection are also present in the cytosol as well as dsRNA from manual injection. All short dsRNA molecules in the cytosol are processed in the same way. An RNAse III enzyme, Dicer, creates a 3' overhang of the dsRNA duplex (Buckingham *et al.* 2004). The RNA is unwound and one half of the duplex incorporated into an RNA induced silencing complex (RISC) protein (Buckingham *et al.* 2004). The multi-subunit RISC protein containing the single strand RNA binds complementary mRNA sequences, ultimately resulting in the silencing or cleavage of the mRNA.

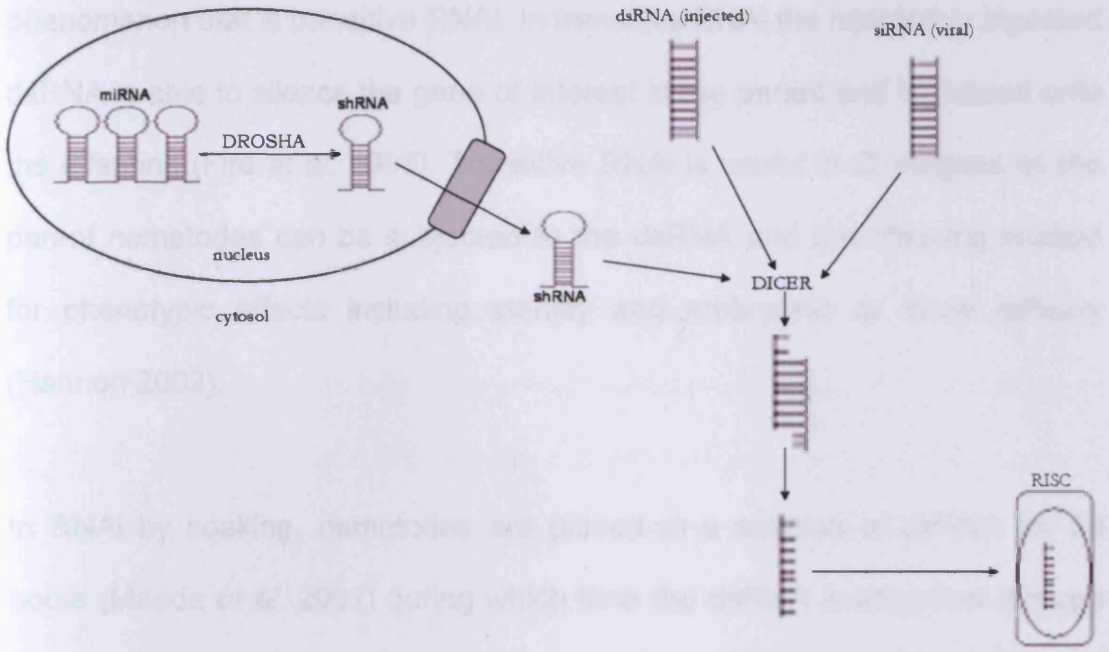

Figure 7.1: Mechanism of RNA interference. The nucleus contains micro RNAs (miRNA). Single hairpin loops of 21 nucleotides are cleaved and exported from the nucleus. In the cytosol there are many types of short double stranded RNAs, including short interfering RNAs (siRNA) from viral infections. All dsRNAs are cleaved by an RNAse enzyme, Dicer, and after being unwound one strand is incorporated into a multi-subunit RNA induced silencing complex (RISC) protein. The RISC-RNA complex can then cleave complementary sequences. Adapted and re-drawn from Meister and Tuschl (2004).

Initially synthetic dsRNA was inserted directly into cells via microinjection. As dsRNA can cross cell membranes the point of injection is not highly critical (Kamath *et al.* 2000). However, microinjection is a laborious process as only one gene can be injected at a time. Additionally, early adult *C. elegans* are used in injections; consequently, the occurrence of sterile phenotypes is reduced as there is less time for the germline to be affected by injected RNA prior to the onset of reproduction (Kamath *et al.* 2000; Kamath and Arhringer 2003). Two other methods to expose dsRNA to *C. elegans* have been developed both of which can be modified for high throughput RNAi. These methods are soaking and feeding (Kamath *et al.* 2000). All three mechanisms

of dsRNA exposure in *C. elegans* (injection, feeding and soaking) rely on the phenomenon that is transitive RNAi. In transitive RNAi the injected or ingested dsRNA is able to silence the gene of interest in the parent and is passed onto the offspring (Fire *et al.* 1998). Transitive RNAi is useful in *C. elegans* as the parent nematodes can be subjected to the dsRNA and the offspring studied for phenotypic effects including sterility and embryonic or larval lethality (Hannon 2002).

In RNAi by soaking, nematodes are placed in a solution of dsRNA for 24 hours (Maeda *et al.* 2001) during which time the dsRNA is absorbed through the cuticle and via ingestion. Following soaking, nematodes are transferred to a new NGM plate and the progeny studied for phenotypic effects (Maeda *et al.* 2001). The process of RNAi by feeding was first described in 1998 (Timmons and Fire 1998). RNAi by feeding involves feeding L3 stage nematodes the *E. coli* strain HT115(DE3) containing dsRNA for the gene of interest (Kamath and Arhringer 2003). Nematodes are then incubated at 20°C and the offspring monitored for phenotypic effects. RNAi by feeding relies on the dsRNA for the gene of interest being eaten, absorbed through the gut and incorporated into somatic and germ line cells (Kamath *et al.* 2000). RNAi by feeding and soaking methods has an advantage over injection in that feeding nematodes RNAi or soaking them in RNAi allows more time for the gonad or germline cells to be affected by the dsRNA (Kamath *et al.* 2000; Kamath and Arhringer 2003). Both RNAi by soaking and feeding have a similar effectiveness of gene silencing but they are less efficient than silencing by injection (Maeda *et al.* 2001; Tabara *et al.* 1998). The disadvantage of RNAi by soaking and

feeding is that although genes in somatic cells are silenced efficiently, the genes in the nervous system are not. In addition silencing by feeding can take longer to have an effect and can potentially be more variable (Kamath *et al.* 2000).

C. elegans is ideally suited for RNAi screens primarily because the genome of this model organism has been fully sequenced and annotated (Buckingham *et al.* 2004). As a result of the *C. elegans* sequencing project an RNAi library is available through the Medical Research Council Gene Service. The library contains 16750 bacterial strains corresponding to 86% of the *C. elegans* genome (Kamath and Arhringer 2003). Briefly, the library was created by amplifying all predicted genes and cloning the PCR products into the vector L4440 (Kamath and Arhringer 2003). The L4440 vector contains T7 promoter sites and in the presence of isopropyl-β-D-thiogalactopyranoside (IPTG) the expression of T7 RNA polymerase is induced (Kamath and Arhringer 2003). The feeding vector was transformed into an RNase III deficient strain of *E. coli* namely HT115(DE3). Induction of T7 polymerase in HT115(DE3) by IPTG generates dsRNA of the gene of interest (Kamath and Arhringer 2003). The H115(DE3) bacteria are fed to nematodes and, following digestion of the bacteria, dsRNA is absorbed through the intestinal wall. The dsRNA extends throughout the nematode and into any offspring via transitive RNAi (Kamath and Arhringer 2003). The nematodes are allowed to reproduce and the offspring studied for any phenotypic effects (Kamath and Arhringer 2003).

7.1.2 Yeast one Hybrid (Y1H) approach

The yeast one hybrid (Y1H) system is a powerful way to identify protein-DNA interactions following the isolation of individual targets from an RNAi screen (Izumchenko *et al.* 2007; Lopato *et al.* 2006). The advantage of the Y1H system is that the DNA-protein interactions take place *in vivo* and as such the proteins and DNA are in the native conformation (Lopato *et al.* 2006). The presence of two vectors is central to the Y1H mechanism. One vector contains a transcription factor of interest while the second vector contains a reporter gene fused in-frame to a *cis*-acting element. Both vectors are co-transformed into the yeast *Saccharomyces cerevisiae*. When the transcription factor binds to the *cis*-acting element in the promoter, the reporter gene is expressed (Figure 7.2) (Izumchenko *et al.* 2007).

Figure 7.2: The mechanism of action of the yeast one hybrid system. The transcription factor containing activation and DNA binding domains will bind to a *cis*-acting element within the gene promoter. The promoter is fused in-frame to a reporter gene such as *LacZ*. Upon induction of the gene, when bound by the transcription factor, β-galactosidase is transcribed. β-galactosidase cleaves the colourless OPNG (*ortho*-nitrophenyl-β-D-galactoside) to nitrophenol, a yellow product, which can be measured colorimetrically. Adapted from Izumchenko *et al.* (2007) and Serebriiskii and Golemis (2000).

The reporter gene used in Y1H experiments is commonly *LacZ*. The *LacZ* gene codes for the enzyme β-galactosidase whose activity can be measured colorimetrically (Serebriiskii and Golemis 2000). The colourless substrate

OPNG (*ortho*-nitrophenyl-β-D-galactoside) is cleaved by β-galactosidase to the yellow coloured product nitrophenol which can be quantitatively assayed (Serebriiskii and Golemis 2000). The induction of *LacZ* is representative of the level of transcriptional activation the transcription factor has on the *cis*-acting element (Serebriiskii and Golemis 2000).

7.2 Aims

An RNAi by feeding screen was used to identify potential transcription factors which affect the transcription of *mtl-1* and *mtl-2*. The screen was performed in the presence and absence of cadmium (12 µM) using the transgenic strains P*mtl-1*::GFP and P*mtl-2*::GFP. Potential candidate genes were validated by Q-PCR. Finally, the inductive potential for each validated transcription factor on the promoters of *mtl-1* and *mtl-2* were investigated using a Y1H system.

7.3 Results

7.3.1 The RNAi screen

An RNAi screen was carried out to identify any potential candidates which affect the transcriptional control of either *mtl-1* or *mtl-2*. A targeted subset of the RNAi library was produced by identifying transcription factors which bound DNA in response to a cellular signal using gene ontology, or GO terms. GO terms annotate and group genes within a limited set of attributes. Broadly, genes are organised into groups based on their involvement in biological processes, molecular functions and those which are cellular components. In this study the GO terms of interest are those which contain the most inclusive set of daughter terms related to transcriptional regulation and DNA binding. AmiGo (www.amigo.geneontology.org), an online database controlled by NCBI, was used to search for genes within the two GO terms of interest.

The parental GO term GO:0003677 corresponds to DNA binding functions and has 5383 member proteins in 7 daughter terms (Box 7.1). Transcriptional regulation is defined by the term GO:0030528 and includes any proteins with regulator activity or activity which is required to initiate transcription in 14 daughter terms, 3315 members in total (Box 7.1). Gene products can be included under more than one GO term thus duplicates were removed. In addition, a number of genes identified in this manner cause embryonic or larval lethal phenotypes when silenced in RNAi screens. Consequently lethal genes were removed from the screen. The targeted subset based on the two

GO terms with duplicates and lethal genes removed resulted in 406 potential effectors of *C. elegans* MT gene transcription.

■ DNA Binding GO:0003677
□Structure-specific DNA binding (GO:0043566) comprising of 41 members
□Damaged DNA binding (GO:0003684) comprising of 79 members
□DNA bending activity (GO:0008301) comprising of 2 members
□DNA clamp loader activity (GO:0003689) comprising of 2 members
□DNA topoisomerase activity (GO:0003916) comprising of 93 members
□Sequence-specific DNA binding (GO:0043565) comprising of 2211 members
□Transcription factor activity (GO:0003700) comprising of 3550 members

■ Transcriptional Regulation GO:0030528
□Two-component response regulator activity (GO:0000156), 13 members
□Transcription factor activity (GO:0003700) comprising of 3550 members
□RNA polymerase I transcription factor activity (GO:0003701), 2 members
□RNA polymerase II transcription factor activity (GO:0003702), 116 members
□RNA polymerase III transcription factor activity (GO:0003709), 3 members
□Transcriptional elongation regulator activity (GO:0003711), 22 members
□Transcription cofactor activity (GO:0003712) comprising of 80 members
□Transcription termination factor activity (GO:0003715), 10 members
□Transcriptional activator activity (GO:0016563) comprising of 84 members
□Transcriptional repressor activity (GO:0016564) comprising of 61 members
□Transcription initiation factor activity (GO:0016986), 38 members
□Transcription initiation factor antagonist activity (GO:0016988), 4 members
□Negative regulator of basal transcription activity (GO:0017163), 2 members
□Transcription anti-terminator activity (GO:0030401) comprising of 4 members

Box 7.1: List of the inclusive daughter members related to DNA binding, GO:0003677 and transcriptional regulation, GO:0030528. DNA binding comprises 5383 members in 7 daughter terms and transcriptional regulation has 3315 members in 14 daughter terms. Any lethal phenotypes were removed as were duplicated genes. Ultimately there were 406 potential regulators of transcription identified from these two terms.

Two GFP strains of *C. elegans* were used, namely P*mtl-1*::GFP and P*mtl-2*::GFP (Chapter 3). Age synchronised nematodes were grown on NGM plates from the L1 stage. Nematodes (L3/L4 stage) were washed off NGM plates with M9 buffer (Table 2.3), pelleted (2000g, 2 minutes) and resuspended in sufficient M9 buffer to ensure that 1-2 nematodes were present in 1 µl M9

buffer (Section 2.14.2). Each well on a multi-well plate was seeded with a single *E. Coli* feeding strain containing one of the 406 genes of interest. Nematodes (5 µl) were distributed into each well and incubated at 20°C. The offspring were monitored for fluorescence at the L2/L3 stage (Figure 7.3). The screen was performed in the presence and absence of cadmium (12 µM).

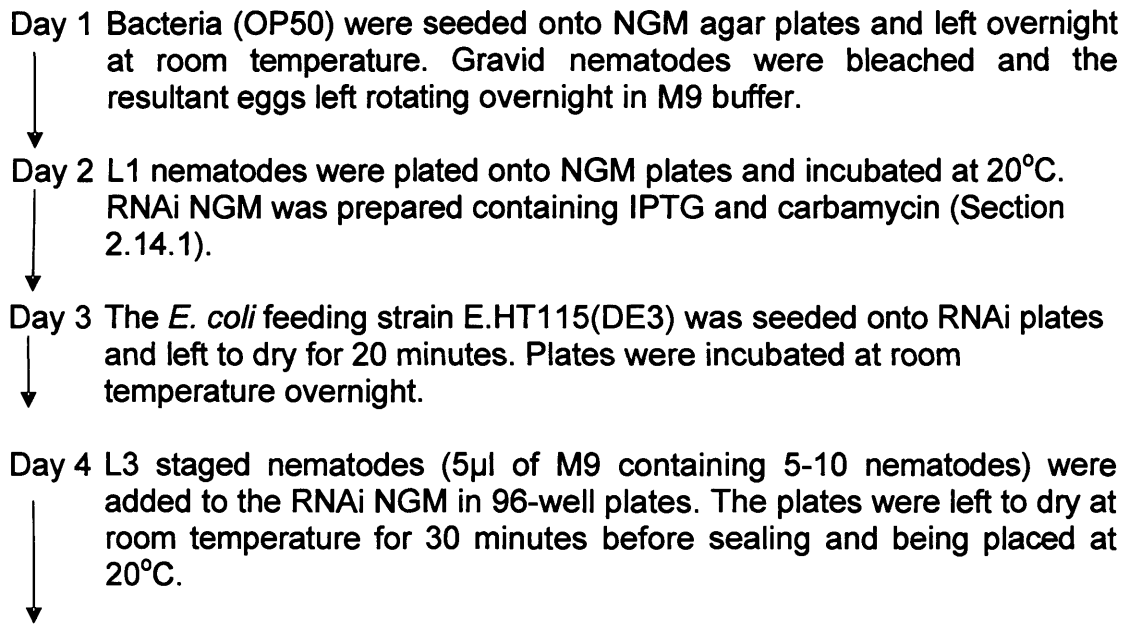

Figure 7.3: Flow diagram describing the RNAi screen. The protocol was adapted from Kamath and Arhringer (2003) using the GFP expressing *C. elegans* strains P*mtl-1*::GFP and P*mtl-2*::GFP provided by Dr Stephen Stürzenbaum (King's College London). More details of the experiment are given in Chapter 2 Section 2.14.

Fluorescent signals were recorded on a scale of 0 to 3 for the pharynx and intestine of *mtl-1* and the intestinal GFP expression of *mtl-2*. Genes which caused no response had a score of 0, for example when the intestinal *mtl-1* and *mtl-2* are "off" in the absence of cadmium. As the GFP signal increased in intensity, a higher value was recorded. A score of 3 was given if the GFP

signal was "superbright". "Superbright" indicated a fluorescence which was much stronger than the norm and could occur in the presence or absence of cadmium for either MT isoform. A diagram showing the strength of the GFP signal and the corresponding score is given in Figure 7.4.

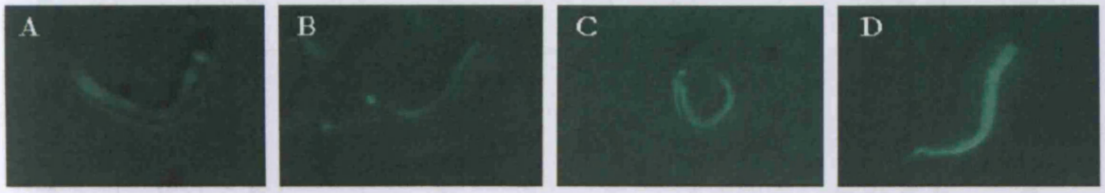

Figure 7.4: Digital images to explain the scoring system used to measure GFP intensity. The images were taken using a Nikon microscope and camera with the same optics as would be used when observing fluorescence during the RNAi screen. Panel A shows the pharynx and intestine with a score of "1" for both as the fluorescence is minimal. Panel B shows P*mtl-1*::GFP where the pharynx has a GFP intensity of "2" while the intestinal intensity is recorded as "1". Panel C indicates two P*mtl-1*::GFP nematodes with both pharynx and intestine of an intensity recorded as "2". Finally Panel D is the strain P*mtl-2*::GFP which is "superbright", an intensity of "3".

The targeted RNAi screen with 406 genes was repeated in triplicate in the presence and absence of cadmium. The genes which consistently affected MT transcription were isolated and screened again. From this second screen, 10 genes were identified which were of interest. These genes were screened in triplicate to remove false positives. Each successive screen reduced the number of potential genes which affected transcription leaving five candidate genes. The raw data from each screen are given in Appendix 3, with the average of the final results for the five candidate genes shown in Table 7.1.

Gene	Location	Cadmium Concentration	GFP signal					
			Control	*cey-1 (F33A8.3)*	*nhr-64 (C45E1.1)*	*ceh-5 (C16C2.1)*	*his-3 (T10C6.12)*	*C25F9.5*
mtl-1	Pharynx	0 µM	**1 or 2**	1	2	1	2	1
mtl-1	intestine	0 µM	**0**	1	2	2	1	1
mtl-2	intestine only	0 µM	**0**	2	3	2	2	2
mtl-1	pharynx	12 µM	**1 or 2**	2	2	2	1	2
mtl-1	intestine	12 µM	**1 or 2**	2	2	2	2	2
mtl-2	intestine only	12 µM	**1 or 2**	2	3	3	2	3

Table 7.1: Results of the RNAi screen. Each P*mtl*::GFP fusion strain was studied in the presence and absence of 12 µM cadmium. P*mtl-1*::GFP was monitored for fluorescence in the pharynx and intestine and P*mtl-2*::GFP in the intestine. Age synchronised L3/L4 nematodes were fed HT115(DE3) containing a dsRNA for one of the transcription factors identified by gene ontology. The offspring were monitored for a fluorescent signal. Each number represents relative fluorescent signal as observed manually and detailed in Figure 7.5. The scale of fluorescence is from 0-3 where 0 is no observed GFP signal and 3 is "superbright" (see Figure 7.4).

The pharyngeal *mtl-1* GFP signal in the RNAi knockdown of *ceh-5(C16C2.1), cey-1(F33A8.1)* and *C25F9.5* was present at low levels in the absence of cadmium. Following exposure to the heavy metal, the expression of pharyngeal *mtl-1* was marginally increased. The inducibility of pharyngeal *mtl-1* expression was lost in *nhr-64(RNAi)*. In *his-3(T0C6.1)* the fluorescent signal in the pharynx decreased following cadmium exposure. With the exception of *C25F9.5(RNAi)* and *ceh-5(RNAi)*, the knockdown by RNAi in the absence of cadmium resulted in the intestinal *mtl-1* expression to be "on", at low levels (Table 7.1). Exposure to cadmium resulted in the fluorescent signal of intestinal *mtl-1* to increase but not to "superbright" levels.

The RNAi induced knockdown of the five candidate genes resulted in the observation of a GFP signal from *mtl-2* in intestinal cells in the absence of cadmium (Table 7.1). The presence of cadmium increased fluorescence to "superbright" levels during the knockdown of *ceh-5(C16F9.5)* and *C25F9.5*. The remaining three genes (*nhr-64(C45E1.1), cey-1(F33A8.3)* and *his-3(T10C6.1)*) did not show metal inducibility of *mtl-2* gene expression.

7.3.2 Quantitative polymerase chain reaction

Two of the genes from the screen were available as deletion mutant strains which were both obtained from the CGC. The mutant RB1592 contained the deletion allele *C45E1.1(ok1957)* (Figure 7.5A) and the deletion allele *F33A8.3(ok1805)* was in the mutant strain VC1310 (Figure 7.5B). No deletion strains were available for *ceh-5(C16C2.1), his-3(T10C6.12)* and *C25F9.5*.

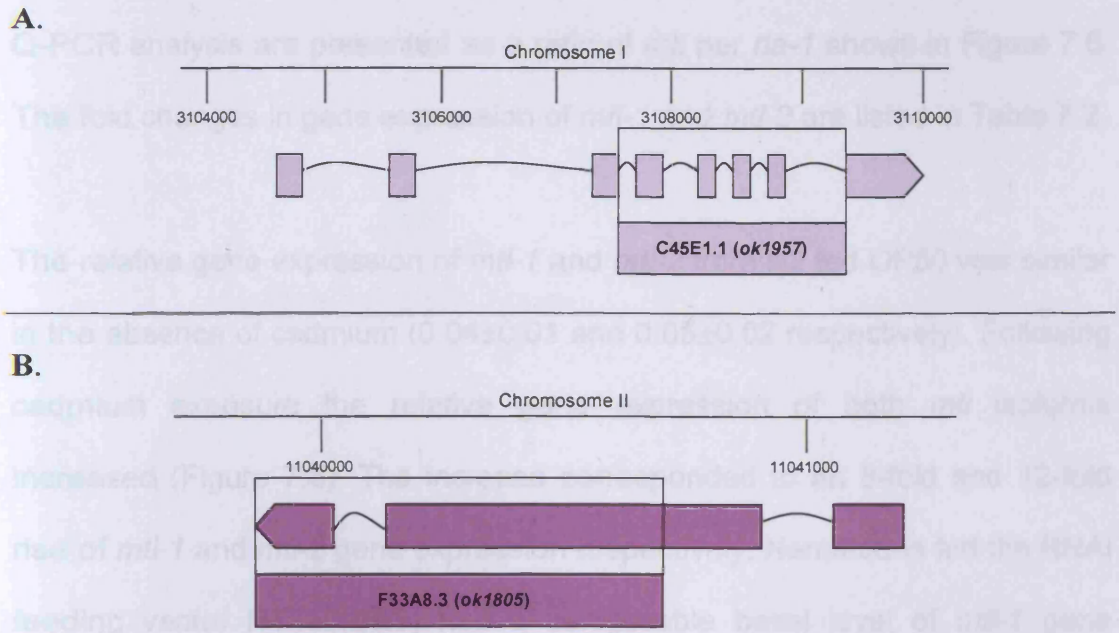

Figure 7.5: Schematic representations of the knockout strains provided from the *Caenorhabditis* Genetics Centre (CGC). The strain RB1592 is a deletion of *C45E1.1(ok1957)* where 4 exons are deleted from the centre of the transcript (Panel A). The CGC provided the deletion allele *F33A8.3(ok1805)* as the mutant strain VC1310 (Panel B). In VC1310, the entire first exon and part of the second coding exon are deleted.

The deletion strains *nhr-64(ok1957)* and *cey-1(ok1805)* were age synchronised and grown from L1 to L4 on OP50 seeded NGM plates in the presence and absence of cadmium (12 µM) prior to Q-PCR analysis. For those genes where deletion strains were not available, staged L1 Bristol N2 nematodes were placed on RNAi plates (Section 2.14.1) seeded with the HT115(DE3) feeding vector containing the dsRNA for the gene of interest, namely *ceh-5(C16F9.5), his-3(T10C6.12)* or *C25F9.5(C25F9.5).* In all cases nematodes were washed off the plates with M9 buffer when they had developed to the L4 stage. RNA extraction by the Tri®-reagent method and cDNA synthesis with MMuLV was performed as in Sections 2.11 and 2.13. Taqman® Q-PCR analysis was undertaken for the genes, *mtl-1* and *mtl-2* with *rla-1* measured by Q-PCR as a housekeeping (control) gene using the

protocol as described in Section 2.15 and Chapter 6. The results of the Q-PCR analysis are presented as a ratio of *mtl* per *rla-1* shown in Figure 7.6. The fold changes in gene expression of *mtl-1* and *mtl-2* are listed in Table 7.2.

The relative gene expression of *mtl-1* and *mtl-2* from N2 fed OP50 was similar in the absence of cadmium (0.04±0.01 and 0.05±0.02 respectively). Following cadmium exposure the relative gene expression of both *mtl* isoforms increased (Figure 7.6). The increase corresponded to an 8-fold and 12-fold rise of *mtl-1* and *mtl-2* gene expression respectively. Nematodes fed the RNAi feeding vector HT115(DE3) had a comparable basal level of *mtl-1* gene expression to OP50 fed nematodes. Following metal exposure for 48 hours the relative expression of *mtl-1* increased 18-fold. Under control conditions the expression of *mtl-2* from nematodes fed HT115(DE3) was greater than OP50 fed N2s (0.09±0.08 compared to 0.05±0.02) and the presence of cadmium increased *mtl-2* gene expression 8-fold.

The RNAi knockdown of *ceh-5(C16F9.5)* and *his-3(T10C6.12)* resulted in the basal levels of *mtl-1* and *mtl-2* gene expression to be greater than in controls (N2 fed HT115(DE3)). In all RNAi knockdown experiments, the expression of *mtl-1* was similar to or greater than *mtl-2* gene expression (Figure 7.6). In contrast the deletion strains *cey-1(ok1805)* and *nhr-64(ok1957)* had a lower basal expression of *mtl-1* and *mtl-2* than in control nematodes (N2 fed OP50).

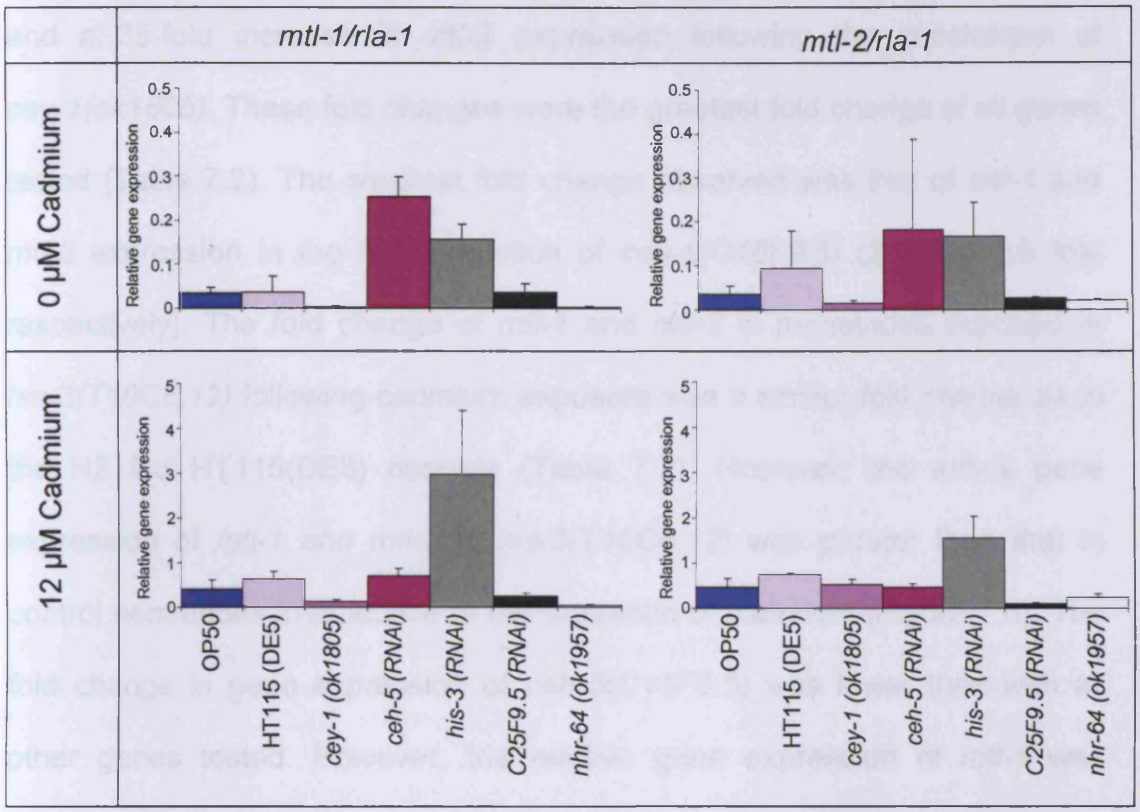

Figure 7.6: Quantitative PCR results. Deletion strains (*cey-1(ok1805)* and *nhr-64(ok1957)*) were grown on OP50 seeded NGM from L1 to L4 stage. N2 were grown on RNAi NGM with the dsRNA for *ceh-5(C16C2.1)*, *his-3(T10C6.12)* or *C25F9.5*. When L4, all nematodes were washed off the plates, pelleted and RNA extracted (Section 2.11) and cDNA synthesised (Section 2.13). The relative gene expression of *mtl-1*, *mtl-2* and *rlp-1* in the presence of cadmium were measured. Note the difference in scales.

Strain or RNAi knockout	*mtl-1/rla-1*		*mtl-2/rla-1*	
	average	error	average	error
OP50	8.2	2.3	12.4	4.0
HT115 (DE5)	17.7	4.7	7.9	0.6
cey-1 (ok1805)	47.6	11.0	34.9	8.1
nhr-64 (ok1957)	17.0	2.3	10.7	3.9
ceh-5 (RNAi)	2.8	0.6	2.5	0.6
his-3 (RNAi)	19.1	9.1	9.4	2.8
C25F9.5 (RNAi)	6.9	1.7	3.9	1.0

Table 7.2: The fold change in gene expression following cadmium exposure. Following Q-PCR analysis and normalisation, the change in gene expression of *mtl-1/rla-1* and *mtl-2/rla-1* was tabled. Errors are standard deviations.

The presence of cadmium resulted in a 47-fold increase in *mtl-1* expression and a 35-fold increase in *mtl-2* expression following the knockdown of *cey-1(ok1805)*. These fold changes were the greatest fold change of all genes tested (Table 7.2). The smallest fold change observed was that of *mtl-1* and *mtl-2* expression in the RNAi deletion of *ceh-5(C16F9.5)* (2.8 and 2.5 fold respectively). The fold change of *mtl-1* and *mtl-2* in nematodes exposed to *his-3(T10C6.12)* following cadmium exposure was a similar fold change as in the N2 fed HT115(DE3) controls (Table 7.2). However, the actual gene expression of *mtl-1* and *mtl-2* in *his-3(T10C6.12)* was greater than that in control nematodes irrespective of the presence of cadmium (Figure 7.6). The fold change in gene expression of *ceh-5(C16F9.5)* was lower than with all other genes tested. However, the relative gene expression of *mtl-1* was greater than in nematodes fed HT115(DE3) in the presence and absence of cadmium.

Two of the genes, *C25F9.5* and *nhr-64(ok1957)* identified from the RNAi screen were not validated by Q-PCR. The RNAi knockdown of *nhr-64* resulted in a "superbright" fluorescent signal of *mtl-2* in the presence and absence of cadmium while the *mtl-1* fluorescent signal remained constant (Table 7.1). Conversely the Q-PCR analysis showed that relative *mtl-1* expression was extinguished and the expression of *mtl-2* was not greater than in control nematodes fed HT115(DE3) (Figure 7.6). In the case of the *C25F9.5* RNAi knockdown, the fluorescent GFP signal of *mtl-1* in the pharynx and intestine increased following cadmium exposure (Table 7.1). Q-PCR analysis revealed that the relative gene expression of *mtl-1* was similar to the HT115(DE5)

control gene expression irrespective of the presence of cadmium (Figure 7.6). The RNAi screen showed that the fluorescent signal of *mtl-2* in the presence of cadmium was "superbright" indicating the transcription factor induced gene expression (Table 7.1), however, this was not observed in the Q-PCR analysis (Figure 7.6). As a result these two genes were omitted from further study. The remaining three genes were investigated further by Y1H analysis to identify their inductive potential.

7.3.3 Yeast spot assay

Prior to Y1H analysis, the toxic concentration of cadmium to yeast cells was identified by performing a spot assay. To determine the LC_{50} the presence, size and number of colonies were observed over a range of cadmium concentrations. *S. cerevisiae* was grown on minimal media supplemented with the required amino acids (Section 2.16.2). The media contained increasing concentrations of cadmium ranging from 1 µM to 500 µM. Yeast was "spotted" onto the plates using a custom made replicator in a 5-fold serial dilution with the starting concentration of $1x10^7$ cells per ml (Section 2.19). Following incubation at 30°C for two days, images of the colonies were taken.

In the absence of cadmium, the yeast grew well (Figure 7.7). The size of the patch was reduced as the yeast became more diluted but the size of individual colonies was still large. At 1, 12 and 50 µM cadmium the yeast showed a similar survival to control conditions. There was a reduction in number of colonies in patches at cell densities of $8x10^4$ and $1.6x10^4$ cells per ml compared to control conditions.

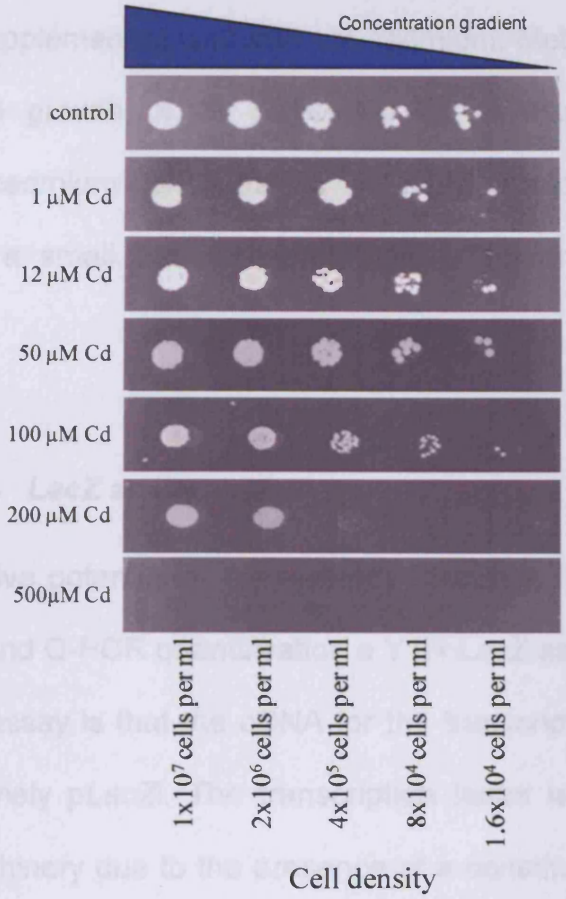

Figure 7.7: The yeast spot assay. Serial dilutions of yeast were "spotted" on control and cadmium supplemented plates using a custom made replicator (Section 2.19). Each plate contained minimal media supplemented with all required amino acids (Section 2.16). Cadmium was added to the media to cover a concentration range from 0 - 500 µM. Plates were incubated at 30°C for 2 days and then photographed.

The growth of *S. cerevisiae* on media supplemented with 12 and 50 µM cadmium was affected at a cell density of $4x10^5$ cells per ml when individual colonies could be observed in the patch (Figure 7.7). Concentrations of cadmium greater than 50 µM seriously affected the growth of yeast. There was growth in all dilutions when yeast was exposed to 100 µM cadmium, however at this concentration the colonies were smaller and reduced in number. No growth was observed at dilutions of $8x10^4$ or $1.6x10^4$ cells per ml on 200 µM cadmium plates and there was a significant reduction in growth at

cell densities of $4x10^5$ cells per ml. The individual yeast colonies were very small on plates supplemented with 200 µM cadmium. Metal concentrations of 500 µM inhibited growth of *S. cerevisiae* at all dilutions (Figure 7.7). Consequently, a cadmium concentration of 12 µM was chosen for the *LacZ* assay as it had a small but not detrimental effect on the growth of *S. cerevisiae*.

7.3.4 *LacZ* assay

To test the inductive potential of the three transcription factors isolated from the RNAi screen and Q-PCR quantification a Y1H *LacZ* assay was performed. The basis of the assay is that the cDNA for the transcription factor is cloned into a vector, namely p*LacZ*i. The transcription factor is transcribed by the yeast cellular machinery due to the presence of a constitutive promoter, such as alcohol dehydrogenase. The transcription factor will bind to a *cis*-acting element within the promoter of the gene of interest, in this case either *mtl-1* or *mtl-2*. As the promoter is fused in frame to the *LacZ* gene on a second vector, when activated transcription of β-galactosidase will be induced. The activity of β-galactosidase can be colorimetrically measured. The substrate for β-galactosidase is OPNG which is colourless and the enzyme converts this to a yellow coloured solution of nitrophenol. The effect of cadmium on the transcription factor can be measured by exposing the yeast cells to cadmium prior to the *LacZ* assay.

Yeast cells (strain Y0000) were co-transformed with two vectors (Section 2.17). One vector, p*LacZ*i (provided by Dr Stephen Stürzenbaum, King's

College London), contained the selection markers URA3 and ampicillin resistance. This vector contained the *LacZ* reporter gene fused in-frame to the MT promoter. The P*mtl-1::LacZ* construct consisted of 553 bp of *mtl-1* promoter while the P*mtl-2::LacZ* construct contained 826 bp of the *mtl-2* promoter. The second vector was pAD-GAL4-2.1 (provided by Dr Hilary Rodgers, Cardiff University, UK) which contained a GAL-4 activation domain, LEU2 and ampicillin resistance selection markers. In addition, an alcohol dehydrogenase promoter is present which drives expression of the GAL-4 and an alcohol dehydrogenase terminator (Figure 7.8). The GAL-4 domain was removed by restriction digest (section 2.10.1) and a newly designed multiple cloning site was inserted. The new vector was digested and the cDNA for each of the three transcription factors was ligated into the vector (Section 2.10.2).

The three candidate genes that were isolated from the RNAi screen and Q-PCR analysis (*his-3, ceh-5* and *cey-1*) were successfully amplified from age synchronised N2. RNA was extracted by the Tri®-reagent method and MMuLV used to synthesise cDNA. The cDNAs were confirmed by sequencing then ligated into the modified pAD-GAL4-2.1 vector. In addition, three controls were generated for use in this assay. Firstly Y0000 was co-transformed with a p*LacZ*i vector which did not contain an MT promoter together with a second vector containing a LEU2 selection marker only. A second control consisted of P*mtl-1::LacZ* and a LEU2 selection marker on a second vector and a third control was comprised of the P*mtl-2::LacZ* co-transformed with a vector containing only the LEU2 selection marker.

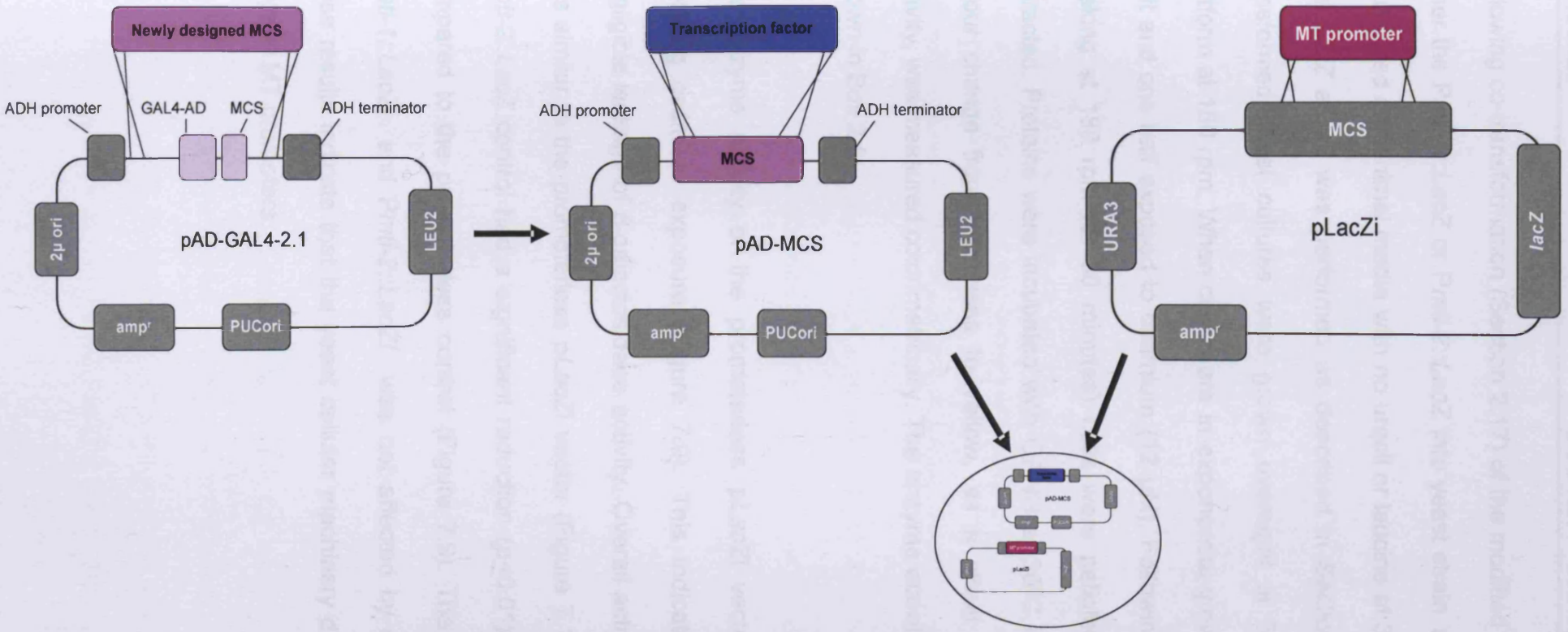

Figure 7.8: Diagram of the vectors co-transformed into yeast for the *LacZ* assay. The pAD-GAL4-2.1 vector (provided by Dr Rodgers, Cardiff University) had the GAL4 and multiple cloning site (both pale purple) was removed by restriction digest (Section 2.10.1) and a newly designed MCS inserted (light purple). The PCR amplified cDNA (blue) of the transcription factor of interest was inserted into the MCS. Expression of the transcription factor is driven by the alcohol dehydrogenase (ADH) promoter. The p*LacZ*i vector (provided by Dr Stürzenbaum, King's College London) contains the minimal promoter elements of *mtl-1* and *mtl-2* which drive *LacZ* expression when activated. Both vectors were co-transformed into the yeast strain Y0000 (Section 2.17) and maintained on minimal media plates (no uracil, no leucine) as described in Section 2.18.

Following co-transformation (Section 2.17) of the modified pAD-GAL4-2.1 and either the P*mtl-1*::*LacZ* or P*mtl-2*::*LacZ* into yeast strain Y0000, strains were maintained on minimal media with no uracil or leucine at 30°C (Section 2.18). The *LacZ* assay was performed as described in Section 2.20. Briefly, co-transformed yeast cultures were grown overnight at 30°C on a shaking platform at 180 rpm. When cells were in exponential growth, the culture was split and one half exposed to cadmium (12 µM). Following incubation (30°C, shaking at 180 rpm for 30 minutes) cells were pelleted and the proteins extracted. Proteins were incubated with OPNG at 30°C for 10 minutes. The colour change from colourless to yellow, as a result of β-galactosidase activity, was measured colorimetrically. The enzyme activity was calculated as shown in Box 2.5.

The enzyme activity of the promoterless p*LacZ*i vector did not change following cadmium exposure (Figure 7.9). This indicated that there was negligible leakage of β-galactosidase activity. Overall activity of P*mtl-1::LacZ* was similar to the promoterless p*LacZ*i vector (Figure 7.10). In contrast, the P*mtl-2::LacZ* control had a significant reduction ($p \leq 0.01$) in enzyme activity compared to the promoterless control (Figure 7.9). The enzyme activity of P*mtl-1::LacZi* and P*mtl-2::LacZi* was not affected by cadmium. Together these results indicate that the yeast cellular machinery does not activate *C. elegans* MT promoters.

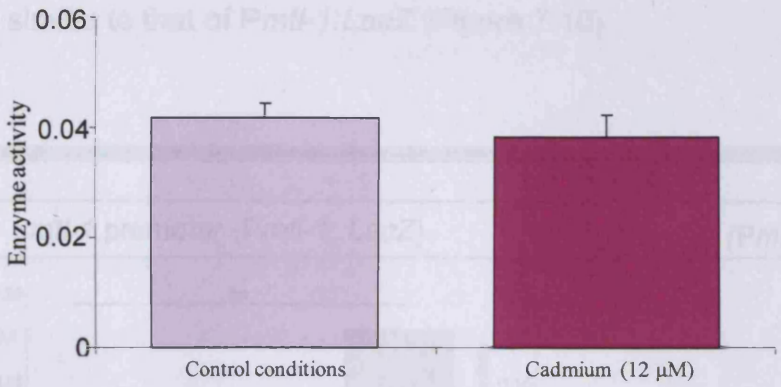

Figure 7.9: Enzyme activity of the promoterless p*LacZi* vector. The p*LacZi* vector was co-transformed into the yeast strain Y0000 with a second vector containing only a LEU selection marker. Yeast cultures in exponential growth were incubated at 30°C on a shaking platform (180 rpm). Cells were harvested and proteins extracted for the *LacZ* assay. The *LacZ* assay consisted of measuring the colour change of OPNG to nitrophenol colorimetrically by the action of β-galactosidase.

In all cases the β-galactosidase activity of P*mtl-1::LacZ* co-transformed with each transcription factor was much greater than the controls (Figure 7.10). A small but not significant increase in enzyme activity was observed when the transcription factors *cey-1* and *ceh-5* were present. In the absence of the heavy metal, activity of β-galactosidase was significantly increased when *his-3* was present ($p \leq 0.01$). Following cadmium exposure, the enzyme activity of *cey-1(F33A8.3)* and *ceh-5(C16C2.1)* was not affected. Enzyme activity was reduced by half in the presence of a vector containing *his-3(T10C6.12)* co-transformed with P*mtl-1::LacZi* following cadmium exposure. The presence of *ceh-5(C16C2.1)* and *his-3(T10C6.12)* in Y0000 co-transformed P*mtl-2::LacZ* did not alter the level of enzyme activity in comparison to the control. The activity of β-galactosidase in the co-transformant P*mtl-2::LacZ* with *cey-1(F33A8.3)* was significantly increased ($p \leq 0.01$) to an level greater than the P*mtl-2::LacZ* control in the absence of cadmium. Following exposure to

the metal, enzyme activity increased significantly ($p \leq 0.01$) although not to the same level similar to that of P*mtl-1:LacZ* (Figure 7.10).

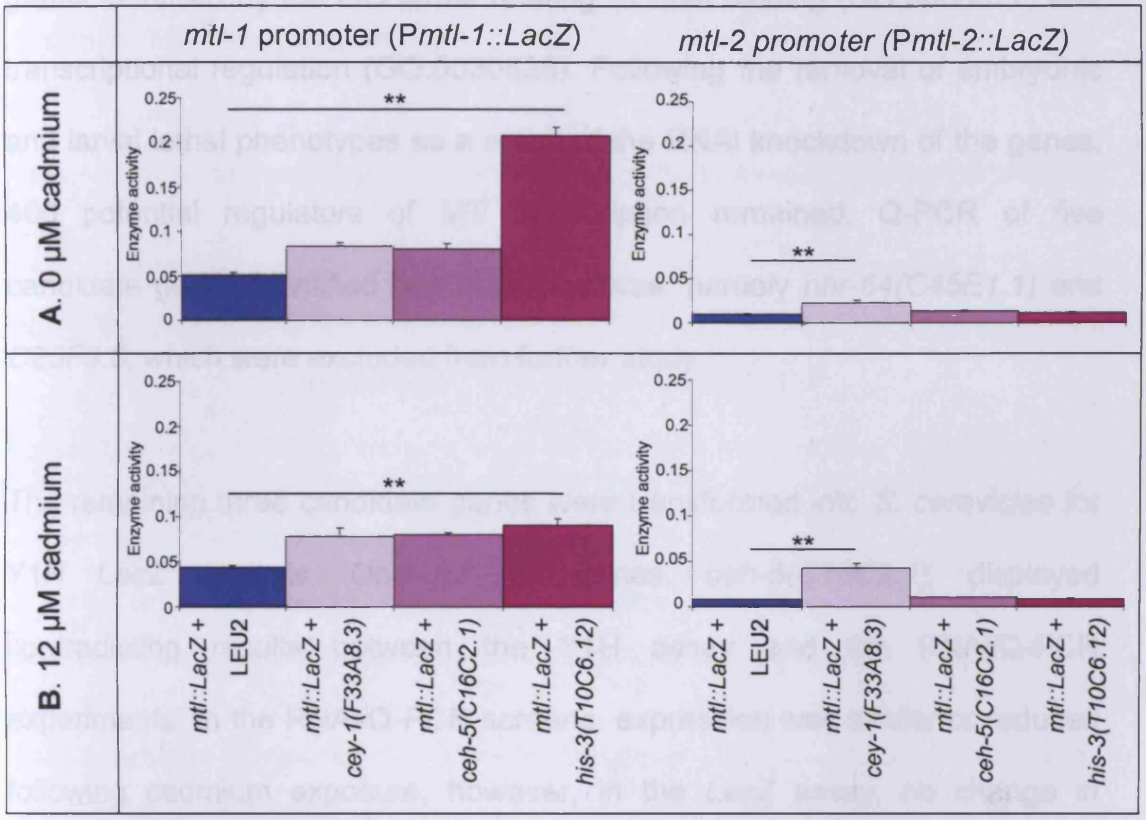

Figure 7.10: Enzyme activity of β-galactosidase in the absence (Panel A) and presence of cadmium (Panel B). Yeast cultures in exponential growth were incubated at 30°C on a shaking platform (180 rpm). Cells were harvested and proteins extracted for the *LacZ* assay. The *LacZ* assay consisted of measuring the colour change of OPNG to nitrophenol colorimetrically by the action of β-galactosidase. Both P*mtl-1::LacZ* and P*mtl-2::LacZ* were tested with a vector containing only a LEU selection marker (blue) and vectors containing *cey-1 (F33A8.3)* (pale purple), *ceh-5(C16C2.1)* (light purple bars) and *his-3(T10C6.12)* (dark purple bars) in the presence and absence of 12 µM cadmium. The errors are standard deviations. Statistical analysis was performed using the ANOVA test with significance indicated by ** where $p \leq 0.01$.

7.4 Discussion

The aim was to identify possible transcription factors which affect the regulation of MT. A targeted RNAi by feeding screen was performed using genes identified by the GO terms relating to DNA binding (GO:0003677) and transcriptional regulation (GO:0030528). Following the removal of embryonic and larval lethal phenotypes as a result of the RNAi knockdown of the genes, 406 potential regulators of MT transcription remained. Q-PCR of five candidate genes identified two false positives, namely *nhr-64(C45E1.1)* and *C25F9.5*, which were excluded from further study.

The remaining three candidate genes were transformed into *S. cerevisiae* for Y1H *LacZ* analysis. One of the genes, *ceh-5(C16C2.1),* displayed contradicting results between the Y1H assay and the RNAi/Q-PCR experiments. In the RNAi/Q-PCR screens, expression was similar or reduced following cadmium exposure, however, in the *LacZ* assay, no change in enzyme activity was observed. A possible reason for these differences may be due to the different promoter lengths used in each method (Figure 7.11). The GFP transgenic nematodes used in the RNAi screen had either 1143 bp of *mtl-1* promoter or 826 bp of the *mtl-2* promoter fused in-frame to the GFP gene. Conversely, the Q-PCR screen quantified transcription of RNA. In these experiments the *mtl* genes are controlled by *cis*-acting elements which could be located from further upstream of the promoter, in introns and in the 3' untranscribed region. In contrast, the length of promoters used in the *LacZ* assay was much shorter. The vector p*LacZ*i contained a promoter sequence of 553 bp for *mtl-1* or 484 bp of *mtl-2* promoter fused to the β-galactosidase

gene. As a consequence of the reduced promoter size in the p*LacZ*i fusion vectors, it is conceivable that the *cis*-acting element to which *ceh-5(C16C2.1)* binds is outside the shorter *mtl-1* and *mtl-2* promoters but within the longer promoters used in the RNAi/Q-PCR screens. Ultimately *ceh-5(C16C2.1)* was discarded from further study.

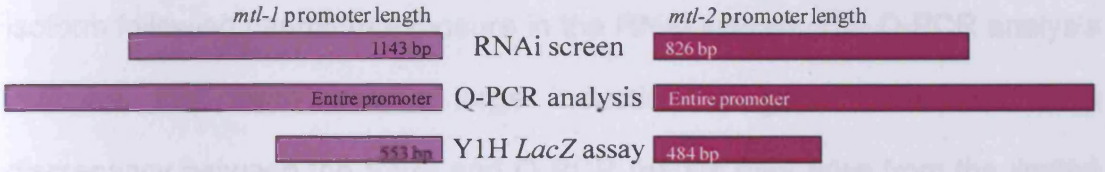

Figure 7.11: The promoter lengths used in the *mtl-1* (light purple) and *mtl-2* (dark purple) fusions. The Q-PCR experiment uses whole nematode populations and any *cis*-acting elements present in the whole genome may affect MT transcription. The P*mtl*::GFP fusions contain 1143 bp of *mtl-1* promoter and 824 bp of *mtl-2* promoter. The p*LacZ*i vectors have *mtl* promoters of approximately half the length of the GFP fusion promoters. The promoters in the p*LacZ*i vector are fused to the β galactosidase gene.

Two candidate genes for MT transcriptional regulation were identified, *his-3 (T10C6.12)* and *cey-1(F33A8.3)*. The first gene isolated, *his-3(T10C6.12)*, is located on Chromosome V within a cluster of genes referred to as the HIS1 cluster. It was interesting to note that the gene is on the same chromosome as both *mtl* isoforms. The knockdown of *his-3(T10C6.12)* increased basal expression of *mtl-1* and *mtl-2*. Following cadmium exposure, the expression of both isoforms was increased. However, there was repression of *mtl-1* following cadmium exposure in the Y1H *LacZ* assay. Thus the presence of *his-3(T10C6.12)* is likely to be associated with the repression of *mtl-1* in the presence of cadmium. The protein coded by *his-3(T10C6.12)* is H_2A, one of four components which comprise the nucleosome. The H_2A protein has a

specific role in chromatin condensation and provides structural integrity to the nucleosome.

The second gene identified as a regulator of MT transcription was *cey-1(F33A8.3).* The basal activity of *mtl-1* and *mtl-2* was reduced when *cey-1(F33A8.3)* was deleted by either RNAi knockdown or in the chromosomal deletion mutant. There was a small induction of each MT isoform following cadmium exposure in the RNAi screen. The Q-PCR analysis indicates that there was a large induction of gene expression. This discrepancy between the RNAi and Q-PCR results may arise from the limited discriminatory power of the RNAi screen. The change in fluorescent signal from the GFP transgenic *C. elegans* strains in the RNAi screen was measured by eye (Figure 7.3) over successive RNAi experiments consequently this method may have been susceptible to subtle changes in fluorescence being missed. In contrast, Q-PCR is highly sensitive method of monitoring the exact change in gene expression by measuring the level of fluorescence as a proportion of PCR product. Secondly, differences in the screens may arise from incomplete silencing by RNAi (Kamath *et al.* 2000) consequently the gene may still be expressed to some level. In contrast, the Q-PCR method used a deletion mutant for this gene, *ok1805.* This partial chromosomal deletion has 100% silencing of the gene due to the removal of one complete and one partial exon (Figure 7.5).

The decrease in basal activity of *mtl-2* in the RNAi/Q-PCR analysis was the opposite of the Y1H *LacZ* screen. Following cadmium exposure the activity of

the enzyme increased but only with the *mtl-2* promoter. There was no effect by *cey-1(F33A8.3)* on *mtl-1* in the Y1H *LacZ* assay. The gene *cey-1(F33A8.3)* codes for a *C. elegans* Y-box protein which is able to bind DNA and regulate transcription of a gene.

7.4.1 Speculative model of MT control

The RNAi, Q-PCR and Y1H screens have isolated two potential transcription factors which may affect the regulation of mtl-1 and mtl-2 in the presence and absence of a heavy metal, namely cadmium. The histone gene *his-3* reduced basal *mtl-1* expression while *cey-1*, which codes for a Y-box protein, increased *mtl-2* expression in the presence of cadmium. This section proposes a mode of action for each of these putative transcription factors.

Nucleosomes have been shown to affect transcription of a gene by packaging DNA to prevent the pre-initiation complex from accessing the TATA box and consequently inhibiting transcription (Hoffmann *et al.* 1997). It is possible that the presence of H_2A allows DNA to condense forming an "open" structure (Hoffmann *et al.* 1997). The "open" formation would present the transcription initiation site, allowing easy access for the pre-initiation complex to bind and begin transcription. Following cadmium exposure, the metal ion can bind to zinc fingers in H_2A and prevent it from forming a complex with DNA. As a result the DNA is not packaged properly and becomes a "closed" (Hoffmann *et al.* 1997). In the "closed" state, the transcription initiation site is not easily accessible and consequently the pre-initiation complex cannot form as readily. Transcription is therefore reduced. As only *mtl-1* is affected by *his-3*

(T10C6.12) it is possible that this is an observation for the control of pharyngeal expression. As the expression of *mtl-1* decreases following cadmium exposure in the presence of *his-3(T10C6.12)*, transcriptional activation of *mtl-2* may be enhanced. In addition, metals ions would induce the generation of PC from PC synthase in the pharynx which would be distributed throughout the gut to chelate metal ions. Therefore there are more metal chelating proteins present to prevent toxicity. The absence of *his-3 (T10C6.12)*, as in RNAi/Q-PCR analysis, removes the potential for *mtl-1* regulation.

Human Y-box binding proteins have been shown to contain a DNA binding domain (Wu *et al.* 2006). Thus, the Y-box protein can regulate cell proliferation as a consequence of the DNA/protein interactions through the DNA binding domain (Wu *et al.* 2006). Within the DNA binding domain is a serine residue which can be phosphorylated (Wu *et al.* 2006) by metals such as cadmium (Saydam *et al.* 2002) and consequently the ability of the Y-box binding protein to interact with DNA is altered. As the *C. elegans* gene *cey-1 (F33A8.3)* is also a Y-box protein which potentially acts in a similar way to the human Y-box protein, it can be hypothesised that CEY-1 binds to an as yet unidentified *cis*-acting element within the MT promoter. Transcription of MT is up regulated. Following exposure to cadmium, the serine within the DNA binding domain become phosphorylated by the action of the metal ion (Saydam *et al.* 2002) and the ability of CEY-1 to bind DNA is enhanced. Ultimately MT transcription is increased and more metal chelating protein is produced.

It is possible that *in vivo* the action of CEY-1 is more complex. A Y-box binding protein (YB-1) regulates expression of gelatinase A in hepatoma cells by the coordinated action of the YB-1 and an AP-2 transcription factor (Mertens *et al.* 1998). The binding of the YB-1/AP-2 complex induces a conformational change in the DNA to stimulate transcription of gelatinase A (Mertens *et al.* 1998). As both *C. elegans* promoters contain AP-1 binding sites, it could be postulated that CEY-1 and AP-1 form a complex which acts on the AP-1 *cis*-acting element of MT in the same way as in gelatinase A. The presence of cadmium could enhance the formation and binding of the CEY-1/AP-1 complex to enhance MT transcription. This type of gene regulation would not have been observed in these experiments as the RNAi and Q-PCR screens only involved the knockdown of one gene at a time and the Y1H *LacZ* assay was concerned with the effect of one transcription factor on the *mtl* promoter.

The speculative modes of action for *his-3* and *cey-1* require further study to fully investigate the extent of their action on the transcriptional regulation of *C. elegans mtl-1* and *mtl-2*.

7.5 Conclusion

The method of using an RNAi by feeding screen to identify potential effectors of transcription and their subsequent validation by Q-PCR was, at least in part, successful. In addition, the use of a *LacZ* assay in yeast cells to quantify the inducability of the positive effectors provides valuable information. Two candidate genes were identified which may be involved in the regulation of *mtl* genes.

It was hypothesised that the presence of the H_2A component of the nucleosome, coded by *his-3(T10C6.12)*, re-models the DNA into a structure which aids the binding of the pre-initiation complex to stimulate transcription. Cadmium then reduces the ability of the nucleosome to bind to DNA. Consequently the *cis*-acting element is not easily accessible for formation of the pre-initiation complex and therefore transcription is reduced. In addition *cey-1(F33A8.3),* a *C. elegans* Y-box protein, was found to stimulate basal transcription of both metallothionein isoforms and in the case of *mtl-2* increase transcription following exposure to cadmium. The potential for binding of CEY-1 to a *cis*-acting element and the subsequent rearrangement of the DNA into a conformation which stimulates transcription was proposed. The presence of cadmium may be involved in the phosphorylation of serine residues within the CEY-1 protein. This may either enhance the binding of CEY-1 to DNA or change the conformation of DNA to allow improved binding of CEY-1. In either case, transcription would be augmented.

The two genes identified in this chapter as regulators of *mtl* transcription require further study to find the locations and specific DNA sequences to which they bind in the promoters of *mtl-1* and *mtl-2*. There may be more factors which affect transcription and the mechanism of transcription may be more complex than in vertebrates. However, the isolation of two potential candidates for transcriptional control of *C. elegans* MT is a step further in the understanding of how this process may be regulated.

CHAPTER EIGHT

GENERAL DISCUSSION

To date, metallothioneins (MT) have been considered to be the primary mechanism of heavy metal detoxification. MTs were first identified in horse kidney in 1960 (Kägi and Vallee 1960) and since then have been isolated from many species including prokaryotes (Huckle *et al.* 1993), plants (Zimeri *et al.* 2005) and higher eukaryotes (Chapman *et al.* 1999; Kugawa *et al.* 1994; Riordan and Vallee 1991). MTs are small cysteine rich proteins which can act as metal chelators and donators as well as possessing antioxidant properties whereby MTs can bind free radicals and reactive oxygen species. The *C. elegans* genome contains two MT isoforms, *mtl-1* and *mtl-2.*

The promoters of *mtl-1* and *mtl-2* have 50.8% sequence identity containing some similar elements, for example, the *cis*-acting elements AP-1 and VPE-2 (Chapter 3). Similarly, the coding regions are 58.6% identical with 18 cysteine residues highly conserved between the two isoforms. Comparison of *C. elegans* and *C. briggsae* MT show that the isoforms are highly conserved between species, with MTL-1 having 88% sequence similarity. Although the protein has a varied sequence between species, the cysteine residues are highly conserved throughout the prokaryotic and eukaryotic kingdoms (Kägi and Schaffer 1988).

The use of transgenic nematodes expressing a green fluorescent protein (GFP) (Swain *et al.* 2004) provided a simple method to observe the

expression pattern of *mtl-1* and *mtl-2 in vivo*. It was confirmed that *mtl-1* was expressed constitutively in the pharynx, specifically in the second pharyngeal bulb. Following exposure to cadmium, *mtl-1* expression increased marginally in the pharynx and was induced in intestinal cells. There was no basal expression of *mtl-2*. Following exposure to cadmium, *mtl-2* expression was induced throughout the intestine. Although cadmium was a strong transcriptional activator of MT, zinc also induced MT. The presence of copper also enhanced transcription of both isoforms of MT, but not to the same extent as cadmium or zinc. A depleted copper environment was achieved through the addition of bathocuproinedisulphonic acid (BCS) to the media. Nematodes exposed to an environment lacking copper showed a slight increase in the transcription of *mtl*. Together these data suggest that the metals which enhance *mtl* transcription can be placed in the order of cadmium $\geq$ zinc > copper. This is different to what has been recorded previously for mammalian MT (Kägi and Schaffer 1988; Klaassen *et al.* 1999) as copper should enhance MT transcription to a greater extent than zinc. In all cases cadmium has been found to be the most potent activator of transcription.

Nematodes were exposed to elevated and depleted metal environments to investigate the phenotypic effects of each MT isoform. NGM was supplemented with cadmium (12 µM), zinc (160 µM), copper (190 µM) and BCS (500 µM). The phenotypic effects of exposure to metals were studied, namely brood size, growth and lifespan. Deletions of either MT isoform, as in the strains containing the genotypes *mtl-1(tm1770)* and *mtl-2(gk125)*, resulted in phenotypic differences which were interchangeable (Chapter 5). This

suggested that there was some degree of compensation for the removal of one MT isoform. Single *mtl* knockouts were used to generate a double MT mutant, *mtl-1;mtl-2(zs1)*, as discussed in Chapter 3 and in Hughes and Stürzenbaum (2007). MTs are widely perceived to be essential and to have a significant role in metal detoxification and homeostasis (Camakaris *et al.* 1999; Klaassen *et al.* 1999; Palmiter 1998; Roesijadi 1992; Vallee 1995). As a consequence it was surprising that the double MT knockout mutants were viable and reproduced. However, the reproduction of *mtl-1;mtl-2(zs1)* was significantly inhibited on NGM which contained trace levels of copper and zinc. This suggests that although MTs are involved in metal detoxification, they are not an essential component of the mechanism.

Cadmium was shown to be a potent stimulator of *mtl-1* and *mtl-2* transcription and induced serious phenotypic effects, namely a reduction in growth and brood size to half that of nematodes grown under optimal laboratory conditions. Cadmium is a teratogen and can cause sterility (Alvarez *et al.* 2005; Jager *et al.* 2005) which can explain the decrease in brood size following exposure to the metal. There was no effect on phenotype in the presence of zinc. A lack of phenotypic effects on *mtl* and *pcs-1* null mutants has been found previously in nematodes and other organisms (Cobbett and Goldsbrough 2002; Cui *et al.* 2007; Egli *et al.* 2003; Ha *et al.* 1999; Ibaim and Grant 2005). Thus MT and PC do not appear to be an important aspect of zinc regulation. The presence of copper in the environment at elevated levels resulted in a significant decrease in brood size with strain specific differences between wild type and MT mutants and the *pcs-1* null nematodes. Volumetric

area was also reduced in the presence of excess copper. The final size of copper exposed nematodes was similar to those exposed to cadmium. The reason for this may be a consequence of the increase in free radicals and reactive oxygen species (ROS) generated in the presence of excess heavy metals (Camakaris *et al.* 1999; Waisberg *et al.* 2003; Valko *et al.* 2005). The ROS are able to irreversibly damage DNA and proteins, leading to cell death. Conversely, a copper depleted environment did not significantly affect the volumetric size or lifespan of any nematode strain. The main consequence of the copper chelator, BCS, on reproduction was to decrease the total brood size in all strains, most significantly *pcs-1(tm1748)* and *mtl-1;mtl-2;pcs-1(zs2),* and to delay the onset of reproduction. Together these data indicates that PCs do play a role in copper homeostasis, possibly to a greater extent than MTs.

The perceived lack of phenotypic differences observed between wild type and MT mutant nematodes in Chapter 5 were mirrored in NMR experiments (Chapter 4). Multivariate analysis of the MT deletion strains showed that with regards to the metabolome, there were no differences between genotypes. In contrast, a significant separation of groups occurred following cadmium exposure irrespective of genotype. Computer aided peak fitting was performed using NMR Suite 5.0 to identify a selection of metabolites. Four metabolites were identified which remained constant and the average of these were used as a normalisation factor (Vandesompele *et al.* 2002). The relative concentration of metabolites of interest, glutathione, methionine, trehalose and cystathionine, were measured and normalised. The concentration of

methionine was similar in wild type and single MT deletion strains in the presence and absence of cadmium. The concentration of methionine showed a non-significant decrease in the double MT deletion strain. Cystathionine had a significant decrease in the relative concentration following cadmium exposure in all nematode strains. The metabolite cystathionine was found to be the cause of the separation of the samples based on cadmium exposure in the PLS-DA scores plot. Thus cystathionine was considered to be a suitable candidate for further investigation.

Cystathionine is the key intermediate in the transsulfuration pathway which generates methionine from cysteine. It has been proposed that cadmium inhibits the enzyme which generates this intermediate, cystathionine-β-synthase by binding to exposed thiol groups on the enzyme (Houghton and Cherian 1991; Sugiura *et al.* 2005; Sura *et al.* 2006). The observations in Chapter 4 correspond to previous observations whereby the presence of cadmium decreases the level of cystathionine while glutathione concentration remains constant (Sugiura *et al.* 2005). The decrease in methionine in *mtl-1;mtl-2(zs1)* may be as a consequence of the incorporation of sulphur from methionine into the generation of new antioxidant peptides, such as PC (Stein *et al.* 1987). Consequently the decrease in cystathionine concentration results in the transsulfuration pathway ceasing to function with a consequent increase in cysteine concentration. Physiological concentration of cysteine cannot exceed 0.2 mmol/l (Rao *et al.* 1990) and therefore the amino acid must be utilised in another reaction or in the generation of cysteine rich proteins. During inhibition of the transsulfuration pathway by inhibition of cystathionine-

β-synthase, MT levels have been shown to be increased with an increase in cystathionine (Stein *et al.* 1987). However, the double MT knockout strain does not contain the gene for either isoform of *mtl.* Consequently the generation of MT cannot occur in *mtl-1;mtl-2(zs1)*. Therefore other peptides must be generated, such as glutathione or PC. Glutathione is synthesised from the intermediate γ-glutamylcysteine which itself is generated from glutamate and cysteine (Mendoza-Cózatl *et al.* 2005). Thus the channelling of excess cysteine into the formation of glutathione maintains the cysteine pool at or below optimal physiological concentrations. The maintenance of glutathione levels was observed by Sugiura *et al.* (2005) and may result from the negative feedback loop generated by the production of glutathione. The antioxidant can prevent its own production by inhibiting the action of γ-glutamylcysteine synthetase (Mendoza-Cózatl *et al.* 2005). As a result glutathione must be utilised in the generation of proteins to prevent it from inhibiting the synthetase enzyme. Proteins which may be generated from glutathiones are PC (Mendoza-Cózatl *et al.* 2005) and MT (Stein *et al.* 1987; Sura *et al.* 2006). As the strain with the genotype *mtl-1;mtl-2(zs1)* cannot generate MT, glutathione must be channelled into the generation of PC.

PC is a long chain polypeptide with the general formula $[\gamma\text{-Glu-Cys}]_n\text{-Gly}$ where n is between 2 and 11 repeats (Lee and Korban 2002). PCs are enzymatically generated from PC synthase. In 2001 *C. elegans* was shown to contain a functional PC synthase coded by the gene *pcs-1* (Clemens *et al.* 2001; Vatamaniuk *et al.* 2001). PC are thought to function solely in metal detoxification and in plants have been shown to form complexes with

cadmium and will direct the removal of the metal to the vacuole (Rea *et al.* 2004). Using GFP fusion constructs (Hope *et al.* 2004), the basal expression of *pcs-1* was identified in four cells; two cells at the pharyngeal/intestinal valve and two cells at the intestinal/rectal valve (Chapter 3). The addition of cadmium, or other heavy metal cations, did not affect the GFP signal intensity. This is because PC synthase is post-translationally stimulated by cations via a metal dependent step in PC generation (Cobbett 2000a). A proposal for the location of PC synthase at either end of the intestine is that from here the newly synthesised PC can be circulated through the intestine where they can bind ingested heavy metals. The metal bound PC complexes can be transported across the apical membranes of the intestinal cells via a specific transporter, possibly HMT-1 (Vatamaniuk *et al.* 2005). The complexes can then be disposed of and the metal ions cannot exert their toxic effects.

It was previously suggested that the concentration of glutathione was maintained at a constant level irrespective of cadmium exposure as a result of the metabolite being channelled into the generation of other sulphur rich proteins. As the double MT knockout cannot generate MT, it was proposed that the generation of PC was increased to maintain glutathione levels. Mass spectrometry (UPLC-TOF/MS) was performed to identify the presence of PC compounds *in vivo*. Based on the structure of *C. elegans* PC proposed by Clemens *et al.* (2001), the use of MS allowed the identification two types of PC (Chapter 4). One, PC_2, had a structure of γ-Glu-Cys-γ-Glu-Cys-Gly ($C_{18}H_{30}N_5O_{10}S_2$) with a corresponding mass of 540. The second PC identified was PC_3 with a mass of 772 and the formula $C_{26}H_{42}N_7O_{14}S_3$ (with a structure

of γ-Glu-Cys-γ-Glu-Cys-γ-Glu-Cys-Gly). The MS quantification of the two types of PC were significantly increased following cadmium exposure, with PC_2 present in higher concentrations than PC_3. This provides sound evidence that more PCs are generated following exposure to cadmium. To summarise the hypothesis: the cadmium inhibition of cystathionine-β-synthase increases cysteine which is used to generate glutathione to maintain cysteine concentrations at 0.2 mmol/l. Glutathione is then used as a substrate for PC synthesis as well as providing a means to transport the metal ion required for enzyme activity to the synthase.

Previous studies have shown that the two metal detoxification systems (PC and MT) function together but it was not known to what extent. PC are enzymatically synthesised from PC synthase (Cobbett 2000a; Lee and Korban 2002) while MT are transcriptionally controlled (Maroni *et al.* 1987; Roesijadi 1992; Swain *et al.* 2004; Timmermans *et al.* 2005). To investigate the contribution of MT and PC to metal detoxification, the MT mutants (single knockouts) and a *pcs-1* null strain were used in Q-PCR analysis as detailed in Chapter 6. The expression of *mtl-1* and *mtl-2* increased with increasing exposure to cadmium (Chapter 6). This supported findings from previous reports (Gonzalez-Mendoza *et al.* 2007; Swain *et al.* 2004; Zhang *et al.* 2005). The expression of *mtl-1* did not increase following the loss of *mtl-2* and vice versa which points to a previously proposed theory that the two MT isoforms function independently (Swain *et al.* 2004). The lack of upregulation following the deletion of one MT isoform by the remaining MT indicates that another factor may act as a compensatory mechanism. Although PC could not be

analysed by Q-PCR, the *pcs-1* null strain nematodes were used to quantify the relative gene expression of *mtl-1* and *mtl-2*. Gene expression of both *mtl* was shown to drastically increase in *pcs-1(tm1748)* compared to controls. Consequently this supports the hypothesis that PC are present and upregulated during cadmium exposure. This was a similar hypothesis to the mechanism of metal detoxification in the yeast *S. pombe* and in plants (Gonzalez-Mendoza *et al.* 2007; Yu *et al.* 1994; Zhang *et al.* 2005; Zhou and Goldsbrough 1994).

Q-PCR experiments included a 48 hour exposure to cadmium (12 µM) from the L1 stage to the L4 larval stage of development. This measurement could not be taken for *pcs-1(tm1748)* as these nematodes were hypersensitive to cadmium. In addition, *mtl-1;mtl-2;pcs-2(zs2)* showed signs of extreme cadmium hypersensitivity (Chapter 5). The hypersensitivity to cadmium in *pcs-1* null nematodes has been noted previously (Vatamaniuk *et al.* 2001) and in other organisms (Clemens *et al.* 1999; Cobbett 2000a; Cobbett 2000b; Cobbett and Goldsbrough 2002). In *pcs-1(tm1748)* and *mtl-1;mtl-2;pcs-1(zs2),* cadmium concentration had to be reduced significantly to allow the nematodes to survive and reproduce. The single *pcs-1* null nematode could survive at 0.5 µM but the triple knockout nematode could not survive above 0.05 µM cadmium (Chapter 5). In addition, *pcs-1* null nematodes were more sensitive to elevated or depleted copper environments compared to MT mutants (Chapter 5). Together this suggested that the proposed hypothesis that, at least in *C. elegans*, PC are important players in the detoxification of cadmium, possibly more than MTs. This proposal goes against the widely

accepted dogma of metal detoxification in vertebrates, not least because a functional PC synthase has not been identified in many vertebrate species (Clemens 2006). However, over the past decade PC synthase genes, identified via homolog database searches, have been found to be widely distributed throughout the animal kingdom (Clemens 2006). PC synthase genes have been identified in all higher plants and has representatives in a wide range of eukaryotic species (Figure 8.1) (Clemens 2006). Bacteria have been shown to have PC synthase-like proteins, similar only at the N-terminal (Clemens 2006).

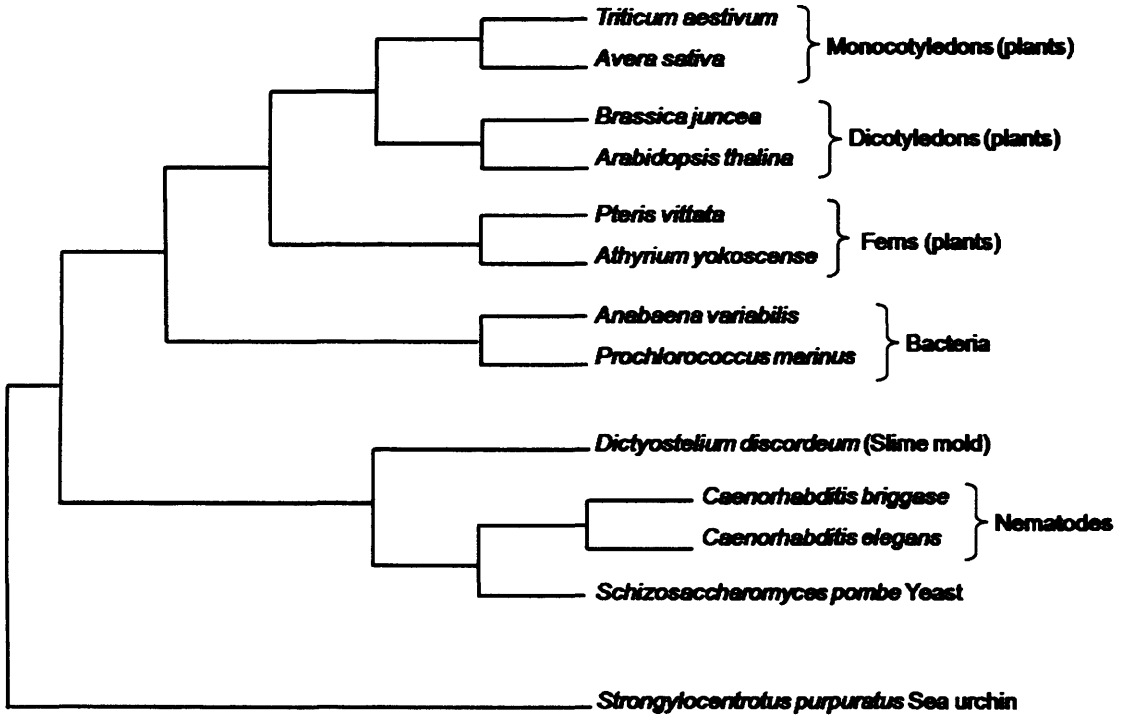

Figure 8.1: Phylogenetic tree of PC synthase genes. Bacterial and eukaryotic PC synthase identified via BLASTp and tBLASTn then aligned by ClustalW. Adapted and redrawn from Clemens (2006).

Due to the broad range of species in which MT and PC synthase are jointly expressed, it is easy to imagine that the proteins function in a co-ordinated fashion to protect the organism from metal toxicity. The degree of response of either MT or PC may vary between species depending on metal challenge. The potential for a varied co-ordinated response to metal detoxification has been illustrated in *S. pombe* and other organisms and described previously (Gonzalez-Mendoza *et al.* 2007; Yu *et al.* 1994; Zhang *et al.* 2005; Zhou and Goldsbrough 1994).

In contrast to PC synthase, MTs are transcriptionally stimulated by the presence of metals (Dallinger 1996; Maroni *et al.* 1987; Swain *et al.* 2004; Timmermans *et al.* 2005). It is generally accepted that MT transcription occurs by the binding of a cation to a metal responsive transcription factor (MTF-1) to form a complex which in turn can bind to a *cis*-acting element within the MT promoter (Saydam *et al.* 2002). The *cis*-acting element is a 7 base pair sequence referred to as a metal responsive element (MRE). The *C. elegans* genome does not contain MTF-1 (Freedman *et al.* 1993) and consequently some other factor must be responsible for the transcriptional stimulation of *mtl*. Although *mtl-2* does contain a single MRE sequence it is not functional and the *mtl-1* promoter does not contain any functional or non-functional MREs (Freedman *et al.* 1993). As such, some other factor must provide the metal inducability of *C. elegans* MT. To identify potential transcription factors which could regulate MT transcription, an RNA interference screen was performed (Chapter 7). The RNAi screen was undertaken in the presence and absence of cadmium (12 µM) using transgenic nematodes expressing GFP

(Swain *et al.* 2004). The change in fluorescence was assessed by eye and positive potential effectors of MT regulation were validated by Q-PCR. Subsequent Y1H analysis identified two potential candidate genes which may affect MT transcription.

The first candidate gene was *his-3(T10C6.12)*, identified as a transcription factor which increased basal expression of *mtl-1*. The gene *his-3(T10C6.12)* codes for the H_2A component of the nucleosome and has a variety of functions including DNA binding. The primary function of nucleosomes is to package DNA. A varying degree of packaging can affect the ability of the transcriptional machinery to bind the DNA and initiate transcription. It was hypothesised that the nucleosome arrangement affects transcription of the pharyngeal *mtl-1* expression. Under normal conditions the DNA is packaged into an "open" formation by the presence of H_2A (Hoffmann *et al.* 1997). This allows the transcriptional machinery access to the transcriptional start site. Following cadmium exposure the nucleosomes are remodelled preventing either the "open" DNA structure or the formation of the pre-initiation complex (Hoffmann *et al.* 1997) reducing the level of transcription. It was proposed that the inhibition of *mtl-1* following cadmium exposure allows more PC to be synthesised. PCs would then be distributed into the top of the intestine together with ingested bacteria where the PCs can bind and chelate metal ions. Thus PCs become the first line of defence against cadmium toxicity. Supporting this argument is the presence of PCs which has been shown to be of more importance than MT in cadmium detoxification as a consequence of hypersensitivity of *pcs-1* null mutants to cadmium (Chapter 5).

A second putative transcription factor of *mtl-2* transcription was *cey-1*(F33A8.3), identified as a transcription factor which increased basal expression of *mtl-2.* Gene expression was further enhanced following cadmium exposure. The *C. elegans* Y box protein has DNA binding properties and has been implicated in DNA dependent transcriptional control. The suggested activation of *mtl-2* by CEY-1 was based upon the observation of a similar Y box protein involved in breast cancer (Wu *et al.* 2006). The premise was that in *C. elegans,* CEY-1 will bind to an as yet unknown *cis*-acting element to enhance basal transcription. The presence of cadmium would phosphorylate serine residues located in the DNA binding domain (Saydam *et al.* 2002). This may induce a conformational change in CEY-1 to enhance binding augmenting transcription. It was also proposed that transcriptional control involving CEY-1 may be more complex. A Y-box protein has been shown to form a complex with AP-2 to enhance gelatinase A transcription (Mertens *et al.* 1998). As *C. elegans mtl* promoters contain AP-1 binding sites, it is conceivable that CEY-1 bind AP-1 which as a complex bind the AP-1 *cis*-acting elements. The phosphorylation of CEY-1 as a result of cadmium exposure (Saydam *et al.* 2002) would then enhance transcription.

In summary, the observation that the double MT knockout survives on basal NGM which contains trace levels of metal indicates that MT are not essential for survival. Little is understood about the transcriptional control of *C. elegans* MT but via an RNAi screen two candidate genes, *his-3* and *cey-1*, were identified which may affect the regulation of *mtl-1* and *mtl-2* transcription respectively. In addition, a functional PC synthase (*pcs-1*) was found not to be

essential for life. However the presence of PC synthase is required for the ability to generate PCs for continual survival and reproduction in environments where there is an excess of heavy metals, specifically cadmium. Although the two *C. elegans* isoforms of MT function independently, they become up regulated when the generation of PCs is compromised.

The reason for *C. elegans*, a relatively simple multicellular organism, to have two different metal detoxification systems (MT and PC) remains elusive. It is conceivable that PCs are omnipresent, although yet to be identified in many organisms. Thus *C. elegans* may not be unusual in utilising MT and PC in metal detoxification.

SCIENTIFIC OUTPUT

Publications

Hughes, S.*, Bundy, J.G.*, (*contributed equally), Want, E.J., Kille, P. and Stürzenbaum, S.R. The metabolomic responses of *Caenorhabditis elegans* to cadmium are largely independent of metallothionein status, but dominated by changes in cystathionine and phytochelatins (submitted to the Journal of Proteome Research, January 2009).

Calafato, S., Swain, S., Hughes, S., Kille, P. and Stürzenbaum, S.R. (2008). Knock down of *Caenorhabditis elegans cutc-1* exacerbates the sensitivity toward high levels of copper. Toxicological Sciences **106**(2): 384-391. Work was not included in the thesis.

Hughes, S. and Stürzenbaum, S.R. (2007). Single and double metallothionein knockout in the nematode *C. elegans* reveals cadmium dependent and independent toxic effects on life history traits. Environmental Pollution **145**(2): 395-400.

Conference attendance

Hughes S, Kille, P and Stürzenbaum, S.R (2007). Life History and Cadmium Toxicosis in the Global Metallothionein Knockout Nematode *Caenorhabditis elegans.* Poster presentation at the 16th International *C. elegans* Meeting, University of California, Los Angeles.

Hughes S, Kille, P and Stürzenbaum, S.R (2007). The knockout of metallothionein and phytochelatin synthase in *C. elegans*: metal induced effects on life history and gene expression. Invited poster presentation at the Society for Experimental Biology (SEB) Metals Symposium, King's College London, UK.

Hughes S. (2007). Caenorhabditis elegans: A model to study developmental biology. An invited oral presentation at University of East Anglia.

Hughes S, Kille, P and Stürzenbaum, S.R (2006). The knockout of metallothionein in *C. elegans*: metal induced effects on life history. Poster presentation at the Postgraduate Research Symposium Cardiff University, UK which won First Prize.

Hughes S. (2006). Knockout of metallothionein(s) in the nematode *Caenorhabditis elegans:* effectors of life history traits. Oral presentation at The Society of Environmental Toxicology and Chemistry (SETAC) Europe 16th Annual Meeting, The Hague, Netherlands.

BIBLIOGRAPHY

Alt, M. (1990). Exploring hyperspace: a non-mathematical explanation of multivariate analysis. London: McGraw-Hill.

Alvarez, O.A., Jager. T., Kooijman, S.A.L.M. and Kammenga, J.E. (2005). Responses of stress of *Caenorhabditis elegans* populations with different reproductive strategies. Functional Ecology **19**: 656-664.

Andrews, G.K. (2000). Regulation of metallothionein gene expression by oxidative stress and metal ions. Biochemical Pharmacology **59**: 94-104.

Andrews, G.K., Bittel, D., Dalton, T., Hu, N., Chu, W., Daggett, M., Li, Q. and Johnson, J. (1999). New insights into the mechanisms of cadmium regulation of mouse metallothionein-I gene expression. Metallothionein IV. Editor: C.D. Klaassen. Basal, Switzerland, Birkhauser: 227-232.

Atherton, H.J., Jones, O.A.H., Malik, S., Miska, E.A. and Griffin, J.L. (2008). A comparative metabolomic study of NHR-49 in *Caenorhabditis elegans* and PPAR-alpha in the mouse. FEBS Letters. **582**(12): 1661-1666.

Bailey, N.J.C., Oven, M., Holmes, E., Nicholson, J.K. and Zenk, M.H. (2003). Metabolomic analysis of the consequences of cadmium exposure in *Silene cucualus* cell cultures via 1H NMR spectroscopy and chemometrics. Phytochemistry **62**: 851-858.

Beck, A., Lendzian, K., Oven, M., Christmann, A. and Grill, E. (2003). Phytochelatin synthase catalyzes key step in turnover of glutathione conjugates. Phytochemistry **62**(3): 423-431.

Beckonert, O., Keun, H.C., Ebbels, T.M.D., Bundy, J., Holmes, E., Lindon, J.C. and Nicholson, J.K. (2007). Metabolic profiling, metabolomic and

metabonomic procedures for NMR spectroscopy of urine, plasma, serum and tissue extracts. Nature Protocols **2**(11): 2692-2703.

Bedair, M. and Sumner, L.W. (2008). Current and emerging mass-spectrometry technologies for metabolomics. Trends in Analytical Chemistry **2**(3): 238-250.

Bertin, G. and Averbeck, D. (2006). Cadmium: cellular effects, modifications of biomolecules, modulation of DNA repair and genotoxic consequences (a review). Biochimie **88**: 1549-1559.

Blaise, B.J., Giacomotto, J., Elena, B., Dumas, M.E., Toulhoat, P., Ségalat, L. and Emsley, L. (2007). Metabotyping of *Caenorhabditis elegans* reveals latent phenotypes. Proceedings of the National Academy of Sciences USA **104**(50): 19808-19812.

Blencowe, D. K. and Morby, A.P. (2003). Zn (II) metabolism in prokaryotes. FEMS Microbiology Reviews **27**: 291-311.

Brenner, S. (1974). The genetics of *Caenorhabditis elegans*. Genetics **77**: 71-94.

Buckingham, S.D., Esmaeili, B., Wood, M. and Sattelle, D.B. (2004). RNA interference: from model organisms towards therapy for neural and neuromuscular disorders. Human Molecular Genetics **13**(2): R275-R288.

Bundy, J.G., Sidhu, J.K., Rana, F., Spurgeon, D.J., Svendsen, C., Wren, J.F., Stürzenbaum, S.R., Morgan, A.J. and Kille, P. (2008). 'Systems toxicology' approach identifies coordinated metabolic responses to copper in a terrestrial non-model invertebrate, the earthworm *Lumbricus rubellus*. BMC Biology **6**(25).

Byerly, L., Cassada, R.C. and Russell, R.L. (1976). The life cycle of the nematode *Caenorhabditis elegans*. Developmental Biology **51**: 23-33.

Camakaris, J., Voskoboinik, I. and Mercer, J.F. (1999). Molecular mechanisms of copper homeostasis. Biochemical and Biophysical Research Communications **261**: 225-232.

Chapman, G.A., Kay, J. And Kille, P. (1999). Structural and functional analysis of the rat metallothionein III genomic locus. Biochimica et Biophysica Acta: Gene Structure and Expression **1445**(3): 321-329.

Choi, D.W., Yokoyama, M. And Koh, J. (1988). Zinc neurotoxicity in cortical cell culture. Neuroscience **24**(1): 67-79

Clemens, S. (2006). Evolution and function of phytochelatin synthases. Journal of Plant Physiology **163**: 319-332.

Clemens, S., Schroeder J.I. and Degenkolb, T. (2001). *Caenorhabditis elegans* expresses a functional phytochelatin synthase. European Journal of Biochemistry/FEBS **268**(13): 3640-3643.

Clemens, S., Kim, E.J., Neumann, D. and Schroeder, J.I. (1999). Tolerance to toxic metals by a gene family of phytochelatin synthases from plants and yeast. The EMBO Journal **18**(12): 3325-3333.

Cobbett, C. and Goldsbrough, C. (2002). Phytochelatins and metallothioneins: Roles in heavy metal detoxification and homeostasis. Annual Review of Plant Biology **53**: 159-182.

Cobbett, C.S. (2000a). Phytochelatins and their roles in heavy metal detoxification. Plant Physiology **123**: 825-832.

Cobbett, C.S. (2000b). Phytochelatin biosynthesis and function in heavy metal detoxification. Current Opinion in Plant Biology **3**: 211-216.

Coen, M., Holmes, E., Lindon, J.C. and Nicholson, J.K. (2008). NMR-based metabolic profiling and metabonomic approaches to problems in molecular toxicology. Chemical Research in Toxicology **21**: 9-27.

Consortium, The *C. elegans* sequencing consortium. (1998). Genome sequence of the nematode *C. elegans*: a platform for investigating biology. Science **282**(5396): 2012-8.

Cousins, R.J., Blanchard, R.K., Popp, M.P., Lui, L., Cao, J., Moore, J.B. and Green, C.L. (2003). A global view of the selectivity of zinc deprivation and excess on genes expressed in human THP-1 mononuclear cells. Proceedings of the National Academy of Sciences **100**(12): 6952-6957.

Cui, Y., McBride, S.J., Boyd, W.A., Alper, S. and Freedman, J.H. (2007). Toxicogenomic analysis of *Caenorhabditis elegans* reveals novel genes and pathways involved in the resistance to cadmium toxicity. Genome Biology **8**(6): R122.

Dallinger, R. (1996). Metallothionein research in terrestrial invertebrates: Synopsis and perspectives. Comparative Biochemistry and Physiology **113**(2): 125-133.

De Schamphelaere, K.A.C., Canli, M., Van Lierde, L.V., Forrez, I., Vanhaecke, F. and Janssen, C.R. (2004). Reproductive toxicity of dietary zinc to *Daphnia magna*. Aquatic Toxicology **70**(3): 233-244.

Egli, D., Selvaraj, A., Yeposkoposyan, H., Zhang, B., Hafen, E., Georgiev, O. and Schaffner, W. (2003). Knockout of 'metal-responsive transcription factor' MTF-1 in *Drosophila* by homologous recombination reveals its central role in heavy metal homeostasis. The EMBO Journal **22**(1): 100-108.

Egli, D., Yeposkoposyan, H., Selvaraj, A., Balamurugan, K., Rajaram, R., Simons, A., Multhaup, G., Mettler, S., Vardanyan, A., Georgiev, O. and Schaffner, W. (2006). A family knockout of all four *Drosophila* metallothioneins reveals a central role in copper homeostasis and detoxification. Molecular and Cellular Biology **26**(6): 2286-2296.

Eisenstein, R.S. (2000). Iron regulatory proteins and the molecular control of mammalian iron metabolism. Annual Review of Nutrition **20**: 627-662.

Fire, A., Xu, S., Montgomery, M.K., Kostas, S.A., Driver, S.E. and Mello, C.C. (1998). Potent and specific genetic interference by double-stranded RNA in *Caenorhabditis elegans*. Nature **391**(6669): 806-811.

Freedman, J.H., Slice, L.W., Dixon, D., Fire, A. and Rubin, C.S. (1993). The novel metallothionein genes of *Caenorhabditis elegans*. The Journal of Biological Chemistry **268**(4): 2554-2564.

Garg, A.K., Kim, J.K., Owens, T.G., Ranwala, A.P., Choi, D.Y., Kochian, L.V. and Wu, R.J. (2002). Trehalose accumulation in rice plants confers high tolerance levels to different abiotic stresses. Proceedings of the National Academy of Sciences USA **99**(25): 15898-15903.

Gedamu, L., Samson, S.L.A., Schieman, S. and Paramchuk, W. (1999). Metallothionein V. Editor: C. Klaassen. pp253-259

Giulietti, A., Overbergh, L., Valckx, D., Decallonne, B., Bouillon, R. and Mathieu, C. (2001). An Overview of real-time quantitative PCR: Applications to quantify cytokine gene expression. Methods **25**(4): 386-401.

Gonzalez-Mendoza, D., Moreno, D.Q. and Zapata-Perez, O. (2007). Coordinated response of phytochelatin synthase and metallothionein

genes in black mangrove, *Avicennia germinans*, exposed to cadmium and copper. Aquatic Toxicology **83**(4): 306-314.

Goodacre, R., Vaidyanathan, S., Dunn, W.B., Harrigan, G.G. and Kell, D.B. (2004). Metabolomics by numbers: acquiring and understanding global metabolite data. Trends in Biotechnology **22**(5): 245-252.

Griffin, J.L. (2006). The Cinderella story of metabolic profiling: does metabolomics get to go the functional genomics ball. Philosophical Transactions of the Royal Society of London. Series B: Biological Sciences **361**(1465): 147-161.

Grill, E., Löffler, S., Winnacker, E.L. and Zenk, M.H. (1989). Phytochelatins, the heavy metal binding peptides of plants, are synthesised from glutathione by a specific gamma-glytamycysteine dipeptidyl transpepidase (phytochelatin synthase). Proceedings of the National Academy of Sciences USA **86**(18): 6838-6842.

Grill, E., Winnacker, E.L. and Zenk, M.H. (1987). Phytochelatins, a class of heavy metal binding peptides from plants, are functionally analogous to metallothioneins. Proceedings of the National Academy of Sciences, USA **84**(2): 439-443.

Grivet, J.P., Delort, A.M. and Portais, J.C. (2003). NMR and microbiology: from physiology to metabolomics. Biochemie **85**(9): 823-840.

Ha, S.B., Smith, A.P., Howden, R., Dietrich, W.M., Bugg, S., O'Connell, M.J., Goldsbrough, P.S. and Cobbett, C.S. (1999). Phytochelatin synthase genes from *Arabidopsis* and the yeast, *Schizosaccharomyces pombe*. Plant Cell **11**(6): 1153-1164.

Hannon, G.J. (2002). RNA interference. Nature **418**: 244-251.

Harris, T.W., Chen, N., Cunningham, F., Tello-Ruiz, M., Antosheckin, I., Bastiani, C., Bieri, T., Blasiar, D., Bradnam, K., Chan, J., Chen, C., Chen, W.J., Davis, P., Kenny, E., Kishore, R., Lawson, D., Lee, R., Muller, H., Nakamura, C., Ozersky, P., Petcherski, A., Rogers, A., Sabo, A., Schwarz, E.M., Van Auken, K., Wang, Q., Durbin, R., Spieth, J., Sternberg, P.W. and Stein, L.D. (2004). WormBase: a multi-species resource for nematode biology and genomics. Nucleic Acids Research **32**(Database issue): D411-D417.

Hirata, K., Tsuji, N. and Miyamoto, K. (2005). Biosynthetic regulation of phytochelatins, heavy metal binding peptides. Journal of Bioscience and Bioengineering **100**(6): 593-599.

Hoffmann, A., Oelgeschläger, T. and Roeder, R.G. (1997). Considerations of transcriptional control mechanisms: Do TFIID–core promoter complexes recapitulate nucleosome-like functions? Proceedings of the National Academy of Sciences USA **94**(17): 8928-8935.

Hope, I.A., Stevens, J., Garner, A., Hayes, J., Cheo, D.L., Brasch, M.A. and Vidal, M. (2004). Feasibility of genome-scale construction of promoter:: reporter gene fusions for expression in *Caenorhabditis elegans* using a Multisite Gateway recombination system. Genome Research **14**(10B): 2070-2075.

Houghton, C.B. and Cherian, M.G. (1991). Effects of inhibition of cystathionase activity on glutathione and metallothionein levels in the adult rat. Journal of Biochemical Toxicology **6**(3): 221-228.

Huckle, J.W., Morby, A.P., Turner, J.S. and Robinson, N.J. (1993). Isolation of a prokaryotic metallothionein locus and analysis of transcriptional control by trace metal ions. Molecular Microbiology **7**(2): 177-187.

Hughes, S. and Stürzenbaum, S.R. (2007). Single and double metallothionein knockout in the nematode *C. elegans* reveals cadmium dependent and independent toxic effects on life history traits. Environmental Pollution **145**(2): 395-400.

Ibaim, U. and Grant, A. (2005). RNA/DNA ratios as a sub lethal endpoint for large-scale toxicity tests with the nematode *Caenorhabditis elegans*. Environmental Toxicology and Chemistry **24**(5): 1155-1159.

Izumchenko, E., Wolfson, M., Golemis, E.A. and Serebriiskii, I.G. (2007) Yeast Gene Analysis. Methods in Microbiology Volume 36, 2nd edition, Academic Press. Editors: I. Stansfield and M.J.R. Stark pp117-118.

Jaeckel, P., Krauss, G., Menge, S., Schierhorn, A., Rucknagel, P. and Krauss, G.J. (2005). Cadmium induces a novel metallothionein and phytochelatin 2 in an aquatic fungus. Biochemical and Biophysical Research Communications **333**(1): 150-155.

Jager, T., Alvarez, O.A., Kammenga, J.E. and Kooijman, S.A.L.M. (2005). Modelling nematode life cycles using dynamic energy budgets. Functional Ecology **19**: 136-144.

Jiang, H., Fu, K. and Andrews, G.K. (2004). Gene- and cell-type-specific effects of signal transduction cascades on metal-regulated gene transcription appear to be independent of changes in the phosyphorylation of metal-response-element-binding transcription factor-1. Biochemical Journal **382**(Part 1): 33-41.

Johnson, T.E. and Hutchinson, E.W. (1993). Absence of strong heterosis for life span and other life history traits in *Caenorhabditis elegans*. Genetics **134**(2): 465-474.

Jones, O.A.H., Walker, L.A., Nicholson, J.K., Shore, R.F. and Griffin, J.K. (2007). Cellular acidosis in rodents exposed to cadmium is caused by adaptation of the tissue rather than an early effect of toxicity. Comparative Biochemistry and Physiology Part D: Genomics and Proteomics **2**(4): 316-321.

Kadandale, P. and Singson, A. (2004). Oocyte production and sperm utilisation patterns in semi fertile strains of *Caenorhabditis elegans*. BMC Developmental Biology **4**:3.

Kägi, J.H.R. and Schaffer, A. (1988). Biochemistry of metallothionein. Biochemistry **27**(23): 8509-8515.

Kägi, J.H.R. and Vallee, B.L. (1960). Metallothionein: a cadmium- and zinc-containing protein from equine renal cortex. The Journal of Biological Chemistry **235**(12): 3460-3465.

Kamath, R.S. and Arhringer, J. (2003). Genome-wide RNAi screening in *Caenorhabditis elegans*. Methods **30**(4): 313-321.

Kamath, R.S., Martinez-Campos, M., Zipperlen, P., Fraser, A.G. and Ahringer, J. (2000). Effectiveness of specific RNA-mediated interference through ingested double-stranded RNA in *Caenorhabditis elegans*. Genome Biology **2**(1). E-publication.

Kammenga, J.E., van Koert, P.H.G., Riksen, J.A.G., Korthals, E.W. and Bakker, J. (1996). A toxicity test in artificial soil based on the life-history

strategy of the nematode *Plectus acuminatus*. Environmental Toxicology and Chemistry **15**: 722-727.

Klaassen, C.D., Liu, J. and Choudhuri, S. (1999). Metallothionein: An intracellular protein to protect against cadmium toxicity. Annual Review of Pharmacological Toxicology **39**: 267-94.

Kojima, Y., Berger, C., Vallee, B.L. and Kägi, J.H.R. (1976). Amino-acid sequence of equine renal metallothionein-1B. Proceedings of the National Academy of Sciences USA **73**(10): 3413-3417.

Kugawa, F., Yamamoto, H., Osada, S., Aoki, M., Imagawa, M. and Nishihara, T. (1994). Metallothionein genes in the nematode *Caenorhabditis elegans* and metal inducability in mammalian culture cells. Biomedical and Environmental Sciences **7**(3): 222-231.

Larin, D., Mekios, C., Das, K., Ross, B., Yang, A. and Gilliam, T.C. (1999). Characterisation of the interaction between the Wilson and Menkes Disease proteins and the cytoplasmic copper chaperone, HAH1p. The Journal of Biological Chemistry **274**(40): 28497-28504.

Le Belle, J.E., Harris, N.G., Williams, S.R. and Bhakoo, K.K. (2002). A comparison of cell and tissue extraction techniques using high-resolution 1H-NMR spectroscopy. NMR in Biomedicine **15**(1): 37-44.

Lee, S. And Korban, S.S. (2002). Transcriptional regulation of *Arabidopsis thaliana* phytochelatin synthase (AtPCS1) by cadmium during the early stages of plant development. Planta **215**(4): 689-693.

Li, Y., Kandasamy, M.K. and Meagher, R.B. (2001). Rapid isolation of monoclonal antibodies. Monitoring enzymes in the phytochelatin synthesis pathway. Plant Physiology **127**(3): 711-719.

Liao, V.H., Dong, J. and Freedman, J.H. (2002). Molecular characterisation of a novel, cadmium-inducible gene from the nematode *Caenorhabditis elegans*. The Journal of Biological Chemistry **277**(44): 40249-42059.

Liao, V.H. and Freedman, J.H. (1998). Cadmium-regulated genes from nematode *Caenorhabditis elegans.* The Journal of Biological Chemistry **273**(48): 31962-31970.

Lichtlen, P. and Schaffner, W. (2001). Putting its fingers on stressful situations: the heavy metal-regulatory transcription factor MTF-1. Bioessays **23**(11): 1010-1017.

Lin, C.Y., Wu. H., Tjeerdema, R.S. and Viant, M.R. (2007). Evaluation of metabolite extraction strategies from tissue samples using NMR metabolomics. Metabolomics **3**(1): 55-67.

Lopato, S., Bazanova, N., Morran, S., Milligan, A.S., Shirley, N. and Langridge, P. (2006). Isolation of plant transcription factors using a modified yeast one-hybrid system. Plant Methods **2**: 3

Maeda, I., Kohara, Y., Yamamoto, M. and Sugimoto, A. (2001). Large-scale analysis of gene function in *Caenorhabditis elegans* by high-throughput RNAi. Current Biology **11**(3): 171-176.

Maret, W. (2005). Zinc coordination environments in proteins determine zinc functions. Journal of Trace Elements in Medicine and Biology **19**(1): 7-12.

Margoshes, M. and Vallee, B.L. (1957). A cadmium protein from equine kidney cortex. Journal of the American Chemical Society **79**(17): 4813-4814.

Maroni, G., Wise, J., Young, J.E. and Otto, E. (1987). Metallothionein gene duplications and metal tolerance in natural populations of *Drosophila melanogaster*. Genetics **117**(4): 739-744.

Mattie, M.D. and Freedman, J.H. (2004). Copper-inducible transcription: regulation by metal- and oxidative stress responsive pathways. American Journal of Physiology - cell physiology **286**(2): C293-C301.

Meister, G. and Tuschl, T. (2004). Mechanisms of gene silencing by double-stranded RNA. Nature **431**(7006): 343-349.

Mendoza-Cózatl, D., Loza-Tavera, H., Hernandez-Navarro, A. and Moreno-Sánchez, R. (2005). Sulfur assimilation and glutathione metabolism under cadmium stress in yeast, protists and plants. FEMS Microbiology Reviews **29**(4): 653-671.

Mertens, P.R., Alfonso-Jaume, M.A., Steinmann, K. and Lovett, D.H. (1998). A Synergistic interaction of transcription factors AP2 and YB-1 Regulates Gelatinase A enhancer-dependent transcription. Journal of Biological Chemistry **273**(49): 32957-32965.

Moilanen, L.H., Fukushige, T. and Freedman, J.H. (1999). Regulation of metallothionein gene transcription. The Journal of Biological Chemistry **274**(42): 29655-29665.

Moore, M.N. (2002). Biocomplexity: the post-genome challenge in ecotoxicology. Aquatic Toxicology **59**(1-2): 1-15.

Nicholson, J.K., Lindon, J.C. and Holmes, F. (1999). 'Metabonomics' : Understanding the metabolic responses of living systems to pathophysiological stimuli via multivariate statistical analysis of biological NMR spectroscopic data. Xenobiotica **29**(11): 1181-1189.

Ogra, Y., Aoyama, M. and Suzuki, K.T. (2006). Protective role of metallothionein against copper depletion. Archives of Biochemistry and Biophysics **451**(2): 112-118.

Palmiter, R.D. (1998). The elusive function of metallothioneins. Proceedings of the National Academy of Sciences USA **95**(15): 8428-8430.

Prasad, A.S. (1985). Clinical, endocrinological and biochemical effects of zinc deficiency. Clinics in endocrinology and metabolism **14**(3): 567-589.

Qiagen Manual (2006) Critical factors for successful Real-Time PCR.

Raamsdonk, L.M., Teusink, B., Broadhurst, D., Zhang, N.S., Hayes, A., Walsh, M.C., Berden, J.A., Brindle, K.M., Kell, D.B., Rowland, J.J., Westerhoff, H.V., van Dam, K. and Oliver, S.G. (2001). A functional genomics strategy that uses metabolome data to reveal the phenotype of silent mutations. Nature Biotechnology **19**(1): 45-50.

Rao, A.M., Drake, M.R. and Stiplanuk, M.H. (1990). Role of the transsulfuration pathway and of gamma-cystathionase activity in the formation of cysteine and sulfate from methionine in rat hepatocytes. The Journal of Nutrition. **120**(8): 837-845

Rea, P.A., Vatamaniuk, O.K. and Rigden, D.J. (2004). Weeds, worms and more. Papain's long lost cousin, Phytochelatin synthase. Plant Physiology **136**(1): 2463-2474.

Reo, N.V. (2002). NMR-based metabolomics. Drug and Chemical Toxicology **25**(4): 375-382.

Ringner, M. (2008). What is principle component analysis? Nature Biotechnology **26**(3): 303-304

Riordan, J.F. and Vallee, B.L. (1991). Metallothioneins and related compounds. Methods in Enzymology. **205** Academic Press Inc, San Diego

Robertson, D.G. (2005). Metabonomics in toxicology: A review. Toxicological Sciences **85**(2): 809-822.

Roesijadi, G. (1992). Metallothioneins in metal regulation and toxicity in aquatic animals. Aquatic Toxicology **22**: 81-114.

Roth, U., von Roepenack-Lahaye, E. and Clemens, S. (2006). Proteome changes in *Arabidopsis thaliana* roots upon exposure to Cd^{2+}. Journal of Experimental Botany **57**(15): 4003-4013.

Sarry, J.E., Kuhn, L., Ducruix, C., Lafaye, A., Junot, C., Hugouvieux, V., Jourdain, A., Bastien, O., Fievet, J.B., Vailhen, D., Amekraz, B., Moulin, C., Ezan, E., Garin, J. and Bourguignon, J. (2006). The early responses of *Arabidopsis thaliana* cells to cadmium exposure explored by protein and metabolite profiling analyses. Proteomics **6**(7): 2180-2196.

Saydam, N., Adams, T.K., Steiner, F., Schaffner, W. **and** Freedman, J.H. (2002). Regulation of metallothionein transcription by the metal-responsive transcription factor MTF-1. The Journal of Biological Chemistry **277**(23): 20438-20445.

Serebriiskii, I.G. and Golemis, E.A. (2000). Uses of lacZ to study gene function: Evaluation of beta-galactosidase assays employed in the yeast two-hybrid system. Analytical Biochemistry **285**(1): 1-15.

Shaw, C.A. (1998). Multiple roles of glutathione in the nervous system. In Glutathione in the nervous system, Editor: C.A.Shaw Taylor and Francis, Washington DC.

Sijen, T., Fleenor, J., Simmer, F., Thijssen, K.L., Parrish, S., Timmons, L., Plasterk, R.H.A. and Fire, A. (2001). On the role of RNA amplification in dsRNA-triggered gene silencing. Cell **107**(4): 465-476.

Smith, C.A., Want, E.J., O'Maille, G., Abagyan, R. and Siuzdak, G. (2006). XCMS: Processing mass spectrometry data for metabolite profiling using nonlinear peak alignment, matching and identification. Analytical Chemistry **78**(3): 779-787.

Stein, A.F., Bracken, W.M. and Klaassen, C.D. (1987). Utilisation of methionine as a sulfhydryl source for metallothionein synthesis in rat primary hepatocyte cultures. Toxicology and Applied Pharmacology **87**(2): 276-283.

Steinkühler, C., Carri, M.T., Micheli, G., Kneopfel, L., Weser, U. and Rotilio, G. (1994). Copper-dependent metabolism of Cu,Zn-superoxide dismutase in human K562 cells. Lack of specific transcriptional activation and accumulation of a partially inactivated enzyme. Biochemical Journal **302**(Part 3): 687-694.

Stillman, M.J., Shaw, C.F. and Suzuki, K.T. (1992). Metallothioneins: synthesis, structure and properties of metallothioneins, phytochelatins and metal-thiolate complexes. New York, Wiley-VCH Publishers.

Stuart, G.W., Searle, P.F., Chen, H.Y., Brinster, R.L. and Palmiter, R.D. (1984). A 21-base pair DNA motif that is repeated several times in metallothionein gene promoters confers metal regulation to a heterologous gene. Proceedings of the National Academy of Sciences USA **81**(23): 7318-7322.

Stürzenbaum, S.R. and Kille, P. (2001). Control techniques in quantitative molecular biological techniques: the variability of invariance. Comparative Biochemistry and Physiololgy Part B **130**(3): 281-289.

Stürzenbaum, S.R., Kille, P. and Morgan, A.J. (1998). The identification, cloning and characterisation of earthworm metallothionein. FEBS letters **431**(3): 437-442.

Sugiura, Y., Kashiba, M., Maruyama, K., Hoshikawa, K., Sasaki, R., Saito, K., Kimura, H., Goda, N. and Suematsu, M. (2005). Cadmium exposure alters metabolomics of sulfur-containing amino acids in rat testes Antioxidants and redox signalling **7**(5-6): 781-787.

Sura, P., Ristic, N., Bronowicka, P. and Wrobel, M. (2006). Cadmium toxicity related to cysteine metabolism and glutathione levels in frog *Rana ridibunda* tissues. Comparative Biochemistry and Physiology Part C: Toxicology and pharmacology **142**(1-2): 128-135.

Suzuki, K.T., Someya, A., Komada, Y. and Ogra, Y. (2002). Roles of metallothionein in copper homeostasis: responses to Cu-deficient diets in mice. Journal of Inorganic Biochemistry **88**(2): 173-182.

Swain, S.C., Keusekotten, K., Baumeister, R. and Stürzenbaum, S.R. (2004). *C. elegans* metallothioneins: New insights into the phenotypic effects of cadmium toxicosis. Journal of Molecular Biology **341**(4): 951-959

Sze, D.Y. and Jardetzky, O. (1994). High-resolution proton NMR studies of lymphocyte extracts. Immunomethods **4**(2): 113-126.

Tabara, H., Grishok, A. and Mello, C.C. (1998). RNAi in *C. elegans*: Soaking in the genome sequence. Science **282**(5388): 430-431.

Tapia, L., González-Agüero, M., Cisternas, M.F., Suazo, M., Cambiazo, V., Uauy, R. and González, M. (2004). Metallothionein is crucial for safe intracellular copper storage and cell survival at normal and supra-physiological exposure levels. Biochemical Journal **378**(Part 2): 617-624.

Thumann, J., Grill, E., Winnacker, E.L. and Zenk, M.H. (1991). Reactivation of metal-requiring apoenzymes by phytochelatin-metal complexes. FEBS Letters **284**(1): 66-69.

Timmermans, M.J.T.N., Ellers, J., and van Straalen, N.H. (2005). Metallothionein mRNA expression and cadmium tolerance in metal stressed and reference populations of the Springtail *Orchesella cincta*. Ecotoxicology **14**(7): 727-739.

Timmons, L. and Fire, A. (1998). Specific interference by ingested dsRNA. Nature **395**: 854.

Tsuji, N., Hirayanagi, N., Iwabe, O., Namba, T., Tagawa, M., Miyamoto, S., Miyasaka, H., Takagi, M., Hirata, K. and Miyamoto, K. (2003). Regulation of phytochelatin synthesis by zinc and cadmium in marine green alga, *Dunaliella tertiolecta*. Phytochemistry **62**(3): 453-459.

Valko, M., Morris, H. and Cronin, M.T.D. (2005). Metals, toxicity and oxidative stress. Current Medicinal Chemistry **12**(10): 1161-1208.

Vallee, B.L. (1995). The function of Metallothioneins. Neurochemical International **27**(1): 23-33.

van der Werf, M.J., Jellema, R.H. and Hankemeier, T. (2005) Microbial metabolomics: replacing trial-and-error by the unbiased selection and ranking of targets. Journal of Industrial Microbiology and Biotechnology. **32**(6): 234-252.

Vandesompele, J., De Preter, K., Pattyn, F., Poppe, B., Van Roy, N., De Paepe, A. and Speleman, F. (2002). Accurate normalisation of real-time quantitative RT-PCR data by geometric averaging of multiple internal control genes. Genome Biology **3**(7): Research 0034.1-0034.11.

Vasak, M. (2005). Advances in metallothionein structure and functions. Journal of Trace Elements in Medicine and Biology **19**(1): 13-17.

Vatamaniuk, O.K., Bucher, E.A., Sundaram, M.V. and Rea, P.A. (2005). CeHMT-1, a putative phytochelatin transporter, is required for cadmium tolerance in *Caenorhabditis elegans*. The Journal of Biological Chemistry **280**(25): 23684-23690.

Vatamaniuk, O.K., Bucher, E.A., Ward, J.T. and Rea, P.A. (2001). A new pathway for heavy metal detoxification in animals. The Journal of Biological Chemistry **276**(24): 20817-20820.

Vatamaniuk, O.K., Bucher, E.A., Ward, J.T. and Rea, P.A. (2002). Worms take the 'phyto' out of 'phytochelatins'. Trends in Biotechnology **20**(2): 61-64.

Vatamaniuk, O.K., Mari, S., Lu, Y. and Rea, P.A. (2000). Mechanism of heavy metal ion activation of phytochelatin (PC) synthase: blocked thiols are sufficient for PC synthase catalysed transpeptidation of glutathione and related thiol peptides. The Journal of Biological Chemistry **275**(40): 31451-31459.

Waisberg, M., Joseph, P., Hale, B. and Beyersmann, D. (2003). Molecular and Cellular mechanisms of cadmium carcinogenesis. Toxicology **192**(1-2): 95-117.

Wang, T. and Brown, M.J. (1999). Differential expression of adenylyl cyclase subtypes in human cardiovascular system Molecular and Cellular Endocrinology **223**(1-2): 55-62.

Want, E., Cravatt, B.F. and Siuzdak, G. (2005). The expanding role of mass spectrometry in metabolote profiling and characterisation. Chembiochem **6**(11): 1941-1951.

Want, E.J., Nordstrom, A., Morita, H. and Siuzdak, G. (2007). From exogenous to endogenous: The inevitable imprint of mass spectrometry in metabolomics. Journal of Proteome Research **6**(2): 459-468.

West, A.K., Stallings, R., Hildebrand, C.E., Chiu, R., Karin, M. and Richards, R.I. (1990). Human metallothionein genes: Structure of the functional locus at 16q13. Genomics **8**(3): 513-518.

Williams, D. H. and Fleming, I. (1995). Spectroscopic methods in organic chemistry. London, The McGraw Hill Companies.

Wimmer, U., Wang, Y., Georgiev, O. and Schaffner, W. (2005). Two major branches of anti-cadmium defence in the mouse: MTF-1/metallothioneins and glutathione. Nucleic Acids Research **33**(18): 5715-5727.

Wood, W.B. (1988). The nematode *Caenorhabditis elegans.* Cold Spring Harbour Laboratory Press.

Wu, J., Lee, C., Yokom, D., Jiang, H., Cheang, M.C.U., Yorida, E., Turbin, D., Berquin, I.M., Mertens, P.R., Iftner, T., Gilks, C.B. and Dunn, S.E. (2006). Disruption of the Y-Box Binding Protein-1 Results in Suppression of the Epidermal Growth Factor Receptor and HER-2. Cancer Research **66**(9): 4872-4879.

Yan, C.H. and Chan, K.M. (2004). Cloning of zebrafish metallothionein gene and characterisation of its gene promoter region in HepG2 cell line. Biochemica et Biophysica Acta **1679**(1): 47-58.

Yu, W., Santhanagopalan, V., Sewell, A.K., Jensen, L.T. and Winge, D.R. (1994). Dominance of metallothionein in metal ion buffering in yeast capable of synthesis of (gamma-EC)nG isopeptides. The Journal of Biological Chemistry **269**(33): 21010-21015.

Zenk, M. H. (1996). Heavy metal detoxification in higher plants - a review. Gene **179**(1): 21-30.

Zhang, H., Xu, W., Guo, J., He, Z. and Ma, M. (2005). Coordinated responses of phytochelatins and metallothioneins to heavy metals in garlic seedlings. Plant Science **169**: 1059-1065.

Zhou, J. and Goldsbrough, P.B. (1994). Functional homologs of fungal metallothionein genes from *Arabidopsis*. The Plant Cell **6**(6): 875-884.

Zhu, B.Z. and Chevion, M. (2000). Copper-mediated toxicity of 2,4,5-trichlorophenol: biphasic effect of the copper(I)-specific chelator neocuproine. Archives of Biochemistry and Biophysics **380**(2): 267-273.

Zimeri, A.M., Dhankher, O.P., McCaig, B. And Meagher, R.B. (2005). The plant MT1 metallothioneins are stabilized by binding cadmiums and are required for cadmium tolerance and accumulation. Plant Molecular Biology **58**(6): 839-855.

APPENDIX ONE

LIST OF BINS USED IN NMR ANALYSIS

NMR spectra were analysed in iNMR v.2 (Nucleomatica, Italy) as detailed in Section 2.21.2. Spectra were manually binned into 96 regions using the iNMR integration function. A list of the bins are given below.

Bin number	ppm
1	0.09..0.09
2	0.93..0.95
3	0.95..0.98
4	0.98..1.01
5	1.01..1.03
6	1.03..1.06
7	1.06..1.09
8	1.24..1.25
9	1.32..1.35
10	1.45..1.47
11	1.47..1.50
12	1.52..1.55
13	1.66..1.69
14	1.70..1.76
15	1.76..1.80
16	1.92..1.93
17	1.98..1.99
18	2.01..2.07
19	2.07..2.09
20	2.10..2.19
21	2.23..2.27
22	2.34..2.38
23	2.40..2.41
24	2.43..2.48
25	2.52..2.54
26	2.54..2.59
27	2.64..2.66
28	2.66..2.71
29	2.71..2.76
30	2.79..2.84
31	2.84..2.89
32	2.94..2.95
33	2.95..2.96
34	2.97..2.99
35	3.00..3.04
36	3.04..3.07

Bin number	ppm
37	3.07..3.10
38	3.10..3.13
39	3.13..3.14
40	3.14..3.16
41	3.16..3.19
42	3.20..3.21
43	3.22..3.23
44	3.23..3.24
45	3.24..3.25
46	3.26..3.28
47	3.29..3.31
48	3.35..3.37
49	3.38..3.40
50	3.40..3.41
51	3.44..3.48
52	3.54..3.55
53	3.56..3.57
54	3.57..3.58
55	3.59..3.60
56	3.60..3.60
57	3.61..3.63
58	3.64..3.67
59	3.67..3.69
60	3.71..3.73
61	3.73..3.75
62	3.75..3.80
63	3.81..3.84
64	3.84..3.89
65	3.90..3.92
66	3.94..3.97
67	3.97..4.00
68	4.00..4.02
69	4.09..4.14
70	4.24..4.27
71	4.35..4.39
72	5.19..5.21

Bin number	ppm
73	5.96..6.01
74	6.03..6.05
75	6.08..6.10
76	6.15..6.17
77	6.52..6.53
78	6.89..6.92
79	7.11..7.13
80	7.13..7.15
81	7.19..7.21
82	7.31..7.35
83	7.38..7.40
84	7.42..7.44
85	7.46..7.49
86	7.95..7.96
87	7.96..7.98
88	8.18..8.18
89	8.24..8.27
90	8.27..8.28
91	8.43..8.44
92	8.45..8.47
93	8.54..8.55
94	8.60..8.61
95	9.33..9.36
96	9.60..9.63

APPENDIX TWO

NMR SPECTRA

NMR samples were analysed as described in (Beckonert et al. (2007) on a 600 MHz Bruker Avance DRX600 spectrometer (Section 2.21). Data was processed in iNMR v.2 (Nucleomatica, Italy) and manually binned (Appendix 1). All spectra were normalised to TSP to allow for direct comparison of the compound intensities. Samples were extracted using a glass bead disruption of the sample with methanol solvent extraction (Section 4.3.3). The figure below is the enhanced region of spectra of all samples (in no particular order) between 2.3 and 3 ppm. This diagram highlights that there was very little difference between spectra on initial inspection. Note similar peaks for glutamaine (2.45 ppm), succinate (2.4 ppm) and glutamate (2.35 ppm). However, one difference is apparent. Namely at 2.75 ppm which corresponds to peaks for cystathionine.

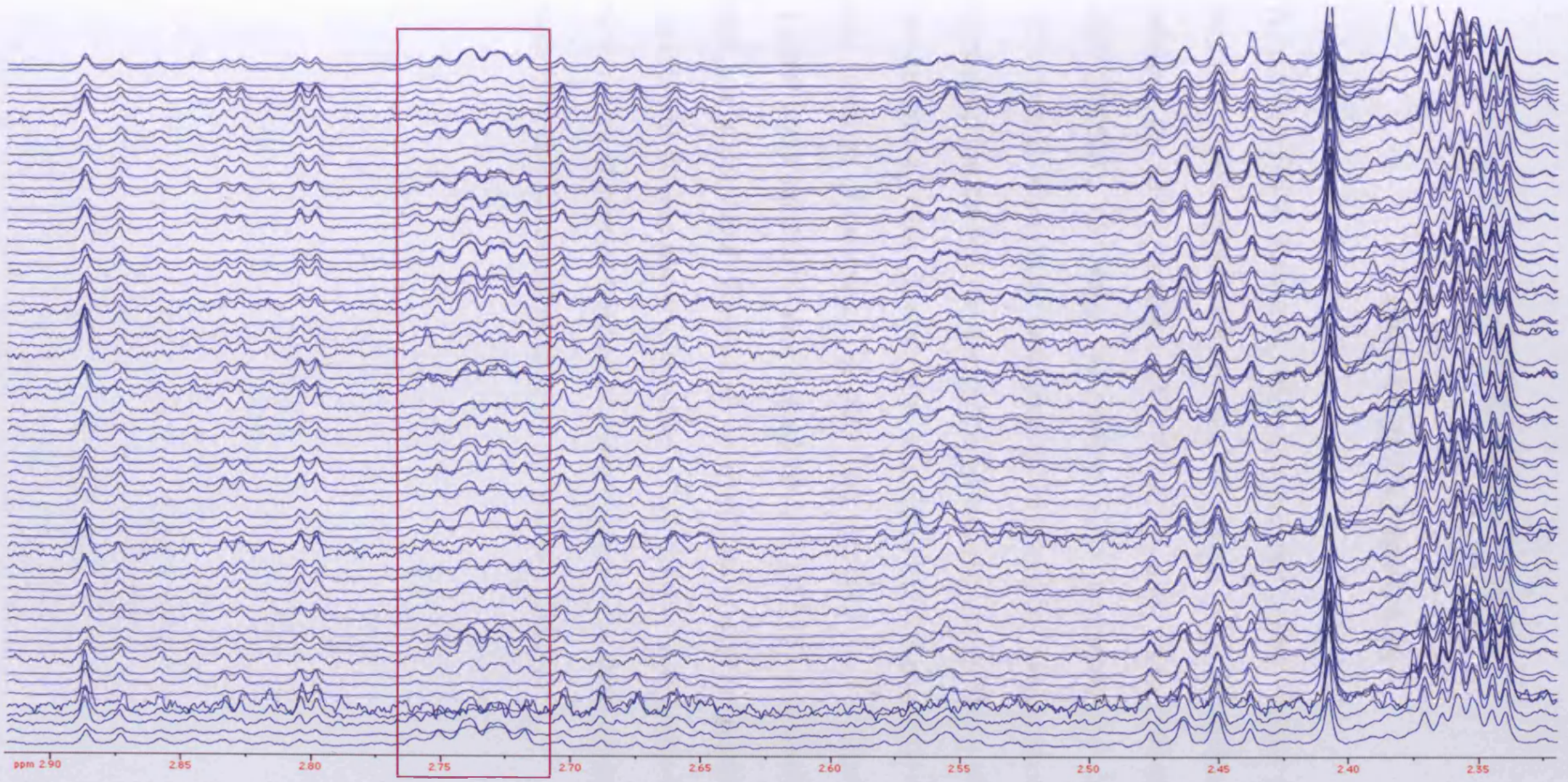

Enlarged spectra for all samples in the presence and absence of cadmium (2.3-3 ppm). Age synchronised nematodes were plated onto 5x 90mm Petri dishes per replicate. When nematodes were at the L4 stage, they were washed off the plates using M9 buffer and pelleted (centrifuged at 2000rpm, 2 minutes). The supernatant was removed and the pellet resuspended in 200 µl M9 buffer. Samples were extracted using the glass bead extraction method with methanol as the solvent. Note the absence of any particular order in the spectra. There was very few differences between samples, with the set of peaks for cystathionine at 2.75 ppm (purple box) do have differences between samples indicating that this metabolite is variable.

APPENDIX THREE

RNAI SCREEN RAW DATA

A targeted RNAi screen by feeding was performed. Genes (406) for the targeted screen were identified on the basis of GO terms for those genes relating to DNA binding (GO:0003677) and transcriptional regulation (GO:0030528). L3 stage nematodes were subjected the *E. coli* strain HT115(DE3). Nematodes were in single wells on 96-well plates with each well containing the dsRNA for one of the genes. The first screen consisted of 406 genes over 4 plates. The screen was repeated in triplicate in the presence and absence of cadmium (12 μM). The intensity of GFP signal from P*mtl-1*::GFP and P*mtl-2*::GFP was scored on a scale of 0 - 3 where 0 is no signal and 3 is "superbright" (Figure 7.4). Positive genes were isolated and screened again (one 96-well plates consisting of 41 genes). Ten genes were isolated which were of interest but half of these proved to be false positives. The raw data from each screen is given over the following pages.

First Screen (406 genes) – plate 1 in triplicate

gene	location	Cadmium concentration	location	A1	A2	A3	A4	A5	A6	A7	A8	A9	A10	A11	A12	B1	B2	B3	B4	B5	B6	B7	B8	B9	B10	B11	B12	C1	C2	C3	C4	C5	C6	C7	C8	C9
			Sequence Name	C46E1.1	F57B10.6		C39F7.1	F10G8.7	W02D9.3	W07E6.6	K12H6.1	C18A3.1	R10H1.3	T18H9.3	C06A1.5	Y44E3B.1	H06O01.2	DY3.3	C18G2.1	C28A1.11	B0019.2	Y39F10A.4	T10C4.6	C18A3.6	C28F5.5	Y53C12C.1	R08F8.6	C43E11.1	F22D6.2	DY3.4	Y97A6A.2	ZC247.3	F47G4.8	ZC204.2	C49D10.2	F10C1.5
mt-1	pharynx	0 µM	rep 1	1	1		2	1		2	1	1		2	2	1	1	1	1	2	1	2	2	1	2	1	1	1	2	1	1	1	2	1	1	2
mt-1	pharynx	0 µM	rep 2	1	1			1	1	2	0	2	1	1		1	1	1		1	1	1	1	1	0	2	1	1	1	1	1		1	1	1	
mt-1	pharynx	0 µM	rep 3	2	2	1	2	1	1	2		1	1	0	2	1	2	2	0	2	1		0		1	2	1	1	2	2	1	3	1	2	1	1
mt-1	intestine	0 µM	rep 1	1	1		2	1		2	1	1		2	1	1	1	1	0	2	0	2	1	1	1	0	1	1	1	1	1	1	1	1	1	1
mt-1	intestine	0 µM	rep 2	1	1			1	1	2	0	2	1	1		1	1	1		1	1	1	1	1	0	2	1	0	0	1	1			0	1	1
mt-1	intestine	0 µM	rep 3	1	1	1	2	1	1	2		1	1	0	1	1	2	1	0	2	1		0		1	0	1	1	1	2	1	3	1	1	1	1
mt-2	intestine only	0 µM	rep 1	0	1	2	1	2	0	1	0	1	2	1		1	1	1	1	0		1	1	1	1	1	1	1	2	2	1	1		0	1	2
mt-2	intestine only	0 µM	rep 2		1	3	1	1	3	1		1	2	2	2	1	1	1	2	1	1	2		1	2	1	2	1	1	3	1	2	1	1		
mt-2	intestine only	0 µM	rep 3	3	2			2	2	2	2	1	2	2		3	2	2	2	1		2	0	1	2		0	1		2		1		2	2	
mt-1	pharynx	12 µM	rep 1	1		3	0	2	3	0	2	3	3	2	3	3	2	2	3			1	2	2	3	2	2	2	3	2	2			1	3	2
mt-1	pharynx	12 µM	rep 2	2	2	2	2	2	2	2	2	2	2	2	2	1	1	2	2	2	2	2	2	2	2	2	2	1	1	1		2	2	2	2	2
mt-1	pharynx	12 µM	rep 3	1		2	2	1	2	2		1			1	0			2	1	1					2	0		2	0	2	2			1		2
mt-1	intestine	12 µM	rep 1	2		3	3	2	2	2	2	3	3	2	3	3	2	2	3			1	2	2	3	2	2	2	2	2	2	2		1	3	2
mt-1	intestine	12 µM	rep 2	0	2	2	2	2	2	2	2	2	2	2	2	1	1	2	2	2	2	2	2	2	2	2	2	1	1	1		2	2	2	2	2
mt-1	intestine	12 µM	rep 3	1		2	2	1	2	2		1			1	0			2	1	1					2	0		2	0	2	2			1		2
mt-2	intestine only	12 µM	rep 1	0		2	1	2	2	2		2	2	2	0		2	2	1	2	2	2	2	2	2	2	2		3	2	2	3	2	2	2	1
mt-2	intestine only	12 µM	rep 2	1		2	1		3	2	2	1	2		2	2	2	2	1	1	2	1	3	2	2	2	2		2	1	2	1	1	1	3	1
mt-2	intestine only	12 µM	rep 3	2	3	3	0	2	2	2		2	0	3	2	3	3	3	2	3	2	1	2	2	3	3		2	2	2		1	2	2	2	3

gene	location	Cadmium concentration	location	C10	C11	C12	D1	D2	D3	D4	D6	D6	D7	D8	D9	D10	D11	D12	E1	E2	E3	E4	E5	E6	E7	E8	E9	E10	E11	E12	F1	F2	F3	F4	F5	F6
			Sequence Name	T05H10.2	F26C11.2	F33A8.3	C43E11.2	K10D8.3	F38A2.10	K10C3.6	F46H11.4	ZK909.4	F45C12.2	R03H10.9	K08A1.4	C34O6.8	F27E5.2	F33A8.4	C27A12.6	C01H6.5	F32H2.1	T23H4.2	F26H2.13	F33H2.1	F45C12.3	C01F1.1	F18C5.2	K08F8.2	F33H1.1	T08D8.2	C46E7.2	F56D12.3	W08D4.6	T23D8.5	C36E7.9	C01B12.2
mt-1	pharynx	0 µM	rep 1	3	1	2	1	1	2	2	1	1	1	1			1	2	2	1	2	1	1	1		2	1	1	1	1	2	1	1	1	1	2
mt-1	pharynx	0 µM	rep 2		1	1			1	1	1		0			1		1		1	0	1	2	1		1	1		2	1	1		1		1	1
mt-1	pharynx	0 µM	rep 3	1			2	2	2	2	1	1	1	2	1	1	1	1	2	3	1	2	1	1		2		2		2	3	2	2	2	2	2
mt-1	intestine	0 µM	rep 1	3	1	2	1	1	2	2	1	1	0	1			0	1	2	1	1	1	1	1		2	1	0	1	1	2	0	0	1	0	1
mt-1	intestine	0 µM	rep 2		1	0			1	0	1		0			1		1		1	0	1	1	1		1	1		2	1	1		1		1	1
mt-1	intestine	0 µM	rep 3	1			2	1	2	1	1	1	1	1	1	1	1	1	2	1	1	1	1	1		2		2		2	3	1	1	1	2	2
mt-2	intestine only	0 µM	rep 1	1		0	1	2	2	0	1	2		0	1	1	1			2		0	1		1	0	0		1		0	2	1	2	1	1
mt-2	intestine only	0 µM	rep 2	1	1	1	2	2	2	1	1		1	2	2	1	2	2	1	0	1	1	1	2	2		1	1	2	1	1	1	1	1		2
mt-2	intestine only	0 µM	rep 3	1	2	1		2	1	0	3		1	1	1	1	1		2		2	1	2	1	2	1	0	1			1	1	2	2		
mt-1	pharynx	12 µM	rep 1	2	2	3	3	1	2	2	2	3	2	2	3	2	3	2	2	2	3	2	0	3	2	2	2	1	3	3		2	2	1	2	
mt-1	pharynx	12 µM	rep 2	2	2	2	1	1	2	2	2	2	2	2	2	2	2	2	1	1	0	2		2	2	1	2	2	2	2	2	1	2	2	1	2
mt-1	pharynx	12 µM	rep 3	1	2	2				3	2	2	0	3	1	2	3	2	2	1	1	3	2	2	2	3	1	2	3	2	2	3			2	2
mt-1	intestine	12 µM	rep 1	2	2	3	3	2	2	2	2	3	2	2	3	2	3	2	2	2	3	2	1	3	2	2	2	1	3	3		2	2	2	2	
mt-1	intestine	12 µM	rep 2	2	2	2	1	1	2	2	2	2	2	2	2	2	2	2	1	1	0	2		2	2	1	2	2	2	2	2	1	2	2	1	2
mt-1	intestine	12 µM	rep 3	1	0	2				3	2	2	0	3	1	2	3	2	2	1	1	3	2	2	2	3	1	2	3	2	2	3			2	2
mt-2	intestine only	12 µM	rep 1	2	2	2	2		2	2	3	2	2		2	0	2	2	2		3	3	3	2	2	2	2	0	2	2			2	3	2	2
mt-2	intestine only	12 µM	rep 2	2	1	2		2	1	1	2	3	1		2	1		1	3		3	1	2	2	1	2		1	2	2	1	3	2	2	2	
mt-2	intestine only	12 µM	rep 3	2	3	2				3	2	3	3	2	3	2	3	2	3		2	3	3	2	2	2	2	3	3	2	2	3	3	2	3	3	2

gene	location	Cadmium concentration	location	F7	F8	F9	F10	F11	F12	G1	G2	G3	G4	G5	G6	G7	G8	G9	G10	G11	G12	H1	H2	H3	H4	H5	H6	H7	H8	H9	H10	H11	H12
			Sequence Name	F46C12.15	B0304.1	F18C6.7	T24B8.6	T01E8.2	Y17G7A.1	T23H2.3	F56D12.4	C17E4.6	T23G6.6	Y62B11A.4	C01B12.8	C33C12.9	C27D8.4	F31E8.3	T24H10.1	C07E3.5	Y57A10B.4	T23H2.5	ZK265.4	C41G7.5	T23D8.8	Y53C10A.12	F25F1.1	F42G2.8	C17G3.8	F21D12.1	ED2H1.7	C07E3.6	F15D4.1
mt-1	pharynx	0 µM	rep 1	2	2	1	2	0	2	1	2	1	1	1		1		1		1	3	3		1	2		2	1					2
mt-1	pharynx	0 µM	rep 2		1	1	1		2	2	1	2	1	1	1		1		1		2	1	2	1	2	1	1		1	1	2		1
mt-1	pharynx	0 µM	rep 3	1		1	2		1		2	2	2	1	2						0	2	2	1		1	1	2	2		2		
mt-1	intestine	0 µM	rep 1	1	2	0	1	0	1	1	0	1	1	1			0		1		1	3	1		1	0		1	1				0
mt-1	intestine	0 µM	rep 2		1	1	1		2	1	1	2	1	1	1		1		1		2	1	2	1	1	1	1		1	1	2		1
mt-1	intestine	0 µM	rep 3	1		1	1		1		2	2	0	1	1						0	2	2	1		1	0	2	2		2		
mt-2	intestine only	0 µM	rep 1	2	1	1		1	2	1	1	1	2	1	1	1	2	1	0		1	1	1	2	2	1	1	1	1	1	1	1	1
mt-2	intestine only	0 µM	rep 2		1	1	1	1	1	0	2	1	2	2	2	1	2	1	1	2	1	1	1	1	1	2	1	1	1	1	1	1	1
mt-2	intestine only	0 µM	rep 3	3	2	1	2	1	1	2			1	0	1	2	2	1	2	2				3		1	1	2	2	2				
mt-1	pharynx	12 µM	rep 1	1	3	2	3	3	2	2	1	2	2	3	2	2	2	1	2	2	2	2	2	2	3	1	1	0	2	2	2		1
mt-1	pharynx	12 µM	rep 2	2	2	2	2	2	2	2	2	2	2	2	2	2	2	2	2	2	2		1	2	2	2	2		2	2	2	2	
mt-1	pharynx	12 µM	rep 3	2	2	2	2	1		2	2		2	2	2	1		1	2		3	2	0	3	2	2		0				1	
mt-1	intestine	12 µM	rep 1	1	3	2	3	3	2	1	1	2	2	2	2	2	2	1	2	2	2	2	2	2	3	1	1	2	2	2	2		1
mt-1	intestine	12 µM	rep 2	2	2	2	2	2	2	2	2	2	2	2	2	2	2	2	2	2	2		1	2	2	2	2	2	2	2	2	2	
mt-1	intestine	12 µM	rep 3	2	2	2	2	1		2	2		2	2	2	1		1	2		3	2	0	3	2	2		0				1	
mt-2	intestine only	12 µM	rep 1	2	2	2	2	2	3	2	1	2	2	2	2	2	2	2	2	2	2	3	2	3	2	3		2		2	2		2
mt-2	intestine only	12 µM	rep 2	2	3		2	2	2		3	1	1	1	2	2	2	2	2	2	2	3	3		2		2	2	3		2	2		3
mt-2	intestine only	12 µM	rep 3	2	2	2	3	3	2	3	3	3	2	3	2	2	2	2	3	2	2	3	2	2	0	3	3			2	3	2	2

First Screen (406 genes) – plate 2 in triplicate

gene	location	Cadmium	location	A1	A2	A3	A4	A5	A6	A7	A8	A9	A10	A11	A12	B1	B2	B3	B4	B5	B6	B7	B8	B9	B10	B11	B12	C1	C2	C3	C4	C5	C6	C7	C8	C9
		concentration	Sequence Name	F15D4.7	C48D5.1	C28B5.4	F23F12.9	R13A5.5	R06D3.11	T05G5.2	Y69A7A.5	C37F5.1	C45E5.8	C26B2.3	C28D4.1	Y49B8A.14	C44F1.2	K10D2.1	F27B3.5	ZK783.4	C13G5.1	M03C11.2	Y75B8A.1	C09G12.1	F38A5.13	C28B2.4	H27C11.1	C01G12.1	E03A3.4	ZC196.2	K04C2.2	C06C3.1	F54F2.9	M03C11.8	Y75B8A.6	F28F9.1
mt-1	pharynx	0 µM	rep 1	1	0	2	1	1	1	2	2	2	2	2	2	2	3	3	1	2	1	1	2	1	2	1	1	1	1	1	1	1	2	1	1	1
mt-1	pharynx	0 µM	rep 2	2	2	2	2	2	2	2	2	2	1	2	1	2	2	2	2	2	2	2	1	2	2	2	2	2	2	2	2	1	1	2	2	1
mt-1	pharynx	0 µM	rep 3				2	1		1	1	2	1	1	2	1		2	2	1		1	2	2	2	1	2	2		2	2	2				2
mt-1	intestine	0 µM	rep 1	1	0	1	0	1	1	1	1	2	1	0	1	1	3	3	1	1	1	1	2	1	1	1	1	1	0	0	0	1	2	1	1	1
mt-1	intestine	0 µM	rep 2	0	2	2	2	2	1	2	2	2	1	2	1	1	2	2	2	2	2	1	1	2	2	2	2	1	2	2	2	1	1	0	1	1
mt-1	intestine	0 µM	rep 3				2	1		1	1	1	1	1	2	1		2	2	1		1	2	1	1	1	2	1		2	0	2				2
mt-2	intestine only	0 µM	rep 1	0		1	1	2		1		1		2	2	1		1	1	1		1		1	1	2		1		1	1	1		1	1	1
mt-2	intestine only	0 µM	rep 2			1	2			3	1		1	2						2	1	2	1	2		2	2		1	2	2	1	2	2	2	1
mt-2	intestine only	0 µM	rep 3	2	1	1	1	1	1		2		2	2	2	2	2	2	2	2	2	2	2	2	2	2	2	2	1		2		2	2	2	2
mt-1	pharynx	12 µM	rep 1	3			2	1				2	1	0	0			1	0	1		1	1	2	1	2	0	0		1	1	2	1	1	1	2
mt-1	pharynx	12 µM	rep 2	2	3	3	1	2	3	2	2	2	3	3	2	1	2	2	1	3	1	1	2	2	3	2	2		2	2		3	1	1	2	2
mt-1	pharynx	12 µM	rep 3	2	3	2	3	2	3	3	3	1	3	3	3	3	3	3	2	2	3	3	3	3	3	2	2		3	3	2	2	3	3	3	3
mt-1	intestine	12 µM	rep 1	3			2	1				2	1	0	0			1	0	1		1	1	2	1	2	0	0		1	1	2	1	1	1	2
mt-1	intestine	12 µM	rep 2	2	3	3	1	2	3	2	2	2	3	3	1	1	2	2	1	3	1	1	2	2	3	2	2		2	2		3	1	1	2	2
mt-1	intestine	12 µM	rep 3	2	3	2	3	2	3	3	3	1	3	3	3	3	3	3	2	2	3	3	3	3	3	2	2		3	3	2	2	3	3	3	3
mt-2	intestine only	12 µM	rep 1	2	2	2		2	2	2	2	2	0		2	3	2			2	2	2	2	2	2			2	2	3	2	2	2	2	2	
mt-2	intestine only	12 µM	rep 2			2	2		2				2		2	3	3	3	1	2	3		1	2	2	3	1				2	2	2	2		2
mt-2	intestine only	12 µM	rep 3	2	2		2	3	2	2	3		3	3	3		3	3	3	3	3	2		3	2	3	3		2	2		3	3	2	0	3

gene	location	Cadmium	location	C10	C11	C12	D1	D2	D3	D4	D5	D6	D7	D8	D9	D10	D11	D12	E1	E2	E3	E4	E5	E6	E7	E8	E9	E10	E11	E12	F1	F2	F3	F4	F5	F6
		concentration	Sequence Name	C01B10.5	T09A12.4	T13F2.2	H10E21.3	R74.1	C34E10.7	B0280.8	C08C3.3	F44E2.2	Y39A1A.5	F53A2.5	W02C12.3	C17H12.9	C26C12.6	F32B6.1	F40G9.11	R74.3	W03A3.1	R151.6	ZK862.5	B0464.7	Y39A1C.3	F45G2.3	F55F10.1	T05A12.4	C27B7.4	K08F4.1	K02F3.4	R10E4.5	C56G2.4	T20B12.8	C14B9.6	F56A4.7
mt-1	pharynx	0 µM	rep 1	1	2	2	2	1	1	1			1	1	2	2	1	1	2	1	1	1	0	1	2	1	1	1	1		1	1	1	2	1	2
mt-1	pharynx	0 µM	rep 2	1	2	2	2	2	2	2	2		2	1	1	2	2	2	2	2	2		2	2	2	2	2	1	2	2	2	2	2	2	1	2
mt-1	pharynx	0 µM	rep 3	1	1	2	2		2	2	1		2	2	2	1	1	2	1	2	1	2	1	2	1	2	2			2	2	1	1	1	3		
mt-1	intestine	0 µM	rep 1	1	2	1	1	1	0	1			1	0	1	1	0	1	1	0	0	1	0	1	2	1	1	1	1		0	1	1	1	1	2
mt-1	intestine	0 µM	rep 2	1	2	2	1	2	1	2	2		1	1	1	0	1	2	2	2	2		2	2	2	1	1	1	1	2	2	2	2	1	1	2
mt-1	intestine	0 µM	rep 3	1	1	2	1		2	1	1		2	2	2	1	1	2	1	1	1	0	1	1	1	1	0			1	2	1	1	1	3		
mt-2	intestine only	0 µM	rep 1		2			2		2		0	1	1		1	0	0	1	2	1	1	1	2	1	1		2	2	1	1	1	1	1	1	2
mt-2	intestine only	0 µM	rep 2		2	1		2	2		2	2	1		2	2	1	2		1			2	1		2	2	2	2	2	1	2		2	2	2
mt-2	intestine only	0 µM	rep 3	2	2	2	2	2	2	2	2	2	2	1	2	2	2	2	2	2	2	2	2	2	2		2	1	2	2	2	2	2	2	2	2
mt-1	pharynx	12 µM	rep 1	1	1	1		2	1	1	1	0			0	0	1	0	2	2	2	3	2	3	0	1	0	1	2	2	2	2	2	2	2	2
mt-1	pharynx	12 µM	rep 2	3	2	3	2	2	2	2	3	2	1	3	2	2	2	3	2	3	2	2	2	3	2	1	1	1	1	2	2	3	2	2	2	3
mt-1	pharynx	12 µM	rep 3	2	2	2		3	3	2	2	3	3	2	2	3	2	3	2	3	2	2	2	3	2	3	2	3	3	2	3	3	2	2	3	3
mt-1	intestine	12 µM	rep 1	1	1	1		2	1	1	1	0			0	0	0	1	0	2	2	2	3	2	3	0	1	0	1	2	2	2	2	2	2	2
mt-1	intestine	12 µM	rep 2	2	2	2	2	2	2	2	3	2	1	3	2	2	2	2	2	3	2	2	2	3	2	1	1	1	1	2	2	3	2	2	2	3
mt-1	intestine	12 µM	rep 3	2	2	2		3	3	2	2	3	3	2	2	3	2	3	3	2	2	2	2	2	3	3	2	3	3	2	3	3	2	2	3	3
mt-2	intestine only	12 µM	rep 1	3	2		3	1		2	2	2	2	2	2	2	2	3	2					2	2	2	2		2		0	2		2	2	2
mt-2	intestine only	12 µM	rep 2	2	2	2		2		2	2	2	2	0	3		2	2	1	2	2	2	2		2			1	2	2	2	2	1		2		
mt-2	intestine only	12 µM	rep 3	2	2	3	3	2	3	3	3	3	3	3	3	3	3	3	2	3	2	2		3	2	3	3	2	3	3	3	3	2	3	2	

gene	location	Cadmium	location	F7	F8	F9	F10	F11	F12	G1	G2	G3	G4	G5	G6	G7	G8	G9	G10	G11	G12	H1	H2	H3	H4	H5	H6	H7	H8	H9	H10	H11	H12
		concentration	Sequence Name	M142.4	F45G2.3	R08C7.3	C08G3.1	ZC410.1	R11A8.4	F23H11.2	R07E5.6	C16A3.1	T20B12.8	C30A5.7	F56A4.9	Y47D3B.7	T07A9.5	R11E3.5	F45E4.9	ZK1251.1	F01D4.6	E02H9.6	C38D4.9	T28A5.8	C07H6.7	R05D3.1	F56A4.11	Y47D3B.9	K11H12.1	AC8.1	F33D4.1	K01H12.3	ZK593.4
mt-1	pharynx	0 µM	rep 1	1	2	1	1	1	1	1	1		1	2	2	3	3	2	1	2	1	1	1	1	0	2	1	0	2	1	2	1	1
mt-1	pharynx	0 µM	rep 2	2	1	2	2	2		1	1	2	1	1	1	2	0	1	2	2	1	2	1	2	1	1	1	2	2	2	2	2	2	2
mt-1	pharynx	0 µM	rep 3	2	1	2	2	1	2	1		1		2		2	1			1	1	1				2		1	2	3	2	3	1
mt-1	intestine	0 µM	rep 1	1	2	1	1	0	1	0	1		0	1	1	3	2	0	1	0	1	1	1	0	0	1	1	0	2	1	2	0	0
mt-1	intestine	0 µM	rep 2	0	1	2	2	2		0	1	2	0	1	1	2	0	1	1	2	1	1	1	1	0	1	1	2	2	2	2	1	2
mt-1	intestine	0 µM	rep 3	2	1	2	2	1	1	1		1		1		1	1			1	1	1				2		1	2	3	2	2	1
mt-2	intestine only	0 µM	rep 1	1	1	1	0	1	1	0	2	1	2	1	2	1	1		1	1	0	1	1	1	1		1		2			1	0
mt-2	intestine only	0 µM	rep 2			2	2	3	2	1			1		2	2	3	1	2	2	2	1	1	2	2	1		2	0	2		2	
mt-2	intestine only	0 µM	rep 3	2	2	2	2	2	2	2	2	2	0	2	2	1	2	2	1	2	2				0	0	0	2	2	2	2	2	2	2
mt-1	pharynx	12 µM	rep 1	1	1	2	3	2	2	0	1		1	1	2	0	1	0	1	1		2	1	1		2		2	1	1	1	1	1
mt-1	pharynx	12 µM	rep 2	2	2	2	1	2	2	2	2	2	2	2	3	2	2	2	2	2	2	2	2	2	2	0	2	3	2	2	1	2	2
mt-1	pharynx	12 µM	rep 3	2	2	3	2	3	3	3	2	2	2	3	2	3	2	3	3		3	2		3	1	1	2	2	3	1	3	3	3
mt-1	intestine	12 µM	rep 1	1	1	2	3	2	2	0	1		1	1	2	0	1	0	1	1		2	1	1		2		2	1	1	1	1	1
mt-1	intestine	12 µM	rep 2	1	2	2	1	2	2	2	2	1	2	2	3	1	2	1	1	2	1	2	2	2	2	0	2	3	2	2	1	2	2
mt-1	intestine	12 µM	rep 3	2	2	3	2	3	3	3	2	2	1	3	2	3	2	3	3		3	2		3	1	1	2	2	3	1	3	3	3
mt-2	intestine only	12 µM	rep 1		1		1	2			3	2	2	2	2	2	2	2	2		2	2	2	2	2	2	2		1		2	1	
mt-2	intestine only	12 µM	rep 2	2	2	2	2	2		2	2	2	2	0	3		2	2	1	2	2	2	2		2		2	2	1	2	1		2
mt-2	intestine only	12 µM	rep 3	2	2	3	3	2	3	3	3	3	3	3	3	3	3	3	2	3	2	2		3	2	3	3	2	3	3	3	3	2

First Screen (406 genes) – plate 3 in triplicate

gene	location	Cadmium	location	A1	A2	A3	A4	A5	A6	A7	A8	A9	A10	A11	A12	B1	B2	B3	B4	B5	B6	B7	B8	B9	B10	B11	B12	C1	C2	C3	C4	C5	C6	C7	C8	C9
		concentration	Sequence Name	T05E11.4	H02I12.7	F13G11.1	T01G6.4	T27B7.2	F47C10.4	T08D8.4	C33G8.6	D1014.8	H18N07.4	R07B7.16	C50B8.6	F01G4.1	F22B3.1	Y57G11C.19	T01G8.7	T27B7.3	C17E7.8	C24G6.4	C03G6.8	F20D6.9	T19B10.8	C13C4.1	T01D3.2	C08F8.6	H21P03.1	F38C2.2	Y116A8C.13	R13D11.6	C39C6.9	F36H12.3	F44E7.8	C03G6.10
mdt-1	pharynx	0 µM	rep 1				0			1			2	0	1						1	1	1		1	1	0			0		1	1	0	1	1
mdt-1	pharynx	0 µM	rep 2	2	2					1						1	1				2	2	2	2				1	1		2		1	2	2	2
mdt-1	pharynx	0 µM	rep 3	2	2	2	2	2	2	3	3	2	2	2	2	2	2	3	2	2	2	3	2	2	2	2	2	2	2	2	2	2	2	2	2	2
mdt-1	intestine	0 µM	rep 1				0			0			1	0	1						1	1	1		1	1	0			0		1	1	0	1	1
mdt-1	intestine	0 µM	rep 2	2	2					1						1	1				1	2	1	1				1	1		2		1	2	1	1
mdt-1	intestine	0 µM	rep 3	2	2	2	2	2	0	3	3	2	2	1	2	1	2	3	2	2	2	3	2	2	2	2	1	2	2	2	2	2	2	2	2	2
mdt-2	intestine only	0 µM	rep 1	0	1	0	1	2	1	0	2		1	0	0	0	0	1	1	0	0	0	1	3	3	0	2	0	1	1	0	3	3	0	1	0
mdt-2	intestine only	0 µM	rep 2		1		2	2			2	1	1	1	1		0	2	1	1	1	1	1	1	1	1	2	0	2	3	1	1	1	1	0	2
mdt-2	intestine only	0 µM	rep 3		1	2	3	2	3	3	2	2	2	2	3	2	2	3	2	2	2	2	3	2	2	1	2	1	2	2	2	2	2		2	2
mdt-1	pharynx	12 µM	rep 1	2	0	1	0			2	2	0	1	3	1	2	0		2	0		2	2	2	1	2	2	1	1		1	0		2	2	1	
mdt-1	pharynx	12 µM	rep 2	1	3	3	3	3	1	3	3	2	2	2	2	1	2	2	1	2	2	2	2	2	2	3	1		2	2	1	2		3	2	2
mdt-1	pharynx	12 µM	rep 3	2	2	3	2	1	3	3	3	2	3	3		3	3	3	3	3	3	3	3	3	3	3	3	2	3	3	3	1	3	3	3	2
mdt-1	intestine	12 µM	rep 1	2	0	1	0			2	2	0	1	2	1	2	0		2	0		2	2	2	1	2	2	1	1		1	0		2	2	1	
mdt-1	intestine	12 µM	rep 2	1	3	3	3	3	1	3	3	2	2	2	2	1	2	2	1	2	1	2	2	2	2	3	1		2	2	1	2		3	2	2
mdt-1	intestine	12 µM	rep 3	2	2	3	2	1	3	3	3	2	3	3		3	3	3	3	3	3	3	3	3	3	3	3	2	3	3	3	1	3	3	3	2
mdt-2	intestine only	12 µM	rep 1	2			1	3	3	2	0	2	2	3	2	0			0	1	1	2	2	2	2	2	3	3	2		0		1	2	2	2	2
mdt-2	intestine only	12 µM	rep 2	3	3	2	2	2	3		3	2	2	2	2		1	2	1	2	1	2	2	2	2	2		2	2	1		2	3		2	1	
mdt-2	intestine only	12 µM	rep 3	2	3	3	3	2	2	3	3	3		3	3	3	2	3	3	3	0		2	3	3	2	2	1	3	2	3	2		2			2

gene	location	Cadmium	location	C10	C11	C12	D1	D2	D3	D4	D5	D6	D7	D8	D9	D10	D11	D12	E1	E2	E3	E4	E5	E6	E7	E8	E9	E10	E11	E12	F1	F2	F3	F4	F5	F6
		concentration	Sequence Name	ZK882.4	T19B10.11	C13C4.2	F55B12.1	R07H5.10	T22B3.1	Y116A8C.13	C39F7.4	T28A11.14	F13A2.8	F25F12.7	C03G6.12	F44A2.1	H12C20.3	C13C4.3	F09F3.10	F54D1.4	C25G4.4	Y116A8C.22	C38C3.9	T24A6.8	C18G1.5	F29G9.4	F25E5.8	C50H2.2	T27F2.4	W05B10.1	ZC376.4	B0035.1	C39E9.12	C52D10.5	F59A7.8	T22F3.11
mdt-1	pharynx	0 µM	rep 1	0	0	0		1	1		2	1	1	1	1		0	1	1	2	1	1	1	2	1	2	1	1		1	1	1	1	2	1	
mdt-1	pharynx	0 µM	rep 2	1		1	2	1	1	0		2			1	1	1	1		1			2	1	2			2			1	2	1	0	2	
mdt-1	pharynx	0 µM	rep 3	2	2	2	2	3	2	2	1	2	2	2	2	1	2	3	2	3	3	2	1	2	0	2	2	1	2	1	2	2	3	2	1	2
mdt-1	intestine	0 µM	rep 1	0	0	0		1	1		1	0	0	1	1		0	1	1	1	0	1	0	1	1	2	1	1		0	1	1	1	1	1	
mdt-1	intestine	0 µM	rep 2	1		1	2	1	0	0		1			1	1	1	1		1			1	1	2			1			1	1	1	0	1	
mdt-1	intestine	0 µM	rep 3	2	2	1	2	3	2	2	1	2	1	2	2	1	2	3	2	3	3	2	1	2	0	2	2	1	1	1	2	2	3	2	0	2
mdt-2	intestine only	0 µM	rep 1	0	0	1	2	2	2	3	3	1	1	1	1	3	2	1		1	0	0	2	1	1	3	1	2	1	0	0	1	1	2	3	2
mdt-2	intestine only	0 µM	rep 2	2			1	1	2	0	3			1	1	1	2		1	2			2	1	1	2		2			0		1	2	0	3
mdt-2	intestine only	0 µM	rep 3	2	2	1	2	2	2	2	1	2		2	2	2	2	2	2	2	1		1	2	0	2	2	2	2	1	1	1	1	2	2	2
mdt-1	pharynx	12 µM	rep 1	1	1	0			2	2		2	3	2		2	2	2	2	2	2	2		2	2	2		2	2	2	2	0	2	2	2		3
mdt-1	pharynx	12 µM	rep 2	2	3		2	2	1	1	1	2	2	1	2	2	2	1	2	2	2	2	3	1	1	1			2	1	2		0		2	
mdt-1	pharynx	12 µM	rep 3	3	3	3	3	2	3	3	2	3	3	3	2	3	3	3	3	3	2	3	2	2	0	3	2	3	3	3	3	3	2	2	2	2
mdt-1	intestine	12 µM	rep 1	1	1	0			2	2		2	3	2		2	0	2	2	2	2	2		2	2	2		1	2	2	0	2	2	2		3
mdt-1	intestine	12 µM	rep 2	2	2		2	2	1	1	1	2	2	1	2	2	2	1	2	2	2	2	3	1	1	1			2	1	2		0		2	
mdt-1	intestine	12 µM	rep 3	3	3	3	3	2	3	3	2	3	3	3	2	3	3	3	3	3	2	3	2	2	0	3	2	3	3	3	3	3	2	2	2	2
mdt-2	intestine only	12 µM	rep 1	2	3	2	0	1	2	3	2	0	2	2	2	2	1	2	1	3	1	2	3	2	2	2	2	2	2	2	1	0	2	3	2	3
mdt-2	intestine only	12 µM	rep 2	1	2		2	2	1	3	2	1	3	2	2	1	2	0		2	3	3	3	2	2		1		3	2	2	1		2	3	2
mdt-2	intestine only	12 µM	rep 3	2	3	2	2	3	2	2	1	3	3	2	2	1	2	0		3	3	3	2	2	3	2	3	1	2		3	2	3	1	2	2

gene	location	Cadmium	location	F7	F8	F9	F10	F11	F12	G1	G2	G3	G4	G5	G6	G7	G8	G9	G10	G11	G12	H1	H2	H3	H4	H5	H6	H7	H8	H9	H10	H11	H12
		concentration	Sequence Name	C06F5.5	F17A9.3	F19F10.1	F57A8.5	R07B7.13	C34D1.1	F58A12.1	F54E12.2	B0564.10	C49C3.5	F44C8.2	F59B1.7	C10G8.8	F17A9.8	F19F10.5	R04B5.3	R07B7.14	C34D1.2	C30G7.1	H02I12.8	Y37A1B.1	R02C2.4	F44C8.5	T27C4.4	C10G8.7	F44C4.2	C12D8.2	F29F11.5	R07B7.15	C34D1.5
mdt-1	pharynx	0 µM	rep 1	2	1		1	1	1	1	1	1	1			1	1	1		1	0	1	0	1	0	1	2	1	1	0			
mdt-1	pharynx	0 µM	rep 2	1	0		2	2	2				1	0	1	2	2	1	2	1	0	0		0	1	2	1	2	2	1	2	1	1
mdt-1	pharynx	0 µM	rep 3	2	1	2	2	2	2	2	2	2	2	1	2		1	1	2			2	2	1	2	2	3	2	1	3	2	2	
mdt-1	intestine	0 µM	rep 1	0	1		1	1	1	1	0	1	0			1	1	1		1		0	0	1	0	1	0	1	1	0			
mdt-1	intestine	0 µM	rep 2	0	0		1	1	2				0	0	1	2	2	1	0		0	0		0	1	2	1	2	0	1	2	1	1
mdt-1	intestine	0 µM	rep 3	2	1	2	1	2	2	2	2	2	2	1	2		1	1	1			1	2	2	3	2	1	2	1	3	2	1	
mdt-2	intestine only	0 µM	rep 1	0	1	1	1	0	2	1	2	2	3	0	1	2	1	1	3	3	0	2	2	0	1	2	3	3	2	2	1	0	0
mdt-2	intestine only	0 µM	rep 2	1	1	1	1	2	1	1	2	2	2	2	2		2	1	2		1		2	0	1	1	2	1	0	2		0	2
mdt-2	intestine only	0 µM	rep 3	2	2	1	3	2	1	2	2	2	2	1	2	2	2	2		1	2	2	1	1	1	2	2	2	2	2	2	2	2
mdt-1	pharynx	12 µM	rep 1		3		2	2	2		0	2	3		0		1	2	2	2	2		1		2		1				2	2	2
mdt-1	pharynx	12 µM	rep 2	3	2	1	1			2		2	1	2		2	2	3	3	0	1		1		2	2	3	3	2			2	2	3
mdt-1	pharynx	12 µM	rep 3	2	2	2	3	3	3	3	3	3	2	2		1	2	2	3	2	3	3	2	2	3	3	2	3	3	2	3	3	3
mdt-1	intestine	12 µM	rep 1		3		2	2	2		0	2	3		0		1	2	1	2	2		1		2		1				2	2	2
mdt-1	intestine	12 µM	rep 2	3	2	1	1			2		2	1	2		2	2	3	2	0	1		1		2	2	3	3	2			2	2	3
mdt-1	intestine	12 µM	rep 3	2	2	2	3	3	3	3	3	3	2	2		1	2	2	3	2	3	3	2	2	3	3	2	3	3	2	3	3	3
mdt-2	intestine only	12 µM	rep 1	2	2	2	2	2	3	0	0	1	3	1	2	2	2	2	3	3		2	0	2	2	2	2	2	2	1	2	2	
mdt-2	intestine only	12 µM	rep 2	1	2	1	3	2	2		2		3	2	2	1		2		3	1				2	2	2	2	2	2	1	2	2
mdt-2	intestine only	12 µM	rep 3	2	3	2	2	3	2	3	3	3	1	1	3		2	2	3		0	3		2	2	2	3	1	3	1	1	3	

First Screen (406 genes) – plate 4 in triplicate

gene	location	Cadmium concentration	location Sequence Name	A1 K08B4.7	A2 F44G3.9	A3 Y113G7B.14	A4 K08A8.2	A5 C12D12.5	A6 F22A3.1	A7 C02B8.4	A8 ZK466.8	A9 T14G8.1	A10 F28H6.4	A11 C18B12.3	A12 F31A3.4	B1 K08B4.8	B2 T13F3.3	B3 F38A6.3	B4 T26C11.5	B5 C02F12.5	B6 F22A3.5	B7 F22F1.1	B8 C44C10.8	B9 K03A11.3	B10 C37E2.5	B11 C33A11.4	B12 F67A10.5	C1 T20B3.3	C2 Y44A6D.3	C3 T28C11.6	C4 T14G12.5	C5 C25B8.6	C6 T01B10.4	C7 C40H5.5	C8 K09A11.1	C9 M163.3
mt-1	pharynx	0 µM	rep 1		1	2	1	2	2	1	2	2	2	2	2	1	2	2	1	1	1	1	2	2	2	2	2	2	1	2	2	2	1	1	1	2
mt-1	pharynx	0 µM	rep 2		2	3			2	0		0				2		2	0	1	2						1		1	2	1	1	2	1	0	2
mt-1	pharynx	0 µM	rep 3		2		3		3	2	2	2	2	2			0	1		2	2		0	1	3	2	1		1			1	2	2	2	2
mt-1	intestine	0 µM	rep 1		1	2	1	1	1	1	1	2	2	2	2	1	2	2	1	1	1	1	2	2	2	1	0	1	1	2	2	2	1	1	1	2
mt-1	intestine	0 µM	rep 2		2	3			2	0		0				2			2	0	0	1					1		1	2	0	1	1	1	0	2
mt-1	intestine	0 µM	rep 3		2		2		3	2	1	2	2	2			0	1		1	2		0	0	3	2	1		1			0	2	2	1	2
mt-2	intestine only	0 µM	rep 1	2	3	2	2	2	2	1	2	1		1	2	2	1	1	1	1	2	1	2		1	1	2	1	1	2	1		2	1	2	1
mt-2	intestine only	0 µM	rep 2	2	2	2	2	2	2	2	2	2	2		2	3	2	2	2	2	2	2	3	2	2	2	2	2	2	2	2	2	2	2	1	2
mt-2	intestine only	0 µM	rep 3	2		2		2		2		2	1	2	2		2	2		2	0	2	2	1	2	2	2	3		2		2	2	2	2	2	2
mt-1	pharynx	12 µM	rep 1	1	2	1	2		2	0			1		1	2	1	0		2	1	2	1	1	2	1	1			1			2		0	2
mt-1	pharynx	12 µM	rep 2	2	2	2	2	1	2	3		1	3		2			3				2		3	2	1	3			0		1	2	2	2	2
mt-1	pharynx	12 µM	rep 3	2					3				2		3			0	2		2		2	2	3	3			2	2	3	2	2			0
mt-1	intestine	12 µM	rep 1	1	2	1	2		2	0			1		1	2	1	0		2	1	2	1	1	2	1	1			1			2		0	2
mt-1	intestine	12 µM	rep 2	2	2	2	2	1	2	3		1	3		2			3				2		3	2	1	2			0		1	2	2	2	2
mt-1	intestine	12 µM	rep 3	2					3				2		3			0	2		2		2	2	3	3			2	2	3	2	2			0
mt-2	intestine only	12 µM	rep 1	2	2	2	2	3	2	2	3	3	3	2	2		1	2	1	2	2	1	3	1	2	2	2	2	2	3	1	2	3	2	2	2
mt-2	intestine only	12 µM	rep 2	1	2	1	3		2	2		2	3	3	2	0	2	3			3	2	2	1	3	3	3	2	3	2	2		3	2	2	2
mt-2	intestine only	12 µM	rep 3	2	0	3	2	0	2	3	2	3	2			0	3	0		2	3	3	2	2	3	2			3	2	3	3	0	3	3	2	3

gene	location	Cadmium concentration	location Sequence Name	C10 F53H4.1	C11 T08C12.7	C12 F08C6.8	D1 R04A9.5	D2 T14F9.5	D5 ZC64.3	D4 C56E10.1	D6 T25B8.2	D8 F17A2.5	D7 F46G10.3	D8 H01A20.1	D9 F53H4.5	D10 F36D8.12	D11 F09C6.9	D12 F57C12.3	E1 C43H6.8	E2 ZC64.4	E3 R173.2	E4 R07B1.1	E5 F46E6.2	E6 F46G10.8	E7 F40E10.2	E8 T23C6.5	E9 T10C6.12	E10 Y51A2D.17	E11 F57C12.4	E12 T02C5.5	F1 T23F2.2	F2 K03A1.6	F3 F44A6.2	F4 C02B4.2	F5 F46G10.7	F6 Y116A8A.1
mt-1	pharynx	0 µM	rep 1	1	2	1	1	1	2	2	1	2	1	2	3	2	2	1	2	1	1	1	1	2	1	2	3	2	1	2	1	1	2	2	2	1
mt-1	pharynx	0 µM	rep 2	1		2	2	2	2	1	2	1	2	2	1	2	2	2	2	2	2	1	2	3	0	1		2			2	2	2	2	1	2
mt-1	pharynx	0 µM	rep 3	2	2	2	2					2	2		2		2	1		0	2	2	1		2	2	2	2	2	1	2				2	2	2
mt-1	intestine	0 µM	rep 1	1	1	0	1	1	2	1	1	2	1	2	2	2	1	0	1	1	1	0	1	2	1	2	2	2	1	1	1	1	1	2	2	1
mt-1	intestine	0 µM	rep 2	1		2	2	1	1	1	2	1	2	2	1	2	2	2	2	1	2	1	1	3	0	1		1			2	2	1	2	1	2
mt-1	intestine	0 µM	rep 3	2	2	1	2					2	2		2		2	1		0	1	2	0		2	2	2	2	2	1	2				2	2	1
mt-2	intestine only	0 µM	rep 1	1	1	0	1	1	1	2	0	1	1	1	1	1	1	0	1	1	1	2	0		2	1	2	1		1	1	1	2	1	1	1
mt-2	intestine only	0 µM	rep 2		2	2		1	2	2	1	2	2	2	2	2	2	2	2	2	2	2	2	1	1	2	1	1	2	1	2	2	2	2	2	2
mt-2	intestine only	0 µM	rep 3		2		2		2	2	1	2			2		2		2		2		1		3	2		2	2		2			2	2	2
mt-1	pharynx	12 µM	rep 1	2	0	1			1		1	2	2	2	2	2	1	0	1	2	2		2	1	2	2	1	2	2	2	2	2	2		2	1
mt-1	pharynx	12 µM	rep 2	1	2	2	3		3	2	1	1	3	2	1	2	2	2	3	2	2	2	2		3	1	2	2	2	2	1	2	2	3	1	1
mt-1	pharynx	12 µM	rep 3	3	3				3	3				2	0	2	3								2			2		2	2	3		3	3	2	1
mt-1	intestine	12 µM	rep 1	2	0	1			1		1	1	2	2	2	2	1	0	1	2	2		2	1	2	2	1	2	2	1	2	2	2		2	1
mt-1	intestine	12 µM	rep 2	1	2	2	3		3	2	1	1	3	2	1	2	2	2	3	2	2	1	2		3	1	2	2	2	2	3	2	1	3	1	1
mt-1	intestine	12 µM	rep 3	3	3				3	3				2	0	2	3							2		2	2		2	2	3		3	3	2	1
mt-2	intestine only	12 µM	rep 1	1	2	1	1	2	2	2	2	3	2	2	1	2	1	1	1	1	2	1	2	2	1	2	2	1	2	2	2	2	2	2	2	2
mt-2	intestine only	12 µM	rep 2	3	3	2	3	3	2	2	3	3	2	3	2	3	2	2	2	3	3		2	2	2	3	3		3	3	2	2	2	2	0	2
mt-2	intestine only	12 µM	rep 3	2		2		0		3		3	3	2		2	2	2	3	3	3	3	3	3		3	3	2	0	2	3	2	3		3	3

gene	location	Cadmium concentration	location Sequence Name	F7 T25G12.9	F8 T10C8.13	F9 Y17D7A.3	F10 ZK402.2	F11 C33D12.1	F12 T22B7.1	G1 K08A8.2	G2 F14F3.1	G3 K11E4.5	G4 T04C10.4	G5 R09G11.2	G6 R09G11.2	G7 T10C6.14	G8 C25F9.5	G9 D1005.3	G10 F56E3.4	G11 T13C6.4	G12 F45E1.8	H1 F11A1.3	H2 T22H6.8	H3 F28H6.2	H4 C27C12.8	H5 F31A3.2	H6 F31A3.2
mt-1	pharynx	0 µM	rep 1	2	2	2	1	1		1	2	2	2	2	1	1	1	2	1	1	2	1	2	2	2	2	2
mt-1	pharynx	0 µM	rep 2	2	0	2	1	0	2	2	0	3	2	1	2		2		0	0		2	1	1	3	0	
mt-1	pharynx	0 µM	rep 3	2		2	2	2	2	0			1	1	2	2			2	3		2	2	2		2	
mt-1	intestine	0 µM	rep 1	1	1	2	1	1		1	1	2	2	1	1	1	1	2	1	1	2	1	1	2	2	2	2
mt-1	intestine	0 µM	rep 2	2	0	1	0	0	2	2	0	3	0	1	1		2		0	0		2	1	1	3	0	
mt-1	intestine	0 µM	rep 3	2		2	2	2	2	0			1	1	2	2			2	3		2	1	2		2	
mt-2	intestine only	0 µM	rep 1	1	2	1	2	1	1	1	1	1	1	2	1	1		2	1	1	1	2	2		1	2	2
mt-2	intestine only	0 µM	rep 2	1	2	2	2		2	2	2	2	2		1	0		2	1	2	2	2	2	2	3	3	2
mt-2	intestine only	0 µM	rep 3	2	2	1	2		2	2	2	2	2	2	2	2	2	2	2	2	2	3		2	1	0	
mt-1	pharynx	12 µM	rep 1	2	2	2	0	2	3	2	2	1	2	2	2	1	2	2	2	1	0	1	2	2	3	1	2
mt-1	pharynx	12 µM	rep 2	1	2	2	1	2	3	3	2	0	2	2	2	0		2	1	2	2	2	2		2	2	2
mt-1	pharynx	12 µM	rep 3	2	2	1		2	3	2			2		3		2	0	2	2	2		3	2			2
mt-1	intestine	12 µM	rep 1	2	2	2	0	1	3	2	2	1	2	2	2	1	2	2	2	1	0	1	2	2	3	1	2
mt-1	intestine	12 µM	rep 2	1	2	2	1	2	3	3	2	0	2	2	2	0		2	1	2	2	2	2		2	2	2
mt-1	intestine	12 µM	rep 3	2	2	1		2	3	2			2		3		2	0	2	2	2		3	2			2
mt-2	intestine only	12 µM	rep 1	2		2	3	2	1	2	2	1		2	2	2		2	2	2	2	2	3	2	2	1	2
mt-2	intestine only	12 µM	rep 2	2	2	2	3	1	3	2	3	2	3			2	2	3	3	3	3	3	3	3	2	3	3
mt-2	intestine only	12 µM	rep 3		3	3		3	2			3		2	3	3	3		3	0	2	3	3				3

Second screen (41 genes) – one plate with 1 replicate

gene	location	Cadmium concentration	Previous location Sequence Name	1A1 C45E1.1	1B4 ZK265.4	1C2 C16C2.1	1C5 T23H4.2	1C7 T23D8.6	1D10 C01B12.2	1 E2 Y39F10A.4	1 E5 F54C12.3	1G9 T15H9.3	1H7 F33A8.3	1H12 F15D4.1	2B4 C38D4.9	2B7 ZC155.2	2C1 F23F12.9	2C6 T20B12.8	2D8 F44E2.2	2 E8 Y47D3B.9	2 E9 Y66A7A.5	2 E10 Y75B8A.1	2H5 C28D4.1	2H9 K08F4.1
mtl-1	pharynx	0 µM	rep 1	2	2	1	2	2	2	1	2	2	2	2	2	2	1	1	2	1	2	2	2	2
mtl-1	intestine	0 µM	rep 1	2	2	1	1	1	2	2	1	1	1	2	2	1	1	1	1	0	1	2	1	1
mtl-2	intestine only	0 µM	rep 1	3	2	2	2	2	2	2	2	2	3	3	3	2	2	2	2	2	2	2	2	2
mtl-1	pharynx	12 µM	rep 1	0	2	0	1	2	0	0	2	2	1	2	2	2	2	2	2	2	2	2	2	2
mtl-1	intestine	12 µM	rep 1	3	3	2	3	3	3	3	3	0	3	3	3	2	3	2	2	3	3	2	2	2
mtl-2	intestine only	12 µM	rep 1	3	3	3	3	3	3	3	3	3	3	3	3	3	3	3	3	3	3	2	3	2

gene	location	Cadmium concentration	Previous location Sequence Name	2H10 R11A8.4	3B3 B0564.10	3B6 Y57G11C.19	3B12 R02C2.4	3D6 F38H12.3	3 E7 F17A9.6	4A5 T10C6.12	4B1 Y51A2D.17	4B2 Y17D7A.3	4B3 C25F9.5	4B4 Y113G7B.14	4C8 C12D12.5	4D2 T22B7.1	4D5 F22A3.5	4D9 K03A1.6	4D12 C02B8.4	4F6 K09A11.1	4F10 K11E4.5	4G3 H01A20.1	4G7 C27C12.6
mtl-1	pharynx	0 µM	rep 1	2	2	2	1	1	2	2	2	1	1	2	2	2	2	2	1.5	2	1	2	2
mtl-1	intestine	0 µM	rep 1	1	1	2	1	0	1	1	1	0	0	1	1	1	2	2	0.5	1	1	2	1
mtl-2	intestine only	0 µM	rep 1	2	2	2	2	2	3	2	2	2	2	2	2	2	2	2	2	2	2	2	2
mtl-1	pharynx	12 µM	rep 1	2	2	2	2	2	2	0	2	2	1	2	2	2	2	2	2	2	2	2	2
mtl-1	intestine	12 µM	rep 1	2	3	2	2	2	3	3	3	2	3	2	3	3	3	3	1.7	3	2	2.5	3
mtl-2	intestine only	12 µM	rep 1	2	2	2	3	3	3	3	3	3	3	3	3	3	2	3	2	3	2	3	3

Third screen (10 genes) – one plate with 3 replicates

gene	location	Cadmium concentration	location Sequence Name	1A1 C45E1.1	1C2 C16C2.1	1C5 T23H4.2	1D10 C01B12.2	1 E2 Y39F10A.4	1H7 F33A8.3	3B3 B0564.10	4A5 T10C6.12	4B3 C25F9.5	4D5 F22A3.5
mtl-1	pharynx	0 µM	rep 1	2	1	1	1	1	1	1	1	0	1
mtl-1	pharynx	0 µM	rep 2	2	1	1	1	1	1	1	1	0	1
mtl-1	pharynx	0 µM	rep 3	2	1	1	1	1	1	1	1	1	1
mtl-1	intestine	0 µM	rep 1	2	0	1	1	1	1	0	0	0	0
mtl-1	intestine	0 µM	rep 2	2	1	1	1	0	1	0	0	0	0
mtl-1	intestine	0 µM	rep 3	2	0	0	1	0	0	0	1	0	0
mtl-2	intestine only	0 µM	rep 1	2	2	2	2	2	2	1	2	0	2
mtl-2	intestine only	0 µM	rep 2	2	2	2	2	2	2	1	2	1	2
mtl-2	intestine only	0 µM	rep 3	2	2	2	2	2	2	1	0	1	2
mtl-1	pharynx	12 µM	rep 1	2	2	2	2	2	2	1	2	2	2
mtl-1	pharynx	12 µM	rep 2	2	2	3	2	2	2	1	2	2	2
mtl-1	pharynx	12 µM	rep 3	2	2	2	2	2	2	1	2	2	2
mtl-1	intestine	12 µM	rep 1	2	3	2	2	2	2	2	2	2	2
mtl-1	intestine	12 µM	rep 2	2	2	3	3	2	2	2	2	2	2
mtl-1	intestine	12 µM	rep 3	3	3	3		2	2	2	2	2	
mtl-2	intestine only	12 µM	rep 1	3	3	3	3	2	2	3		3	
mtl-2	intestine only	12 µM	rep 2	3	3	3		2	3	3	3	3	3
mtl-2	intestine only	12 µM	rep 3	3	3	3	2	2	3	3	3	2	2

MANUSCRIPTS

1) Hughes, S.L.*, Bundy, J.G.* (*contributed equally), Want, E.J., Kille, P. and Stürzenbaum, S.R. (2009). The metabolomic responses of Caenorhabditis elegans to cadmium are largely independent of metallothionein status, but dominated by changes in cystathionine and phytochelatins. Submitted to Journal of Proteome Research

2) Hughes, S. and Stürzenbaum, S.R. (2007). Single and double metallothionein knockout in the nematode *C. elegans* reveals cadmium dependent and independent toxic effects on life history traits. Environmental Pollution **145**(2): 395-400.

3) Calafato, S., Swain, S., Hughes, S., Kille, P. and Stürzenbaum, S.R. (2008). Knock down of *Caenorhabditis elegans cutc-1* exacerbates the sensitivity toward high levels of copper. Toxicological Sciences **106**(2): 384-391. Work was not included in the thesis.

The metabolomic responses of *Caenorhabditis elegans* to cadmium are largely independent of metallothionein status, but dominated by changes in cystathionine and phytochelatins.

Samantha L. Hughes[1,2,3]§, Jacob G. Bundy[4]§, Elizabeth J. Want[4], Peter Kille[2], Stephen R. Stürzenbaum[1]*

1: School of Biomedical and Health Sciences, Pharmaceutical Sciences Division, King's College London, Franklin Wilkins Building, Stamford Street, London SE1 9NH, UK

2: School of Biosciences, University of Cardiff, Main Building, Park Place, Cardiff CF10 3TL, UK

3: Current address: Genetics Unit, Department of Biochemistry, University of Oxford, South Parks Road, Oxford OX1 3QU, UK

4: Department of Biomolecular Medicine, Division of Surgery, Oncology, Reproductive Biology, and Anaesthetics, Faculty of Medicine, Imperial College London, Sir Alexander Fleming Building, London SW7 2AZ, UK

§Joint first authors

*Corresponding author

Email: stephen.sturzenbaum@kcl.ac.uk

Telephone: +44 (20) 78484406

Key words: phytochelatin, metallothionein, metabolomics, metabonomics, cadmium, UPLC-MS

Abstract

Cadmium is a widely-distributed toxic environmental pollutant. Using proton NMR spectroscopy and UPLC-MS, we obtained metabolic profiles from the model organism *C. elegans* exposed to sub-lethal concentrations of cadmium. Neither in the presence nor absence of cadmium did the metallothionein status (single or double *mtl* knockouts) markedly modulate the metabolic profile. However, independent of strain, cadmium exposure resulted in a decrease in cystathionine concentrations and an increase in the non-ribosomally synthesized peptides phytochelatin-2 and phytochelatin-3. This suggests that a primary response to low levels of cadmium is the differential regulation of the *C. elegans* trans-sulfuration pathway, which channels the flux from methionine through cysteine into phytochelatin synthesis. These results were backed up by the finding that phytochelatin synthase mutants (*pcs-1*) were at least an order of magnitude more sensitive to cadmium than single or double metallothionein mutants. However, an additive sensitivity towards cadmium was observed in the *mtl-1; mtl-2; pcs-1* triple mutant.

INTRODUCTION

Cadmium is a toxic heavy metal that is released into the environment as a consequence of man-made activities[1]. In humans, prolonged exposure to cadmium can result in many detrimental effects, including proteinuria, osteomalacia, osteoporosis, renal damage, and development of prostate cancer[2]. The biological responses to cadmium are complex, and thus are far from being fully understood.

Cadmium has been shown to alter the expression of approximately 300 genes in the model organism *Caenorhabditis elegans*[3]. This highlights that cadmium affects multiple targets and/or that the nematode may utilize multiple mechanisms to control cadmium concentrations, and so prevent the onset of toxic effects. Primary candidates for protective responses are metallothioneins (MTs), small (6-7 kDa) cysteine-rich metal-binding proteins[4, 5], which have been identified in all prokaryotes and eukaryotes[6] and are thought to function in copper and zinc homeostasis[5], protect against oxidative damage[7], and play a significant role in the detoxification of the non-essential metal cadmium[8]. *C. elegans* contains two MT isoforms, *mtl-1* and *mtl-2*, both located on chromosome 5[9]. However, deletion of *mtl-1* and/or *mtl-2* demonstrated that both isoforms contribute to cadmium detoxification, but are not essential for life[10].

Metabolic profiling (metabolomics/metabonomics) has been widely used for functional studies, including mechanistic toxicology[11-13]. It has been successfully used for the analysis of cadmium toxicity in a range of organisms, including plants,

microbes, invertebrates, and mammals[14-20]. Given the importance of *C. elegans* as a model organism, there have been surprisingly few metabolomic studies. Blaise *et al.*[21] applied metabolomics at a proof-of-principle level for evaluation of gene function, and other studies have used metabolomics as a component of functional studies of *C. elegans* knockout strains[22, 23]. We are not aware of any studies that have used metabolomics to investigate the effects of an external stress, such as a toxic compound, in *C. elegans*. Here, we used both ^{1}H NMR and UPLC-MS to carry out an untargetted metabolomic analysis of *C. elegans* responses to cadmium, with the aims of, firstly, identifying the metabolic fingerprint of sub-lethal cadmium exposure; secondly, characterizing the metabolic phenotype of metallothionein deletion mutants; and thirdly, determining if one modulated the other by identifying any metabolic interactions between cadmium exposure and metallothionein status.

MATERIALS AND METHODS

C. elegans strains

Wild type (Bristol N2) and *gk125(vc128)* were obtained from the *Caenorhabditis* Genetics Centre (CGC) at the University of Minnesota, USA. The strains *mtl-1 (tm1770)* and *pcs-1(tm1748)* were provided by the Mitani Laboratory at the Tokyo Women's Medical University School of Medicine, Japan. The metallothionein double knockout *mtl-1;mtl-2(zs1)* was previously generated as detailed in Hughes and Stürzenbaum[10], a method that we used here to create the triple mutant *mtl-1;mtl-2;pcs-1*. Briefly, back-crossed *pcs-1(tm1748)* hermaphrodites were heat shocked (30 °C for 5.5 hours) and resultant male offspring isolated. At least five males were placed with a single back crossed *mtl-1;mtl-2(zs1)* hermaphrodite. The progeny were allowed to grow to reproducing adults and screened for *mtl-1, mtl-2* and *pcs-1* using standard nested genomic PCR on single worms. Offspring from parents with all three genes knocked out were isolated, and homozygotes confirmed over four successive generations.

Sample treatment and metabolite extraction

Nematodes were maintained on NGM using *Escherichia coli* OP50 as a food source. Each strain was grown either on control NGM agar in the presence or absence of 12 µM cadmium. Each replicate (8 per condition) consisted of approximately 8000 individuals. Samples for NMR and mass spectrometry analysis were generated from wild type, single and double MT knockouts. In detail, gravid nematodes were bleached and rotated overnight. The following day, age synchronised nematodes

were placed onto NGM (± Cd) as L1. The nematodes were incubated at 20 °C for 48 hours to allow the nematodes to develop to the L4 stage. When at the L4 stage, nematodes were washed off the plates using M9 buffer. The nematodes were pelleted by centrifugation (2000 rpm, 2 minutes) and the supernatant removed. The pellet was resuspended in 200 µl M9 buffer and metabolites directly extracted. An equal volume (approximately 0.3 g) of acid washed glass beads (Sigma, UK) was added to the nematode pellet with 100% methanol (800 µl). The sample was vortexed for 3 minutes and the supernatant transferred to a fresh 2 ml micro-centrifuge tube. The remaining glass beads were vortexed in 80% methanol (1 ml) for 1 minute and the supernatant transferred to the micro-centrifuge tube. Following centrifugation (3000 rpm, 2 minutes) the supernatant was stored at -80 °C until required.

Life history analysis

Gravid *mtl-1;mtl-2(zs1), pcs-1(tm1748), mtl-1;mtl-2;pcs-1(zs2)* and wild type adults were bleached to release eggs. Following overnight incubation, the age synchronised L1 stage nematodes were distributed onto cadmium dosed NGM. After 24 hours, single nematodes were transferred to individual wells of a multi-well plate and transferred daily until reproduction had ceased. All incubations were at 20 °C. The total number of offspring from each nematode was determined. Nematodes were monitored daily throughout development and post-reproduction to determine death. Death was recorded when there was no movement of the nematode following repeated probing with a hair.

NMR spectroscopy

Samples were analysed essentially as described in Beckonert *et al.* [24]. Briefly, all samples were analysed on a 600 MHz Bruker Avance DRX600 spectrometer equipped with a triple-axis inverse-geometry probe and a BACS tube-changer autosampler (Bruker BioSpin, Rheinstetten, Germany). The samples were held at 300K during acquisition. A Bruker Avance 'NOESYPRESAT' pulse sequence with 100 ms mixing time was used to suppress the peak from residual water protons; the $\pi/2$ pulse length and spectrometer tuning and matching were set using a typical sample. Data were acquired over a 12 kHz spectral width into 32K data points; an additional 3.5 s relaxation recovery delay was included for each pulse, giving a 5.0 s recycle time. 256 scans were acquired per sample, giving an approximate acquisition time of 22 minutes.

The spectra were initially processed in iNMR v.2 (Nucleomatica, Molfetta, Italy). Free induction decays were zero-filled by a factor of 1.5 and an exponential apodization function of 0.5 Hz applied, followed by Fourier transformation. Phase correction and first-order polynomial baseline correction were carried out using the software proprietary algorithms. Spectra were manually binned for further data analysis into 96 separate regions, using the iNMR integration function. Selected compounds were analysed using the software package NMR Suite 5.0 (Chenomx, Edmonton AB, Canada), i.e. comprehensive fitting of all peaks in the spectra was not performed. This software enables computer-aided manual fitting of spectra of individual compounds (combinations of Lorentzian lineshapes based on authentic standards) to the mixture spectra[25], thus allowing both deconvolution and quantification of

specific metabolites, including methionine, glutathione, cystathionine, trehalose, succinate, glutamate, alanine, and betaine. All of these compounds were present in the Chenomx metabolite library except for trehalose, which we added as a standard to the library.

Mass spectrometry

An aliquot of the supernatant was placed in a sample glass vial (Waters, USA) and maintained at 4 °C prior to injection of 5 µl onto the column. Chromatographic separations were performed on a Waters 2.1mm x 100mm ACQUITY (Waters, USA) 1.7 µm C18 BEH column maintained at 40 °C. Reverse phase chromatography conditions were employed using a 26 minute gradient with mobile phase A being 0.1% formic acid (FA) in water and mobile phase B 0.1% FA in acetonitrile. The composition was maintained at 99.9% A for the first 2 minutes, then increased linearly from 0.1 to 50% B over 10 minutes. A 50% composition of B was held for 1 minute and then increased to 99.9% B over the next 4 minutes. Mobile phase B was held at 99.9% for 4 minutes and then returned to 99.9% A and held until 26 minutes.

Electrospray (ESI) mass spectrometry experiments were performed on a Micromass LCT Premier (Waters, USA) operated in both positive and negative ionisation modes. The mass spectrometer was calibrated across the mass range 50-2000 Da using a solution of sodium formate. All analyses were acquired using the lock spray to ensure accuracy and reproducibility; 200 pg/µl leucine-enkephalin in water:acetonitrile at a 50:50 ratio was used as the lock mass with a flow rate of 30 µl/min. Data were collected in centroid mode, the lockspray frequency was set at 5

seconds, and data were averaged over 10 scans. The mass spectrometer was operated with a capillary voltage of 2.4 kV in negative ion mode and 3.2 kV in positive ion mode, using a cone voltage of 35 V, nebulizer gas flow of 900 l/h, desolvation temperature of 350°C, and source temperature of 120°C. The instrument was set to acquire over the mass range *m/z* 50-2000 with an acquisition time of 1 second and an interscan delay of 100 ms.

The raw data were processed using the open-source freeware XCMS which is able to detect and align metabolite peaks. After correcting for retention time, the relative metabolite ion intensities are directly compared[26]. Following data input, the samples were divided into 8 groups (i.e four strains ± cadmium) and the chromatograms directly compared. The chromatograms were judged to contain well-retained peaks from 1.5 to 17 minutes, and so only data from these regions were used for multivariate analysis. Negative and positive mode data were analysed as separate datasets.

Multivariate analysis

The binned data were used for NMR and the peak table generated by XCMS was used for the UPLC-MS data. All analyses were performed using SIMCA-P+ v11.5 (Umetrics, Umeå, Sweden). Both sets of data were mean-centred before analysis; in addition, the UPLC-MS data were scaled to unit variance (autoscaling), and the NMR data were log-transformed by log(x + 1). We used both unsupervised (principal component analysis) and supervised methods (partial least squares discriminant analysis, PLS-DA) to interrogate the data.

RESULTS AND DISCUSSION

The metallothionein and phytochelatin knockout strains

A triple knockout (*mtl-1;mtl-2;pcs-1*(*zs2*)) was generated by crossing and PCR based selection of progeny. Deletions are as follows: *mtl-1* lacks 186 bp of promoter, the entire coding region and 47 bp of the 5' UTR; *mtl-2* has 208 bp of promoter, the entire coding region and 585 bp of the 5' UTR removed and *pcs-1* 416 bp of the promoter, the first exon and 45 bp of the first intron. Wild type and *mtl-1, mtl-2* and *pcs-1* deletion strains were identified by nested PCR followed by agarose gel electrophoresis (Figure S1, supporting information). All strains were viable under laboratory conditions, with no gross differences in phenotype.

The cystathionine pool in *C. elegans* is cadmium-responsive and independent of metallothionein status

NMR spectroscopy gives information on high-concentration metabolites. Nonetheless, the universal nature of NMR detection means that it is a valuable and true non-targetted profiling approach across all metabolite classes. In addition, changes in high-concentration metabolites are also likely to have physiological significance. Hence, NMR was used to identify the metabolic changes occurring as a result of cadmium exposure in *C. elegans* wild-type and MT mutants. Nematodes were exposed to 12 µM cadmium, a low sub-lethal concentration previously shown to stimulate MT transcription in *C. elegans*[27] and display subtle effects on life-history parameters[10]. At this dose, the effects can be expected to be limited to cadmium-specific biochemical responses, rather than general toxicity/stress responses as

identified, for example, in nematodes exposed to 100 µM cadmium but not at lower concentrations[3].

We carried out an initial unsupervised pattern-recognition analysis – principal components analysis – to determine if there were large treatment- or genotype-related effects. However no significant differences were observed between the genotypes, the exposures, or genotype/cadmium interactions (data not shown). In contrast, supervised techniques can be more powerful in detecting differences in complex multivariate data. Partial least squares discriminant analysis (PLS-DA) deals well with correlated data and complex omic data sets, and is often used with spectral data[28, 29]. As for the unsupervised analysis, there was no separation of genotypes in the presence or absence of cadmium, i.e. we were not able to fit any robust models separating strains, as judged by cross-validation (data not shown). Conversely, the samples could be separated according to cadmium exposure irrespective of genotype (Fig. 1), i.e. perhaps surprisingly, the wild-type and metallothionein knockout nematodes displayed a similar metabolic response to cadmium.

Inspection of the variable loadings identified cystathionine and trehalose as potential responders, but the loadings for the variables assigned as cystathionine were aligned more directly with the cadmium treatment effect. In addition, upon visual inspection of the full-resolution spectra no clear metabolite differences, other than cystathionine, were observed (data not shown). Finally, individual metabolites were quantified by fitting spectra based on authentic standards. As betaine, alanine,

glutamate and succinate levels did not fluctuate following cadmium exposure, these four metabolites were averaged and used as an internal normalization factor against which to report cystathionine levels. The use of selected multiple control variables has been used to normalize between samples for gene transcript data[30]. In addition to cystathionine, we were *a priori* interested in the concentrations of glutathione and, *a posteriori*, methionine (given the cystathionine response, and the close biochemical relatedness of methionine; other S-containing metabolites such as cysteine and homocysteine would also have been of interest, but were not detected by 1D NMR) and trehalose (given the multivariate analysis results). However, methionine and trehalose concentrations did not change significantly following cadmium exposure. In contrast, cystathionine was significantly reduced by cadmium across all strains (two-way ANOVA, $P = 0.001$; Fig. 2).

UPLC-MS

We observed a large number of distinct peaks (Table S1, Supporting Information), although these will not all represent independent metabolites as peaks from the same compound (for instance, adducts) are not combined. We have not attempted to identify the majority of peaks, but the data can still be used in the first instance to judge overall phenotypic response patterns, and secondly, to identify key responsive metabolites. As was the case for the NMR data, the UPLC-MS metabolic profiling did not highlight clear differences between the genotypes, either in the presence or absence of cadmium (data not shown). However, and again similarly to the NMR results, exposure to cadmium induced clear metabolic effects, regardless of the genetic background (Fig. 1).

Inspection of the loadings highlighted variables assigned as phytochelatins (PCs) with two peaks in the chromatograms with retention times of 212 and 252 seconds (Fig. 3). The dominant peak at 212 s with an *m/z* of 540.142 corresponds to $[MH]^+$ for PC_2, with the molecular formula $C_{18}H_{30}N_5O_{10}S_2$, and a predicted molecular weight of 540.143. The peak at 252 s was PC_3 with an *m/z* of 772.196 (predicted 772.195) and formula for $[MH]^+$ of $C_{26}H_{42}N_7O_{14}S_3$. In addition, a characteristic ion was observed two mass units below the [MH]+ molecular ion, which we assume is formed by loss of H_2 to give an oxidized cyclic metabolite, i.e. with a disulphide bridge. The fact that the [M-H]+ ion was also observed by Clemens *et al.* for a single peak, despite using different chromatographic conditions[31], might indicate that this is a neutral loss that takes place in the mass spectrometer source; however, the [MH]+ and [M-H]+ ions clearly elute at slightly different retention times for PC_3 (Fig. 3). A peak at -4 mass units (loss of $2H_2$) might well be observed for PC_4, with four –SH groups, and perhaps corresponding mass losses of *2n* for higher PCs. Further univariate analysis of the PC levels, log-transformed to give normally distributed data, confirmed that the PC response was significantly affected by cadmium but not metallothionein status (two-way ANOVA; $P < 0.001$ for PC_2 and $P = 0.002$ for PC_3; Fig. 4).

PCs are non-ribosomal peptides, $(GluCys)_nGly$, synthesized from glutathione, with the smallest PC being the pentapeptide PC_2[32, 33]. PCs were first identified in plants[34], but a functional orthologue of *C. elegans* phytochelatin synthase (PCS) orthologue was later identified and characterized[31, 35-38]. We are able to demonstrate, for the first time, increased levels of PC_2 and PC_3 directly in *C. elegans* on cadmium exposure. This increase as detected by UPLC-MS cannot explain all the observed metabolomic changes, if only because the reduction in cystathionine is not matched by a

quantitatively equivalent NMR-visible increase in other metabolites. Furthermore, the observed decrease in cystathionine in both wild-type and MT-null strains cannot be explained by incorporation of cysteine into MTs. Based on the metabolomic data, it is conceivable that nematodes excrete PC-bound cadmium as an organism-level detoxification mechanism, thus representing a novel pathway for removal of cadmium in *C. elegans*; alternatively, sequestration of high-molecular-weight cadmium-bound PCs might also explain the reduction in cystathionine levels. These hypotheses should be investigated in future experiments.

Cystathionine is a central intermediate in the sulphur amino acid metabolism sitting within the methionine transsulfuration pathway[19, 39] which, in animals, is the sole route for the production of cysteine. Since cysteine is an essential substrate for phytochelatin and glutathione production[40], cystathionine is intimately linked to all potential sulphur-based ligands (MT, PCS and GSH) exploited for cadmium detoxification. The level of cystathionine is controlled by two key enzymes, namely, cystathionine-β-synthase (CβS) and cystathionine-γ-lyase (CγL) (Fig. 5), and *C. elegans* orthologues (Wormbase WS198: CβS, F13B12.4 and ZC373.1; CγL, *cth-1* and *cth-2*) have been identified. The levels of transsulfuration intermediates, such as cystathionine, is a composite function of the kinetics of each step within the pathway. i.e. the pathway flux. The reaction catalysed by CβS is key to the commitment of the cell to convert sulphur within the methionine pool to cysteine via homocysteine and cystathionine, whilst CγL is responsible for the final step which generates cysteine. The steady state levels of cystathionine attained are therefore a direct function of the rate of CβS and CγL; the equilibrium between substrate and product attained by CγL is innately influenced by the concentration of free cysteine. In situations where free

cysteine is removed by being rapidly incorporated into protein and/or converted to GSH or PC, as is the case upon cadmium challenge, the equilibrium will favour product production and reduce levels of cystathionine, as observed in this study. The impact of heavy metal challenge on sulphur amino acid metabolism has been comprehensively studied in yeast, protists and plants, all of which use MT and PC for metal detoxification. These studies are in line with our observations showing a reduction in cystathionine caused by a suppression of CβS and an elevation in the activity of CγL. The most comprehensive study was performed in yeast using isotopic label for demonstrating flux of sulphur as well as proteomic and metabolic profiling approaches. This study showed a clear increase in flux of sulphur amino acids away from protein synthesis and into glutathione production (although possible conversion into PCs was not measured)[41]. A major difficulty with extrapolating from these studies is the ability of yeast to utilize inorganic sulphur in the generation of cysteine and methionine. However, supporting observations indicating conservation of the opposing effect of cadmium on CβS and CγL can be found in rat testes and in the kidneys and brain of the frog *Rana ridibunda*[19, 42] – although it should be noted that Sugiura *et al.* interpreted the observed decrease of cystathionine levels in rat as a result of flux from cysteine to H_2S via cystathionine[19]. Further preliminary evidence in support of a direct impact of cadmium on transsulfuration in *C. elegans* is given by a separate transcriptomic study of chronic cadmium exposure of *C. elegans*, in which 20 μM cadmium caused a 2-fold reduction of CγL and a 1.7-fold increase in CβS expression[43]. Clearly, these data will need to be further verified but must also take into account that cadmium effects may also involve impacts on protein function. Therefore, a complete interpretation will require a future integrated assessment of gene regulation, protein activity, and effects on metabolic pathway flux.

Cadmium-dependent transcription of PCS has been reported for the annelid *Eisenia fetida*[44], and although PC production was not measured, it was argued that PC synthesis was at least partly regulated under transcriptional control. However, in contrast, previous studies in *C. elegans* observed no increase in *pcs-1* transcription, nor of the PC transporter *hmt-1*[3]. As shown in several plant and microbe species, PCS activity depends on heavy metal ions such as cadmium[45]; and in some organisms, PC synthesis is regulated by changes in PCS activity rather than changes in expression[46, 47]. We hypothesize that a similar regulatory mechanism holds for *C. elegans*, and our data provide a clear example of how metabolome analysis can complement transcriptomic data to unravel biological responses that are not controlled by changes in gene expression.

PCs and MTs both contribute to protection against cadmium toxicity in *C. elegans*

Both NMR- and MS-based metabolomic datasets indicated that the MT genotype did not significantly modulate the metabolic profile. However, exposure to cadmium resulted in an increase of PCs. In an attempt to dissect the functional responses of MTs and PCs, *pcs-1(tm1748)*, *mtl-1;mtl-2(zs1)* and *mtl-1;mtl-2;pcs-1(zs2)* were subjected to increasing concentrations of cadmium. Even in control conditions (i.e. no cadmium), all mutant strains showed a significant reduction in total brood size (ANOVA, $p \leq 0.01$). Figure 6 clearly shows an overall progression in sensitivity to cadmium for brood size, with the *pcs-1(tm1748)* knockout more sensitive than the double MT knockout *mtl-1;mtl-2(zs1)*, and the PC/MT triple knockout *mtl-1;mtl-2;pcs-1(zs2)* the most sensitive of all. At a cadmium concentration of 0.5 µM, the triple

mutant produced no viable offspring, and at higher concentrations both the *pcs-1(tm1748)* and the triple mutant were not viable, with stalled development during early larval stages leading to early death. Thus our results confirm earlier observations that knockdown of *pcs-1* confers hypersensitivity to cadmium in *C. elegans*[37]. Furthermore, the results show that, although PCs are more protective against cadmium toxicosis, MTs have a contributory protective role: in PC-null strains, the presence of MTs clearly confers additional protection when brood size is considered as an endpoint, although lifespan is not obviously affected (Fig. 6).

CONCLUSIONS

Metallothioneins are believed to play a key role in organisms' responses to and protection against toxic soft metal ions such as cadmium. We have confirmed earlier observations that phytochelatin synthase is required in *C. elegans* for protection against cadmium, by demonstrating the production of phytochelatins (PC_2 and PC_3) directly in tissue extracts of cadmium-exposed *C. elegans*. Functional assays with appropriate knockout strains showed that metallothioneins do help protect against cadmium toxicity, but not to the same extent as phytochelatins. Furthermore, NMR- and UPLC-MS-based metabolomic analyses imply that (at least in phytochelatin synthase-normal nematodes) the main physiological responses to cadmium are independent of metallothionein status, and result in an increased production of phytochelatins by altered flux through the methionine transsulfonation pathway. *C. elegans* is an important model organism, but cannot be used for mechanistic toxicology studies unless its responses to toxic compounds are well understood. Our results here show that attempts to understand the effects of metallothioneins in isolation on cadmium toxicity in *C. elegans* without also considering compensatory

phytochelatin responses may well be flawed. This might also hold true for other metals and metalloids (e.g. copper, zinc, arsenic) known to induce phytochelatin production in plants and microbes.

ACKNOWLEDGEMENTS

We would like to thank the *C. elegans* KnockOut Consortium for the isolation of the *gk125(vc128)* allele; the *Caenorhabditis* Genetics Centre, which is funded by the National Institutes of Health National Centre for Research Resources, for the supply of N2 and *mtl-2(gk125)*; and the Mitani laboratory (Tokyo Women's Medical University School of Medicine, Japan) for the isolation of *mtl-1(tm1770)* and *pcs-1(tm1748)*. SLH was supported by a Natural Environment Research Council (NERC) studentship (NER/S/A/2005/13135). SRS thanks the Royal Society and EJW thanks Waters Corp. for additional support.

REFERENCES

(1) Nriagu, J. O. Global inventory of natural and anthropogenic emissions of trace metals to the atmosphere. *Nature*. **1979**, *279*, 409-411.

(2) Nordberg, G. F.; Nogawa, K.; Nordberg, M.; Friberg, L. Cadmium. In *Handbook on the Toxicology of Metals*; Nordberg, G. F.; Fowler, B.A.; Nordberg, M.; Friberg, L., Eds.; Academic Press: London, 2007; pp. 446-479.

(3) Cui, Y.; McBride, S. J.; Boyd, W. A.; Alper, S.; Freedman, J. H. Toxicogenomic analysis of *Caenorhabditis elegans* reveals novel genes and pathways involved in the resistance to cadmium toxicity. *Genome Biol.* **2007**, *8*, R122.

(4) Kagi, J. H.; Valee, B. L. Metallothionein: a cadmium- and zinc-containing protein from equine renal cortex. *J Biol Chem.* **1960**, *235*, 3460-3465.

(5) Klaassen, C. D.; Liu, J.; Choudhuri, S. Metallothionein: an intracellular protein to protect against cadmium toxicity. *Annu Rev Pharmacol Toxicol.* **1999**, *39*, 267-294.

(6) Kugawa, F.; Yamamoto, H.; Osada, S.; Aoki, M.; Imagawa, M.; Nishihara, T. Metallothionein genes in the nematode Caenorhabditis elegans and metal inducibility in mammalian culture cells. *Biomed Environ Sci.* **1994**, *7*, 222-231.

(7) Camakaris, J.; Voskoboinik, I.; Mercer, J. F. Molecular mechanisms of copper homeostasis. *Biochem Biophys Res Commun.* **1999**, *261*, 225-232.

(8) Palmiter, R. D. The elusive function of metallothioneins. *Proc Natl Acad Sci U S A.* **1998**, *95*, 8428-8430.

(9) Freedman, J. H.; Slice, L. W.; Dixon, D.; Fire, A.; Rubin, C. S. The novel metallothionein genes of Caenorhabditis elegans. Structural organization and inducible, cell-specific expression. *J Biol Chem.* **1993**, *268*, 2554-2564.

(10) Hughes, S.; Sturzenbaum, S. R. Single and double metallothionein knockout in the nematode C. elegans reveals cadmium dependent and independent toxic effects on life history traits. *Environ Pollut.* **2007**, *145*, 395-400.

(11) Coen, M.; Holmes, E.; Lindon, J. C.; Nicholson, J. K. NMR-based metabolic profiling and metabonomic approaches to problems in molecular toxicology. *Chem Res Toxicol.* **2008**, *21*, 9-27.

(12) Goodacre, R.; Vaidyanathan, S.; Dunn, W. B.; Harrigan, G. G.; Kell, D. B. Metabolomics by numbers: acquiring and understanding global metabolite data. *Trends Biotechnol.* **2004**, *22*, 245-252.

(13) Robertson, D. G. Metabonomics in toxicology: a review. *Toxicol Sci.* **2005**, *85*, 809-822.

(14) Bailey, N. J.; Oven, M.; Holmes, E.; Nicholson, J. K.; Zenk, M. H. Metabolomic analysis of the consequences of cadmium exposure in Silene cucubalus cell cultures via 1H NMR spectroscopy and chemometrics. *Phytochemistry.* **2003**, *62*, 851-858.

(15) Griffin, J. L.; Walker, L. A.; Shore, R. F.; Nicholson, J. K. Metabolic profiling of chronic cadmium exposure in the rat. *Chem Res Toxicol.* **2001**, *14*, 1428-1434.

(16) Griffin, J. L.; Walker, L. A.; Troke, J.; Osborn, D.; Shore, R. F.; Nicholson, J. K. The initial pathogenesis of cadmium induced renal toxicity. *FEBS Lett.* **2000**, *478*, 147-150.

(17) Guo, Q.; Sidhu, J. K.; Ebbels, T. M. D.; Rana, F.; Spurgeon, D. J.; Svendsen, C.; Stürzenbaum, S. R.; Kille, P.; Morgan, A. J.; Bundy, J. G. Validation of metabolomics for toxic mechanism of action screening with the earthworm *Lumbricus rubellus*. *Metabolomics.* **2009**, *10.1007/s11306-008-0153-z*,

(18) Sarry, J. E.; Kuhn, L.; Ducruix, C.; Lafaye, A.; Junot, C.; Hugouvieux, V.; Jourdain, A.; Bastien, O.; Fievet, J. B.; Vailhen, D.; Amekraz, B.; Moulin, C.; Ezan, E.; Garin, J.; Bourguignon, J. The early responses of Arabidopsis thaliana cells to cadmium exposure explored by protein and metabolite profiling analyses. *Proteomics.* **2006**, *6*, 2180-2198.

(19) Sugiura, Y.; Kashiba, M.; Maruyama, K.; Hoshikawa, K.; Sasaki, R.; Saito, K.; Kimura, H.; Goda, N.; Suematsu, M. Cadmium exposure alters metabolomics of sulfur-containing amino acids in rat testes. *Antioxid Redox Signal.* **2005**, *7*, 781-787.

(20) Tanaka, Y.; Higashi, T.; Rakwal, R.; Wakida, S.; Iwahashi, H. Quantitative analysis of sulfur-related metabolites during cadmium stress response in yeast by capillary electrophoresis-mass spectrometry. *J Pharm Biomed Anal.* **2007**, *44*, 608-613.

(21) Blaise, B. J.; Giacomotto, J.; Elena, B.; Dumas, M. E.; Toulhoat, P.; Segalat, L.; Emsley, L. Metabotyping of *Caenorhabditis elegans* reveals latent phenotypes. *Proc Natl Acad Sci U S A.* **2007**, *104*, 19808-19812.

(22) Atherton, H. J.; Jones, O. A.; Malik, S.; Miska, E. A.; Griffin, J. L. A comparative metabolomic study of NHR-49 in *Caenorhabditis elegans* and PPAR-α in the mouse. *FEBS Lett.* **2008**, *582*, 1661-1666.

(23) Falk, M. J.; Zhang, Z.; Rosenjack, J. R.; Nissim, I.; Daikhin, E.; Nissim, I.; Sedensky, M. M.; Yudkoff, M.; Morgan, P. G. Metabolic pathway profiling of mitochondrial respiratory chain mutants in *C. elegans*. *Mol Genet Metab.* **2008**, *93*, 388-397.

(24) Beckonert, O.; Keun, H. C.; Ebbels, T. M.; Bundy, J.; Holmes, E.; Lindon, J. C.; Nicholson, J. K. Metabolic profiling, metabolomic and metabonomic procedures

for NMR spectroscopy of urine, plasma, serum and tissue extracts. *Nat Protoc.* **2007**, *2*, 2692-2703.

(25) Weljie, A. M.; Newton, J.; Mercier, P.; Carlson, E.; Slupsky, C. M. Targeted profiling: quantitative analysis of 1H NMR metabolomics data. *Anal Chem.* **2006**, *78*, 4430-4442.

(26) Smith, C. A.; Want, E. J.; O'Maille, G.; Abagyan, R.; Siuzdak, G. XCMS: processing mass spectrometry data for metabolite profiling using nonlinear peak alignment, matching, and identification. *Anal Chem.* **2006**, *78*, 779-787.

(27) Swain, S. C.; Keusekotten, K.; Baumeister, R.; Sturzenbaum, S. R. C. elegans metallothioneins: new insights into the phenotypic effects of cadmium toxicosis. *J Mol Biol.* **2004**, *341*, 951-959.

(28) Boulesteix, A. L.; Strimmer, K. Partial least squares: a versatile tool for the analysis of high-dimensional genomic data. *Brief Bioinform.* **2007**, *8*, 32-44.

(29) Trygg, J.; Holmes, E.; Lundstedt, T. Chemometrics in metabonomics. *J Proteome Res.* **2007**, *6*, 469-479.

(30) Vandesompele, J.; De Preter, K.; Pattyn, F.; Poppe, B.; Van Roy, N.; De Paepe, A.; Speleman, F. Accurate normalization of real-time quantitative RT-PCR data by geometric averaging of multiple internal control genes. *Genome Biol.* **2002**, *3*, 7.

(31) Clemens, S.; Schroeder, J. I.; Degenkolb, T. Caenorhabditis elegans expresses a functional phytochelatin synthase. *Eur J Biochem.* **2001**, *268*, 3640-3643.

(32) Cobbett, C.; Goldsbrough, P. Phytochelatins and metallothioneins: roles in heavy metal detoxification and homeostasis. *Annu Rev Plant Biol.* **2002**, *53*, 159-182.

(33) Cobbett, C. S. Phytochelatins and their roles in heavy metal detoxification. *Plant Physiol.* **2000**, *123*, 825-832.

(34) Grill, E.; Winnacker, E. L.; Zenk, M. H. Phytochelatins: the principal heavy-metal complexing peptides of higher plants. *Science.* **1985**, *230*, 674-676.

(35) Clemens, S.; Kim, E. J.; Neumann, D.; Schroeder, J. I. Tolerance to toxic metals by a gene family of phytochelatin synthases from plants and yeast. *EMBO J.* **1999**, *18*, 3325-3333.

(36) Ha, S. B.; Smith, A. P.; Howden, R.; Dietrich, W. M.; Bugg, S.; O'Connell, M. J.; Goldsbrough, P. B.; Cobbett, C. S. Phytochelatin synthase genes from Arabidopsis and the yeast Schizosaccharomyces pombe. *Plant Cell.* **1999**, *11*, 1153-1164.

(37) Vatamaniuk, O. K.; Bucher, E. A.; Ward, J. T.; Rea, P. A. A new pathway for heavy metal detoxification in animals. Phytochelatin synthase is required for cadmium tolerance in Caenorhabditis elegans. *J Biol Chem.* **2001**, *276*, 20817-20820.

(38) Vatamaniuk, O. K.; Mari, S.; Lu, Y. P.; Rea, P. A. AtPCS1, a phytochelatin synthase from Arabidopsis: isolation and in vitro reconstitution. *Proc Natl Acad Sci U S A.* **1999**, *96*, 7110-7115.

(39) Rao, A. M.; Drake, M. R.; Stipanuk, M. H. Role of the transsulfuration pathway and of gamma-cystathionase activity in the formation of cysteine and sulfate from methionine in rat hepatocytes. *J Nutr.* **1990**, *120*, 837-845.

(40) Houghton, C. B.; Cherian, M. G. Effects of inhibition of cystathionase activity on glutathione and metallothionein levels in the adult rat. *J Biochem Toxicol.* **1991**, *6*, 221-228.

(41) Lafaye, A.; Junot, C.; Pereira, Y.; Lagniel, G.; Tabet, J. C.; Ezan, E.; Labarre, J. Combined proteome and metabolite-profiling analyses reveal surprising insights into yeast sulfur metabolism. *J Biol Chem.* **2005**, *280*, 24723-24730.

(42) Sura, P.; Ristic, N.; Bronowicka, P.; Wrobel, M. Cadmium toxicity related to cysteine metabolism and glutathione levels in frog Rana ridibunda tissues. *Comp Biochem Physiol C Toxicol Pharmacol.* **2006**, *142*, 128-135.

(43) Swain, S. C.; Wren, J.; Sturzenbaum, S. R.; Kille, P.; Jager, T.; Jonker, M. J.; Hankard, P. K.; Svendsen, C.; Chaseley, J.; Hedley, B. A.; Blaxter, M.; Spurgeon, D. J. Linking toxicants' mechanism of action and physiological mode of action in *Caenorhabditis elegans*. *BMC Biol.*, submitted.

(44) Brulle, F.; Cocquerelle, C.; Wamalah, A. N.; Morgan, A. J.; Kille, P.; Lepretre, A.; Vandenbulcke, F. cDNA cloning and expression analysis of Eisenia fetida (Annelida: Oligochaeta) phytochelatin synthase under cadmium exposure. *Ecotoxicol Environ Saf.* **2008**, *71*, 47-55.

(45) Grill, E.; Loffler, S.; Winnacker, E. L.; Zenk, M. H. Phytochelatins, the heavy-metal-binding peptides of plants, are synthesized from glutathione by a specific gamma-glutamylcysteine dipeptidyl transpeptidase (phytochelatin synthase). *Proc Natl Acad Sci U S A.* **1989**, *86*, 6838-6842.

(46) Hirata, K.; Tsuji, N.; Miyamoto, K. Biosynthetic regulation of phytochelatins, heavy metal-binding peptides. *J Biosci Bioeng.* **2005**, *100*, 593-599.

(47) Mendoza-Cozatl, D.; Loza-Tavera, H.; Hernandez-Navarro, A.; Moreno-Sanchez, R. Sulfur assimilation and glutathione metabolism under cadmium stress in yeast, protists and plants. *FEMS Microbiol Rev.* **2005**, *29*, 653-671.

(48) Wylie, T.; Martin, J.; Abubucker, S.; Yin, Y.; Messina, D.; Wang, Z.; McCarter, J. P.; Mitreva, M. NemaPath: online exploration of KEGG-based metabolic pathways for nematodes. *BMC Genomics*. **2008**, *9*, 525.

FIGURE LEGENDS AND FIGURES

Figure 1. Partial least squares discriminant analysis of NMR (A–C) and UPLC-MS (D–F) data.

A: Scores plot, NMR data. Point shape indicates cadmium treatment and colour indicates strain. Circles: 12 µM cadmium. Squares: controls (no cadmium). Black: N2 wild-type. Blue: *mtl-2* knockout. Red: *mtl-1* knockout. Yellow: *mtl-1;mtl-2* double knockout.

B: Loadings plot, NMR data. Variables corresponding to resonances from trehalose (blue) and cystathionine (red) are marked directly on the plot.

C: Validation plot, NMR data. The ordinate shows the distribution of R^2 (solid line, triangles) and Q^2 values (dashed line, squares) for 50 permutations of the original data order. The abscissa shows the correlation of the permuted data order with the original data order.

D: Scores plot, UPLC-MS data. Symbols are the same as for panel A.

E: Loadings plot, UPLC-MS data. Variables corresponding to peaks from phytochelatin-2 and phytochelatin-3 (blue) are marked directly on the plot.

F: Validation plot, UPLC-MS data. Symbols are the same as for panel C.

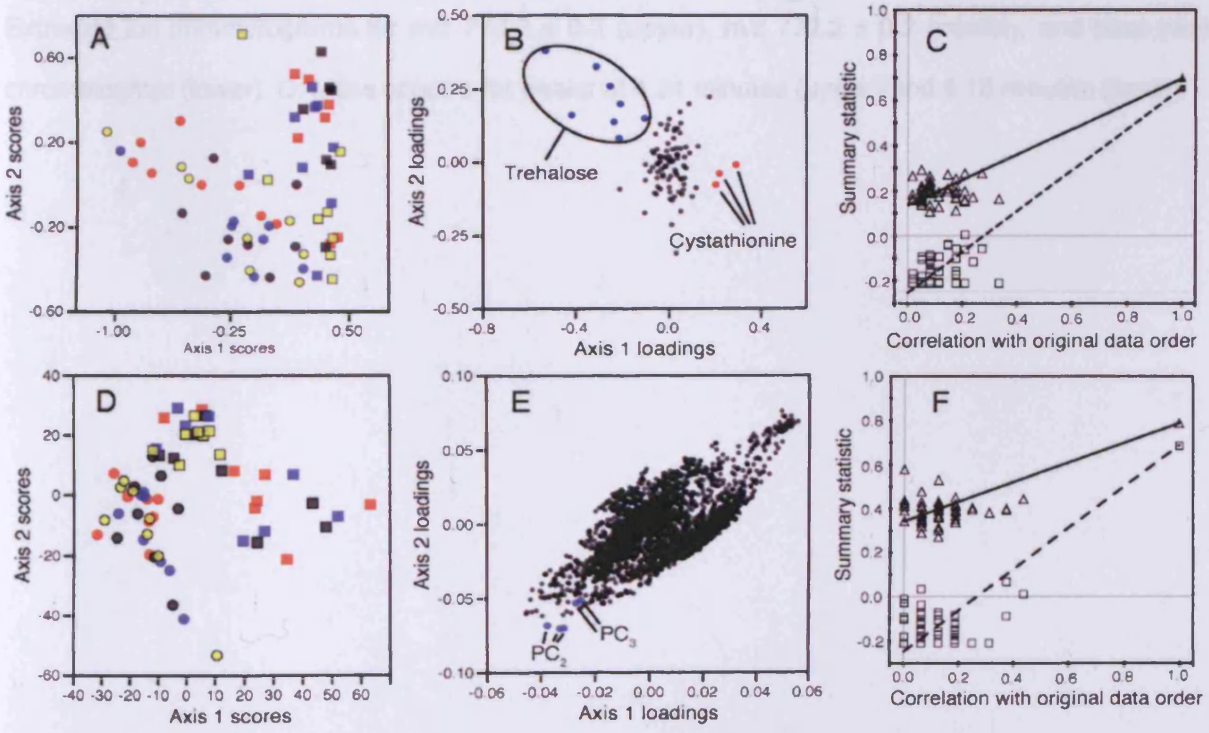

Figure 2. Cadmium exposure causes a decrease in cystathionine levels. Black bars: cystathionine (expressed on dimensionless scale, relative to a mean of four other abundant metabolites) in the absence of cadmium. Grey bars: cystathionine in the presence of 12 μM cadmium. Error bars represent SEM (n = 8).

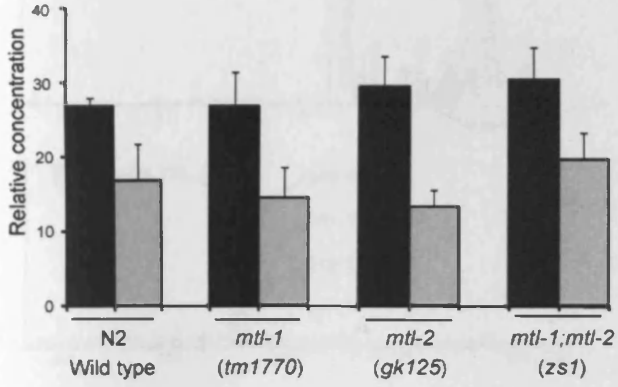

Figure 3. Detection of phytochelatins by UPLC-MS. A: Extracted ion chromatogram for m/z 540.1 ± 0.2 (upper) and base-peak chromatogram (lower). B: mass spectrum of peak at 3.60 minutes. C: Extracted ion chromatograms for m/z 770.2 ± 0.2 (upper), m/z 772.2 ± 0.2 (middle), and base-peak chromatogram (lower). D: Mass spectra for peaks at 4.34 minutes (upper) and 4.18 minutes (lower).

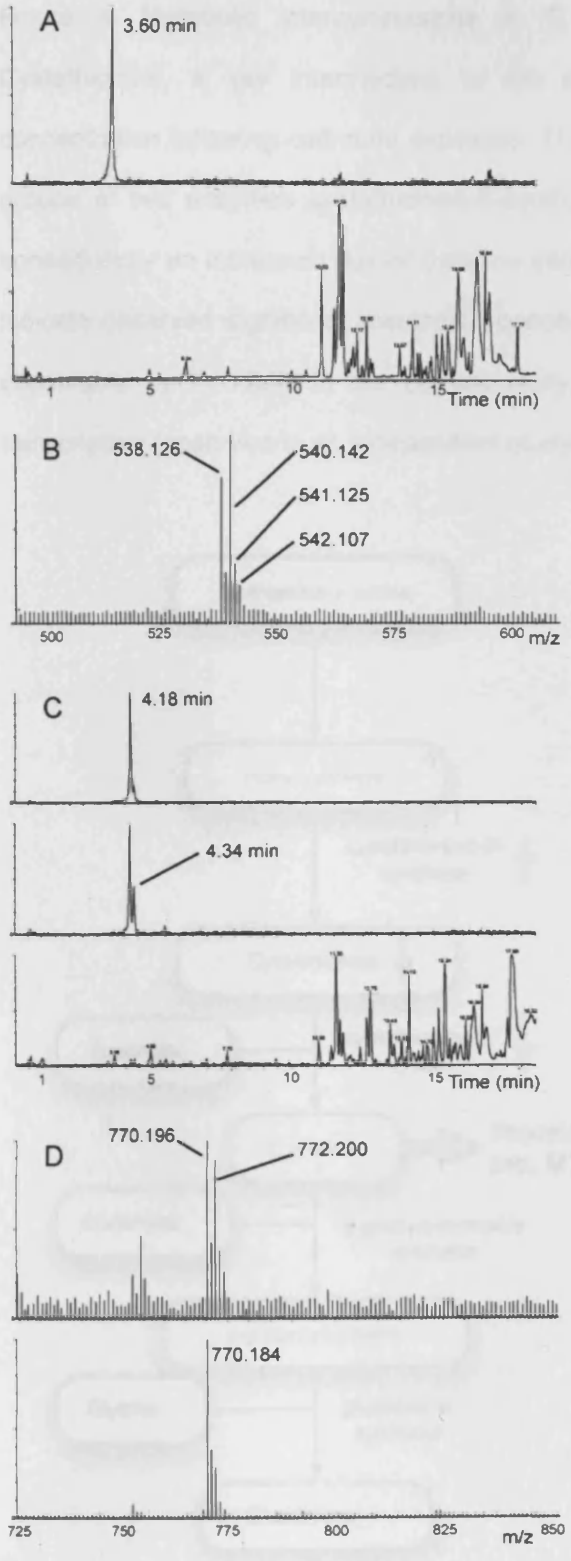
A
3.60 min
1
5
10
15
Time (min)
B
538.126
540.142
541.125
542.107
500
525
550
575
600
m/z
C
4.18 min
4.34 min
1
5
10
15
Time (min)
D
770.196
772.200
770.184
725
750
775
800
825
m/z
850

Figure 4. Metabolic interconversions in *C. elegans* (based on information in NemaPath[48]). Cystathionine, a key intermediate in the transsulfuration pathway, significantly decreased in concentration following cadmium exposure. This is due to the inhibition by cadmium at the free thiol groups of two enzymes cystathionine-β-synthase (CβS) and cystathionine-γ-lyase (CγL). There is consequently an increased flux of cysteine into glutathione synthesis and phytochelatin. Blue arrows indicate observed significant metabolite concentration changes. Metabolite names in grey were not observable by ^{1}H NMR in our current study. Red arrows represent proposed changes in gene transcription (observed in an independent study).

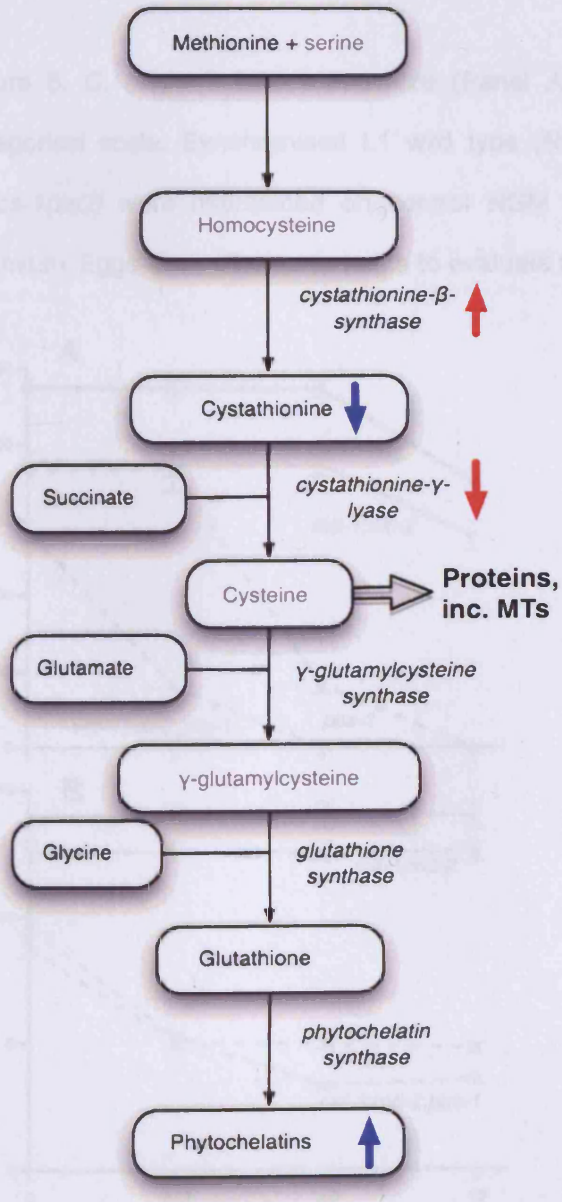

Figure 5. Phytochelatins are increased in *C. elegans* tissue extracts by cadmium exposure: UPLC-MS integrals, log_{10} transformed. Black bars: control. Grey bars: 12 µM cadmium. Error bars ± SEM (n = 8). A: m/z 540 (PC_2). B: m/z 770 (PC_3).

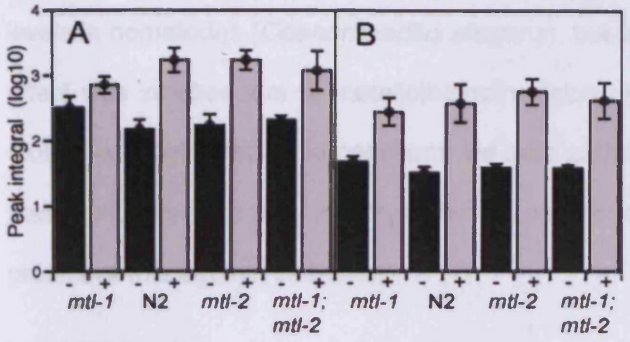

Figure 6. *C. elegans* total brood size (Panel A) and lifespan (Panel B); NB the abscissa is a categorical scale. Synchronised L1 wild type (N2), *mtl-1;mtl-2(zs1), pcs-1(tm1748)* and *mtl-1;mtl-2;pcs-1(zs2)* were maintained on control NGM supplemented with 0.05 µM, 0.5 µM or 12 µM cadmium. Eggs were allowed to hatch to evaluate the total viable offspring. Error bars ± SEM (n=32).

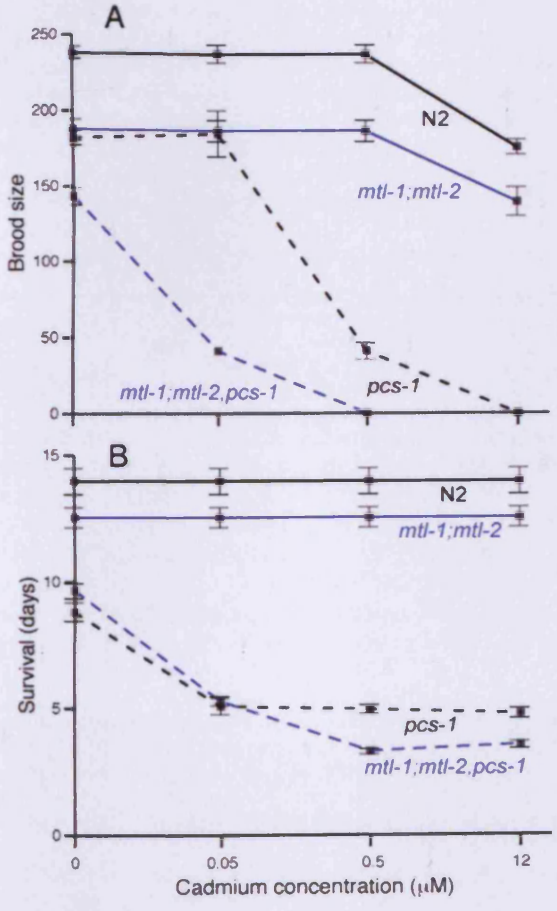

TOC graphic and synopsis:

Metabolic profiling by NMR and UPLC-MS showed that cadmium exposure decreased cystathionine levels in nematodes (*Caenorhabditis elegans*), but increased concentrations of phytochelatins. As this effect was independent of metallothionein status, and given that the phytochelatin synthase (*pcs-1*) mutant is hypersensitive to cadmium, we infer cadmium resistance in *C. elegans* is dependent on the trans-sulfuration pathway for phytochelatin production. In addition, metallothionein confers an additive protective role against cadmium.

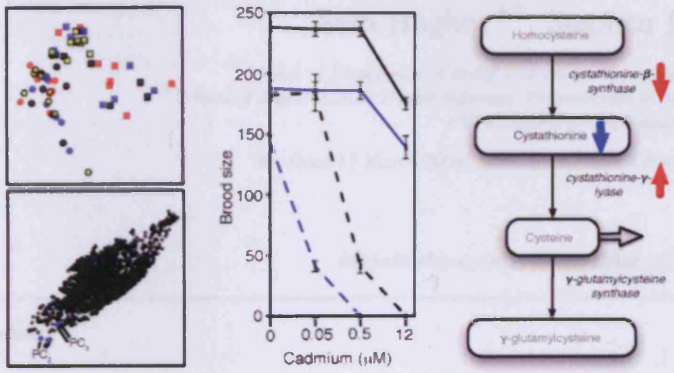

Available online at www.sciencedirect.com
ScienceDirect
Environmental Pollution 145 (2007) 395–400
ENVIRONMENTAL POLLUTION
www.elsevier.com/locate/envpol

Rapid Communication

Single and double metallothionein knockout in the nematode *C. elegans* reveals cadmium dependent and independent toxic effects on life history traits

Sam Hughes [a,b], Stephen R. Stürzenbaum [a,b,*]

[a] *School of Biosciences, Cardiff University, Main Building, Park Place, Cardiff CF10 3TL, UK*
[b] *School of Biomedical & Health Sciences, Pharmaceutical Sciences Research Division, King's College London, 150 Stamford Street, London SE1 9NH, UK*

Received 17 March 2006; received in revised form 17 May 2006; accepted 15 June 2006

Metallothionein is a modifier of life-history parameters.

Abstract

The genome of the nematode *Caenorhabditis elegans* contains two metallothionein genes, both involved in metal homeostasis and/or detoxification. Single metallothionein knockout mutants have been created and now, for the first time, a double mutant has been isolated. Life history studies in the presence or absence of cadmium showed that all metallothionein mutants are viable. Although cadmium did not influence longevity, a dose dependent reduction in total brood size and volumetric growth was observed in wild type animals, which was magnified in single knockouts and further exacerbated in the double knockout. However, the metallothionein deletion caused two effects that are independent of cadmium exposure, namely all knockout strains displayed a reduced total brood size and the deletion of both metallothionein loci caused a significant reduction in volumetric growth. In summary, metallothionein is undoubtedly an important player in cadmium detoxification, but evidently also an important factor in cadmium independent pathways.

Keywords: Metallothionein; Knockout; Cadmium; Nematode; *C. elegans*

1. Introduction

Metallothioneins (MTs) are cadmium-, zinc- and copper-containing sulphur rich proteins typically 6–7 kDa in molecular weight (Freedman et al., 1993) with an omnipresent phylogenetic distribution ranging from plants (Zimeri et al., 2005) and prokaryotes (Daniels et al., 1998) to higher eukaryotes (Chapman et al., 1999). Identified functions of MT include the metabolism and homeostasis of essential trace metals such as zinc and copper (Klaassen et al., 1999), the protection against oxidative damage (Colangelo et al., 2004), acting as chaperones for protein folding (Plamiter, 1998) and the protection from cadmium and other toxic stressors (Beattie et al., 2005).

In mammalian cells more than ten isoforms have been identified which have been grouped in four primary subdivisions. Whilst MT-1 and MT-2 are expressed ubiquitously, MT-3 is specific to the brain and MT-4 is limited to stratified tissues (West et al., 1990). In mammals, MT is thought to be primarily involved in copper sequestration and in the protection from reactive oxygen species. Mammalian MT-1 and MT-2 have been extensively studied and the promoter regions are well characterized, both containing metal responsive elements and glucocorticoid responsive elements. Gene activation is mediated via a metal responsive transcription factor (MTF-1) that binds to multiple metal response elements

* Corresponding author. School of Biomedical & Health Sciences, Pharmaceutical Sciences Research Division, King's College London, 150 Stamford Street, London SE1 9NH, UK. Tel.: +44 207 848 4406; fax: +44 207 848 4500.
E-mail address: stephen.sturzenbaum@kcl.ac.uk (S.R. Stürzenbaum).

0269-7491/$ - see front matter © 2006 Elsevier Ltd. All rights reserved.
doi:10.1016/j.envpol.2006.06.003

(MREs) located within the promoter of the metallothionein genes (Vasak, 2005).

In contrast to the well studied mammalian MT-mediated metallo-biology, the function of invertebrate MT is less widely understood. To date, most studies on invertebrate MT have focused on the earthworm (Stürzenbaum et al., 1998, 2001, 2004), the snail (Dallinger et al., 1997, 2005), the fruit fly (Domenech et al., 2003) and the nematode (Freedman et al., 1993; Moilanen et al., 1999; Swain et al., 2004). In many cases, for example the springtail (Timmermans et al., 2005), adaptation to elevated environmental metal concentrations has been achieved through the increased synthesis of MT or via the duplication of metallothionein genes (Stephan et al., 1994; Knapen et al., 2005).

The fully sequenced genome of the nematode *C. elegans* contains two MT isoforms (mtl-1 and mtl-2) both located on chromosome V. Swain et al., (2004) demonstrated that the single chromosomal deletion of mtl-2 and the knockdown of mtl-1 via an RNAi mediated approach, causes significant deleterious effects upon exposure to elevated levels of cadmium. Only recently has a deletion mutant of mtl-1 been isolated, allowing for the first time, an investigation into the effects caused by the chromosomal deletion of both MT loci, thereby creating an invaluable tool to investigate the role MT plays in metal sequestration, trafficking and detoxification.

2. Materials and methods

2.1. Generation of a double (mtl-1 and mtl-2) metallothionein deletion mutant

To create the double MT knockout *mtl-1;mtl-2(zs1)*, *mtl-1(tm1770)* was backcrossed twice and *mtl-2(gk125)* backcrossed six times. Backcrossed *mtl-2(gk125)* were heat shocked (30 °C for 5.5 h) at L4 larval stage and five young resultant male offspring were transferred to a plate containing one single L4 *mtl-1(tm1770)* hermaphrodite. The progeny were singled out into multi-well plates and maintained until maturity (identified by the presence of eggs). Following single worm lysis, a genomic polymerase chain reaction (PCR) was performed to screen and identify double knockout mutants. Homozygous double mutant strains were selected and assessed and confirmed over at least 4 generations. In detail, each single worm lysis was split to allow a two step (nested) PCR of mtl-1 and mtl-2. The primary PCR of mtl-1 was achieved using the sense primer 5′-TGACCAGTGTCGTGAGCGAC-3′ with the anti-sense primer 5′-TAGATGTTTCAGACGTCACC-3′ at optimized conditions with commercial Taq polymerase (Promega, Southampton, UK) as specified in the manufacturer's recommended conditions. The primary PCR product (1 μl) was then used in a nested PCR with sense primer 5′-CAGGGTTTC ATAGTCGGGGT-3′ and anti-sense primer 5′-CCTGTGGAGAAACGT GTAAG-3′. Similarly, the *mtl-2(gk125)* was identified by PCR using the sense primer 5′-TGACCAGTGTCGTGAGCGAC-3′ and anti-sense primer 5′-TAGATGTTTCAGACGTGACC-3′ followed by a nested PCR with sense primer 5′-CAGGGTTTCATAGTCGGGGT-3′ and anti-sense primer 5′-CCTGTGGAGAAACGTGTAAG-3′.

2.2. Brood size and lifespan measurements

All nematodes were grown on agar plates using standardized protocols (Brenner, 1974). Gravid hermaphrodites were bleached to release the eggs and maintained overnight in standard M9 buffer. The resultant staged L1 larvae were placed onto dosed petri dishes and incubated at 20 °C. Following a 24 h exposure period, single animals of the fourth larval stage (L4) were transferred to individual wells of multi-well plates and transferred daily until the brood period was completed. Total brood size and daily reproductive output was determined for each strain at four nominal concentrations of cadmium (0, 2.5, 5 and 12 μM). Counts were performed manually and the mean number (±standard error) of hatched offspring for each strain/category determined (wild type: $n = 38$; *mtl-1(tm1770)*: $n = 44$; *mtl-2(gk125)*: $n = 45$; *mtl-1;mtl-2(zs1)*: $n = 36$). For lifespan measurements, nematodes were monitored daily throughout development and post maturity by tapping the nematode on the head with a hair. Animals were considered dead if no movement was observed following repeated probing. Average lifespan (±standard error) was calculated from all strains (wild type: $n = 35$; *mtl-1(tm1770)*: $n = 37$; *mtl-2(gk125)*: $n = 40$; *mtl-1;mtl2(zs1)*: $n = 30$). The data was statistically analyzed using a 2-tailed 2 sample *t*-test (Minitab Ltd., Coventry, UK).

2.3. Growth measurements

Nematodes (10 individuals per strain, per dose) were photographed using a digital camera attached to a microscope (both Nikon UK Ltd., Kingston upon Thames, UK). Photographs were taken at 24 h time intervals over 142 h (t_0 = L1s transferred to plates). The volumetric area within the perimeter of the nematodes was calculated by means of a graticule and specialist software (Image ProExpress, Media Cybernetics, Wokingham, UK).

2.4. Statistics

Statistical differences ($P \leq 0.05$ and $P \leq 0.01$) between genotype and brood size, growth, lifespan or cadmium dose were identified using ANOVA, followed by the Tukey's *post-hoc* test.

3. Results and discussion

3.1. C. elegans strains

Using the primer sets given in Section 2, wild type and appropriate deletions of the MT gene locus were identified

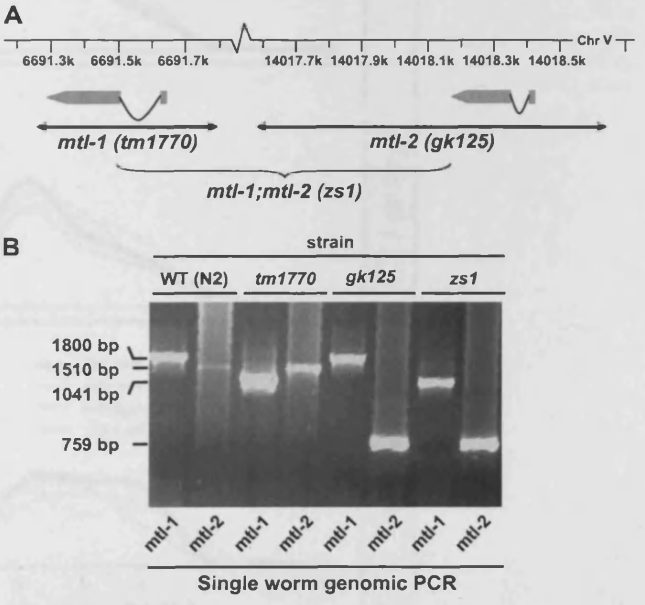

Fig. 1. Schematic diagram of the two *C. elegans* metallothionein loci (mtl-1 and mtl-2) on chromosome V. Indicated are the intron-exon boundaries (grey arrows) and the location of the chromosomal deletion of single metallothioneins (plain arrows) (A). Following the backcrossing of single metallothionein strains, a homozygous double knockout was created and identified by single worm genomic PCR (B).

by nested PCR. In detail, the mtl-1 and mtl-2 amplicons in wild type animals were 1800 bp and 1510 bp, respectively. In *mtl-1(tm1770)*, the mtl-1 amplicon was reduced to 1041 bp, corresponding to a deletion that encompasses 186 bp of the mtl-1 promoter, the entire coding region and 47 bp of the 3′ untranslated region. Similarly, PCR of mtl-2 in *mtl-2(gk125)* amplified a 759 bp product, due to a deletion of 208 bp promoter, the entire coding region and 585 bp of the 3′ untranslated region. As a considerable proportion of the promoter and the entire coding region are deleted in both strains they can be considered to be true null alleles (see Fig. 1A). The newly created, viable, homozygous metallothionein double knockout *mtl-1;mtl-2(zs1)* displayed PCR banding patterns equivalent to *mtl-1(tm1770)* and *mtl-2(gk125)* (see Fig. 1B) and thus is a unique investigative tool for metallo-toxicology. Both single and the double MT knockout mutants are viable, highlighting that MT is not essential for life, cadmium detoxification or essential metal homeostasis.

3.2. Total brood size and brood period measurements

Under optimal conditions, in the absence of cadmium, the wild type strain produced 225 ± 7 viable eggs, a number that is in broad synergy with the expected norm. The egg laying period approximated a normal, bell shaped distribution with the maximum daily output (143 ± 4) peaking on day

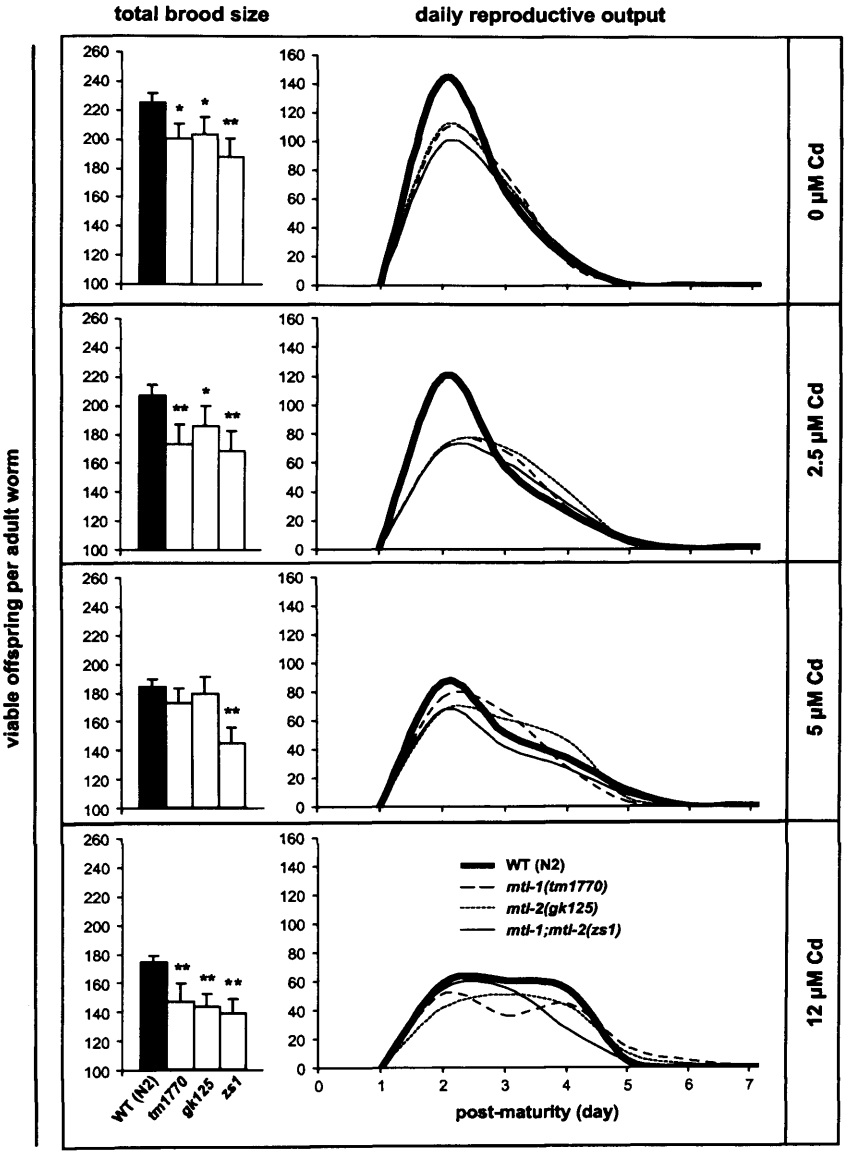

Fig. 2. Total brood size, daily reproductive output and reproductive period of wild type (N2), *mtl-1(tm1770)*, *mtl-2(gk125)* and the double knockout *mtl-1;mtl-2(zs1)* exposed to a cadmium gradient (0, 2.5, 5 and 12 µM Cd). Averages ± standard errors were calculated as described in Section 2. Statistical differences (* = $P \leq 0.05$ and ** = $P \leq 0.01$) between wild type and mtl knockout strains were identified using ANOVA, followed by the Tukey's *post-hoc* test. Note strain specific differences in control conditions as well as dose dependent effects of cadmium.

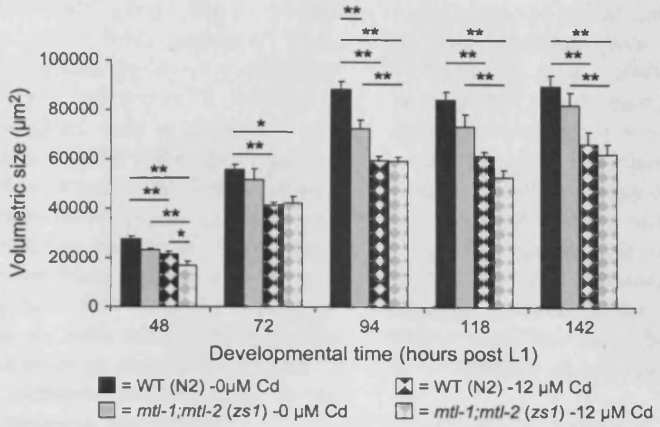

Fig. 3. The effects of cadmium on volumetric growth. Growth over developmental time of wild type (black bars) or *mtl-1;mtl-2(zs1)* (grey bars) in the presence (checkered bars) or absence (solid bars) of 12 µM cadmium. Note the strain specific and dose dependent reductions. Averages (±standard errors) at each time point were determined from 10 individuals per strain, per dose. Statistical differences (* = $P \leq 0.05$ and ** = $P \leq 0.01$) were identified using ANOVA, followed by the Tukey's *post-hoc* test.

two (post L1). With increasing cadmium concentrations, total brood size was reduced in a dose dependant manner with notable changes in the Gaussian distribution, namely the peak becoming lower, broader and flatter at 2.5 µM Cd and 5 µM Cd (Fig. 2). At 12 µM Cd the main reproductive output spanned a 3-day period (approximately 50 eggs/day) with a cumulative total in the control strain reaching 175 eggs ±5. In general, this trend was observed in all three knockout strains, however total reproductive output was consistently lower in mtl knockout animals with the most pronounced reduction observed in the double knockout. Total brood size for *mtl-1(tm1770)*, *mtl-2(gk125)* and *mtl-1;mtl-2(zs1)* was reduced from 201, 203 and 188 eggs at 0 µM cadmium to 148, 144 and 139 offspring at 12 µM cadmium, respectively (all of which were significantly different ($P \leq 0.05$) to corresponding control nematodes (Fig. 2). Whilst the total brood size of *mtl-1;mtl-2(zs1)* was intrinsically lower compared to wild type ($P \leq 0.01$), the single knockouts were indistinguishable from each other and displayed an intermediate total reproductive performance between wild type and the double knockout.

Cadmium is a known teratogen (WHO, 1996), possibly explaining the cadmium-induced effects in wild type animals

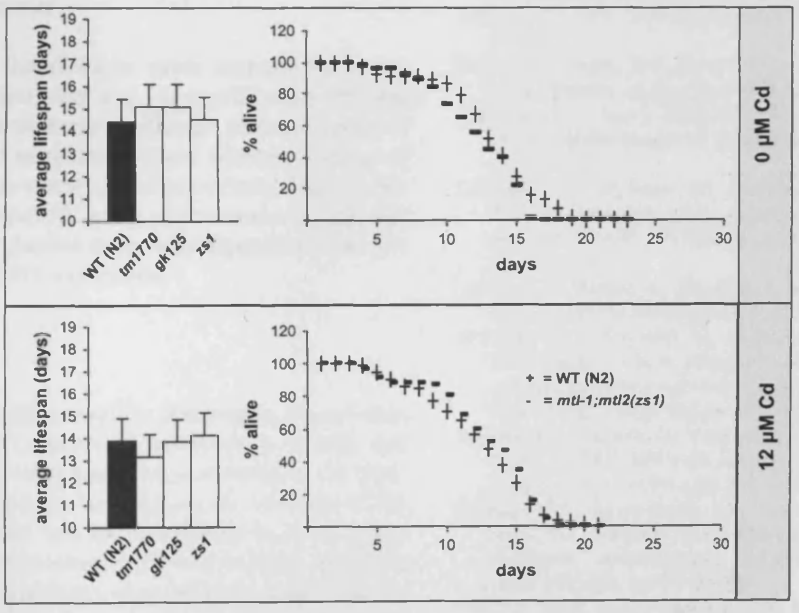

Fig. 4. Lifespan measurements of wild type and metallothionein deletion mutants in the presence or absence of cadmium. Day one was defined as the time when nematodes were at L1 stage and death identified when the nematode did not respond to repeated probing. Averages ± standard errors were calculated as described in Section 2. Note the absence of significant strain specific differences in lifespan.

and mutants lacking one or both MT genes. The *C. elegans* hermaphrodite germ line cells form a finite number of sperm (Jager et al., 2005), thus being the limiting factor in reproductive fertilization, and consequently brood size. It therefore is conceivable that a teratogenic agent, such as cadmium, may effect reproductive success via a negative influence on gamete formation, a notion that has been stipulated by others (Alvarez et al., 2005) and worthy of further investigation. Consequently, it is therefore not surprising that the absence of the cadmium chelator metallothionein, as in the mutants tested, will enhance any cadmium specific teratogenic effect on brood size. However, it is of utmost interest to note that brood size was compromised in MT mutants even in conditions devoid of cadmium, highlighting that cadmium detoxification is not the only modulator of metallothionein functioning.

3.3. Growth measurements

C. elegans goes through four molt stages and growth occurs exponentially between these points until a final plateau phase is reached (Byerly et al., 1976; Jager et al., 2005). However, some toxicants, including cadmium, can act as negative effectors of growth (Alvarez et al., 2005). The systematic measurement of volumetric growth in the presence or absence of cadmium over a 142 h time course confirmed this trend in wild type and all MT mutants in a dose dependent manner (data not shown). No consistent strain-specific differences were observed regarding the growth, bar one exception: compared to wild type, the volumetric growth of *mtl-1;mtl-2(zs1)* was impaired notably in conditions lacking the toxicant (Fig. 3). Clearly this provides further evidence that MTs biological role is not limited to cadmium detoxification.

3.4. Lifespan measurements

At 0 μM cadmium, the wild type strain survived for an average of 14.5 days, a figure that was not significantly different to any of the MT deletion strains. Although elevated levels of cadmium at 12 μM did marginally reduce average lifespan in all strains, the effect was statistically insignificant (Fig. 4A,B). As lifespan was not impaired in any of the strains tested, this indicates that the demographic index is independent from low doses of cadmium and MT expression.

4. Conclusions

Although MT is hailed as a major component in cadmium detoxification, the *mtl-1;mtl-2(zs1)* nematode is viable and thus MT does not seem to be essential to survival in the presence or absence of cadmium. In addition, the viability of the double knockout suggests that MT is unlikely to be an indispensable component of essential metal homeostasis including zinc or copper, both of which are present (in trace amounts) in the NGM medium and have been shown to be weak inducers of mlt transcription (Swain et al., 2004), at least at elevated levels. It is therefore conceivable that other pathways may complement or indeed supplement the cadmium detoxification process. Candidate genes are pcs-1 (a phytochelatin synthase) (Vatamaniuk et al., 2005) or the suite of cdr genes (Dong et al., 2005), all of which have been shown to be powerful responders to cadmium exposure.

Nevertheless, the deletion of both MT loci increased the sensitivity of the nematode in response to cadmium, reflected by a reduction in total brood size and changes in the daily reproductive output. This suggests that MT does provide a protective role from the toxic effects exerted by cadmium. Most striking, however, is the observation that a significantly impaired brood size and volumetric growth were also manifested in the absence of cadmium.

Acknowledgements

We thank the *C. elegans* KnockOut Consortium for the isolation of the *gk125(vc128)* allele, the *Caenorhabditis* Genetics Centre, which is funded by the National Institutes of Health National Centre for Research Resources, for the supply of N2 and *mtl-2(gk125)* and the Mitani laboratory (Tokyo Women's Medical University School of Medicine, Japan) for the isolation of *mtl-1(tm1700)*. This work was supported by a Natural Environmental Research Council (NERC) studentship (NER/S/A/2005/13135) and the Royal Society.

References

Alvarez, O.A., Jager, T., Kooijman, A.L.M., Kammenga, J.E., 2005. Responses to stress of *Caenorhab*ditis *elegans* populations with different reproductive strategies. Funct. Ecol. 19, 656–664.

Beattie, J.H., Owen, H.L., Wallace, S.M., Arthur, J.R., Kwun, I.S., Hawksworth, G.M., Wallace, H.M., 2005. Metallothionein overexpression and resistance to toxic stress. Toxicol. Lett. 16 (157), 69–78.

Brenner, S., 1974. The genetics of *Caenorhabditis elegans*. Genetics 77, 71–94.

Byerly, L., Cassada, R.C., Russell, R.L., 1976. The life cycle of the nematode *Caenorhabditis elegans*. Dev. Biol. 51, 23–33.

Chapman, G.A., Kay, J., Kille, P., 1999. Structural and functional analysis of the rat metallothionein III genomic locus. Biochim. Biophys. Acta 1445 (3), 321–329.

Colangelo, D., Mahboobi, H., Viarengo, A., Osella, D., 2004. Protective effect of metallothioneins against oxidative stress evaluated on wild type and MT-null cell lines by means of flow cytometry. Biometals 17 (4), 365–370.

Dallinger, R., Berger, B., Hunziker, P., Kägi, J.H., 1997. Metallothionein in snail Cd and Cu metabolism. Nature 388 (6639), 237–238.

Dallinger, R., Chabicovsky, M., Hodl, E., Prem, C., Hunziker, P., Manzl, C., 2005. Copper in *Helix pomatia* (Gastropoda) is regulated by one single cell type: differently responsive metal pools in rhogocytes. Am. J. Physiol. Regul. Integr. Comp. Physiol. 289, R1185–R1195.

Domenech, J., Palacios, O., Villarreal, L., Gonzalez-Duarte, P., Capdevila, M., Atrian, S., 2003. MTO: the second member of a Drosophila dual copper-thionein system. FEBS Lett. 533 (1–3), 72–78.

Daniels, M.J., Turner-Cavet, J.S., Selkirk, R., Sun, H., Parkinson, J.A., Sadler, P.J., Robinson, N.J., 1998. Coordination of Zn^{2+} (and Cd^{2+}) by prokaryotic metallothionein. Involvement of his-imidazole. J. Biol. Chem. 273 (36), 22957–22961.

Dong, J., Song, M.O., Freedman, J.H., 2005. Identification and characterisation of a family of *Caenorhabditis elegans* genes that is homologous to the cadmium-responsive gene cdr-1. Biochim. Biophys. Acta 1727, 16–26.

Freedman, J.H., Slice, L.W., Dixon, D., Fire, A., Rubin, C.S., 1993. The novel metallothionein genes of *Caenorhabditis elegans*. J. Biol. Chem. 268, 2554–2564.

Jager, T., Alvarez, O.A., Kammenga, J.E., Kooijman, A.L.M., 2005. Modelling nematode life cycles using dynamic energy budgets. Funct. Ecol. 19, 136–144.

Klaassen, C.D., Liu, J., Choudhuri, S., 1999. Metallothionein: an intracellular protein to protect against cadmium toxicity. Annu. Rev. Pharmacol. Toxicol. 39, 267–294.

Knapen, D., Redeker, E.S., Inacio, I., De Coen, W., Verheyen, E., Blust, R., 2005. New metallothionein mRNAs in *Gobio gobio* reveal at least three gene duplication events in cyprinid metallothionein evolution. Comp. Biochem. Physiol. C Toxicol. Pharmacol. 140 (3–4), 347–355.

Moilanen, L.H., Fukushige, T., Freedman, J.H., 1999. Regulation of metallothionein gene transcription. J. Biol. Chem. 274, 29655–29665.

Plamiter, R.D., 1998. The elusive function of metallothioneins. Proc. Natl. Acad. Sci. USA 95, 8428–8430.

Stephan, W., Rodriguez, V.S., Zhou, B., Parsch, J., 1994. Molecular evolution of the metallothionein gene Mtn in the melanogaster species group: results from *Drosophila ananassae*. Genetics 138 (1), 135–143.

Stürzenbaum, S.R., Kille, P., Morgan, A.J., 1998. The identification, cloning and characterisation of earthworm metallothionein. FEBS Lett. 431, 437–442.

Stürzenbaum, S.R., Winters, C., Galay, M., Morgan, A.J., Kille, P., 2001. Metal ion trafficking in earthworms – identification of a cadmium specific metallothionein. J. Biol. Chem. 276, 34013–34018.

Stürzenbaum, S.R., Georgiev, O., Morgan, A.J., Kille, P., 2004. Cadmium detoxification in earthworms: from genes to cells. Environ. Sci. Technol. 38 (23), 6283–6289.

Swain, S.C., Keusekotten, K., Baumeister, R., Stürzenbaum, S.R., 2004. *C. elegans* metallothioneins: new insights into the phenotypic effects of cadmium toxicosis. J. Mol. Biol. 341, 951–959.

Timmermans, M.J.T.N., Ellers, J., Roelofs, D., Van Straalen, N.M., 2005. Metallothionein mRNA expression and cadmium tolerance in metal stressed and reference populations of the springtail *Orchesella cincta*. Ecotoxicology 14, 727–739.

Vasak, M., 2005. Advances in metallothionein structure and functions. J. Trace Elem. Med. Bio. 19, 13–17.

Vatamaniuk, O.K., Bucher, E.A., Sundaram, M.V., Rea, P.A., 2005. CeHMT-1, a putative phytochelatin transporter, is required for cadmium tolerance in *Caenorhabditis elegans*. J. Biol. Chem. 280, 23684–23690.

West, A.K., Stallings, R., Hildebrand, C.E., Chiu, R., Karin, M., Richards, R.I., 1990. Human metallothionein genes—structure of the functional locus at 16q13. Genomics 8, 513–518.

WHO, 1996. Guidelines for Drinking-Water Quality. In: Health Criteria and Other Supporting Information, second ed., vol. 2. World Health Organization, Geneva.

Zimeri, A.M., Dhankher, O.P., McCaig, B., Meagher, R.B., 2005. The plant MT1 metallothioneins are stabilized by binding cadmiums and are required for cadmium tolerance and accumulation. Plant Mol. Biol. 58 (6), 839–855.

TOXICOLOGICAL SCIENCES 106(2), 384–391 (2008)
doi:10.1093/toxsci/kfn180
Advance Access publication August 22, 2008

Knock down of *Caenorhabditis elegans cutc-1* Exacerbates the Sensitivity Toward High Levels of Copper

Sara Calafato,* Suresh Swain,† Samantha Hughes,†,* Peter Kille,* and Stephen R. Stürzenbaum†,[1]

*School of Biosciences, University of Cardiff, Main Building, Park Place, Cardiff CF10 3TL, UK; and †Pharmaceutical Science Division, School of Biomedical and Health Sciences, King's College London, London SE1 9NH, UK

Received July 2, 2008; accepted August 14, 2008

Copper, though toxic in excess, is an essential trace element that serves as a cofactor in many critical biological processes such as respiration, iron transport, and oxidative stress protection. To maintain this balance between requirement and toxicity, biological systems have developed intricate systems allowing the preservation of homeostasis while ensuring delivery of copper to the appropriate cellular component. The nematode *Caenorhabditis elegans* was exploited to assess the effects of copper toxicity at the population level to identify key changes in life cycle traits including, lethality, brood size, generation time, growth, and life span. To enhance our understanding of the complexities of copper homeostasis at the genetic level, the expression profile and functional significance of a putative copper cytoplasmic metallochaperone *cutc-1* were analyzed. Using quantitative PCR technology, *cutc-1* was found to be downregulated with increasing $CuSO_4$ concentrations. However, although total (whole body) copper levels increased in nematodes exposed to elevated levels of copper, wild-type and knock down of *cutc-1* by RNA-mediated interference (RNAi) were statistically indistinguishable. Nevertheless, RNAi of *cutc-1* affected brood size, growth and induced a marked increase in protruding vulva and bagging phenotypes at higher copper exposures. This indicates that *cutc-1* plays a crucial role in the protection from excess copper.

Key Words: **copper; *C. elegans*; *cutC*; *cutc-1*.**

Copper ions can adopt distinct redox states, oxidized Cu^{2+} or reduced Cu^{+}, allowing the metal to play a pivotal role in cell physiology as a catalytic cofactor in the redox chemistry of enzymes and proteins (Tapiero *et al.*, 2003). These enzymes and proteins carry out fundamental biological functions that are required for growth and development (Linder, 1991). Copper proteins are involved in vital processes such as respiration (mitochondrial oxidative phosphorylation), iron transport, oxidative stress protection (free radical scavenging), blood clotting, hormone production, neurotransmitter synthesis and maturation, elastin crosslinking, and pigmentation (Petris *et al.*, 2003; Puig *et al.*, 2002; Tapiero *et al.*, 2003). As copper-requiring proteins are involved in such a wide variety of biological processes, deficiency can cause an alteration in enzyme activity, often causing disease states or pathophysiological conditions (Mak and Lam, 2008).

Excess copper ions can cause damage to cellular components because of an imbalance between the uptake and efflux of copper ions (Tapiero *et al.*, 2003). Copper is toxic to cells because of its ability to reversibly donate and receive electrons and is responsible for the intracellular generation of superoxide and other reactive oxygen species (Kimura and Nishioka, 1997). In addition, under anaerobic conditions, copper appears to shift from Cu^{++} to the Cu^{+} oxidation state thereby exacerbating the Cu^{+} concentration gradient and increasing its toxicity by facilitating passive or active uptake (Outten *et al.*, 2001). If allowed to engage in uncontrolled redox chemistry in a cell, copper can cause devastating and irreparable damage to proteins, lipids, and DNA (Rees and Thiele, 2004). It is therefore important that organisms have appropriate mechanisms for uptake and detoxification, as well as possessing cellular sensors to ensure that copper is present in the cell to drive the essential biochemical processes while preventing its accumulation to toxic levels (Mufti *et al.*, 2007; Pena *et al.*, 1998).

Several families of proteins have been shown to control the activity and distribution of intracellular metal ions (Rensing and Grass, 2003), including integral transmembrane transporters, metalloregulatory sensors, and diffusible cytoplasmic metallochaperone proteins that protect and guide metal ions to targets (Finney and O'Halloran, 2003). On the basis of the preliminary characterization of Cu-sensitive mutants in *Escherichia coli*, it was proposed that six genes (*cutA*, *cutB*, *cutC*, *cutD*, *cutE*, and *cutF*) are involved in the uptake, intracellular storage, and delivery and efflux of copper. A mutation in one or more of these genes results in increased copper sensitivity (Gupta *et al.*, 1995). A human ortholog of *E. coli* cutC was identified and found to be distributed throughout the cytoplasm, which is consensus with *E. coli* cutC, and suggests that cutC may be a cytoplasmic Cu-binding

[1] To whom correspondence should be addressed at Pharmaceutical Science Division, School of Biomedical and Health Sciences, King's College London, 150 Stamford Street, London SE1 9NH, UK. Fax: +44 207 848 4500. E-mail: stephen.sturzenbaum@kcl.ac.uk.

protein which plays a role in copper homeostasis and acts as a shuttle protein in intracellular copper trafficking (Li *et al.*, 2005).

The aim of this study was to assess the whole organism response of *C. elegans* exposed to copper, identify functional and expression characteristics of *cutc-1*, a putative copper transporter, and utilize RNA-mediated interference (RNAi) technology to knock down *cutc-1* to determine its involvement in copper toxicology.

MATERIALS AND METHODS

Caenorhabditis elegans strains and culture conditions Wild-type (N2, Bristol) *C. elegans* was used in all experiments and maintained on either nematode growth medium (NGM) agar in 55 mm Petri dishes at 20°C in a constant temperature incubator or in NGM liquid culture grown in 50 ml conical flasks within an orbital shaker at 150 rpm maintained at 20°C, according to standard procedures (Brenner, 1974; Lewis and Fleming, 1995; Sulston and Hodgkin, 1988). The bacterial food source was *E. coli* OP50 (an uracil-requiring *E. coli* strain to prevent overgrowth of the bacterial culture).

Metal content of exposure media and nematodes Exposures were performed by supplementing the NGM agar–based support media and the fresh overnight culture of *E. coli* OP50 (immediately prior to seeding on agar plates) and with equimolar amounts of $CuSO_4$. The copper concentration of fully oxidized nitric acid–digested samples was quantified either by Atomic Absorption Spectrophotometry (for NGM agar analysis) using an air-acetylene flame on a Varian SpecrAA-100 (Varian Instruments, Walton-on-Thames, Surrey, UK) with automatic background correction or, for nematodes exposed to copper-containing NGM plates, a Graphite Furnace (41102L, PerkinElmer, Waltham, MA). For the purpose of this study, all copper concentrations stated refer to nominal, not nitric acid extractable, amounts.

Quantitative PCR Nematodes were cultured in 750-ml S-basal media (5.85 g NaCl, 1 g K_2HPO_4, 6 g KH_2PO_4, made up to 999 ml with ddH_20, and following autoclave sterilization and cooling to below 55°C, 1 ml of cholesterol [5 mg/ml] was added) inoculated with 20 ml OP50 and LB broth (250 ml). The flask was incubated at 20°C, shaking at 150 rpm until the population reached approximately 50,000 staged nematodes. After centrifugation at 2000 × g for 2 min, the supernatant was removed to a minimal volume and the culture was split into 15-ml tubes. The nematodes were exposed in S-basal to 0, 100, 500, and 2000μM $CuSO_4$ for 24 h with five biological replicates at each concentration. Total RNA was extracted using a standard Tri-reagent protocol (Sigma, Gillingham, UK), purified and concentrated by ethanol precipitation, and 2 μg was used to generate complementary DNA (cDNA).

Gene-specific primers were used to amplify *cutc-1* (ZK353.7) and rla-1 (Y37E3.7) from *C. elegans* cDNA (Supplementary Table 1). The PCR product was visualized by agarose gel electrophoresis, gel extracted and cloned into pGEM-T (Promega, Southampton, UK). The inserts of the plasmids were sequenced using universal M13 primers to confirm the identity of the insert. Quantitative PCR (qPCR) amplifications were performed using TaqMan probe technology on the ABI Prism 7700 Sequence Detection System exploiting the primers and probes provided in Supplementary Table 1. Calibration standards and samples were quantified in parallel. Five biological replicates were prepared for each test sample, and for each biological replicate, the cDNA samples were analyzed in triplicate.

Preparation of target genes for RNAi Following cDNA synthesis, *cutc-1* was amplified using specific primers (Supplementary Table 1) with *EcoR1* adapters at the 5′ end. The PCR product was purified by gel extraction, ligated into the pGEM-T vector, and transformed into DH5α competent cells. The plasmid was purified, and positive clones were identified by restriction digest with *EcoR1*. The digested DNA was purified by gel extraction and subcloned into the RNAi vector pPD129.36 (an Amp^R plasmid containing an IPTG-inducible T7 RNA promoter). The *cutc-1*–containing plasmid was confirmed by sequencing and transformed into competent HT115 (F-, mcrA, mcrB, IN (rrnD-rrnE)1, lambda-, rnc14::Tn10 (DE3 lysogen:lacUV5 promoter—T7 polymerase)) which are deficient in RNase III, allowing the stable expression of double stranded RNA. For all RNAi experiments, the empty pPD129.36 vector was also transformed into HT115 cells and used as a control.

Caenorhabditis elegans RNAi exposure and sample preparation Nematodes were washed off agar plates using M9 buffer, centrifuged for 2 min at 2000 × g, and the supernatant removed. After pooling the nematodes, they were distributed onto agar plates containing 0, 20, 100, and 500μM $CuSO_4$ streaked with HT115 containing either the empty RNAi vector (pPD129.36) or the *cutc-1* RNAi clone. Once gravid, adults were synchronized using the standard egg preparation protocol and the F1 generation placed back onto the agar plates. When the nematodes reached L4 stage, they were either used to determine the life history parameters or frozen at − 80°C for subsequent RNA extraction.

Total brood size, generation time, life span, and lethality assay The life cycle of *C. elegans* was assessed over a range of copper concentrations in the presence or absence of *cutc-1* RNAi. Typically, staged nematodes were placed on NGM agar plates and replica plated every 24/36 h to a new plate. Brood size ($n = 20$ per dose and RNAi exposure), generation time, the time an egg takes to develop into a reproducing adult ($n = 30$ per dose and RNAi exposure), and life span, the timeframe between egg and death ($n = 100$ per dose and RNAi exposure) were measured by manual counting and observation. As *E. coli* OP50 does not grow on agar plates containing in excess of 1mM $CuSO_4$, the lethality assay was performed in liquid culture. The lethal concentration of $CuSO_4$ (± *cutc-1* RNAi) was determined using staged nematodes placed in M9 buffer (to maintain the pH and minimize the risk of a shift in Cu speciation) supplemented with OP50. The nematodes were rotated at 20°C and the titer determined every 24 h (three biological replicates were used with four titers performed for each exposure), and the average number of nematodes was calculated.

RESULTS

Lethality of Caenorhabditis elegans Exposed to $CuSO_4$ in Liquid Culture

A distinct dose-responsive effect causing detrimental effects on the survival of nematodes with increasing $CuSO_4$ concentrations was observed (Figure 1) where survival was reduced to 50% within 76 h at a nominal concentration of 0.25mM $CuSO_4$. At $CuSO_4$ concentrations of 0.5, 1, 2, and 3mM, the timeframe was reduced to 46, 42, 16, and 13 h, respectively. LC50 concentrations for *C. elegans* were obtained from three independent repeats ± SEM, resulting in an LC_{50} (24 h) of 1.59 ± 0.04mM $CuSO_4$, an LC_{50} (48 h) of 0.47 ± 0.01mM $CuSO_4$, an LC_{50} (72 h) of 0.29 ± 0.01mM $CuSO_4$, and an LC_{50} (96 h) of 0.02 ± 0.01mM $CuSO_4$.

Bioinformatic Analysis of Caenorhabditis elegans cutc-1

The putative copper homeostasis protein CUTC-1 (ZK353.7) is 250 amino acids in length and contains two exons. It is located in the center of an operon containing an ubiquitin regulatory protein and leucine aminopeptidase, a zinc metalloprotease. *C. elegans* CUTC-1 was aligned to human, rat, fly,

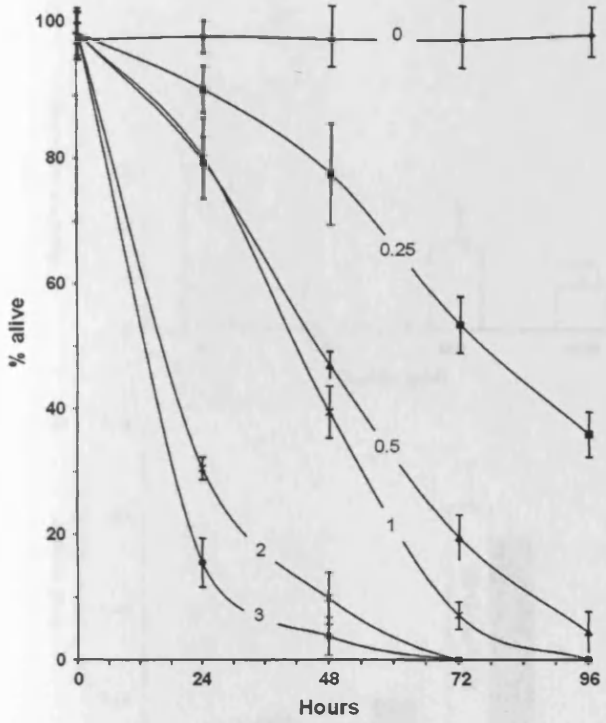

FIG. 1. The effect of copper (0, 0.25, 0.5, 1, 2, and 3mM $CuSO_4$) on the lethality of nematodes maintained in liquid culture over a 4-day exposure period. The data presented are averages from five independent experiments and expressed as mean survival ± SEM.

A:		Hs	Rn	Dm	Ec	Ce	Cb
Hs	% identity	100					
	% similarity	100					
Rn	% identity	90	100				
	% similarity	96	100				
Dm	% identity	45	46	100			
	% similarity	63	63	100			
Ec	% identity	44	43	41	100		
	% similarity	58	59	63	100		
Ce	% identity	39	39	38	38	100	
	% similarity	59	60	58	59	100	
Cb	% identity	37	40	36	38	82	100
	% similarity	60	64	58	58	92	100

B:	Cellular location	Percentage probability
Cytoplasmic		73.9 %
Mitochondrial		8.7 %
Nuclear		8.7 %
Golgi		4.3 %
Cytoskeletal		4.3 %

C:

FIG. 2. Identity/similarity scores of *Caenorhabditis elegans* CUTC-1 (Ce) and corresponding CutC orthologs in *Homo sapiens* (Hs), *Rattus norvegicus* (Rn), *Drosophila melanogaster* (Dm), *Escherichia coli* (Ec), and *Caenorhabditis briggsae* (Cb) were calculated using NCBI's bl2seq algorithm (Panel A). Prediction of the cellular location of *cutc-1* was performed using the ExPASy k-NN program (Panel B). The 3D molecular structure of CUTC-1 was modeled from the x-ray crystallography of the protein from *Shigella flexneri* (Zhu et al., 2005) using SWISS-MODEL (Guex and Peitsch, 1997; Peitsch, 1995; Schwede *et al.*, 2003) and visualized using Swiss-pdbViewer 3.7 (Panel C).

nematode, and bacterial orthologs using the ClustalW algorithm (see Supplementary Fig. 1). The protein family does not contain classic copper-binding motifs such as MXM or MXXXM but instead displays a highly conserved motif, VTFHRAFD, of unknown function. Pair wise comparison, using the bl2seq option of the NCBI BLAST suite, revealed a consistent identity score of 38–39% and similarity score of 58–60% in relation to human, rat, fly, and bacterial counterparts which increased to 82% identity and 92% similarity when compared to the nematode *Caenorhabditis briggsae*, a conservation that is not dissimilar to the conservation between rat and human orthologs (Figure 2, Panel A). Further analysis included a hydrophobicity plot, which indicated that CUTC-1 does not contain transmembrane-bound domains and therefore is unlikely to be located in the membrane (data not shown). Likewise, it was deduced that the *C. elegans* CUTC-1 protein does not have an N-terminal signal peptide, a mitochondrial or nuclear localization site, or an ER retention motif as defined by the EXPASY bioinformatics tools (http://www.expasy.org/tools) but is predicted to be of cytoplasmic nature (Figure 2, Panel B).

A 3D representation of CUTC-1 was generated by homology modeling (SWISS-MODEL; Guex and Peitsch, 1997; Peitsch, 1995; Schwede *et al.*, 2003) using the x-ray crystallography of the CUTC of *Shigella flexneri* as a template (Zhu *et al.*, 2005) and visualized using Swiss-pdbViewer 3.7 (Figure 2, Panel C). The 3D structure of CUTC-1 consists of a series of parallel β-sheets arranged in a barrel formation surrounded by α-helices. The α-helices connect the parallel strands of the β-sheets and run antiparallel to the β-sheets, an overall structure that closely resembles a TIM or α/β barrel protein. The conserved VTFHRA motif is located within the hydrophobic core of the protein with conserved histidine and charged residues reside inside the TIM barrel (see Supplementary Fig. 1) which have previously been predicted to be functionally important for copper binding (Zhu *et al.*, 2005). In addition, two evolutionarily conserved cysteine residues (cys15 and cys32) lie inside the barrel and therefore may potentially be involved in metal binding.

Expression of cutc-1 in Wild-type Caenorhabditis elegans and Efficiency of cutc-1 RNAi

The transcriptional expression of *cutc-1* was quantified in *Caenorhabditis elegans* exposed to different $CuSO_4$ concentrations using TaqMan probe technology and normalized against the control gene *rla-1*. Compared to control nematodes, the relative expression of *cutc-1* was reduced in nematodes exposed for 24 h to 100μM $CuSO_4$ and statistically significantly reduced at 500μM $CuSO_4$ ($p \leq 0.012$) and 2000μM $CuSO_4$ ($p \leq 0.006$) (Figure 3, Panel A). In addition,

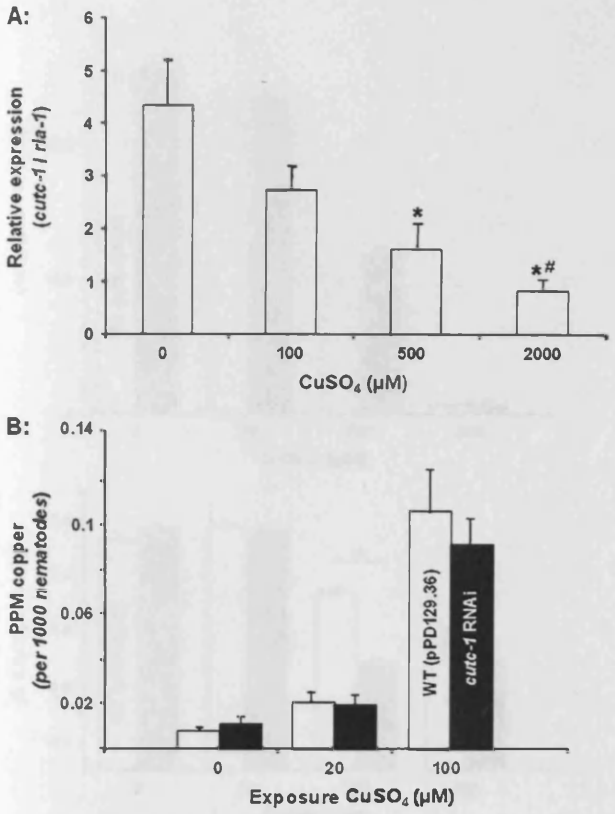

FIG. 3. The relative gene expression of *cutc-1* is reduced in nematodes exposed to copper. * denotes a significant difference ($p \leq 0.05$) from control (0 $CuSO_4$) and # denotes a significant difference from nematodes exposed to 100μM $CuSO_4$ (Panel A). Total (nitric acid extractable) body burden of copper increases with environmental concentrations. Note that there is no statistically significant difference between wild type and the knock down of *cutc-1* (Panel B).

qPCR was used to determine the efficiency of the transcript suppression following the RNAi silencing of *cutc-1* by bacterial feeding. The comparison of *cutc-1* expression in the presence and absence of RNAi demonstrated that *cutc-1* was effectively silenced by 75% (see Supplementary Fig. 2A).

Copper Accumulation in the Presence or Absence of RNAi Silencing of cutc-1

Caenorhabditis elegans was routinely maintained on standard NGM agar which was shown to contain a basal level of 6μM copper when extracted with concentrated nitric acid. Assessment of the nitric acid–extractable concentration of copper in the agar plates was observed to be 40% less than the nominal concentration of $CuSO_4$ added to the agar plates (see Supplementary Table 2). Due to the small physical size of nematodes, it was necessary to tool 1000 individuals to allow the quantification of total, nitric acid–extractable, copper concentrations. A dose-dependent increase was observed, and 100μM $CuSO_4$ caused a statistically significant increase in copper levels. The RNAi of *cutc-1* caused a similar increase that, though marginally lower at the highest concentration tested, was statistically not different to wild-type nematodes (see Figure 3B). This implies that *C. elegans cutc-1* is not the major exporter of excess copper.

Life Cycle Traits Following the Knockdown of cutc-1 by RNAi

Total brood size decreased with increasing $CuSO_4$ concentrations in both the control nematodes and those exposed to *cutc-1* RNAi. In the presence of RNAi of *cutc-1*, nematodes exposed to 100μM $CuSO_4$ produced significantly less progeny than the respective wild-type nematodes ($p \leq 0.05$). It is remarkable that at 500μM $CuSO_4$, the reproductive output was decimated to below 5% of control plates (Figure 4A). Generation time increased with increasing concentrations of $CuSO_4$. The average generation time was 66 h at 0μM $CuSO_4$, increasing to 78 h at 500μM $CuSO_4$. There was no significant difference in the generation time between wild-type nematodes and those exposed to the RNAi of *cutc-1* (see Supplementary Fig. 2B).

Nematode length decreased with increasing $CuSO_4$ concentrations in wild-type and RNAi exposures. Reduction in growth was most marked in nematodes exposed to the two highest concentrations (100 and 500μM $CuSO_4$) during the knock down of *cutc-1* and significantly different to wild-type ($p < 0.000$ and 0.002 for nematodes exposed to 100 and 500μM $CuSO_4$, respectively) (Figure 4, Panel B). The average life span of nematodes generally decreased with increasing $CuSO_4$ concentrations, being significantly shorter at 500μM $CuSO_4$ compared to 0, 20, and 100μM $CuSO_4$ ($p < 0.001$). There was also a significant decrease in the life span from 0 to 100μM $CuSO_4$ and from 20 to 100μM $CuSO_4$ ($p < 0.001$). No differences in life span were observed between wild type and the nematodes exposed to the RNAi of *cutc-1* (see Supplementary Fig. 2C).

Phenotypic Effects of $CuSO_4$ Following RNAi of cutc-1

The phenotypes protruding vulva (pvl) and bag of worms (egl) were frequently encountered in *C. elegans* exposed to $CuSO_4$. The prevalence of these phenotypes over a range of $CuSO_4$ concentrations was observed, and the number of nematodes that perished from bag of worms was determined from over 100 nematodes per dose. Nematodes exposed to the RNAi of *cutc-1* displayed the bagged phenotype at all $CuSO_4$ concentrations with an increasing incidence at elevated $CuSO_4$ concentrations, with 15% of the nematodes displaying the phenotype at 0μM $CuSO_4$, increasing to 74% at 500μM $CuSO_4$. In contrast, bagging in wild-type nematodes occurred only at 100μM $CuSO_4$ and 500μM $CuSO_4$, with 10% and 70%, respectively, of the nematodes developing bag of worms (Figure 5, Panel A). PD4251 (ccls4251 I; dpy-20 (e1282) IV) a strain that produces green fluorescent protein in all body wall and vulval muscles (with a combination of mitochondrial and

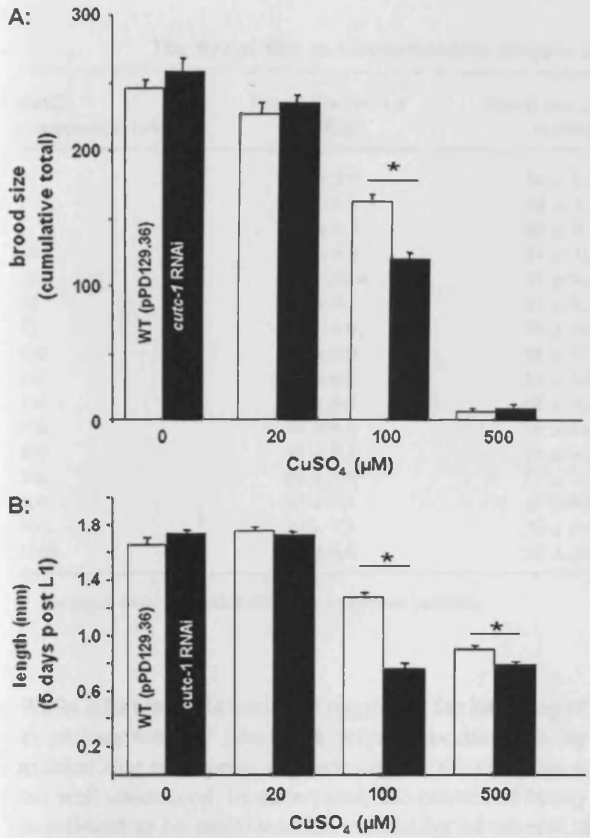

FIG. 4. Total brood size is reduced in nematodes exposed to increasing doses of copper. Following the RNAi of *cutc-1* (black bars), no statistical difference in brood size was observed under control and low copper exposure conditions, but deemed statistically different while exposed to 100μM $CuSO_4$ (Panel A). After a 5-day exposure period, the length of the nematode is reduced in a copper dose-dependent manner, a trend that is amplified in nematodes subjected to the RNAi of *cutc-1* (Panel B). Replicates per dose and condition: brood size $n = 20$; length $n = 15$.

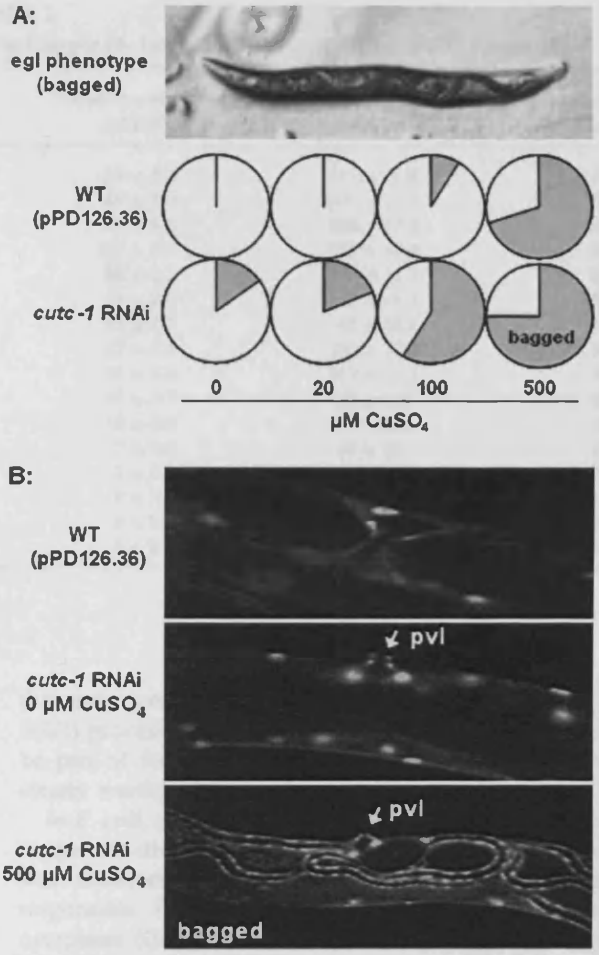

FIG. 5. Copper induces an egg laying–defective (egl) phenotype (leading to the offspring hatching internally, bagging). RNAi of *cutc-1* increases the percentage of bagging, notably also in the absence of $CuSO_4$ (Panel A; $n = 100$). Bagging was frequently caused by a protruding vulva (pvl) phenotype. Panel B illustrates this using PD4251, a transgenic strain that expresses a vulval and body wall muscle green fluorescent protein, in the presence and absence of *cutc-1* RNAi and $CuSO_4$.

nuclear localization) was used to visualize the presence of both phenotypes during $CuSO_4$ exposure and RNAi of *cutc-1* (Figure 5, Panel B). It is, at this stage, not known if the pvl/egl phenotype is an indirect or direct effect of copper toxicosis, a notion that clearly warrants further investigations.

DISCUSSION

Metal analysis highlighted that basal amounts (prior to the addition of $CuSO_4$) approximated 6μM copper in control agar. In *C. elegans*, concentrations of excess $CuSO_4$ induced detrimental effects on brood size (Table 1), life span and an increase in generation time. In addition to the development of phenotypic abnormalities, development (manifested as a reduction in body size and growth) was impaired. The results of whole-organism copper toxicity in nematodes is of course not novel and has been exquisitely documented for *C. elegans*, *Pristionchus pacificus*, and *Panagrellus redivivus* (Boyd and Williams, 2003), results that are concurrent with other soil-inhabiting organisms such as the springtail *Proisotoma minuta* (Nursita *et al.*, 2005) and the earthworm *Lumbricus rubellus* (Spurgeon *et al.*, 2005).

As the minimum inhibitory concentration of *E. coli* on agar medium is 1mM (Spain and Alm, 2003), LC50 experiments were carried out in liquid culture to ensure the bacterial food source was not a limiting factor. The 24-h and 72-h LC50 of $CuSO_4$ in *C. elegans* was determined to be 1.59 and 0.29mM, respectively. This concurs with a previous study in *C. elegans*, where the 24-h LC50 of $CuSO_4$ was predicted to be 1.57mM (Tatara *et al.*, 1998).

The essential yet toxic nature of copper highlights that regulation via a simple copper exclusion system is unlikely.

TABLE 1
The Brood Size of *Caenorhabditis Elegans* Exposed to Copper (0–1mM CuSO4) on Standard NGM Plates

$CuSO_4$ concentration (μM)	Brood size 0–24 h (±SEM)	Brood size 25–48 h (±SEM)	Brood size 49–72 h (±SEM)	Brood size cumulative (±SEM)	Total brood size (% of control)
0	59 ± 5.8	94 ± 8.2	94 ± 5.4	247 ± 11.8	100
1	36 ± 6.8	82 ± 7.5	89 ± 1.0	207 ± 14.9	84
5	33 ± 6.5	85 ± 6.1	106 ± 4.3	224 ± 11.5	91
10	41 ± 5.8	67 ± 11.3	107 ± 5.0	215 ± 19.4	87
25	43 ± 13.4	77 ± 8.0	98 ± 0.5	218 ± 11.5	88
50	41 ± 7.1	83 ± 6.5	78 ± 2.0	202 ± 11.3	82
75	39 ± 3.9	70 ± 10.1	57 ± 4.7	166 ± 14.2	67
100	41 ± 8.9	48 ± 13.2	37 ± 3.5	126 ± 30.3	51
125	31 ± 6.3	51 ± 6.6	35 ± 3.0	117 ± 12.3	47
150	41 ± 5.9	51 ± 3.2	18 ± 2.7	113 ± 9.3	46
200	44 ± 4.4	18 ± 1.6	10 ± 0.0	69 ± 6.2	28
400	48 ± 5.3	16 ± 4.1	3 ± 0.0	67 ± 8.5	27
500	40 ± 5.9	17 ± 7.5	2 ± 0.0	59 ± 12.0	24
600	30 ± 8.9	15 ± 4.8	0 ± 0.0	45 ± 13.6	18
800	30 ± 7.2	20 ± 2.6	0 ± 0.0	50 ± 9.2	20
1000	34 ± 0.6	19 ± 1.5	0 ± 0.0	53 ± 1.9	21

Averages were calculated from six replicates (±SEM).

While information is available regarding the handling of metals in prokaryotes and yeast, the precise mechanisms by which multicellular eukaryotes regulate copper are complex and thus not well understood. In eukaryotes, the control of heavy metals is believed to be multifactorial, consisting of several different pathways, encompassing a whole scope of chaperones, metalloenzymes, permeases, reductases, and transcription factors. The knowledge base has recently expanded significantly through the application of microarray technology, including experimental systems such as yeast (Yasokawa *et al.*, 2008), earthworms (Bundy *et al.*, 2008), and mice (Eun *et al.*, 2008); however, a meaningful and exhaustive bioinformatic analysis remains the major challenge to facilitate the identification of new genes and pathways involved in copper trafficking.

Bioinformatic analysis of *C. elegans* CUTC-1 confirmed its putative role as a cytosolic copper chaperone. The sequence alignment highlighted a conserved VTFHRA motif of unknown function that was conserved in all species. 3D structure prediction placed this motif in the hydrophobic core of the protein, indicating a likely role of importance. Noteworthy is the observation that histidine residues, frequently associated with copper binding (Rogers *et al.*, 1991), are located on either side of the protein pore. The overall structure of the modeled protein closely resembles an α/β barrel typical (but not exclusive) of enzymes that catalyze a very wide range of different reactions but can also have nonenzymatic roles in the cell including binding and transport proteins (Nagano *et al.*, 1999; Reardon and Farber, 1995). CUTC-1 is located in the center of an operon containing the ubiquitin regulatory protein, UBXD2, and *lap-1*, a leucine aminopeptidase. Given that operons are not random gene assemblages but coregulate genes that make proteins with related functions (Blumenthal *et al.*, 2002) provides circumstantial evidence that *cutc-1* may indeed be part of the protein degradation pathway, a notion that is clearly worthy of further investigation.

In *E. coli*, cutC mutants are copper sensitive and accumulate copper but display normal kinetics of copper uptake. The gene was therefore postulated to encode for an efflux protein responsible for the removal of excess copper from the cytoplasm (Gupta *et al.*, 1995). This is in contrast to the data observed for *C. elegans*. Firstly, the concentration of total copper did not change significantly upon the knock down of *cutc-1*. Secondly, transcription of *cutc-1* was downregulated at elevated $CuSO_4$ concentrations, a finding that is in partial agreement with Rodrigues *et al.* (2008) who found that *cutC* was downregulated in biofilm cells of *Xylella fastidiosa* a plant pathogen at 7mM $CuSO_4$ compared to 3 and 5mM. This suggests that *cutc-1* is, at least in the nematode, unlikely to be a positive regulator of bulk copper efflux, *per se*.

By means of RNAi, it was possible to characterize the involvement of *cutc-1* in $CuSO_4$-induced changes in life cycle parameters. Prior to performing the RNAi experiments, the efficiency of *cutc-1* knock down was assessed by qPCR, which showed that *cutc-1* expression could be reduced by over 75% using RNAi. Nematodes exposed to *cutc-1* RNAi were significantly smaller than wild-type nematodes at elevated $CuSO_4$. High levels of copper were also shown to induce vulval abnormalities (pvl and resultant bagging), a phenotype that was more frequently encountered when *cutc-1* was knocked down and was also present at basal copper concentrations. In conclusion, this work suggests that *cutc-1* may have a complex role in the trafficking of copper from the cell or in intracellular

storage of free copper ions. Furthermore, it provides the first tantalizing insights into the biological processes and molecular functions associated with this novel copper metallochaperone within a eukaryotic organism and reveals a substantial diversity in function over its prokaryotic counterparts.

SUPPLEMENTARY DATA

Supplementary data are available online at http://toxsci.oxfordjournals.org/.

FUNDING

UK Natural Environmental Research Council (NER/T/S/2001/00021); Brixham Environmental Laboratory (AstraZeneca); Royal Society to S.R.S.

ACKNOWLEDGMENTS

We thank the *Caenorhabditis* Genetics Centre, which is funded by the National Institutes of Health National Centre for Research Resources, for the supply of N2 and PD4251. In addition, we are grateful to Wendy Williams for her contribution during the early stages of the project and Mr M. O'Riley (Cardiff University) and Dr T. Blackall (King's College London) for metal analyses.

REFERENCES

Blumenthal, T., Evans, D., Link, C. D., Guffanti, A., Lawson, D., Thierry-Mieg, J., Thierry-Mieg, D., Chiu, W. L., Duke, K., Kiraly, M., *et al.* (2002). A global analysis of *Caenorhabditis elegans* operons. *Nature* **417,** 851–854.

Brenner, S. (1974). The genetics of *Caenorhabditis elegans*. *Genetics* **77,** 71–94.

Boyd, W. A., and Williams, P. L. (2003). Comparison of the sensitivity of three nematode species to copper and their utility in aquatic and soil toxicity tests. *Environ. Toxicol. Chem.* **22**(11), 2768–2774.

Bundy, J. G., Sidhu, J. K., Rana, F., Spurgeon, D. J., Svendsen, C., Wren, J. F., Stürzenbaum, S. R., Morgan, A. J., and Kille, P. (2008). 'Systems toxicology' approach identifies coordinated metabolic responses to copper in a terrestrial non-model invertebrate, the earthworm *Lumbricus rubellus*. *BMC Biol.* **6,** 25.

Eun, J. W., Ryu, S. Y., Noh, J. H., Lee, M. J., Jang, J. J., Ryu, J. C., Jung, K. H., Kim, J. K., Bae, H. J., Xie, H., *et al.* (2008). Discriminating the molecular basis of hepatotoxicity using the large-scale characteristic molecular signatures of toxicants by expression profiling analysis. *Toxicology* **249,** 91–106.

Finney, L. A., and O'Halloran, T. V. (2003). Transition metal speciation in the cell: Insights from the chemistry of metal ion receptors. *Science* **300,** 931–936.

Guex, N., and Peitsch, M. C. (1997). SWISS-MODEL and the Swiss-PdbViewer: An environment for comparative protein modeling. *Electrophoresis* **18,** 2714–2723.

Gupta, S. D., Lee, B. T. O., Camakaris, J., and Wu, H. C. (1995). Identification of *cutC* and *cutF (nlpE)* genes involved in copper tolerance in *Escherichia coli*. *J. Bacteriol.* **15,** 4207–4215.

Kimura, T., and Nishioka, H. (1997). Intracellular generation of superoxide by copper sulphate in *Escherichia coli*. *Mutat. Res.* **389,** 237–242.

Lewis, J. A., and Fleming, J. T. (1995). Basic culture methods. In *Caenorhabditis elegans*: Modern Biological Analysis of an Organism (H. F. Epstein and D. C. Shakes, Eds.), pp. 3–29. Academic Press, San Diego, CA.

Li, J., Ji, C., Chen, J., Yang, Z., Wang, Y., Fei, X., Zheng, M., Gu, X., Wen, G., Xie, Y., *et al.* (2005). Identification and characterization of a novel Cut family cDNA that encodes human copper transporter protein CutC. *Biochem. Biophys. Res. Commun.* **337,** 179–183.

Linder, M. C. (1991). In *Biochemistry of Copper*. Plenum Press, New York.

Mak, C. M., and Lam, C. W. (2008). Diagnosis of Wilson's disease: A comprehensive review. *Crit. Rev. Clin. Lab. Sci.* **45,** 263–290.

Mufti, A. R., Burstein, E., and Duckett, C. S. (2007). XIAP: Cell death regulation meets copper homeostasis. *Arch. Biochem. Biophys* **463**(2), 168–174.

Nagano, N., Hutchinson, E. G., and Thornton, J. M. (1999). Barrel structures in proteins: Automatic identification and classification including a sequence analysis of TIM barrels. *Protein Sci.* **10,** 2072–2084.

Nursita, A. I., Singh, B., and Lees, E. (2005). The effects of cadmium, copper, lead, and zinc on the growth and reproduction of *Proisotoma minuta* Tullberg (Collembola). *Ecotoxicol. Environ Saf.* **60**(3), 306–314.

Outten, F. W., Huffman, D. L., Hale, J. A., and O'Halloran, T. V. (2001). The independent *cue* and *cus* systems confer copper tolerance during aerobic and anaerobic growth in *Escherichia coli*. *J. Biol. Chem.* **276,** 30670–30677.

Peitsch, M. C. (1995). Protein modeling by E-Mail. *Biotechnology* **13,** 658–660.

Pena, M. M., Koch, K. A., and Thiele, D. J. (1998). Dynamic regulation of copper uptake and detoxification genes in *Saccharomyces cerevisiae*. *Mol. Cell. Biol.* **18,** 2514–12314.

Petris, M. J., Smith, K., Lee, J., and Thiele, D. J. (2003). Copper-stimulated endocytosis and degradation of the human copper transporter, hCtr1. *J. Biol. Chem.* **11,** 9639–9646.

Puig, S., Lee, J., Lau, M., and Thiele, D. J. (2002). Biochemical and genetic analyses of yeast and human high affinity copper transporters suggest a conserved mechanism for copper transport. *J. Biol. Chem.* **29,** 277.

Reardon, D., and Farber, G. K. (1995). The structure and evolution of alpha/beta barrel proteins. *FASEB J.* **9,** 497–503.

Rees, E. M., and Thiele, D. J. (2004). From aging to virulence: Forging connections through the study of copper homeostasis in eukaryotic microorganisms. *Curr. Opin. Microbiol.* **71,** 1–10.

Rensing, C., and Grass, G. (2003). *Escherichia coli* mechanisms of copper homeostasis in a changing environment. *FEMS Microbiol. Rev.* **2-3,** 197–213.

Rodrigues, C. M., Takita, M. A., Coletta-Filho, H. D., Olivato, J. C., Caserta, R., Machado, M. A., and de Souza, A. A. (2008). Copper resistance of biofilm cells of the plant pathogen *Xylella fastidiosa*. *Appl. Microbiol. Biotechnol* **77**(5), 1145–1157.

Rogers, S. D., Bhave, M. R., Mercer, J. F. B., Camakaris, J., and Lee, B. T. O. (1991). Cloning and characterisation of *cutE*, a gene involved in copper transport in *Escherichia coli*. *J. Bacteriol.* **173,** 6742–6748.

Schwede, T., Kopp, J., Guex, N., and Peitsch, M. C. (2003). SWISS-MODEL: An automated protein homology-modeling server. *Nucleic Acids Res.* **13,** 3381–3385.

Spain, A., and Alm, E. (2003). Implications of microbial heavy metal tolerance in the environment. *Rev. Undergrad. Res.* **2,** 1–6.

Spurgeon, D. J., Svendsen, C., Lister, L. J., Hankard, P. K., and Kille, P. (2005). Earthworm responses to Cd and Cu under fluctuating environmental conditions: A comparison with results from laboratory exposures. *Environ. Pollut.* **136,** 443–452.

Sulston, J. E., and Hodgkin, J. (1988). Methods. In The Nematode *Caenorhabditis elegans* (W. B. Wood, Ed.), pp. 587–606. CSHL Press, Cold Spring Harbor, NY.

Tapiero, H., Townsend, D. M., and Tew, K. D. (2003). Trace elements in human physiology and pathology: Copper. *Biomed. Pharmacother.* **57,** 386–398.

Tatara, C. P., Newman, M. C., McCloskey, J. T., and Williams, P. L. (1998). Use of ion characteristics to predict relative toxicity of mono-, di-, and trivalent metal ions: *Caenorhabditis elegans* LC50. *Aquat. Toxicol.* **42,** 255–269.

Yasokawa, D., Murata, S., Kitagawa, E., Iwahashi, Y., Nakagawa, R., Hashido, T., and Iwahashi, H. (2008). Mechanisms of copper toxicity in Saccharomyces cerevisiae determined by microarray analysis. *Environ. Toxicol.* doi: 10.1002/tox.20406.

Zhu, Y. Q., Zhu, D. Y., Lu, H. X., Yang, N., Li, G. P., and Wang, D. C. (2005). Purification and preliminary crystallographic studies of CutC, a novel copper homeostasis protein from *Shigella flexneri*. *Protein Pept. Lett.* **12,** 823–826.